THE UNIVERSITY
of EDINBURGH

This thesis has been submitted in fulfilment of the requirements for a postgraduate degree (e.g. PhD, MPhil, DClinPsychol) at the University of Edinburgh. Please note the following terms and conditions of use:

This work is protected by copyright and other intellectual property rights, which are retained by the thesis author, unless otherwise stated.
A copy can be downloaded for personal non-commercial research or study, without prior permission or charge.
This thesis cannot be reproduced or quoted extensively from without first obtaining permission in writing from the author.
The content must not be changed in any way or sold commercially in any format or medium without the formal permission of the author.
When referring to this work, full bibliographic details including the author, title, awarding institution and date of the thesis must be given.

The Biological Synthesis of Stable Copper Nanoparticles

Nikolaos Pantidos

Thesis submitted for the degree of Doctor of Philosophy to The University of Edinburgh

2016

Abstract

Many nonferrous industries such as mining and surface treatment plants produce co-products that are high in heavy metals and therefore toxic to the environment. A less obvious producer of heavy metal containing co-products is the whisky industry. Current methods of copper removal from such co-products include electrolysis and membrane filtration which are impractical and costly. When copper is found as a salt, current methods of removal include settlement, filtration and precipitation. Alternatives such as biological copper ion removal from effluents has also been shown to be effective.

This study aimed to develop a biological method for the synthesis of stable copper nanoparticles. *Morganella psychrotolerans* was used to reduce Cu^{2+} to insoluble Cu^{0} nanoparticles. The nanoparticles were purified and characterised using X-Ray Photoelectron Spectroscopy (XPS) and High-Resolution Transmission Electron Microscopy (HR-TEM). Whisky distillery co-products were tested as a growth medium for *M. psychrotolerans* with concomitant copper nanoparticle synthesis. The copper nanoparticles were also studied for their application in electronics in order to make conductive circuits.

Genomics studies combined with proteomics, helped develop possible models for copper nanoparticle synthesis by *M. psychrotolerans*, as well as identify proteins and genes not previously thought to be related to this pathway.

The genome sequence of *M. psychrotolerans* obtained in this work allowed for a far more detailed study on the mechanism of copper nanoparticle synthesis than previously possible. This thesis also focused on understanding this mechanism better through proteomics and qRT-PCR. In order to study the identified copper ion reduction pathway in the future, a genetic modification toolkit was developed for *M. psychrotolerans*.

Declaration

I hereby declare that this thesis was composed by me and that the research presented herein is my own work unless otherwise stated. This work has not been submitted for any other degree or professional qualification.

Nikolaos Pantidos

2016

Acknowledgements

First and foremost I would like to thank Dr Louise Horsfall for giving me the opportunity to carry out the research for my Ph.D. and for her constant encouragement to develop as a scientist. Her guidance and supervision was of tremendous help and I greatly appreciate her support for attending numerous conferences and meetings, keeping up to date with current trends in the field. Also, a big thank you to Professor David Arnot for his support and source of wisdom during the project.

I owe a bit thanks to Mike Capeness and Matt Edmundson for their advice, conceptual and technical support throughout the project, and of course the countless laughs we have had these past few years. Also a big thank you to all the Horsfall lab members who make working in the lab a fun environment to be in.

I would like to thank a collaborator, Dr David Clarke for providing his valuable time and expertise to perform MALDI-MS with me. Gerard Cummins for taking the time to perform printing with copper nanoparticles as well as subsequent testing. Also, Ross Blackley and Sam McFadzean for the many hours we spent looking for nanoparticles. A big thank you also to Katsiaryna Usachova for her work on characterising the antibiotic sensitivity of *M. psychrotolerans*.

A big thank you to my friends and family who have kept me sane throughout this work and their constant support and encouragement. A special thanks to Lisa Buttrick who has had to listen to my complaining and for her support and inspiration to go the extra mile.

Finally I would like to thank the BBSRC, Diageo and The University of Edinburgh for financial support.

Abbreviations

°C	Degrees Celcius
µg	Microgram
µl	Microlitre
µm	Micrometre
µM	Micromolar
Bp	Base-pair
BSA	Bovine Serum Albumin
cm	Centimeters
CuNP	Copper nanoparticle
DNA	Deoxyribonucleic acid
g	Gram
h	Hours
HPLC	High performance liquid chromatography
HR-TEM	High Resolution Transmission Electron Microscopy
ICP-OES	Inductively coupled plasma – Optical emission spectroscopy
Kb	Kilobase-pair
kV	Kilovolts
L	Litre
LB_{ns}	Lysogeny Broth without salt
M	Molar
MALDI-MS	Matrix-assisted laser desorption/ionization – mass spectrometry
mg	Milligram
MIC	Minimum inhibitory concentration
min	Minutes
ml	Millilitre

mM	Millimolar
MOPS	3-[N-Morpholino]propanesulphonic acid
ng	Nanogram
nm	Nanometre
OD_{600}	Optical density at 600 nm
PBS	Phosphate Buffered Saline
PCR	Polymerase chain reaction
pH	Power of hydrogen
qRT-PCR	Quantitative Real-Time Polymerase Chain Reaction
rpm	Rotations per minute
SOC	Super Optimal Broth
TAE	Tris-acetate-EDTA
TEM	Transmission Electron Microscopy
UV	Ultra-violet
v/v	Volulme/ volume
x g	Gravitational force
XPS	X-ray photoelectron spectroscopy

Table of Contents

List of Figures

Chapter 1

Chapter 3

Chapter 5

Chapter 6

Chapter 1. Synthesis and Characterisation of Stable Copper Nanoparticles by *Morganella psychrotolerans*

1.1 Introduction

In the past few years the topic of metallic nanoparticles has become a widespread research focus. The term "nano" is derived from the Greek word "nanos" which means dwarf and represents a measurement scale of one-billionth (10^9) of a metre in size (Narayanan and Sakthivel 2010; Thakkar, Mhatre *et al.* 2010). To put in perspective, a regular bacterium is approximately 1-3 μm in diameter (Katz, Alimova *et al.* 2003), a typical virus is around 100 nm wide (Wagner, Plank *et al.* 1992) and a DNA strand is only 2.5 nm in diameter (Lyubchenko and Shlyakhtenko 1997). The exact definition of a nanoparticle varies slightly depending on the size range. The most common definition defines nanoparticles as particulate dispersions of solid particles with at least one dimension in the size range of 10-1000 nm (Mohanraj and Chen 2006; Thakkar, Mhatre *et al.* 2010).

In order to survive in environments containing toxic concentrations of metallic ions, certain microorganisms have evolved and adapted intricate metal resistance mechanisms. Some of these methods of defence involve the chemical alteration of the toxic metal ion that results in an attenuated state of the metal, such as nanoparticles, that do not cause lethal toxicity to the organism producing them. Consequently, nanoparticles are the by-products of the microorganism's defence mechanism against specific metallic ions (Iravani 2014). This natural defence mechanism of microorganisms can be used to generate metallic nanoparticles in a much "greener" way compared to chemical methods that use toxic chemicals (Li, Xu *et al.* 2011). One of the main differences between nanoparticles and their "bulk" counter-parts is their large surface area to volume aspect ratio resulting from their extremely small size, allowing them to interact with other compounds or particles easier (Narayanan and Sakthivel 2010; Thakkar, Mhatre *et al.* 2010). Nanoparticles exhibit unique optical, chemical, thermal, physical, electrical and magnetic properties when compared to their "bulk" size counter-parts (Durán, Marcato *et al.* 2007; Husseiny, El-Aziz *et al.* 2007). Such properties can be applied for antimicrobials, catalysts, next generation biosensors and electronics (Durán, Marcato *et al.* 2007; Narayanan and Sakthivel 2010).

Biologically synthesised metallic nanoparticles are a widely studied materials group and rightly so, as they show great diversity and can be used in a plethora of applications.

The uses of synthesised nanoparticles, chemically or biologically, depend strongly on the way they have been synthesised. Silver nanoparticles (AgNPs) have been extensively studied for their effective antibacterial properties (Durán, Marcato *et al.* 2007; Krishnaraj, Jagan *et al.* 2010). Nanoparticles made of silver and gold have been proven to inhibit growth of Gram-negative and Gram-positive bacteria, making them potent antibacterial agents (Guzmán, Jean *et al.* 2009; Lima, Guerra *et al.* 2013). Antimicrobial resistance is considered one of the greatest challenges to mankind in the 21st century (Pantidos and Horsfall 2014). Optical sensors have also been developed based on silver nanoparticles which detect the formation of small molecule adsorbates (McFarland and Van Duyne 2003). Catalysts based on platinum (Pt) nanoparticles have demonstrated high activity of formic acid electrooxidation (Waszczuk, Barnard *et al.* 2002). Nanoparticles for such uses are currently most commonly synthesised using wet-chemical methods which are mainly low-cost high-yield. However chemical techniques very often require the use of toxic solvents and the nanoparticles produced are often rendered unsafe for biomedical uses through their contamination by the chemicals still present in the end product (Li, Xu *et al.* 2011). A more environmentally friendly method of synthesising metallic nanoparticles is required to achieve safe implementation in industries. To achieve this result, biological methods have been a focus of study as they generally do not require toxic chemicals or pure starting materials in order for metallic nanoparticle synthesis to occur.

Biological metallic nanoparticle synthesis by many bacteria, fungi and plants has been observed, and each case presents different advantages and disadvantages (Table 1.1) (Suresh, Prabagaran *et al.* 2004; Song and Kim 2009). Research on biological production of metallic nanoparticles is mainly based around Ag and Au. Choosing the right organism may depend on a number of variables. Growth temperature, intracellular or extracellular synthesis, ease of extraction, growth temperature, and ratio of nanoparticle synthesis levels versus levels of metallic ions removed from the environment and synthesis time, all play an important role in the biological production of nanoparticles. Also the specific metal in question is of primary importance, as

organisms generally adapt defence mechanisms to only a small number of metals, therefore limiting the pool of available organisms to work with (Pantidos and Horsfall 2014). Synthetic biology, a nascent field of science is beginning to address such problems by engineering organisms with a wider array of metal resistances, with the ability to synthesise a wider array of metallic nanoparticles (Edmundson, Capeness *et al.* 2014).

Name of organism	Nanoparticles Produced	Synthesis Location	Method	References
A) Bacteria				
Thermomonospora sp.	Au	Extracellular	Reduction	Wiley *et al.* 2004
Rhodococcus species	Au	Intracellular	Reduction	Montazer *et al.* 2014
Escherichia coli	Pd, Pt	Extracellular	Reduction	Waszuczuk *et al.* 2002
Rhodopseudomonas capsulata	Au	Extracellular	Reduction	Mafuné *et al.* 2003
Pseudomonas aeruginosa	Au	Extracellular	Reduction	Narayanan *et al.* 2010
Delftia acidovorans	Au	Extracellular	Reduction	He *et al.* 2007
Bacillus licheniformis	Ag	Intracellular	Reduction	Johnston *et al.* 2013
Shewanella sp.	AsS	Extracellular	Reduction	Ahmad *et al.* 2004
	Se	Extracellular	Reduction	Schülter *et al.* 2014
Desulfovibrio desulfuricans	Pd	Extracellular	Reduction	Lloyd *et al.* 1998
Bacillus sphaericus JG-A12	U, Cu, Pb, Al, Cd	Extracellular	Biosorption and Reduction	McFarland *et al.* 2003
Bacillus sp.	Ag	Intracellular	Reduction	Kalimuthu *et al.* 2008
Klebsiella pneumonia	Ag	Extracellular	Reduction	Pugazhenthiran *et al.* 2009
Escherichia coli	Ag	Extracellular	Reduction	Pugazhenthiran *et al.* 2009
Enterobacter cloacae	Ag	Extracellular	Reduction	Pugazhenthiran *et al.* 2009
Lactobacillus spp.	Ag	Extracellular	Biosorption and Reduction	Shahverdi *et al.* 2007
Enterococcus faecium	Ag	Extracellular	Biosorption and Reduction	Shahverdi *et al.* 2007
Lactococcus garvieae	Ag	Extracellular	Biosorption and Reduction	Shahverdi *et al.* 2007
B) Fungi				
Pediococcus pentosaceus	Ag	Extracellular	Biosorption and Reduction	Shahverdi *et al.* 2007
Fusarium oxysporum	CdS	Extracellular	Enzyme Mediated	Das *et al.* 2014
	Ag	Extracellular	Reduction	Sintubin *et al.* 2009
	Au	Intracellular	Reduction	Pollman *et al.* 2006
Aspergillus fumigatus	Ag	Extracellular	Reduction	Song *et al.* 2009
Neurospora crassa	Pt	Intracellular & Extracellular	Reduction	Sleytr *et al.* 1993
Verticillium sp.	Au	Intracellular	Reduction	Baco-Carles *et al.* 2011
C) Plants & Extracts				
Coriolus versicolor	Ag	Intracellular & Extracellular	Reduction	Ramanathan *et al.* 2013
Aspergillus flavus	Ag	Extracellular	Reduction	Parikh *et al.* 2008
Jatropha curcas latex	Ag	Extracellular	Latex Mediated Reduction	Mukherjee *et al.* 2001
Acalypha indica leaf extract	Ag	Extracellular	Reduction	Durán *et al.* 2007
Medicago sativa seed exudate	Ag	Extracellular	Reduction	Rai *et al.* 2009
Cymbopogon flexuosus extract	Au	Extracellular	Reduction	Ummartyotin *et al.* 2012
Live Alfalfa plants	Au	Intracellular	-	Ahman *et al.* 2002
Magnolia kobus leaf broth	Ag	Extracellular	Reduction	Edmundson *et al.* 2014
Arabidopsis thaliana	Pd	Intracellular	Reduction	Wiley *et al.* 2004

Table 1.1: List of types of metallic nanoparticles formed by various organisms. The synthesis method as well as its location is also described.

Methods of biological metal detoxification fall into two groups. The first is bioreduction, in which the metal ions are reduced chemically into less reactive forms, ie. nanoparticles. This method generally involves dissimilatory metal reduction, in which the reduction of a metal ion is linked with the oxidation of an enzyme provided by the organism (Deplanche, Caldelari *et al*. 2010). The resulting metallic nanoparticles can be found intracellularly, extracellularly or bound to the cell wall or membrane of the organism responsible for the process (Figure 1.1). These nanoparticles are inert and therefore do not react as readily as their ionic counter-parts and may be safely removed from any biological factors through downstream processing (Iravani 2014). The second method is biosorption which involves the direct binding of metal ions from the extracellular environment onto the organism itself, in areas such as the cell membrane and the cell wall. This is a passive process and therefore requires no energy expenditure by the organism which may infer an advantage in some cases (Pantidos and Horsfall 2014).

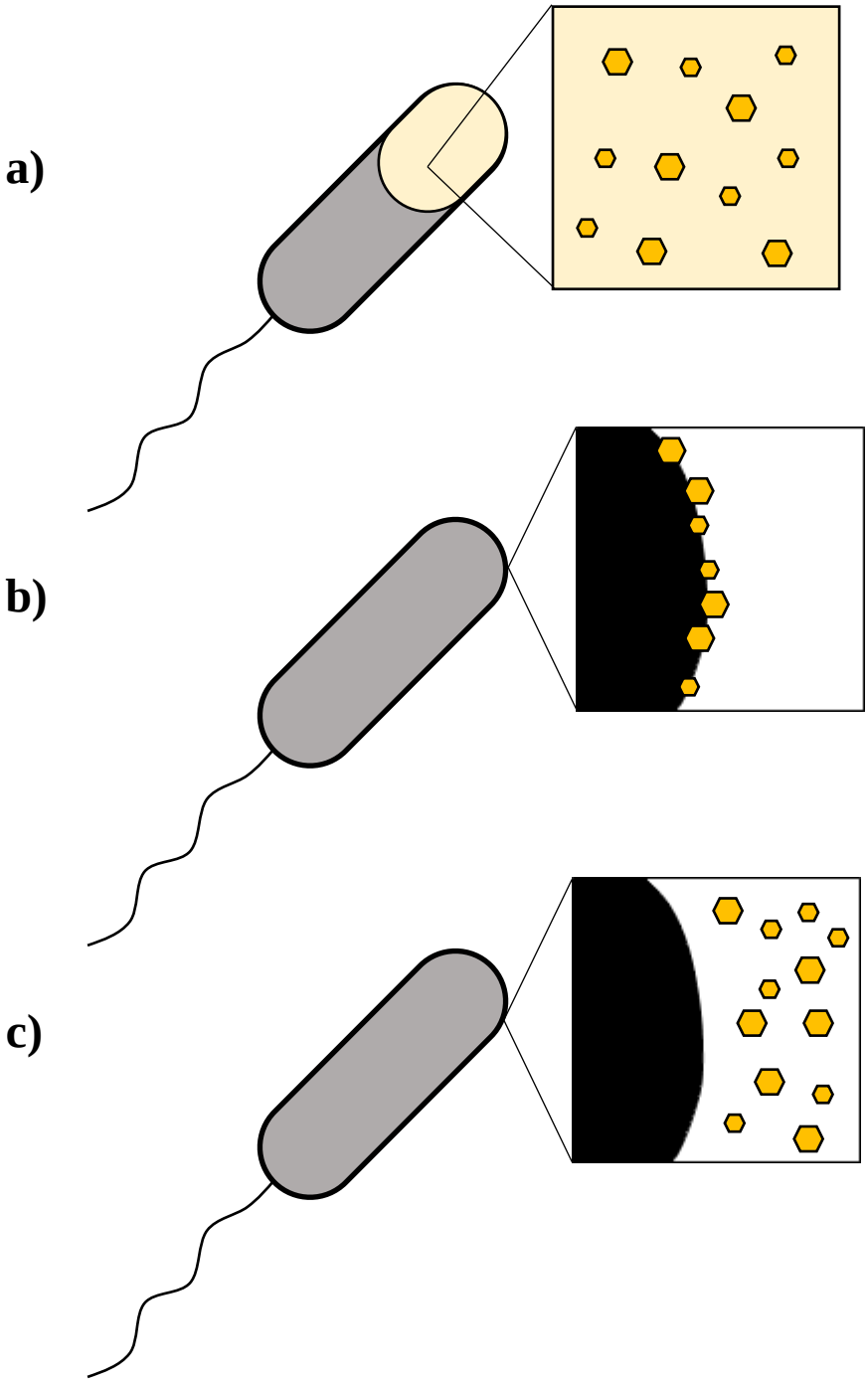

Figure 1.1: Possible locations for nanoparticle synthesis

Biologically synthesised metallic nanoparticles can be localised in three locations. Depending on the type of bacterium used, nanoparticle locations vary and may include a) intracellular, b) on the cell surface and/or c) extracellular.

1.2 Chemical and Physical Methods of Nanoparticle Synthesis

There are several different ways to synthesise metallic nanoparticles. In order to gain a clear understanding of the benefits of biological methods of nanoparticle (NP) synthesis, knowledge of the current chemical and physical methods of NP synthesis is needed. An understanding of the synthesis methods that use toxic chemicals would help in avoiding their use and therefore create a more environmentally friendly method that uses biology as the manufacturer.

The Wiley *et al.* group successfully synthesised cube and tetrahedron shaped AgNPs by heating $AgNO_3$ with Ethylene glycol to 148^{o}C. The ability to control the shape and size of nanoparticles is important when a target application is involved that requires nanoparticles with particular characteristics. This method resulted in NPs of 20-80 nm in diameter which were relatively monodispersed (Wiley, Herricks *et al.* 2004). A difference of 60 nm between the smallest and the largest size nanoparticles obtained is minor, but it may infer different properties in various applications. Therefore it is ideal that the relative size of the resulting NPs be monodispersed to ensure similar properties. The temperature used in this study requires higher energy consumption in order to produce the AgNPs compared to biological methods.

More recently, another group reported the synthesis of AgNPs in the size range of 20 to 150 nm in diameter with an average size of 90 nm (Montazer, Shamei *et al.* 2014). Montazer *et al.* used polyamide fabrics to achieve the AgNP synthesis, in which the fabrics themselves were responsible for the reduction process of the Ag ions. Wound sutures, artificial tendons and medical packaging made of such fabrics may confer antimicrobial protection. The group also noticed that the polyamide fabrics acted as a stabilising agent preventing oxidation of the NPs, which meant that no other NP stabilising agents were required. Montazer *et al.* applied the AgNP coated fabrics on antibacterial assays which showed antibacterial activity as far as after 30 washes.

The stability of metallic nanoparticles limits their application, as oxidation results in a loss of function. The addition of external capping proteins or other chemicals has shown to improve their stability and even improve their antibiotic activity (Yan, Liu *et al.* 2015). Yan *et al.* was able to produce AuNPs using carboxylic curdlan (CC) as both the reducing agent and the stabilising agent, preventing them from oxidation (Yan,

Liu *et al.* 2015). The extremely small size of nanoparticles is what makes them susceptible to oxidation, therefore ligands, either biologically derived or externally added, are often required to maintain their stability (Figure 1.2).

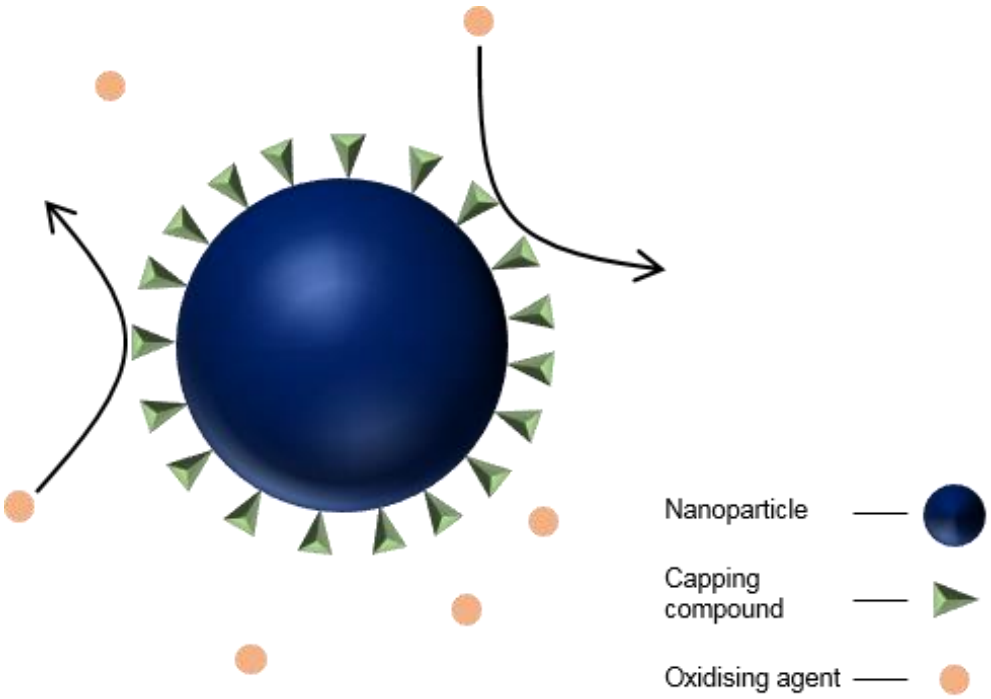

Figure 1.2: Capping compounds of biogenic nanoparticles

The picture shows a nanoparticle stabilised by an externally added stabilising compound. The resulting nanoparticle becomes more resistant to oxidation and other forms of degradation.

A physical method was successfully used to create platinum nanoparticles (PtNPs) in the scale of 1-7 nm (Mafuné, Kohno *et al.* 2003). Mafuné *et al.* performed laser ablation which is a method of creating nanoparticles by using a laser beam to heat up the bulk type of target metal used. SDS and water were used as the solvents in different cases and both showed effective synthesis of PtNPs. The method offered an advantage over other non-biological nanoparticle synthesis method as it used cheap and non-toxic solvents. However due to the size range of the nanoparticles being very small, isolation was not possible via centrifugation (Mafuné, Kohno *et al.* 2003).

1.3 Synthesis of Nanoparticles by Bacteria

Bacteria are one of the most abundant life forms on earth, and therefore, unsurprisingly, they are also one of the most diverse. In the past decade, the focus of research has been the production of metallic nanoparticles using bacteria. Bacteria are used in such research extensively due to their high abundance, fast growth and replication rate, inexpensive, easy of manipulation and for their ability to adapt to extreme conditions (Pantidos and Horsfall 2014). Growth conditions of bacteria can easily be manipulated and kept constant without significant variability, hence allowing for easy reproducibility. Changing growth conditions may also impact on the production of nanoparticles. For instance pH has been shown to have an effect on the nanoparticles themselves or on a particular part of the synthesis process, resulting in nanoparticles of various sizes and shapes (He, Guo *et al.* 2007). Such manipulations of growth conditions allows the creation of nanoparticles with various properties for different applications whilst using the same organism without directly manipulating the organism. Another example of pH effecting the size and shape of nanoparticles is described and shown in chapter 3.

A study by Johnston *et al.* (2013), describes the successful synthesis of elemental gold nanoparticles by *Delftia acidovorans*. The bacterium synthesised a small non-ribosomal peptide named delftibactin which was responsible for the reduction of gold ions into the elemental nanoparticle form (Johnston, Wyatt *et al.* 2013). This method offers the advantage of synthesising nanoparticles using extracellularly secreted compounds without the need for bacteria to be present. Hence less downstream processing is required to purify the nanoparticles. The authors propose that, much like

in other organisms that protect themselves by attenuating the metal into a less toxic form, *D. acidovorans* also produced this delftibactin in order to protect itself from the toxic effects of gold ions. Although many bacteria are known to produce metallic nanoparticles, there have been no established mechanisms for nanoparticle production (Pantidos and Horsfall 2014). In another case, gold nanoparticles were synthesised extracellularly by *Rhodopseudomonas capsulata* (He, Guo *et al.* 2007). The nanoparticles ranged from 10 to 20 nm in size and it was suggested that they were synthesised by an NADH-Dependant Reductase (Figure 1.3). This enzyme has been reported in the past to be a crucial component in reducing metal ions into metallic nanoparticles (Ahmad, Mukherjee *et al.* 2003). However since the process involves the nanoparticle being assembled intracellularly, the size of nanoparticles may be limited to the pore sizes of the cell membrane.

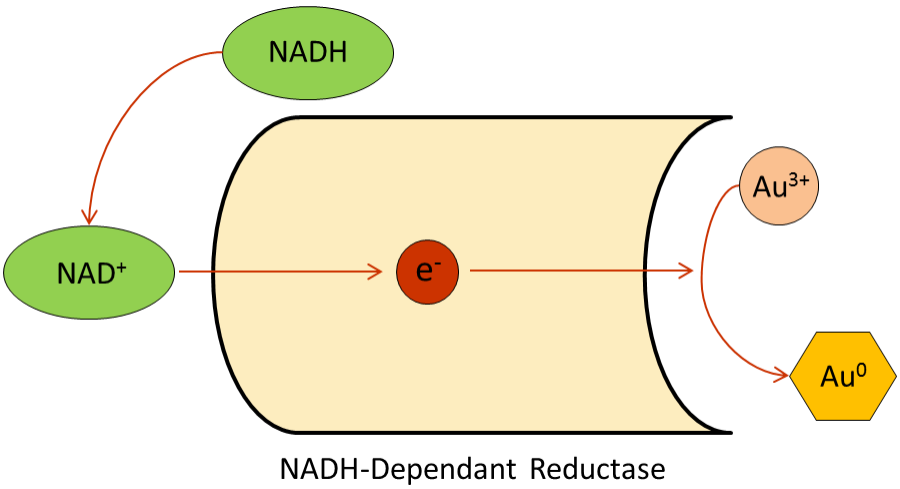

Figure 1.3: NADH-Dependant gold ion reduction

The diagram shows a proposed mechanism for Au ion reduction using the enzyme NADH-Dependant Reductase. The method involves electron donations from NADH molecules onto NADH-Dependant Reductase which then subsequently donates 3 electrons ton each Au^{3+} to form zero valent AuNPs.

Platinum Group Metals (PGM) are a group of metals consisting of ruthenium, rhodium, palladium, osmium, iridium and platinum, which exhibit high catalytic properties and are used in dehalogenation and hydrogenation reactions (Pantidos and Horsfall 2014). It has recently been shown that bacteria isolated from Alpine environments greatly contaminated with heavy metals, are able to synthesise pure zero valent Pd nanoparticles (Schluter, Hentzel *et al.* 2014). Furthermore the same group was able to use these nanoparticles in dehalogenation of tri and tetra-chlorinated dioxin congeners. Although Schlüter *et al.* (2014) tested many types of bacteria from those sites, only *Pseudomonas* species were found to be involved in the production of PdNPs. In an earlier study, Lloyd *et al.* (1998) found that *Escherichia coli* is able to synthesise elemental PdNPs using hydrogenases produced by the bacterium. Similarly, Capeness *et al.* (2015) also achieved synthesis of PdNPs using *Desulfovibrio alaskensis.* In both of these studies, the NPs were deposited on the cell envelope which requires treatment of the cell membrane to "release" the nanoparticles into the extracellular medium.

Sintubin *et al.* was able to produce AgNPs using the lactic acid bacteria *Lactobacillus spp., Lactococcus garvieae, Enterococcus faecium* and *Pediococcus pentosaceus*. The method described was more complicated than the conventional 1-step process from other groups, in that they employed a 2-step method whereby the Ag ions were firstly bound to the cell membrane by biosorption prior to subsequent reduction to form metallic AgNPs (Sintubin, De Windt *et al.* 2009). AgNPs are known to oxidise easily on the surface (Kuzma, Weis *et al.* 2012), therefore their stabilisation is important. In the case of Sintubin *et al.*, they suggested that the AgNPs were stabilised by the cell wall of the bacteria that synthesised them. Moreover, an increase in pH showed increased formation of AgNPs (Sintubin, De Windt *et al.* 2009). This was in agreement with the He *et al.* group where pH showed a significant effect on the nanoparticles' size and shape, and therefore needs to be a vital part of future method designs for nanoparticle synthesis.

Kalimuthu *et al.*, showed their AgNP production intracellularly by *Bacillus licheniformis*. Although the nanoparticles were made from pure elemental Ag, they needed to be extracted in order to analyse them or for use in other applications, therefore an additional extraction step was needed (Kalimuthu, Suresh Babu *et al.*

2008). This presents a disadvantage compared to methods in which nanoparticles are synthesised extracellularly and require less purification; one of the key facts in minimising industry costs. A very different approach to synthesise AgNPs was taken by Shaverdi *et al.*, in which the supernatant of a live bacterial culture was collected and tested for its ability to synthesise AgNPs. By utilising this method, it was possible to create extracellular AgNPs after addition of the Ag ions. Since the cell-free supernatant was used directly to synthesise nanoparticles, no cell removal step was needed (Das, Thomas *et al.* 2014). However the experiment occurred over 72 hours in the presence of light which is known to affect the stability of AgNPs causing them to oxidise. Therefore such a method would not be ideal for producing high quality elemental AgNPs.

There are also a number of studies into other more unconventional metals such as uranium (U) and arsenic (As) (Edmundson and Horsfall 2015). The *Bacillus* species has been the focus of many studies into the bioaccumulation and nanoparticle production and rightly so as they are able to produce nanoparticles of many types of metals (Pollmann, Raff *et al.* 2006; Kalimuthu, Suresh Babu *et al.* 2008; Pugazhenthiran, Anandan *et al.* 2009). *Bacillus sphaericus* is able to biosorpt significant concentrations of Al, Cu, Pb and U metal ions. Proteins located on the S-layer – a porous layer of proteins surrounding the bacterial cell membrane (Figure 1.4) – of the membrane were found to be responsible for the binding of metal ions and concomitant removal from aqueous environments. The S-layer of *B. sphaericus* was found to accumulate U at concentrations of up to 20 mg/g of protein by carboxyl and phosphate group binding (Sleytr, Messner *et al.* 1993).

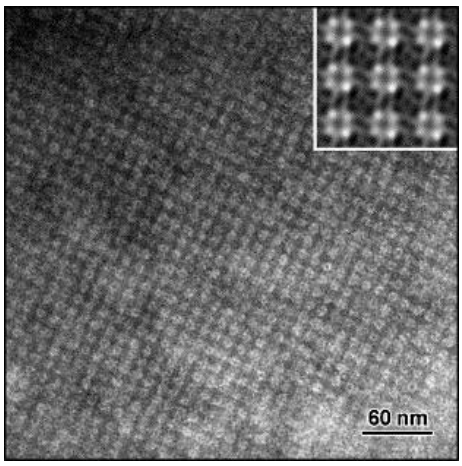

Figure 1.4: Bacterial S-layer from Bacillus sphaericus JG-A12

Transmission Electron Microscopy analysis revealed the porous material where nanoparticles are found. Reprinted from Pollman *et al.*

The biosynthesis of copper nanoparticles (CuNPs) is also possible, however it is widely known that CuNPs are unstable in oxic conditions and they tend to oxidise after synthesis to form copper oxide (CuO). This quick oxidation occurs because Cu is not stable in the nanometer scale and reacts readily with oxygen (Pantidos and Horsfall 2014). Stabilisation methods of CuNPs therefore have been another focus of research. A study by Ramanathan *et al.* described the synthesis of elemental CuNPs by *Morganella morganii*, an organism of clinical relevance. The method suggested involved the uptake of Cu^{2+} ions from the medium by the organism, and their subsequent reduction to CuNPs, prior to expulsion from the cells using an efflux mechanism (Ramanathan, Field *et al.* 2013). This pathway or the related genes however have not been confirmed to be responsible for the production of CuNPs. A similar study by Parikh *et al.*, using *Morganella sp.*, has successfully produced AgNPs extracellularly. The method of synthesis was suggested to be the organism's defence mechanism against Ag ions (Parikh, Singh *et al.* 2008). Analysis of the SilE sequence from *Morganella sp.* and other Ag binding proteins revealed a 99% similarity. Furthermore, a high similarity was also observed between SilE homologues and Cu binding proteins, which suggests that the mechanism involving SilE is similar for the production of both Ag and Cu nanoparticles. A more recent study on the bioproduction of stable CuNPs involved the use of anaerobic *Thermoanaerobacter* sp. X513 bacteria in aqueous environments (Jang, Jacobs *et al.* 2015). In this instance the CuNPs were stabilised by the addition of capping molecules such as organic and inorganic surfactants. The group achieved good stabilisation of CuNPs with only 0.14 of the synthesised fraction oxidised after 20 days with the addition 0.1 vol % of oleic acid (Jang, Jacobs *et al.* 2015).

1.4 Synthesis of Nanoparticles by Fungi

Fungi have been used in research extensively and in metallic nanoparticle synthesis, they are considered to offer certain advantages compared to bacteria (Pantidos and Horsfall 2014). Much like bacteria they are easy to grow, cheap and offer easy downstream processing. Moreover fungi possess mycelia and secrete proteins to significantly higher amounts than bacteria.

AgNPs, as mentioned before, are a great area of research because of their high potential for use as antimicrobial agents or in electronics (Rai, Yadav *et al.* 2009; Ummartyotin, Bunnak *et al.* 2012). *Fusarium oxysporum*, has been used extensively to create metallic nanoparticles such as AgNPs (Pantidos and Horsfall 2014). It has also been shown to produce molybdenum sulphide (MoS), lead sulphide (PbS), cadmium sulphide (CdS) and zinc sulphide (ZnS) nanoparticles in the presence of their respective ions in the medium (Ahmad, Mukherjee *et al.* 2002). All of the nanoparticles produced however were found intracellularly, which presented a problem in their extraction. A more recent study by Ahmad *et al.*, showed the first example of extracellular production of AgNPs using *F. oxysporum* (Ahmad, Mukherjee *et al.* 2003). This presented a much bigger advantage due to the easier purification of the nanoparticles.

Extracellular synthesis of metallic nanoparticles is ideal for uses such as catalysis or antimicrobials. However intracellular synthesis also offers some advantages despite the difficulty in extracting the metal from the fungi. Bioremediation is the process of removing contaminants with the use of microorganisms. In this case fungi that produce nanoparticles intracellularly have an advantage, as they are easier to remove by simple filtration or low speed centrifugation than the nanoparticle themselves, which are much smaller and weigh far less. A study was performed on the fungus *Coriolus versicolor*, in which both intracellular and extracellular AgNPs were produced simply by adjusting the reaction conditions (Sanghi and Verma 2009). This process therefore could be tailored to the specific application that it is destined for.

On the other hand, not much is known about platinum nanoparticle (PtNP) production by fungi. The fungus *Neurospora crassa* was used to intracellularly synthesise PtNPs that formed nanoparticle agglomerates as well as smaller individual nanoparticles. The two different nanoparticle groups that were produced were explained by their production using the *N. crassa* biomass and its extract separately. The group witnessed that the extract was responsible for the formation of the smaller individual nanoparticles, whilst the agglomerates were observed when the nanoparticles were synthesised intracellularly (Castro-Longoria, Moreno-Velazquez *et al.* 2012). Work by Riddin *et al.*, used the well-studied fungus *F. oxysporum* to also produce PtNPs. The nanoparticles were mainly synthesised and found intracellularly and the authors

reported that pH and temperature were critical factors in maintaining the synthesis of nanoparticles by *F. oxysporum* (Riddin, Gericke *et al.* 2006). This is another case of manipulating the size and shape of metallic nanoparticles by changing the conditions of incubation of the metal ions with the biological matrix.

A group of magnetic metallic nanoparticles made from magnetite (Fe_3O_4), a common oxide of iron which contained magnetic properties, has been the focus of a number of studies. The fungi *F. oxysporum* and *Verticillium* sp. have been reported to produce magnetite nanoparticles (MaNPs) (Bharde, Rautaray *et al.* 2006). The magnetic properties of such nanoparticles make them easy to extract using a magnet and they offer great potential in magnetic recording devices and in biomedical applications such as position sensing, oscillation damping and magnetic resonance imaging (Sun and Zeng 2002; Thapa, Palkar *et al.* 2004).

Many of the fungi used to study biological metallic nanoparticle synthesis use pathogenic fungi. Although in some studies the nanoparticles are found extracellularly, there is still great concern on applying nanoparticles derived from pathogenic sources (Spadaro and Gullino 2005). Two studies that used the non-pathogenic fungi *Trichoderma reesei* and *Trichoderma asperellum*, showed the production of AgNPs (Nevalainen, Suominen *et al.* 1994; Mukherjee, Roy *et al.* 2008; Vahabi, Mansoori *et al.* 2011). *T. reesei* has been used extensively in the food industry, pharmaceuticals and textile industry for a long time (Nevalainen, Suominen *et al.* 1994). The organism involved in the production of metallic nanoparticles has to be carefully considered in regards to their application. The use of non-pathogenic organisms is essential to avoid the potential for infection or toxicity, especially in the cases of biomedical applications.

1.5 Synthesis of Nanoparticles by Plants

Bacteria and fungi have been the main focus of research in metallic nanoparticle synthesis, however plants have not been researched as extensively. There has been an increasing volume of research on nanoparticle synthesis by plants in the past decade as there is a need for methods of producing them in an environmentally friendly way (Pantidos and Horsfall 2014). Although the use of bacteria and fungi is also considered "green", the possibility of infecting humans makes them potentially inappropriate for

certain applications. Plants on the other hand lack infectious abilities and therefore it is one of the main advantages over other organisms.

There are numerous studies in which whole plants or plant extracts have been used to illustrate metallic nanoparticle production. A study by Bar *et al.* showed an environmentally friendly method of synthesising AgNPs using *Jatropha curcas* extract. These AgNPs had a relatively homogenous size range of 10-20 nm, which is a much smaller range compared to nanoparticles reported to be made from bacteria or fungi (Bar, Bhui *et al.* 2009). A separate study also showed the synthesis of AgNPs using plants and achieved a homogenous dispersion of nanoparticle between 20-30 nm in diameter (Krishnaraj, Jagan *et al.* 2010), which is useful in certain applications. Extracellular AgNPs made by Krishnaraj *et al.* were tested for antimicrobial activity and they showed bacterial growth inhibition at as low as 10 µg/ml (Pantidos and Horsfall 2014). A study by Luckman *et al.* illustrated the production of AgNPs by extracts of *Medicago sativa* in as little as 1 minute post-exposure to Ag ions. At a temperature of 30^{o}C, 90% of the Ag ions present had been converted into AgNP (Lukman, Gong *et al.* 2011). Although the process of very time and energy efficient, no significant antimicrobial properties were observed by the AgNPs. It was suggested that they could be used with the *M. sativa* extract to synergistically eliminate bacteria (Lukman, Gong *et al.* 2011).

In some rare cases, the exact component of a plant extract that is responsible for the reduction of metallic ions into nanoparticles is known. A study by Kasthuri *et al.* mentioned phyllanthin, a molecule present in extracts of *Phyllanthus amarus*. The group was able to produce Ag and Au nanoparticles using only this molecule, therefore identifying the molecule responsible for the reduction process. Kasthuri *et al.* found that by varying the concentration of phyllanthin, nanoparticles of different size and shape were achieved. Lower concentrations of phyllanthin resulted in hexagonal and triangular AuNPs, whereas higher concentrations resulted in the formation of mainly spherical nanoparticles (Kasthuri, Kathiravan *et al.* 2009).

Park *et al.* described the use of plant derived phytochemicals and polysaccharides for the production of Ag and Au nanoparticles. This method would offer advantages as the compounds responsible for the reduction process would be known and no addition

of harmful toxic chemicals would be needed (Park, Hong *et al.* 2011). Examples of such plant derived compounds that have been successfully utilised in metallic nanoparticle synthesis are chitosan (Laudenslager, Schiffman *et al.* 2008), cellulose (Cai, Kimura *et al.* 2008), soluble starch (Raveendran, Fu *et al.* 2003), dextran (Ma, Li *et al.* 2005), hyaluronic acid (Kemp, Kumar *et al.* 2009) and alginic acid (Saha, Pal *et al.* 2009).

A study by Song *et al.* describes the use of various plants extracts for their ability to produce AgNPs. The extracts from Persimmon, Ginkgo, Pine, Platanus and Magnolia were tested and compared (Song and Kim 2009). The Magnolia extract was shown to be the most effective in creating nanoparticles as it was able to convert 90% of the Ag ions into nanoparticles within 11 minutes of exposure. The reaction conditions had to be carefully adjusted as it was found to impact on the rate, size and shape of the nanoparticles (Song and Kim 2009). At 95^{o}C the synthesis rate was higher with the resulting nanoparticles being small. On the other hand at 25^{o}C the synthesis rate was slower but the nanoparticles were larger. This is once again highlighting the importance of regulating reaction conditions during the synthesis.

Liquid extracts from the lemongrass plant *Cymbopogon flexuosus* had the potential to synthesise AuNPs (Shankar, Rai *et al.* 2004). The resulting nanoparticles were triangular in shape and were formed by aggregates of smaller circular shaped nanoparticles. The fluidity of their shapes was caused by the surface complexation of ketones and/or aldehydes present in the *C. flexuosus* extract. Another group was able to create bimetallic nanoparticles made up of Ag and Au. Extract from the leaves of *Azadirachta indica* was mixed with Au and Ag ions. A rapid bimetallic synthesis was observed with the reaction plateau occurring at approximately 2 hours. The production of bimetallic nanoparticles may infer advantages when more than one metal needs to be removed from a contaminated sample. Biometallic nanoparticles may also offer certain advantages in their applications such as more effective antimicrobials. The compounds responsible for this process were suggested to be terpenoids and flavanones derived from the leaves of the plant and are also suggested to keep the nanoparticles stable (Shankar, Rai *et al.* 2004).

A study by Arooj *et al.* showed the synthesis of long-term stable AgNPs using the fruit *Citrus sinensis* (orange). The reaction time was 2 hours and the resulting nanoparticles showed stability over a five month period (Arooj et al). This was unique as AgNPs are considered relatively unstable and therefore require the use of ligands to induce stability. The group tested these biogenic AgNPs after 5 months of storage for their MIC on *Bacillus subtilis, Shigella, Staphilococcus aureus* and *Escherichia coli*. The nanoparticles were found to still exhibit a strong antimicrobial effect with an MIC of 20 µg/ml for *B. subtilis* and *Shigella* and 30 µg/ml for *E. coli* and *S. aureus* (Arooj *et al.*). This is a prime example of metallic nanoparticles having the potential to be used as new antimicrobials as they present a good MIC as well as long-term stability for storage and effect (Naila, Nadia *et al.* 2014).

There is very little research on PtNPs made by plants. The plant extract of *Diopyros kaki* was used to produce PtNPs with a higher than 90% conversion of Pt ions in 2.5 hours (Song, Kwon *et al.* 2010). It was suggested by Song *et al.* that the reduction of the ions was based on the presence of compounds such as alcohols, amines, carboxylic acids and ketones and not enzymes such as is the case in many other biological syntheses by bacteria and fungi. This hypothesis was also supported by the fact that the reaction was carried out at 95^{o}C and subsequent FTIR analysis did not detect the presence of proteins (Song, Kwon *et al.* 2010).

It is obvious that most of the research involving biological production of metallic nanoparticles by plants, in fact use the plants' extract. A study by Parker *et al.* described a process of creating palladium nanoparticles (PdNPs) using the whole plant *Arabidopsis thaliana*. The plant was fully grown, followed by addition of Pd ions into its growing medium for 24 hours. The result observed was the formation of PdNPs of 2-4 nm size. The nanoparticles were then purified from the plant and were successfully shown to exhibit catalytic activity using the Suzuki-Miyaura coupling reaction. What was notable was that the biogenically created PdNPs in fact showed higher catalytic activity than the commercially available PdNPs created in other means (Parker, Rylott *et al.* 2014).

Another study used Alfalfa plant seeds to grow the plants for two weeks in soil containing various concentrations of Au ions (Gardea-Torresdey, Parsons *et al.* 2002).

The AuNPs found in the plant were then extracted using various methods and analysed, confirming their presence and chemistry. Although this is an example of using whole plants for nanoparticle synthesis, it was not a viable industrial process due to the time it took to grow the plant and allow it to convert the metal ions (Pantidos and Horsfall 2014). An industrially feasible process would need the production time to be significantly shorter than the one reported, however the low cost of production and the lack of need for harsh toxic chemicals give it an advantage over current commercially available methods (Pantidos and Horsfall 2014).

1.6 Applications of Metallic Nanoparticles

There is a significant amount of research into the synthesis of metallic nanoparticles using bacteria, fungi and plants as well as their applications. Biogenic nanoparticles may be used in catalysts, cosmetics, electronics and cancer treatment depending on their nature and element.

Modern day electronics have started taking advantage of AuNPs and AgNPs which are used to print low resistance conductors (Pantidos and Horsfall 2014). The extremely small size of AuNPs gives them several advantages over their "bulk" equivalents such as flexibility and lower sintering temperature. Plastics can therefore be used in electronics as they do not melt in the lower sintering temperatures of AuNPs to form low resistance conductors (Daniel, Frank *et al.* 2003). Stuchinskaya *et al.* has studied the effects of AuNPs on breast cancer tissue cells. The nanoparticles were coated with an antibody that was able to bind specifically to cancerous cells and it in fact provided promising results for specifically targeting and killing breast cancer cells via cytotoxic shock caused by the AuNPs producing a singlet oxygen producer pthalocyanine (Stuchinskaya, Moreno *et al.* 2011).

The continuing rise of antimicrobial resistance in recent years has led to attempts to develop new types of antibiotics to combat it. AgNPs have shown great potential to kill bacteria and have shown therapeutic potential (Pantidos and Horsfall 2014). In a similar way as in the Stuchinskaya *et al.* study, AgNPs were coated with a photosensitizer which was then targeted specifically onto cancerous cells. The nanoparticles then would create free radicals and kill the surrounding cancerous tissue (Dos Santos, Seckler *et al.* 2014). AgNPs have shown great versatility and therefore

have been the focus of many areas of research (Pantidos and Horsfall 2014). The antimicrobial effects of AgNPs have shown great potential for future antibacterials (Zain, Stapley *et al.* 2014). They act by creating reactive oxygen species which subsequently cause deadly damage to surrounding bacteria (Dos Santos, Seckler *et al.* 2014).

Zain *et al.* have shown that CuNPs may be used as antimicrobials also. The group was able to synthesise bi-metallic Ag-Cu nanoparticles and successfully showed an increase in antibacterial potency compared to single species nanoparticles. The size of the nanoparticles also played an important role in the level of antibacterial activity (Zain, Stapley *et al.* 2014).

Whereas Ag, Cu and Au are good metals for synthesising nanoparticles destined for applications such as antibacterials and electronics, PGMs are extremely useful for their catalytic properties. Pt is therefore extensively used for fuel cell applications and acts as the oxygen reducing cathode. In some cases PtNPs can also be used as anodes where it has the potential to oxidise methanol in the methanol oxidation reaction (MOR) as well as other types of fuels (Chen, Lim *et al.* 2009). Another use for PtNPs is catalysis, in which it has been shown to help progress chemical reactions such as hydrogenation processes (Bratlie, Lee *et al.* 2007). PdNPs have also been used for similar catalytic applications.

1.7 *Morganella* sp. and Nanoparticle Synthesis

The Gram-negative, rod-shaped, single flagellated bacterium *Morganella morganii* has been shown to create CuNPs (Ramanathan, Field *et al.* 2013). It is a facultative anaerobe and is generally found in nosocomial infections as well as part of the flora in human intestines (Singla, Kaistha *et al.* 2010).

The instability of CuNPs, as mentioned earlier, is known to be a serious problem for both biogenically created CuNPs as well as chemically synthesised nanoparticles (Pantidos and Horsfall 2014). *M. morganii* creates stable CuNPs that do not oxidise over long periods of time. In fact the Ramanathan *et al.* group was able to create CuNPs that were stable up to 5 weeks post-production. The problem however is that the organism is regarded to be unsafe to work with for industrial purposes. *M. morganii* is

classed as a category 2 opportunistic pathogen by the Leibniz Institute DSMZ-German Collection of Microorganisms and Cell Cultures (DSMZ). This means that it is capable of infecting humans and may pose a pathogenic risk, rendering the organism unsafe for use in industrial processes.

Morganella psychrotolerans U2/3 is an organism related to *M. morganii*, however it presents several advantages over it. *M. psychrotolerans* is classed as a category 1 non-pathogenic organism by DSMZ. Therefore it is regarded as safe to use for industrial applications without the fear of infection as it does not grow at temperatures above 35^{o}C. *M. psychrotolerans* was first isolated in 2006 by the Emborg *et al.* group and was isolated from cold-smoked tuna fish. It is able to grow at temperatures of as low as 0^{o}C (Emborg 2006).

Besides the lack of pathogenicity of *M. psychrotolerans* compared to *M. morganii*, its optimum growth temperature is 20^{o}C, which would require significantly less energy input for growth at large scale. It has a relatively rapid doubling time which also means that it can be easily grown in large quantities when needed.

A study by Ramanathan *et al.* showed the synthesis of AgNPs using *M. psychrotolerans*. The size and shape of the nanoparticles was found to differ depending on the incubation temperature during exposure to Ag ions (Ramanathan, O'Mullane *et al.* 2011). At 4^{o}C the AgNPs were 70-100 nm across and were formed during a long period of 14 days. At 15^{o}C the nanoparticles observed contained less triangularly shaped nanoplates and more circularly shaped nanoparticles. By increasing the incubation temperature to 20^{o}C, the nanoparticles achieved were in the 2-5 nm range in size with the fewest nanoplates observed measured at 100-150 nm. Finally an incubation temperature of 25^{o}C, which was 5^{o}C above the organism's optimal growth temperature, a mixture of nanoplates and nanoparticles was observed (Ramanathan, O'Mullane *et al.* 2011).

The mechanism for nanoparticle synthesis in both *M. morganii* and *M. psychrotolerans* is thought to be similar. Ramanathan *et al.* suggested that *M. morganii* may use the same pathway to produce both Ag and Cu nanoparticles. A Ag/Cu ion production pathway was described (Figure 1.5) which involves the transport of Cu^{2+} into the

cytoplasm using the *CusCFBASR* efflux system, reduction of the ions into elemental CuNPs and subsequent secretion outside the cell using the same efflux pump system (Ramanathan, Field *et al.* 2013). There was however, no supporting data for this hypothesis and therefore the study described in this thesis delves deeper in order to understand the exact mechanism of CuNP synthesis. A new pathway is also suggested based upon supporting data gathered during the study (Chapter 5).

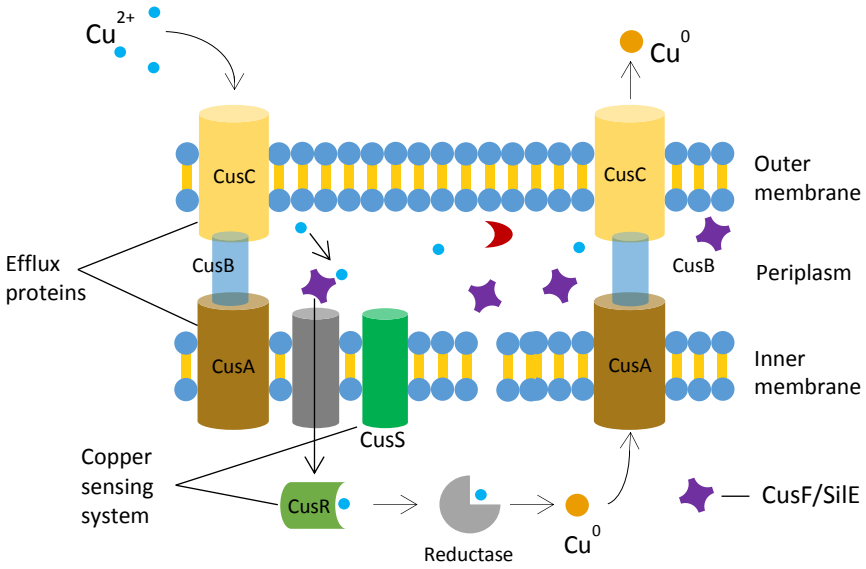

Figure 1.5: Cu/Ag nanoparticle pathway in *Morganella morganii*

Figure adapted from Ramanathan *et al.* (2013).

1.8 Whisky Production and Co-Products

Whisky is one of the world's most popular alcoholic drinks and Scotch whisky alone generates an estimated £3.95 billion from exports for the UK balance of trade. This equates to 38 bottles shipped overseas per second with a total case (12 70 cl bottles at 40% vol) number exported outside of the UK so far exceeding 99 million. Around 20 million casks lie maturing in warehouses all around Scotland. A current total of 115 licensed Scotch whisky distilleries exist for its production (Scotch whisky association).

Taking all of the above into account, it becomes obvious that the Scotch whisky industry is extremely important with a lot of heritage behind it. Of course, just like in any other product making industry, there are by-products created. In the case of whisky, the by-products – alternatively called "co-products" – produced are pot ale (PA) and spent lees (SL). These are derived from the two serial distillations that take place in order to concentrate the ethanol and generate the new make (Figure 1.6).

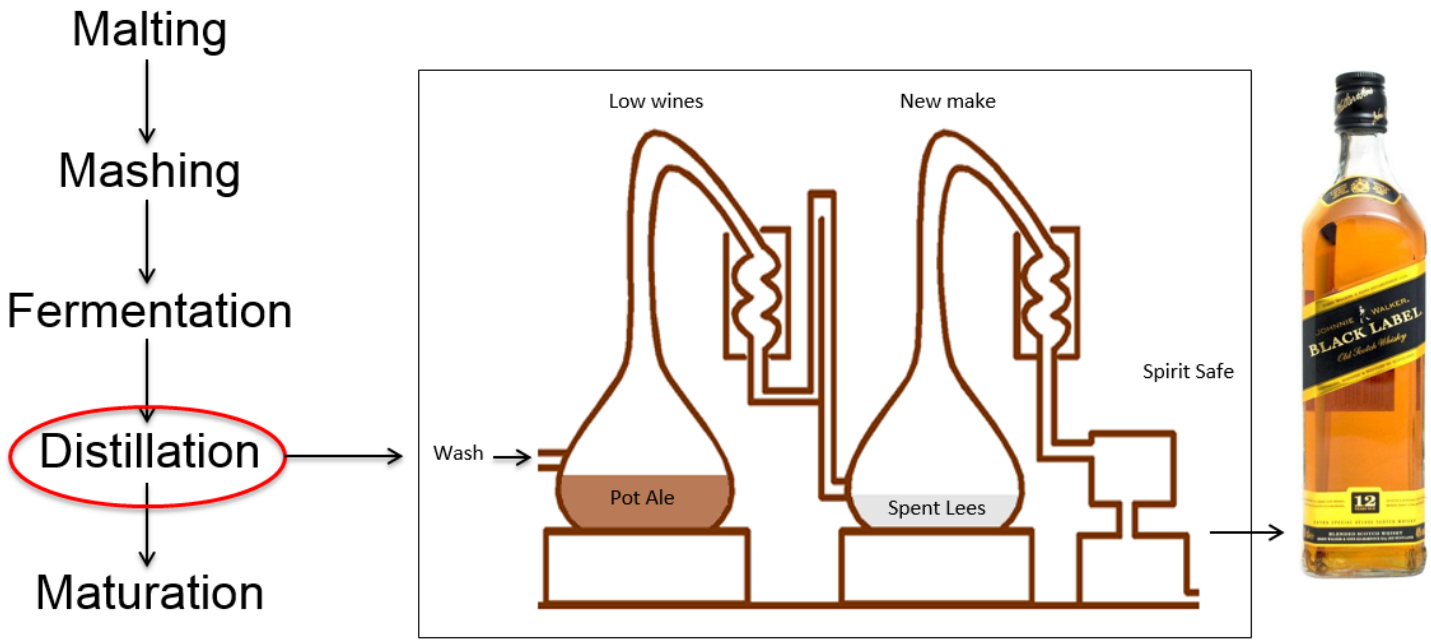

Figure 1.6: Process illustrating the process of whisky production.

The distillation step comprises of two distillations steps. These generate pot ale and spent lees as by-products after the first and second distillation respectively. The “new make” that comes through after the second distillation is then put in casks for ageing.

Chemical analysis of the co-products from various distilleries revealed a high concentration of Cu^{2+} present in PA (approximately 1.1 ppm) and significantly higher in SL (approximately 30 ppm) (See Appendix). Although PA is currently dried down to a syrup and/or granules and fed to cattle due to the highly nutritious value, it is particularly toxic to sheep. Sheep lack the resistance mechanism for Cu ions and therefore Cu ions at the concentrations present in the co-products can be toxic to them. SL contains much higher Cu^{2+} levels and is therefore treated via various methods such as anaerobic fermenters using an anaerobic bacterial mixture or via ion filtration using an ion exchange resin that binds to Cu^{2+}. Anaerobic fermenters can be slow and run into various problems such as infection from external bacteria or fungi, leaks, pipe blockages due to build-up of biofilms and excessive foam.

The resulting treated co-products end up disposed of safely in the rivers flowing adjacent to the distillery that owns the treatment plant. Cu^{2+} ions that have been collected by the resin are then transported to an external chemical company (data collected from Diageo). This strategy however is losing potential income and does not fully fit the "circular economy" concept, in which resources in use are kept for as long as possible in order to maximise value and then products and materials are recovered and recycled on each service cycle. A biological method for creating value from waste material such as whisky distillery co-product would be ideal. A method may be tailored for the use of industrially significant bacteria to reduce the Cu^{2+} from the co-products into valuable CuNPs which can then either be re-used as sacrificial copper during whisky distillation, or in other applications mentioned previously.

1.9 Aims of Research in Presented Thesis

The interest in carrying out this project was led by the high levels of Cu ions found in whisky distillery co-products and the potential of employing a "green" biological method for extracting and reusing this Cu as a valuable material. Initially a number of bacterial species were tested for their Cu bioaccumulation/bioreduction potential. The bacterium *M. psychrotolerans* U2/3 was specifically chosen to carry out this project due to its unique mechanisms for Cu tolerance and production of stable elemental CuNPs.

Due to the lack of scientific research on *M. psychrotolerans*, the organism was characterised, its genome was sequenced and its native plasmid has been partially sequenced. The CuNPs produced by this organism were studied in detail using a variety of elemental analysis techniques. Genetic modification tools were also developed in order to manipulate and enhance the biotechnological application of this metallic nanoparticle producing organism. Potential uses of the synthesised CuNPs were also assessed in microelectronics. The project involved the bioremediation of waste material and transforming it into a useful material that can then be used in other applications, thus contributing in the "circular economy" concept. Finally, the biological stabilising agent was also examined to elucidate the reason of why CuNPs synthesised by *M. psychrotolerans* are stable and resist oxidation.

Chapter 2. Materials and Methods

2.1 Strains

Bacterial strains used in this study were obtained from the Leibniz-Institute DSMZ-German Collection of Microorganisms and Cell Cultures (DSMZ). The bacterial strain used was *M. psychrotolerans* U2/3. *M. psychrotolerans* was grown in LB_{ns} (1% Tryptone, 0.5% yeast extract) for 24 hours at its optimum growth temperature of 20°C and 200 rpm (Emborg 2006). In case of solid medium, *M. psychrotolerans* was grown in LB_{ns} agar medium at 25°C for 48 hours to allow enough time for colony formation.

2.2 Plasmids

The plasmids used in this study are listed in Table 2.1. Plasmids were chosen for their antibiotic resistance cassettes and for their variations in origins of replication.

Plasmid	Features	Source
pUC4K	pMB1 origin, *bla*, *lacZ*, Kn^R, Ap^R	(Taylor and Rose 1988)
pRK415-kn	Kn^R, broad host range	Donated by Dr. Michael Capeness. University of Edinburgh 2014.
pK18mobSacB	pMB1 origin, *oriT*, *SacB*, *lacZα*, Kn^R	(Schäfer, Tauch *et al.* 1994)
pSUP404.2	*repB,E,F*, *repA*, *repC*, *mobC*, *mob*, p15A origin, Kn^R, Cm^R, broad host range	(Priefer, Simon *et al.* 1985)
pRK415	Tc^R, Ap^R, broad host range	(Keen, Tamaki *et al.* 1988)
pSUP202	pMB1 origin, Tc^R, Ap^R, Cm^R	(Simon, Priefer *et al.* 1983)
pSB1C3-RFP	pMB1 origin, Rfp, Cm^R	Donated by Professor Chris French. University of Edinburgh 2014.
pACYC184	p15A origin, Cm^R, Tc^R	Invitrogen, Darmstadt, Germany

Table 2.1: List of plasmids and their features used in this study.

Km, Cm, Tc and Ap stand for kanamycin, chloramphenicol, tetracycline and ampicillin respectively. Growth medium was supplemented with the respective antibiotic depending on the plasmid used for transformation.

2.3 Stock Solutions, Media, Buffers and Primers

All solutions, media and buffers were prepared using de-ionised. pH was measured using a Mettler Toledo pH meter. Sterilisation was performed using an autoclave or filtration through 0.22 µm filter where autoclaving was not possible.

Agarose gel	0.8% Agarose, 0.005% SYBR Safe DNA Gel Stain
BSA Stock Solution	1 mg Bovine Serum Albumin, 1 ml H_2O
Extraction Buffer	10 mM Tris pH 8.0, 100 mM EDTA pH 8.0, 0.5% SDS
GYT Medium	10% Glycerol, 0.125% Yeast Extract, 0.25% Tryptone
LB_{ns} Medium	1% w/v Tryptone, 0.5% w/v Yeast Extract
LB_{ns} Agar Medium	LB_{ns} Medium supplemented with 1.5% agar
MOPS (10x Stock)	0.5 M 3-[N-Morpholino]propanesulphonic acid pH 6.5, 7.5 and 8.5
PBS (Phosphate Buffered Saline)	8.0 g NaCl, 0.2 g KCl, 1.42 g Na_2HPO_4, 0.24 g KH_2PO_4
SOC (Super Optimal Broth)	0.5% w/v Yeast Extract, 2% Tryptone, 10 mM NaCl, 2.5 mM KCl, 20 mM $MgSO_4$, 20 mM Glucose
TAE Buffer (20x Stock)	96.8 g Tris base [tris(hydroxymethyl)aminomethane], 22.8 ml glacial acetic acid, 7.4 g EDTA disodium salt, H_2O_{dd} to 1 L

TE Buffer (10x Stock)	1 M Tris-HCl pH 7.5, 0.5 M EDTA pH 8.0, 880 ml H_2O_{dd}
TSS (Transformation and Transport Solution)	5 g Poly(ethylene glycol) 8000, 1.5 ml 1 M $MgCl_2$, 2.5 ml Dimethyl sulfoxide (DMSO), LB to 50 ml
Urea Buffer	2 M Urea and 6 M Urea stock solutions

2.4 Synthesis and Analysis of Copper Nanoparticles

2.4.1 Synthesis of Copper Nanoparticles

M. psychrotolerans was grown in 20 ml of LB_{ns} at 20°C for 24 hours at 200 rpm. To the fully grown culture, 5 mM $CuSO_4$ final concentration was added and mixed by shaking. The culture was then placed back in the incubator for a further 24 hours at 20°C and 200 rpm. Copper nanoparticle synthesis occurred during the culture's exposure to $CuSO_4$ over a 24 hour period. At the end of the 24 hours, the culture was centrifuged at 3,000 rpm. for 10 minutes using a Sigma 3-16KL centrifuge. The supernatant was carefully collected so as to not disturb the pellet and filtered through a syringe filter of 0.22 µm size to remove any remaining bacteria and larger cell debris. The filtrate which now contained the nanoparticles was ready for further analysis.

2.4.2 Ultracentrifugation of Copper Nanoparticles

After synthesis the CuNPs were then ultracentrifuged to get a more concentrated solution of nanoparticles. The filtrate containing the CuNPs was transferred into Beckman ultracentrifuge tubes. The tubes were centrifuged at 39,000 rpm for 16 hours to allow for the smallest size nanoparticles to form a pellet. The supernatant was carefully removed without disturbing the pellet. The pellet containing the nanoparticles was then resuspended in 500 µl H_2O_{dd} for further analysis.

2.4.3 UV-Vis (Ultraviolet-Visible Spectroscopy) of Copper Nanoparticles

A UV-Vis assay is useful in performing relative quantification of nanoparticles in an aqueous medium. This method was used to examine the rate of CuNP synthesis. Non concentrated CuNPs were used for this analysis. A 350 ml culture of *M. psychrotolerans* was incubated for 24 hours at 20°C and 200 rpm. The procedure was performed in triplicate. After incubation, the culture was centrifuged at 3,000 rpm. to form a pellet and concentrate the cells. The supernatant was removed and 20 ml of fresh LB_{ns} was added to the pellet to resuspend it. 1 ml of the culture at this point was taken to be used as a blank. Then, 5 mM $CuSO_4$ final concentration was added to the culture to start synthesising the CuNPs. A further 1 ml was taken out of the culture containing $CuSO_4$. The rest of the cultures were immediately put back in the incubator at 20°C, 200 rpm. The samples taken out, were centrifuged at 4,500 x g for 10 minutes, filtered through a 0.22 µm syringe filter and the supernatant was transferred into UV-

transparent plastic cuvettes. The first sample not containing $CuSO_4$ was used as a blank for the UV-Vis assay. The sample at 0 hours containing 5 mM $CuSO_4$ was then used to measure the absorbance of a spectrum wavelength ranging from 300-800 nm. Subsequent samples were taken out at 1, 2, 4, 8, 12 and 24 hours and they were then also measured in the same wavelength spectrum. The values were then plotted onto a graph to better visualise the change in absorbance for CuNPs ranging from 580 nm to 620 nm.

2.4.4 Anaerobic CuNP synthesis

With the aerobic synthesis of CuNPs by *M. psychrotolerans* established, a method for producing them anaerobically was also developed. This was used to compare the differences in nanoparticle shape and size post-production.

For anaerobic synthesis, 20 ml of LB_{ns} was inoculated with *M. psychrotolerans* and incubated for 24 hours under aerobic conditions at 20^{o}C and 200 rpm. At the end of the 24 hours, the culture was transferred in to the anaerobic cabinet Whitley A95 anaerobic workstation and the culture was left without a lid for the dissolved oxygen to diffuse out for 20 minutes. 5 mM $CuSO_4$ final concentration was added to initiate the synthesis of CuNPs. The culture was incubated at 30^{o}C for 24 hours at 200 rpm. After 24 hours of synthesis, the culture was taken out of the anaerobic cabinet, centrifuged at 4,500 x g for 10 minutes and filtered through a 0.22 µm syringe filter to remove all bacterial cells. The filtrate containing the anaerobically produced CuNPs was then ready for further analysis.

2.4.5 X-ray Photoelectron Spectroscopy (XPS)

The initial elemental analysis of the synthesised CuNPs was performed using XPS (Sigma Probe, Surface Analysis Instrument, ThermoFisher). Synthesised CuNPs were drop casted onto the surface of a silicon wafer measuring 6 mm x 7 mm. The wafer was allowed to dry in a 37^{o}C incubator for the CuNPs to coat the surface of the wafer. The wafer was then analysed using XPS at a pressure of higher than 1 x 10^{-9} Torr (1 Torr = 1.333 x 10^{2} Pa). A general scan of the spectrum of C 1s, O 1s, N 1s and Cu 2p was performed using un-mono-chromatised MgKα radiation. The final spectrum resolution was at 0.5 eV for measurements. The Shirley algorithm was used to correct for background noise.

2.4.6 Transmission Electron Microscopy

Colloidal solutions of CuNPs obtained after synthesis by *M. psychrotolerans* were drop coated onto carbon coated Cu (TEM) or Ni (HR-TEM) grids. The solution was left to dry for 10 minutes at room temperature prior to removal of remaining liquid using a filter paper, but not touching the top of the grids. The grids were incubated at room temperature for a further 10 minutes to allow any micro-droplets to evaporate. The grids were then mounted onto a Cu probe for TEM and Ni probe for HR-TEM and inserted into the microscope. For TEM the instrument used was a Philips/FEI CM120 Biotwin transmission electron microscope and for HR-TEM the instrument used was a Jeol JEM-2011 transmission electron microscope operated at an accelerating voltage of 80 kV and 200 kV respectively.

2.4.7 pH Effects on CuNPs

M. psychrotolerans just like all other living organisms have an optimum growth pH and in this case for this organism it is pH 7.0. The pH of LB_{ns} after autoclaving is approximately 6.5 as the medium is non-buffered. Manipulating the pH of the medium the CuNPs are found in however does not affect their production and hence allows to study its effect on CuNPs.

The method was adapted from the method of producing concentrated CuNPs described previously. The CuNPs were produced using the same method, however after concentrating them using ultracentrifugation, the supernatant was removed and 500 µl MOPS buffer (50 mM) was added at a specific pH. The buffers used were

MOPS at pH 6.5, 7.5 and 8.5. A separate sample of concentrated CuNPs was used for each buffer. All the samples were then incubated for 24 hours at 4^{o}C. Suitable controls were made including *M. psychrotolerans* grown without the presence of $CuSO_4$ and non-inoculated media with presence and absence of $CuSO_4$.

2.4.8 Inductively Coupled Plasma Optical Emission Spectrometry (ICP-OES)

ICP-OES was employed to measure the Cu concentrations of aqueous samples. The instrument was used to measure the concentration of Cu in the supernatant after the CuNPs had been removed.

M. psychrotolerans was used to produce CuNPs using different starting concentrations of $CuSO_4$ in the growth medium (0.5, 1.0 and 5.0 mM $CuSO_4$). The CuNPs were removed along with the cell pellets by centrifugation and/or ultracentrifugation using the method described previously. In this method, the supernatant was kept and used for Cu content measurements using ICP-OES (Perkin Elmer Optima 5300 DC ICP-OES). At least 3 ml of each sample was transferred into a 15 ml Falcon tube. The samples were sonicated and placed in the tube rack in the ICP-OES instrument (Perkin Elmer Optima 5300 DV ICP-OES) ready for collection by the robot arm. The appropriate buffer or medium not containing any $CuSO_4$ was used as a blank. A standard curve was made using six standards containing 10, 5, 2.5, 1.25, 0.63 and 0.31 mM $CuSO_4$ diluted in H_2O_{dd}. The samples were prepared in triplicates and the measurements were also taken in triplicate for each sample.

2.4.9 Copper nanoparticle printing

Work carried out by Dr Gerard Cummins from the Scottish Microelectronics Centre. Microscope slides (WWR super premium, low iron clear glass) were washed in acetone, IPA and deionised water three times before being dried using compressed deionised air. The CuNPs were filtered through a 0.22 µm Millex syringe filter prior to filling the print head. The slides were placed on a Dimatix DMP 2800 material printer. The printing origin was offset from the top, left hand corner of the slides by 5mm in x and y axis. The plate temperature was set to 60^{o}C to ensure rapid evaporation of the deionised water once deposited to minimise spreading and concentrate the particles over a smaller area to maximise the chance of printing a continuous CuNP

film. The jetting frequency was set to 1 kHz and the CAD file was set to print 3 squares of width 5, 2.5 and 1 mm.

2.4.10 Matrix-Assisted Laser Desorption/Ionization – Mass Spectrometry (MALDI-MS)

MALDI-MS was performed by Dr David Clarke from the University of Edinburgh, School of Chemistry. Experiments were carried out using a 12T SolariX FT-ICR MS (Bruker Dattonics). Mass calibration was performed using built-in protein standards. Samples containing CuNPs were mixed with α-Cyano-4-hydroxycinnamic acid (CHCA) matrix dissolved in a 1:4 v/v solution of acetonitrile and distilled water. After mixing, 2 µl of the sample was loaded onto a MALDI plate and was allowed to dry before inserting into the vacuum chamber. MALDI-MS was performed and peaks were recorded in positive mode.

2.5 Growth of *M. psychrotolerans* in various conditions

2.5.1 Growth in LB_{ns} Agar

To test the tolerance threshold of *M. psychrotolerans* to $CuSO_4$, an assay was developed using agar plates containing $CuSO_4$ at various concentrations. LB_{ns} agar was prepared and autoclaved, after cooling to 55°C, 5 mM $CuSO_4$ final concentration was added and mixed slowly by inverting several times. The agar containing the $CuSO_4$ was then poured onto an empty petri dish. The same was repeated for $CuSO_4$ concentrations of 0.01, 0.1, 0.5 and 1 mM. A control was also set up which did not contain any $CuSO_4$. The agar plates were incubated for 48 hours at 25°C in a static incubator prior to examining for growth.

2.5.2 Growth in Distillery Co-Products (Agar)

Pot ale and spent lees from the Glenkinchie whisky distillery were used for this assay. Both co-products were mixed at different ratios to investigate the optimum growth conditions for *M. psychrotolerans*. The ratios tested are listed in Table 2.2. 2% agar was added to the co-products in order to allow for the medium to solidify. The pH of the co-products was adjusted to 7.0 prior to autoclaving. 20 ml of each co-product as well as co-product mix ratio was poured onto an empty petri dish and allowed to solidify. 10 µl of a *M. psychrotolerans* culture was spotted on the plates at dilutions

ranging from 10^0 to 10^{-6}. The plates were then incubated at 25°C for 48 hours in a static incubator prior to examining for growth.

Plate Number	Pot Ale Ratio	Spent Lees Ratio
1	10	0
2	9	1
3	8	2
4	7	3
5	6	4
6	5	5
7	4	6
8	3	7
9	2	8
10	1	9
11	0	10

Table 2.2: Ratios of co-products tested on agar plates. A final volume of 20 ml was used in each sample.

2.5.3 Growth in Distillery Co-Products (Liquid)

Pot ale and spent lees from the Glenkinchie whisky distillery were also used for this assay. The assay was similar to the agar version described previously, however it was performed in liquid medium rather than adding agar and solidifying it. The same ratios were tested as mentioned in Table 2.2. All co-products were mixed in 50 ml falcon tubes. All the samples were then inoculated with *M. psychrotolerans* and placed in a shaking incubator for 24 hours at 20^{o}C and 200 rpm. After 24 hours of incubation the cultures were taken out of the incubator and their absorbance was determined at O.D.$_{600}$ (Optical density at 600 nm) using a UVmini-1240, Shimadzu spectrophotometer.

2.5.4 Antibiotic Resistance Assays

A culture of *M. psychrotolerans* was grown for 24 hours in LB$_{ns}$ at 20^{o}C, 200 rpm. The culture was then diluted in LBns to 10^{0}, 10^{-1}, 10^{-2}, 10^{-3}, 10^{-4} and 10^{-5}. 10 µl of each dilution was spotted on LBns agar plates containing one antibiotic in specific concentration (each plate contained different concentrations of an antibiotic). Three replicates were performed for each agar plate. The antibiotics tested were Ap 50 µg/ml, Kn 5, 10, 20, 40, 60, 80 µg/ml, Cm, 5, 10, 20, 40, 60, 80 µg/ml, Tc 5, 10, 20, 50 µg/ml and Nx (Nalidixic acid) 50 µg/ml. For each antibiotic tested, a positive control was set up containing no antibiotic.

2.6 Extractions and Stock Preparations

2.6.1 Plasmid Extraction

All plasmid extractions were carried out using a commercially available plasmid extraction kit for small (QIAGEN, QIAprep Spin Miniprep Kit, Catalogue number 27104) and medium scale (QIAGEN, Plasmid Midi Kit, Catalogue number 12145) samples.

2.6.2 Genomic DNA Extraction (Commercial Kit)

Genomic DNA extractions were carried out using a commercially available genome extraction kit (ThermoFisher, Easy-DNA gDNA Purification Kit, Catalogue number K1800-01).

2.6.3 Genomic DNA Extraction (in-house)

Genomic DNA of *M. psychrotolerans* was prepared using an in-house method for obtaining high yield pure gDNA. A 50 ml culture of *M. psychrotolerans* was grown for 24 hours at 20^{o}C at 200 rpm. The culture was then centrifuged at 4,500 x g for 15 minutes to form a pellet and the supernatant was removed. The cell pellet was resuspended in 4 ml of Extraction buffer carefully so as not to induce foam formation (10 mM Tris pH 8.0, 100 mM EDTA pH 8.0, 0.5% SDS). The sample was then incubated at 50^{o}C for 1 hour before addition of proteinase K (50 µg/ml final) and thorough mixing. The mixture was incubated at 50^{o}C for 16 hours. An equal volume of phenol was added to the mixture and mixed carefully by slow inversion for 15 minutes. The mixture was then centrifuged at full speed in a benchtop centrifuge (eppendorf 5417R centrifuge) for 5 minutes. The top phase of the mixture was removed carefully by not disturbing the lower phase and transferred into a new sterile tube. DNA precipitation was performed by adding 1/10 volume 3 M Sodium Acetate (NaOAc) and an equal volume of isopropanol. The tube was mixed by rotation using a benchtop roller (Stuart roller mixer) until DNA formed a visible white precipitate, and until the precipitate became densely concentrated. The precipitate was removed by picking it up with a Pasteur pipette. While the DNA was on the Pasteur pipette, 1 ml of 75% ethanol (EtOH) was pipetted directly onto the DNA to wash it. The DNA was partially dried by forcing air through the pipette onto the DNA. The DNA was then resuspended in 0.7 ml of TE by pipetting it onto the DNA while resting on the tip of the Pasteur pipette. The DNA was gradually resuspended and collected in a microcentrifuge tube. RNA treatment was performed by adding RNase A (10 µl of 10 mg/ml RNase A) and incubation at 42^{o}C for 30 minutes. Phenol:Chloroform extraction was performed twice to remove any trace proteins from the sample and purify the gDNA. 1/10 volume 3 M NaOAc and 1 volume isopropanol was then added to precipitate the gDNA. The sample was rotated in a benchtop roller until a pellet was visible. The sample was centrifuged for 1 minute at full speed on a benchtop centrifuge prior to washing with 75% EtOH. The sample was air dried for approximately 2 minutes and then resuspended in 0.5 ml of H_2O_{dd} to form a concentrated gDNA stock.

2.6.4 PCR Purification

DNA products from restriction digestion reactions were purified using the commercially available kit QIAGEN, QIAquick PCR Purification Kit, Catalogue number 28104.

2.6.5 Agarose Gel DNA Extraction

DNA present in agarose gels was extracted and purified using the kit QIAGEN, QIAquick Gel Extraction Kit, Catalogue number 28704.

2.6.6 Frozen Stock Preparation

Bacterial cultures were grown for 24 hours at their optimum conditions for growth. 0.5 ml of the bacterial culture was transferred to Wheaton polypropylene Cryule Vials. 0.5 ml of 80% Glycerol was added to each tube to get a 40% Glycerol stock. The tubes were mixed by pipetting up and down and snap frozen in liquid nitrogen. They were then transferred into a -80^{o}C freezer quickly to prevent thawing.

2.6.7 RNA Extraction

Extraction of RNA from *M. psychrotolerans* was performed using the commercially available kit illustra RNAspin Mini Kit, GE Healthcare, Catalogue number 25-0500-70. Prior to commencing with the RNA isolation, the bench as well as all the equipment used including pipettes, gloves and centrifuges were wiped with RNase AWAY Decontamination Reagent to prevent extracted RNA contamination. A Bunsen burner was used to ensure sterility.

To ensure RNA eluate obtained was free from genomic DNA derived from the host organism, a further DNase treatment was performed using the commercially available kit DNA-*free* DNA Removal Kit, ThermoFisher, Catalogue number AM1906.

2.7 Genetic Modification

2.7.1 Genetic Analysis

Genome analysis for the bacteria used in this study was performed using the software CLC Sequence Viewer by QIAGEN. Vectors used in this study were mapped and analysed using the software SnapGene and its freeware version SnapGene Viewer. PCR primers were designed either manually or using the online tool Primer3 provided by the Howard Hughes Medical Institute and by the National Institutes of Health. Gene

constructs and vector inserts were designed using the software A Plasmid Editor (ApE) provided by Bio-Soft Net.

2.7.2 Polymerase Chain Reaction (PCR)

The reagents used for PCR were provided by New England Biolabs and Promega. The reaction conditions were based on the protocol provided with the commercially available polymerase Phusion High-Fidelity DNA Polymerase, New England Biolabs, Catalogue number M0530S. Reaction conditions were altered according to the size of the PCR product and the annealing temperatures of the primers used in each reaction as instructed by the provided kit. PCR was performed on a Bio-Rad T100 Thermal Cycler.

2.7.3 Restriction Digestion and Ligation

Restriction digestion was performed using the method provided by New England Biolabs. The reaction volumes were adjusted to 100 µl to obtain higher yields of DNA. 20 units of restriction enzyme was used as well as 5 µg of DNA per reaction. CutSmart Buffer was used for each reaction provided by Promega, Catalogue number B7204S.

Ligation was performed in 20 µl total volume reaction, using the T4 DNA Ligase, ThermoFisher, Catalogue number IVGN210. The vector to insert ratio was 1:3. 5 and 10 µl of a ligation mix was used for transformations of *M. psychrotolerans* and TOP10 *E. coli*, ThermoFisher, Catalogue number C4040-03.

2.7.4 Plasmid mutagenesis

Mutations on plasmids were carried out using the QuikChange Lightning Multi Site-Directed Mutagenesis Kit by Agilent Technologies Catalogue number 210513. DNA primers were designed using Primer3 and were synthesised by Sigma-Aldrich. Verification of the mutations was carried out by Sanger sequencing (Edinburgh Genomics) using primers binding upstream of the mutagenesis site.

2.7.5 Preparing Electrocompetent *M. psychrotolerans*

The following protocol was adapted from (Evans 2001) in order for it to be used on *M. psychrotolerans*. 50 ml of *M. psychrotolerans* grown for 24 hours was split into two and used as an inoculation culture for two flasks containing 475 ml of room temperature LB_{ns}. The cultures were then grown at 20^{o}C and 200 rpm and until they reached an $O.D._{600}$ of 1.0. $O.D._{600}$ measurements were recorded every 40 minutes. When the O.D.600 reached 1.0, the cultures were rapidly transferred into an ice bath and incubated for 15-30 minutes while swirling occasionally to ensure even cooling. The culture was then transferred into pre-chilled 50 ml Falcon tubes and centrifuged at 4^{o}C at 3,000 rpm. for 10 minutes. The supernatant was removed and the cell pellets were resuspended in 1 volume of pre-chilled H_2O_{dd} of the centrifuged culture. Centrifugation and decanting was repeated again followed by resuspension of the cells in a half volume of pre-chilled 10% glycerol. Centrifugation and decanting was then repeated and the supernatant was carefully removed using a pipette. The pellets were resuspended in 1 ml of pre-chilled GYT by gentle swirling as pipetting might disrupt them. The cell concentration was recorded by taking an $O.D._{600}$ measurement of a 1/100 dilution of the cell sample. 50 µl aliquots of the cell suspension was transferred into pre-chilled microcentrifuge tubes prior to snap freezing using liquid nitrogen. The frozen electrocompetent cells were then stored at -80^{o}C for future use.

2.7.6 Preparing Chemically Competent *M. psychrotolerans*

Chemically competent cells of *M. psychrotolerans* and *E. coli* were prepared using a modified version of the Chung *et al.* (1989) method to suit the growth conditions of the organisms used in this study.

5 ml cultures of *M. psychrotolerans* and *E. coli* were diluted 1/100 in LB medium and incubated at a shaking incubator to an $O.D._{600}$ of 0.5, at 20^{o}C and 37^{o}C respectively.

When the $O.D._{600}$ reached 0.5 the cultures were centrifuged at 3,000 rpm. for 10 minutes prior to removing the supernatant. The pellets were resuspended in 10% volume TSS solution. 100-200 µl of the cell suspensions were aliquoted into pre-chilled microcentrifuge tubes before subsequently snap freezing using liquid nitrogen. The chemically competent cells were then stored at -80^{o}C for future use.

2.7.7 Electroporation of *M. psychrotolerans*

50 µl of pre-prepared electrocompetent cells of *M. psychrotolerans* were thawed on ice. Depending on the vector concentration, 1-3 µl of vector DNA was added to the thawed cells and mixed by gentle swirling. The cells were then transferred to pre-chilled electroporation cuvettes with a 2 mm gap (Gene Pulser/MicroPulser Electroporation Cuvettes, 0.2 cm gap, Catalogue number 1652086). The cuvettes were pre-chilled and it was ensured that they were cool enough before adding the cell suspension. After adding the cells, the cuvettes were tapped to ensure any bubbles rose to the top of the suspension. The cuvettes were inserted one by one in the electroporator (Bio-Rad Pulse Controller-Gene Pulser) electrodes while removing the excess moisture from their surface. The cells were pulsed with 2.5 kV and immediately 1 ml of SOC was added to the cells before placing the cuvettes on ice for 2 minutes for recovery. The cells were then transferred into microcentrifuge tubes for incubation at 20^{o}C for over 2 h, at 200 rpm. The transformants were selected by plating the cell suspensions onto LB_{ns} containing the appropriate antibiotic for the vector used (Cm 40 µg/ml, Tc 50 µg/ml or Kn 50 µg/ml). The plates were incubated at 25^{o}C for 24-48 hours.

2.7.8 Transformation of Chemically Competent Cells

Chemically competent cells were thawed on ice and 1-3 µl of vector DNA or 5-10 µl of ligation mix was added to the thawed cells and mixed by gentle swirling. The cells were then incubated on ice for 30 min prior to heat shocking at 42^{o}C for 45 seconds in a heatblock (techne, Dri-Block DB-2D). Immediately after the heat shock, the cells were transferred on ice for 2 min for recovery. 1 ml of room temperature S.O.C. was added to the cells. The tubes containing the cells were incubated at 20^{o}C, 200 rpm. for over 2 hours in the case of *M. psychrotolerans.* In the case of *E. coli* the cells were incubated at 37^{o}C, 200 rpm. for 1 hour. After incubation, transformants were selected

by plating the cells on LB or LB_{ns} plates with the appropriate antibiotic for the vector used and incubated for 24-48 hours at 25°C for *M. psychrotolerans* or 37°C for *E. coli*.

2.7.9 Agarose Gel Electrophoresis

Agarose gels were made to a concentration of 0.8% by adding agarose to 1x TAE buffer. The mixture was then microwaved to boiling temperature until the agarose dissolved completely. 0.005% ml SYBR Safe DNA Gel Stain was added and the gel was left to cool to 55°C in a water bath set to 55°C. The gel was poured onto the casting stand (Geneflow electrophoresis tank) and allowed to set at room temperature. After submerging the gel in 1x TAE buffer in the appropriate gel tank, the gel was ready for use. DNA Electrophoresis was performed between 50-100 V and between 30 min and 3 h depending on size using a Bio-Rad PowerPac HC. Visualisation of DNA in agarose gels was performed using a Syngene, G:Box with a SYBR Safe detection filter.

2.7.10 Markerless Chromosomal Gene Deletions in *M. psychrotolerans*

1 PCR was set up with primers annealing to flanking DNA 500 bp upstream of the gene and the beginning (N-terminus) of the gene:

The tail on the second primer anneals to the end (C-terminus) of the gene. Another PCR was set up with primers annealing to the flanking DNA 500 bp downstream of the gene and the end (C-terminus) of the gene:

The tail on the first primer anneals to the start (N-terminus) of the gene so that the PCR products overlap at the ends. This gave rise to 2 PCR products which had the start and end of the gene and overlapped:

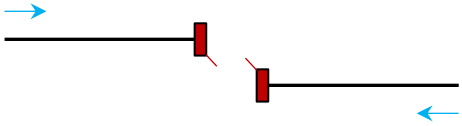

The 2 products were then used as a template with the outer primers to form the deleted gene with flanking regions:

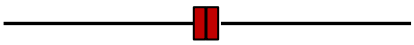

Agarose Gel Electrophoresis was performed with the PCR product in order to separate it, and it was then subsequently extracted and purified using the QIAquick Gel Extraction Kit, Catalogue 28704. Gibson Assembly was performed using the primers HisGib-F and HisGib-R in order to insert the PCR product into pK18mobSacB. The primers were designed using the Gibson Assembly toolkit provided by New England Biolabs (NEB). The plasmid with the PCR product was then inserted into One Shot TOP10 Chemically Competent *E. coli* provided by ThermoFisher, Catalogue C404003,

via transformation. Kanamycin was used as the selection marker to ensure maintenance of the plasmid.

Colonies were screened using PCR for the presence of the vector with the insert. After confirmation, the *E. coli* with the plasmid was cultured in the presence of kanamycin and the plasmid was purified to acquire higher yields. Electrocompetent *M. psychrotolerans* was then transformed with pK18mobSacB+insert using the protocol described previously in this chapter.

Isolates from the transformation were spread on agar plates containing LB and a range of concentrations of sucrose (5-15% sucrose). Surviving colonies would not contain a plasmid copy and therefore were picked and screened by replica plating onto agar plates containing kanamycin or no selection marker. Colonies that did not survive on kanamycin selection but survived on no selection agar plates were picked and screened for the deletion mutation using PCR with primers binding on the flanking regions of the wild-type gene.

2.7.11 Genome Sequencing and Annotation of *M. psychrotolerans*

The genome of *M. psychrotolerans* was sequenced with the help of Edinburgh Genomics. The instrument used was the Illumina MiSeq system which generated up to 300 base reads. Partial genome assembly was performed by Edinburgh Genomics using an automated software. Genome annotation was performed using the software Rapid Annotation using Subsystem Technology (RAST).

2.8 Proteomic Studies on *M. psychrotolerans*

2.8.1 Trypsin Digestion

A 10 ml culture of *M. psychrotolerans* was grown according to normal culturing conditions described earlier. The culture was then centrifuged for 10 min at 3,000 rpm and the supernatant was removed. The cell pellet was washed with PBS buffer, centrifuged again and the supernatant decanted. The cell pellet was washed twice more with PBS to ensure all the growth medium had been removed. The clean cell pellet could then be snap frozen for future use.

To perform a trypsin digestion on the *M. psychrotolerans* pellet, a tube containing the cells was thawed on ice. The pellet was resuspended in 200 µl of 6 M Urea buffer,

vortexed briefly and sonicated for 2 min. A pipette should not be used to resuspend the pellets. Then, 5 µl of DTT reducing reagent was added to the cell mixture, vortexed and incubated for 30-60 min at room temperature. 20 µl of iodoacetamide alkylating reagent was added, the mixture was vortexed and incubated for a further 30-60 min at room temperature. In the next step, 20 µl of DTT reducing reagent was added to the cell mixture, vortexed and incubated at room temperature for 30-60 min. The urea concentration was then reduced by diluting the cell mixture with 775 µl H_2O_{dd} and vortexing to mix. Trypsin was added and mixed carefully in a 1:50 ratio depending on the total protein content of the sample derived from the Bradford assay described later in this chapter. The digestion mix was incubated for 16 h at 37^{o}C.

Peptides from the overnight digestion were cleaned on a Solid Phase Extraction (SPE) reverse phase Bond Elut LMS cartridge, 25 mg (Agilent) and dried for RP-RP (Reversed Phase-Reversed Phase) fractionation (3 fractions). Samples were then reconstituted in 0.06 M ammonium formate buffer pH 10 and subsequently separated on a SPE reverse phase Bond Elut LMS cartridge, 25 mg. The low organic phase buffer A contained 0.06 M ammonium formate at pH 10 and the high organic phase buffer B was 100% acetonitrile. Three elution steps were performed at 15%, 25% and 100% of buffer B. The samples were then dried in a low pressure Speedvac (Thermo Jouan) and stored at -20^{o}C.

2.8.2 Standard Curve for Bradford Assay

Enough Biorad Quick Start Bradford Reagent 1x was aliquoted from the stock and left to stand at room temperature before the start of the method. The BSA stock solution (10 µg/µl BSA) was diluted in H_2O_{dd} at concentrations of 0, 1, 2.5, 5, 7.5 and 10 µg/µl and a final volume for each dilution of 1 ml. 100 µl of each dilution was then mixed with 900 µl of Urea 2 M. In 1 ml plastic disposable cuvettes, 100 µl of each dilution mixed with Urea 2 M was mixed with 1 ml of BioRad Quick Start Bradford Reagent 1x. The cuvettes were incubated at room temperature for 5 minutes before $O.D._{595}$ was measured using a spectrophotometer. The sample containing no BSA was used as the blank. The data gathered was then plotted on a graph and a line of best fit was used to correlate the absorbance measurements with the concentrations of each sample.

2.8.3 Bradford Assay

Enough Biorad Quick Start Bradford Reagent 1x was aliquoted from the stock and left to stand at room temperature before the start of the method. A blank solution was generated containing 5 µl H_2O_{dd} and 45 µl Urea 2 M. For the sample containing the cell suspension, a 1:10 dilution was performed using 5 µl sample and 45 µl Urea 2 M. This solution was diluted twice more by mixing 10 µl of the first dilution and 40 µl Urea 2 M (final 1:50 dilution). The final dilution contained 25 µl of the 1:50 dilution and 24 µl Urea 2 M (final 1:100 dilution). Next, 40 µl of each dilution was mixed with 1 ml of BioRad Quick Start Bradford Reagent 1 x. This procedure was performed in triplicate. The samples were incubated for 5 min at room temperature and then the samples were pipetted up and down twice to mix the samples. The samples were then transferred into 1 ml plastic spectrophotometer cuvettes and their absorbance was read at $O.D._{595}$. The absorbance was proportional to the concentration observed in the standard curve prepared prior to the protein content assay.

2.8.4 High Pressure Liquid Chromatography Mass Spectrometry (HPLC-MS)

The dried peptide containing samples were reconstituted in 0.5% v/v trifluoroacetic acid (dissolved in H_2O_{dd}) to a concentration of 1 µg/ µl. Samples were then filtered using a Millex filter before HPLC-MS analysis. HPLC-MS/MS analysis was performed using a nano-pump (Dionex Ultimate 3000, ThermoFisher) coupled to a QExactive system (ThermoFisher) with a pre-column of 300 µm x 5 mm (Acclaim Pepmap, 5 µm particle size) connected to a column of 75 µm x 50 cm (Acclaim Pepmap, 3 µm particle size). Samples were separated and analysed on a gradient for 90 min in a data dependent analysis (1 survey scan at 70,000 resolution followed by the top 10 MS/MS).

The MS/MS spectra obtained were searched using MASCOT versions 2.4 (Matrix Science Ltd) against an in-house database of *M. psychrotolerans* genomic DNA (3989 sequences) with a maximum missed-cut value of 2. The features used in all searches were:

i) Variable methionine oxidation
ii) Fixed cysteine carbamidomethylation
iii) Precursor mass tolerance of 10 ppm

iv) MS/MS tolerance of 0.05 amu

v) Significance threshold (p) below 0.05 (MudPIT scoring)

vi) A threshold peptide score of 20

Progenesis QI (version 2.0.5387.52102 Nonlinear Dynamics) was used for LC-MS label-free quantification. Only MS/MS peaks with a charge of 2+, 3+ and 4+ were considered for the total number of "Features" (signal at one particular retention time and m/z), the five most intense spectra per "Feature" were taken into account for the analysis. Normalisation was first performed based on the median of the ion intensities of the multicharged ion sets 2+, 3+ and 4+. The associated unique peptide ion intensities for a particular protein were summed to generate an abundance value which was then converted using an ArcSinH function (log transform was not ideal considering the significant amount of near zero measurements generated by the used method of detection). Based on the abundance values observed, means were calculated as well as the fold changes (in comparison to control samples) and were evaluated. One-way ANOVA was used to calculate p-values based on the ArcSinH transformed values. Proteins that were differentially expressed were only considered significant if the following conditions were met:

i) p-values (pair-wise) were less than 0.05

ii) Number of peptides detected and used for quantification per protein was equal or more than 2

iii) Absolute fold change was at least 1.5 (i.e. $\geq$1.5 fold for overabundant proteins and $\leq$0.667 fold for underabundant proteins)

Chapter 3. Synthesis and Characterisation of Stable Copper Nanoparticles by M. psychrotolerans

3.1 Introduction

Metallic nanoparticles differ greatly from their bulk counterparts (Husseiny, El-Aziz *et al.* 2007), for example they can be unstable and readily oxidise due to their uniquely small size (Huang, Yan *et al.* 1997). The stability of synthesised nanoparticles has therefore been a focus of research as it also plays an important role in their activity. Copper nanoparticles (CuNPs) are a prime example of unstable nanoparticles. They tend to oxidise in the presence of oxygen and form copper oxide (CuO) (Baco-Carles, Datas *et al.* 2011).

M. psychrotolerans is a little-studied category 1 non-pathogenic bacterium that is highly tolerant to Cu ions and that we have identified as having the ability to synthesise CuNPs. This is likely to be part of its defence mechanism; it uses Cu^{2+} to synthesise elemental CuNPs which are less reactive and therefore do not pose such a high toxicity risk. It is a facultative anaerobe and can therefore also be used under anaerobic conditions to synthesise CuNPs without oxidation of the nanoparticles occurring. *M. psychrotolerans* grows best at 20^{o}C (Emborg 2006), which makes this organism ideal for nanoparticle synthesis as energy requirements for growth are lower than the majority of non-biogenic methods.

CuNPs of an elemental nature are important as they have the potential to be used in many applications, such as electronics, catalysts and antimicrobials (Pantidos and Horsfall 2014). The use of *M. psychrotolerans* for the production of stable copper nanoparticles was therefore investigated in this study. The aim of this research was to synthesise, characterise and assess the qualities of the stable CuNPs produced by *M. psychrotolerans* and gain insight into the biological mechanisms used. *M. psychrotolerans* might then be utilised for the bioremediation of whisky distillery co-products from various whisky distilleries in Scotland.

3.2 Synthesis of Copper nanoparticles

To assess the ability of *M. psychrotolerans* to synthesise CuNPs the bacterium was grown at 20^{o}C for 24 hours as per the protocol described in the materials and methods. After growth, $CuSO_4$ was added to the LB_{ns} medium to a final concentration of 5 mM and further incubated for 24 hours. The colour of the medium during the incubation stayed dark green and did not change (Figure 3.1). Control experiments with *M. psychrotolerans* grown in LB_{ns}, removed through filtration and $CuSO_4$ added to the spent medium also showed the same colour change of yellow (colour of LB_{ns} medium) to dark green; the colour change in this case happened immediately after the addition of $CuSO_4$. This colour change therefore was shown to be unrelated to the presence of CuNPs in the medium.

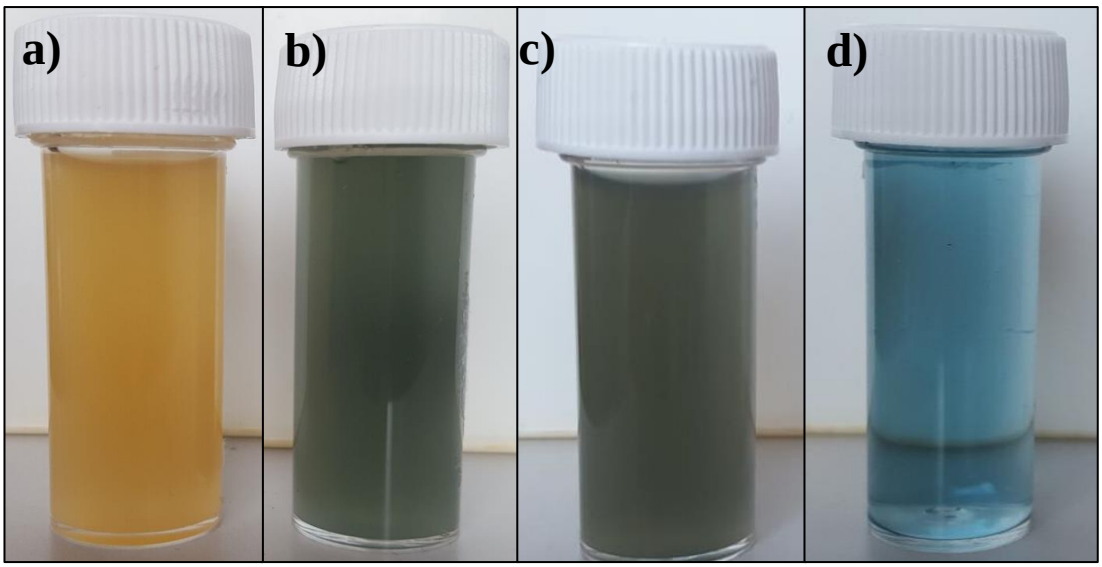

Figure 3.1: Plastic bijou bottles illustrating the colour of *M. psychrotolerans* cultures in the presence and absence of $CuSO_4$

Plastic bijou bottles illustrating the colour of the culture a) before addition of $CuSO_4$, b) immediately after addition of $CuSO_4$, c) 24 hours after addition of $CuSO_4$, d) LB_{ns} with 5 mM $CuSO_4$ after 24 hours of incubation.

The control experiment that contained no bacteria at any time maintained its blue colour throughout incubation at 20ºC for 24 hours; whereas the control experiment that contained LB_{ns} without any $CuSO_4$ added maintained its yellow colour. This meant that the presence of *M. psychrotolerans* in the medium containing $CuSO_4$ caused the medium to turn green over time.

3.3 Purification of Copper nanoparticles

Following the synthesis of CuNPs, they were purified for further characterisation as described in the materials and methods. The resulting pellet (Figure 3.2) contained the CuNPs that were subsequently used for further analysis. LB_{ns} medium contained proteins and cell debris, in addition to any extracellular proteins released by *M. psychrotolerans*, all of which needed to be removed. Any contaminant present would decrease the quality of characterisation results by increasing background noise levels when using analytical techniques or increasing the debris in TEM analysis.

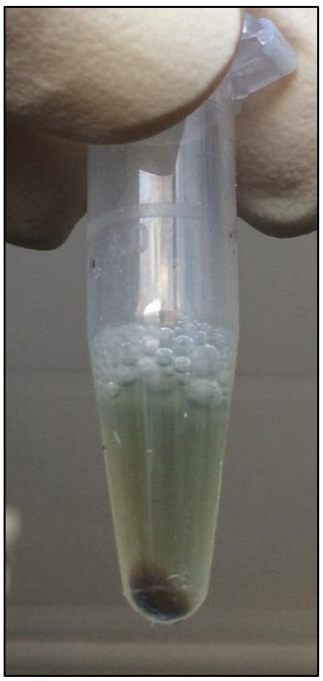

Figure 3.2: CuNP containing pellet synthesised by *M. psychrotolerans*

Picture shows the CuNP containing pellet after 16 hr of centrifugation resuspended in 500 µl of H_2O from an initial 10 ml culture of *M. psychrotolerans*, transferred into a microfuge tube.

3.4 Transmission Electron Microscopy

TEM has been used to visualise the metallic nanoparticles synthesised by the related organism *M. morganii* (Ramanathan, Field *et al.* 2013). The nanoparticles produced were easily seen via the electron microscope with a good resolution. This method was therefore also chosen here to screen and visualise any CuNPs produced by the organism *M. psychrotolerans*.

The nanoparticles were observed under an accelerating voltage of 200 kV. As shown in Figure 3.3, the nanoparticles were somewhat irregular in shape and size. Their size ranged from 4 nm to 60 nm, and by counting the nanoparticles and examining their sizes using ImageJ, the size distribution was determined. The majority of CuNPs were found to be between 10-19 nm across, followed by the next highest distribution groups of 20-29, 30-39, 40-49, 50-59 nm and finally 0-9 nm. The average diameter of the nanoparticles was 25.8 nm (Figure 3.4). There were no nanoparticles observed in the negative control sample containing 5 mM $CuSO_4$ and no bacteria.

Since TEM lacked the resolution to examine the CuNPs in more detail and at higher magnification, High Resolution-TEM (HR-TEM) was performed at the University of St. Andrews. Once again the nanoparticles were produced as described previously without the purification step and this time they were left at 4^{o}C for 6 weeks to verify their stability. A control experiment with $CuSO_4$ at 5 mM but no bacteria was also included. EDX analysis revealed the elemental composition of the nanoparticles and Fast Fourier Transform (FFT) elucidated the crystalline structure of the nanoparticles. The higher magnification of the nanoparticles allowed for improved analysis of the shape and structure. Figure 3.5 shows a CuNP magnified 500,000x. The shape appears hexagonal but without distinct edges, this may be due to the presence of capping proteins that keep the nanoparticles stable in their elemental state. Figure 3.5 also shows a well ordered structure with lattice fringes along the nanoparticle in 1 dimension. The distance between two lattice fringes was measured to be 0.20 nm, which is strongly indicative of elemental Cu and does not support the presence of a copper salt (Parikh, Singh *et al.* 2008).

EDX analysis allowed for the relative quantification of Cu while focusing the electron beam onto a single nanoparticle. The composition of the grid was considered

and a nickel (Ni) grid was used rather than the usual copper grid to analyse the CuNPs to avoid any false positives caused by the grids. However, the probe that the grid was mounted on had a Cu head which did cause a slight increase in the copper levels of the sample. To establish the difference in Cu levels between the background and the CuNPs, the electron beam was focused onto the carbon layer of the grid and an EDX spectrum obtained (Figure 3.6). The electron beam was then focused onto a nanoparticle and a second EDX spectrum was obtained. The difference in Cu levels between the first and the second spectra showed the relative Cu quantity present in the nanoparticles. As shown in Figure 6, when focusing onto one of the nanoparticles present on the carbon coated grid, high levels of copper were found to be present.

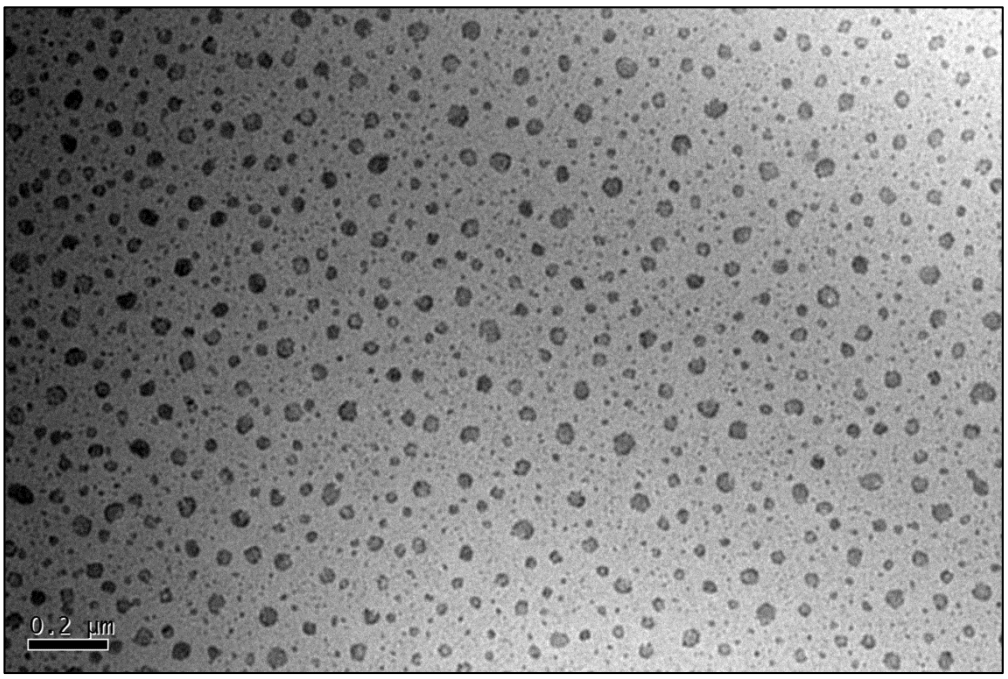

Figure 3.3: CuNPs synthesised by *M. psychrotolerans* visualised by TEM

Low magnification picture of a sample containing copper nanoparticles in supernatant after bacterial synthesis. The nanoparticles were prepared without purification and were visualised 2 days after synthesis.

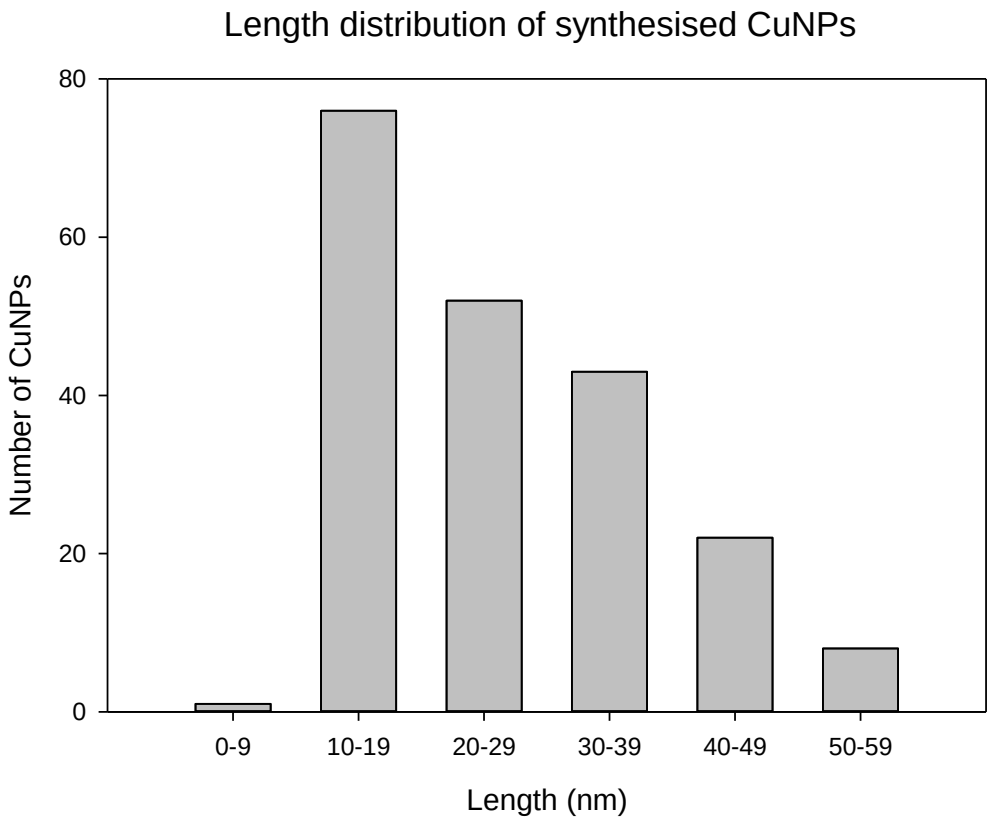

Figure 3.4: Size distribution of CuNPs synthesised by *M. psychrotolerans*

The graph shows the distribution of copper nanoparticles size and the average number of counts per size group measured in ImageJ. The counts were obtained from TEM analysis of non-purified copper nanoparticles synthesised at 20^{o}C, 2 days post-production.

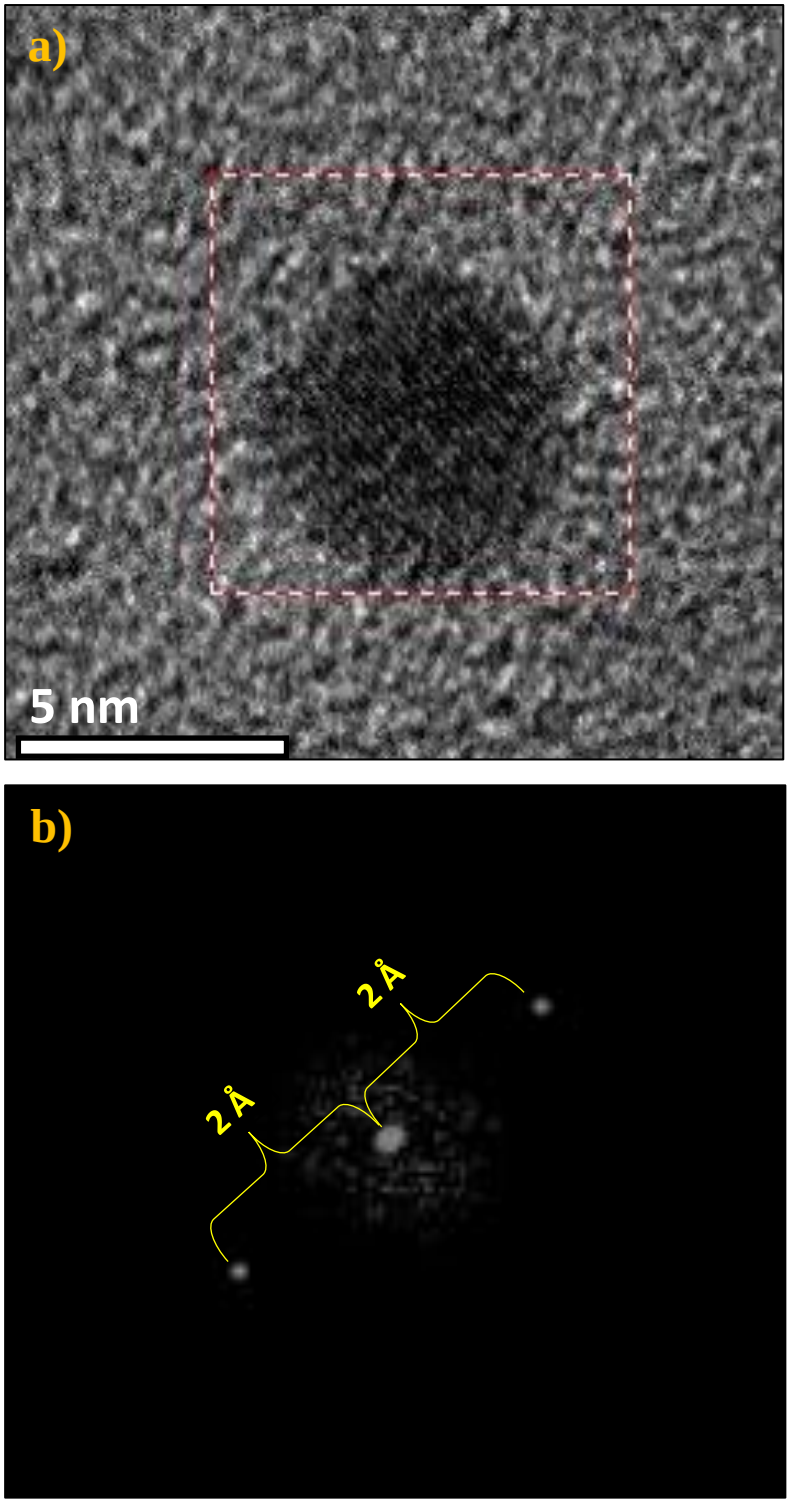

Figure 3.5: HR-TEM of CuNPs

HR-TEM pictures showing non-purified copper nanoparticles synthesised at 20°C, 6 weeks post-production. Pictures show a) one of the nanoparticles at x500,000 magnification and b) FFT of the copper nanoparticle. D-spacings of 0.20 nm indicates the presence of elemental Cu.

a)

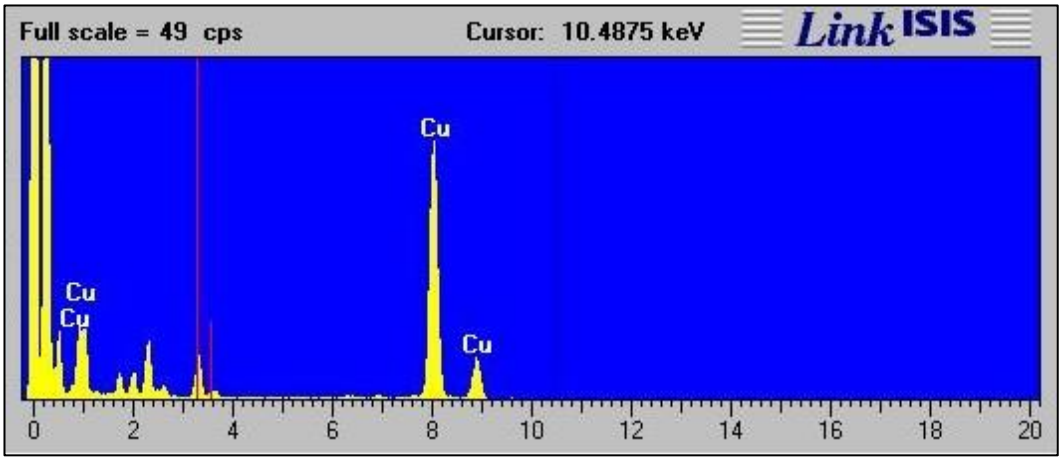

b)

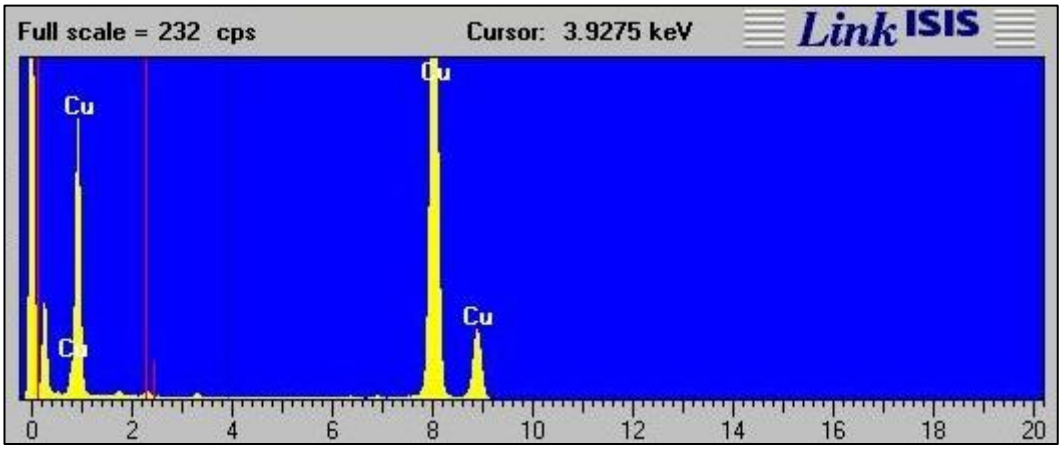

Figure 3.6: EDX spectra of copper nanoparticles

EDX spectra of copper nanoparticles synthesised at 20 ^{o}C overnight by *M. psychrotolerans.* a) Illustrates the background Cu levels caused by the Cu head of the probe that the grids are mounted on and b) shows the relative Cu levels present on the copper nanoparticles. No other elements were found to exist in significant levels suggesting the copper nanoparticles were solely made of copper, and in its elemental form.

3.5 X-ray Photoelectron Spectroscopy

Non-purified CuNPs were used for X-ray Photoelectron Spectroscopy (XPS) analysis. *M. psychrotolerans* was removed after the synthesis of CuNPs and the supernatant containing the nanoparticles was drop casted on a silicon wafer. After the wafer had dried, it was then analysed by XPS.

A full spectrum scan was performed from 0 to 1150 eV. The graph obtained from the data (Figure 3.7) shows three clear peaks that correspond to the three most abundant elements present in every sample, carbon (C), nitrogen (N) and oxygen (O). Copper peaks were also present, however they are very small compared to the reference C, N and O peaks, due to the low abundance of CuNPs present in the sample.

To verify the presence of CuNPs and obtain clearer peaks, a scan between 940 and 970 eV was performed. After 50 scans to reduce the noise levels, two distinct peaks were observed when graphing the data. One was a large peak at 945.3 eV and the other a smaller peak, 19 eV higher, at 964.3 eV (Figure 3.8). The peaks appeared at slightly higher energy values than might be expected for copper but the relative heights of these two peaks and their 19 eV spacing are characteristic of Cu at its zero valent form. The instrument had not been calibrated prior to the analysis commencing and therefore we believe the peaks to have shifted, a common occurrence under such circumstances (Institute 2000). There were no satellite peaks observed, supporting the previous result that the copper nanoparticles were made solely of copper in its elemental form. However the spectrum was rather noisy, caused by sample impurities present due to the samples containing bacterial growth medium as well as any extracellular material released by *M. psychrotolerans* during growth.

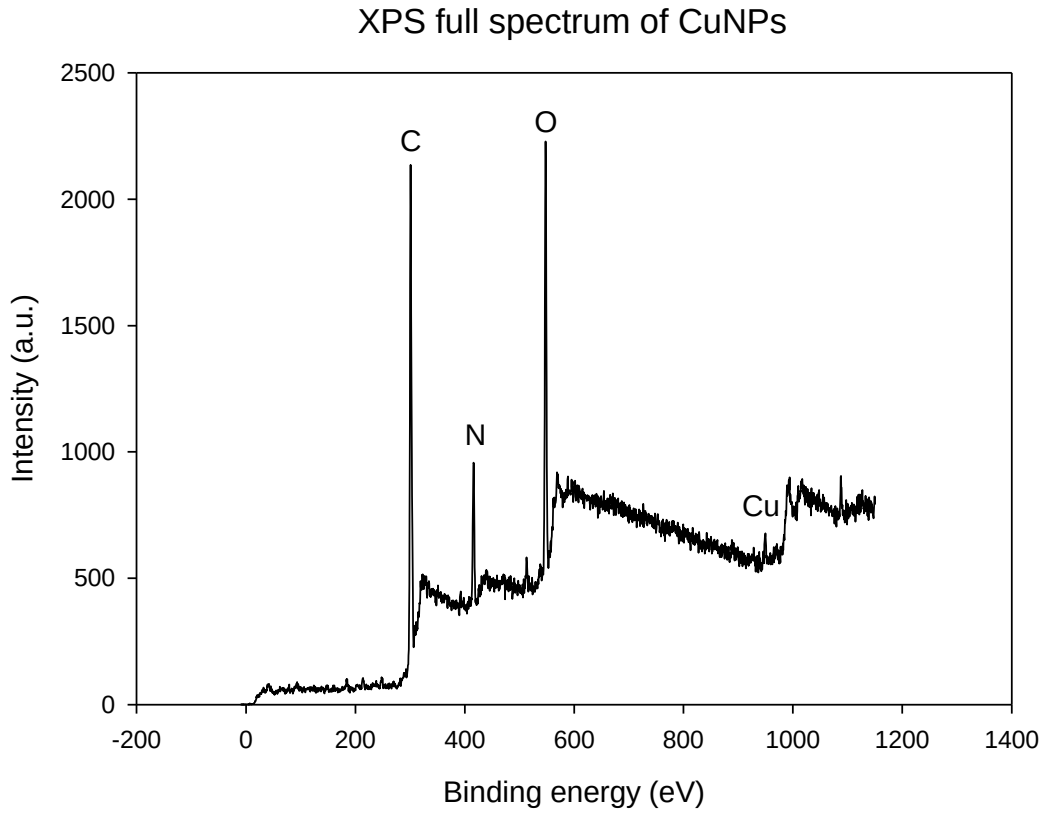

Figure 3.7: XPS full spectrum of CuNPs

Energy level spectrum of the supernatant containing synthesised copper nanoparticles by *M. psychrotolerans*. Peaks for C, N, O and Cu are labelled on the graph.

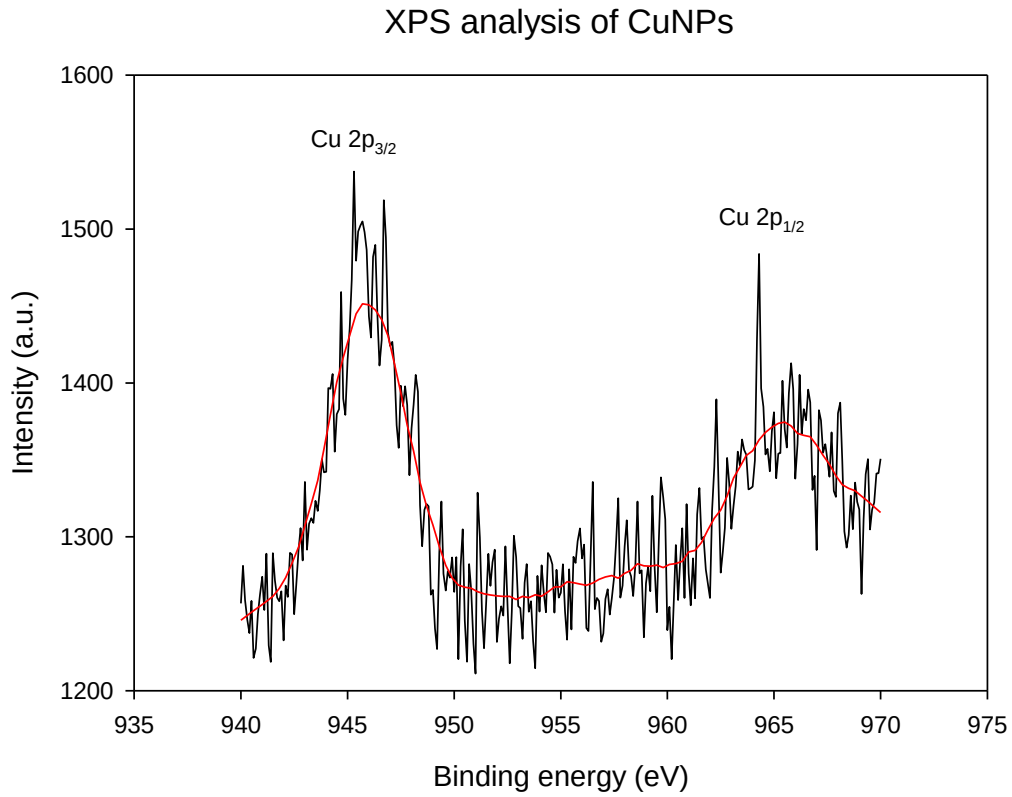

Figure 3.8: XPS analysis of CuNPs

The graph shows the excitation energy levels of a smaller part of the spectrum, specifically looking at the Cu energy levels. The red line is a moving average of the values recorded to highlight the peaks present within the noisy sample. The noise was reduced by performing 50 scans over the sample.

3.6 Inductively Coupled Plasma Optical Emission Spectroscopy

To quantify the levels of Cu ions removed from the original sample through their conversion into CuNPs, Inductively Coupled Plasma Optical Emission Spectroscopy (ICP-OES) was used. ICP-OES is a technique commonly used for quantitative measurement of metallic ions within an aqueous environment (Ren, Chong *et al.* 2015). Using a range of standards, each containing a known concentration of Cu^{2+}, a standard curve was constructed. The absorbance of each sample was then measured at predefined wavelengths set for Cu and the measurement was then correlated to the standard curve to determine the concentration of Cu^{2+} in each sample. This method was chosen for its simplicity and high accuracy for measuring metallic ions in aqueous environments (Merson and Evans 2003) and also because ICP-OES has a detection range within the Cu^{2+} concentrations that were used in this study.

CuNPs were prepared in the same manner as described before. The results after running the samples in the ICP-OES, given in Figure 3.9, show that the Cu levels in the crude supernatant are lower than the ultracentrifuged crude (UC). Ultracentrifugation was used in order to pellet small sized nanoparticles that are otherwise difficult to pellet using slower speed centrifugation. All three replicates produced a similar result.

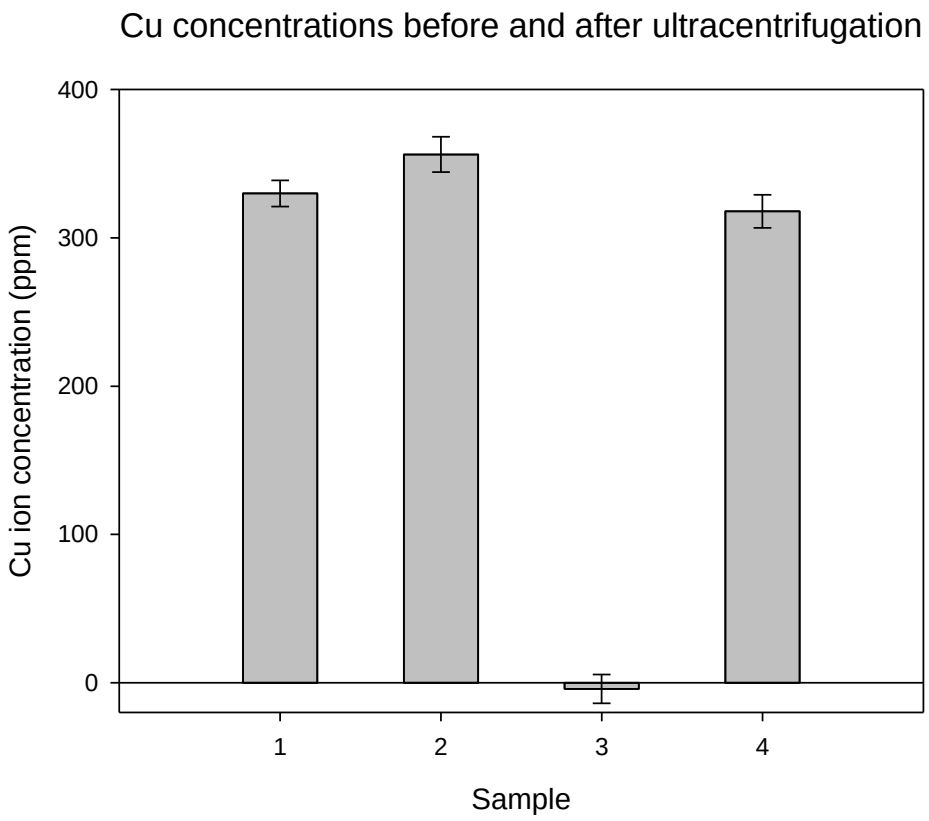

Figure 3.9: ICP-OES of Cu levels before and after ultracentrifugation

ICP-OES concentration values measured before and after removal of copper nanoparticles from the 1) crude supernatant, 2) ultracentrifuged crude, 3) negative control (LB_{ns}), and 4) positive control (LB_{ns} + 5 mM $CuSO_4$). A small difference in the values was observed and shown with error bars.

The experiment was repeated using a similar preparation method for the samples. This time the crude supernatant was split into two separate tubes prior to ultracentrifugation. One tube was ultracentrifuged for 45 minutes at 39,000 rpm before the supernatant was collected (UC_{45}). The second tube was ultracentrifuged for 16 hours at 39,000 rpm before the supernatant was collected (UC_{960}). The ICP-OES copper concentration measurements show a similar result to the first run. All the values obtained were multiplied by their dilution factor of 100 to get the original concentration of the samples. As seen in Figure 3.10, there was no removal of ionic Cu from the UC samples. The observed difference in values between the samples was very small and the experimental error significant therefore this data does not support a change in Cu concentration.

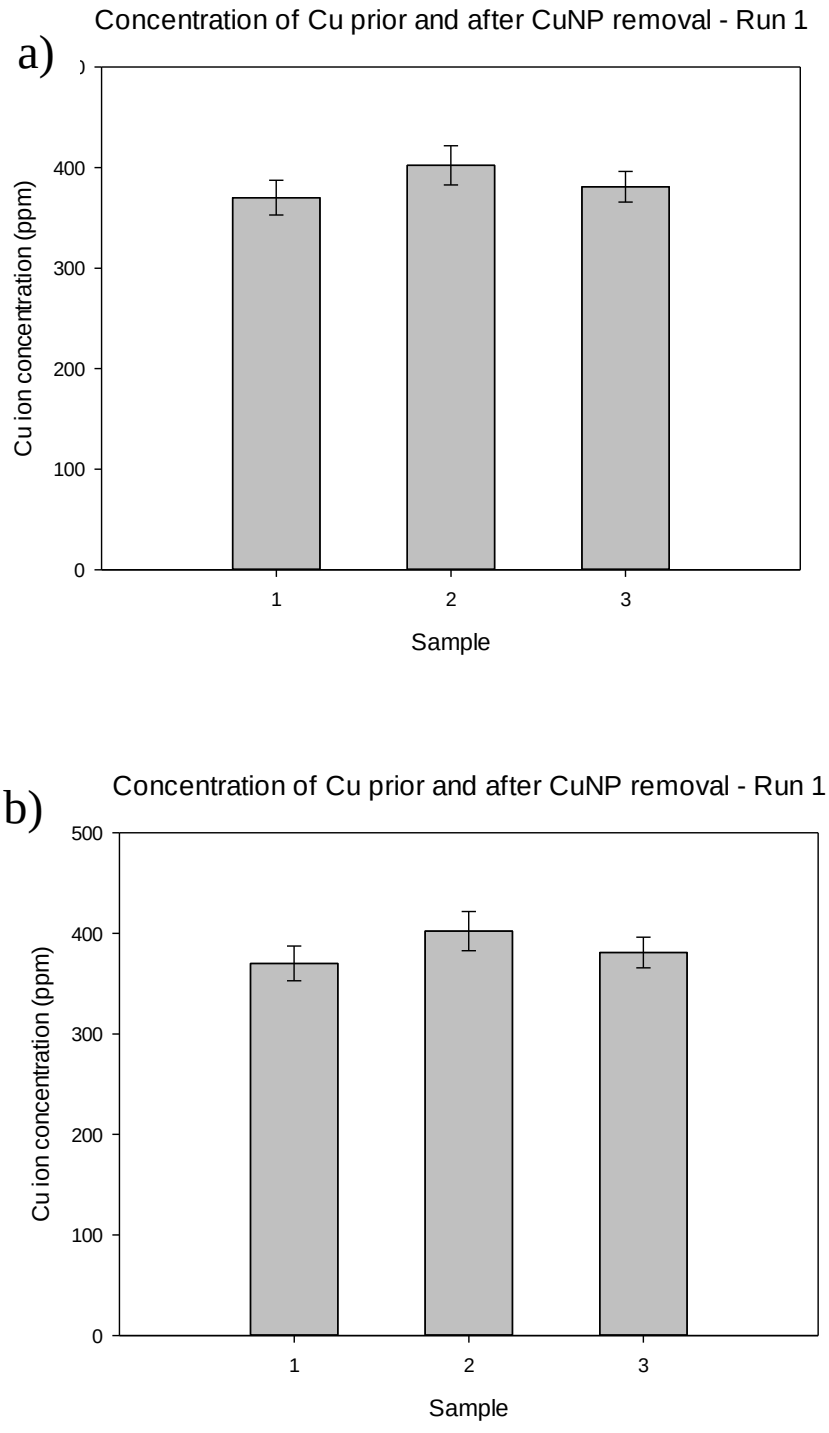

Figure 3.10: ICP-OES of Cu levels before and after ultracentrifugation

Bar chart shows the concentration of Cu found in a) Run 1 and b) Run 2, before and after ultracentrifugation at 39,000 rpm at different intervals. The samples analysed were 1) crude, 2) UC_{45} and 3) UC_{960}.

3.7 pH effect on Copper Nanoparticles

The pH of the solution surrounding the nanoparticles plays a strong role in their stability (He, Guo *et al.* 2007). The synthesised CuNPs were purified using the method described previously in the materials and methods. After the second ultracentrifugation step, the pellet containing the CuNPs was resuspended in solutions of MOPS buffer at differing pH, adjusted with HCl/H_2SO_4.

The nanoparticles initially produced by *M. psychrotolerans* are called 'seeds' as their size and shape were manipulated using buffers. After resuspension of the nanoparticle seeds in their respective buffers, they were incubated for 24 hours at 4^{o}C. Samples were then loaded onto copper grids and examined using TEM. All the nanoparticles exhibited marked differences in their morphology (Figure 3.11).

The nanoparticles resuspended in buffer at pH 7.5 were larger than the seed nanoparticles initially produced by *M. psychrotolerans* and their size more uniform. The majority of the nanoparticles appeared to have a diameter of 100 nm which was significantly larger than the seed particles. No aggregation was observed and their shape was more rounded and uniform.

CuNPs that were resuspended in MOPS buffer at pH 6.5 retained similar physical characteristics to those resuspended in buffer at pH 7.5. The density and the number of nanoparticles observed appeared to be very similar, however nanoparticles were seen to have grown in size or aggregated to form particles with an average diameter of 200 nm (Figure 3.11). To ensure the composition of these nanoparticles, EDX was used, which indeed confirmed they were composed of Cu.

After resuspension at pH 8.5, the morphology of the CuNPs changed completely. The nanoparticles appeared to form rod-like shapes with an average width of 100 nm and length of 2 µm, thus making them microparticles by definition. A precipitate was also observed that was confirmed, using TEM, to contain larger sized rods of width around 300 nm and length of 4 µm (Figure 3.11).

The experiment was repeated three times in total but with limited success at pH 8.5 as the quantities of nanoparticles observed was significantly less, however morphologies

were similar. The results at pH values of 6.5 and 7.5 were reproducible with similar morphologies.

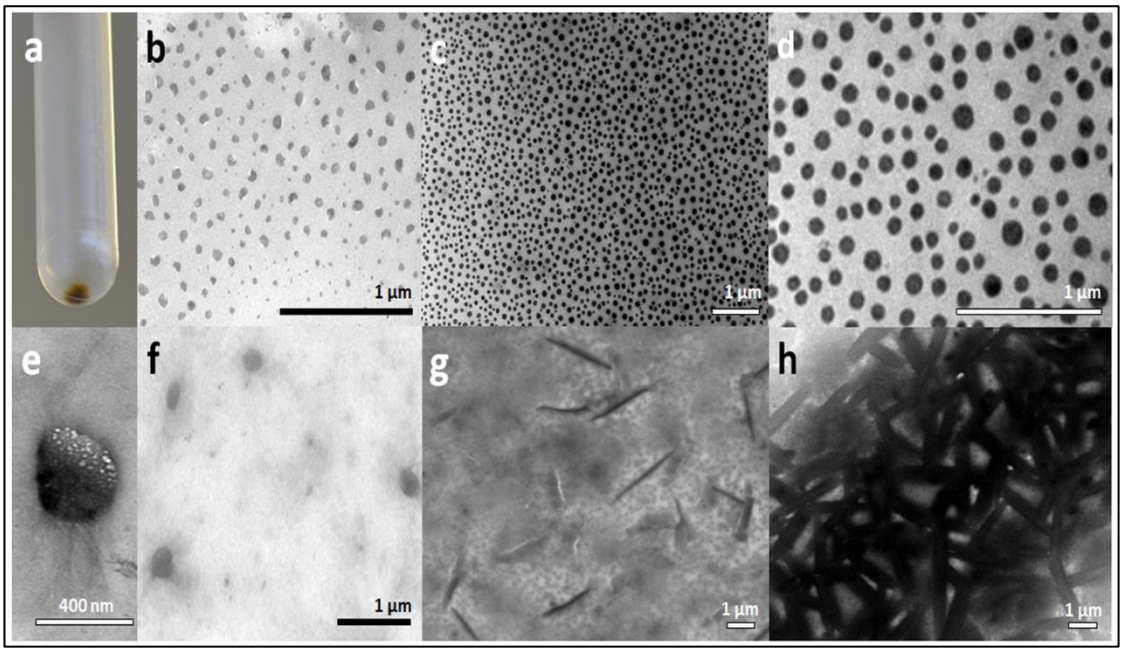

Figure 3.11: pH effects on CuNPs synthesised by *M. psychrotolerans*

Images of CuNPs following purification and nanoparticle manipulation by pH. (a) CuNP pellet formed after over-night ultracentrifugation. (b) Supernatant containing CuNPs following ultracentrifugation for 30 minutes. Debris from the LB medium has largely been removed; the nanoparticles retain the irregular shape and sizes of the nanoparticles produced by *M. psychrotolerans* (Fig. 3a-c). (c) CuNPs following 24 hours of incubation in MOPS buffer pH 7.5. The nanoparticles are now more uniform in shape, and most are around 100 nm. (d) A close-up of a section from (c). (e-f) CuNPs following 24 hours of incubation in MOPS buffer pH 6.5. The nanoparticles are irregular in size and shape but some are bigger than the nanoparticles found before incubation in buffer, up to 400nm in some instances (e). (g-h) CuNPs following 24 hours of incubation in MOPS buffer pH 8.5. The nanoparticles have formed rod-like structures, ranging in size from 100-300 nm in width and 2-4 µm in length.

3.8 Zetasizer measurements of Copper nanoparticles

Zeta potential is a measure of the magnitude of the electrostatic forces between particulate matter and plays an important role in stability (Hanaor, Michelazzi *et al.* 2012). To identify the zeta potential of the synthesised nanoparticles a zetasizer was used. CuNPs were synthesised by incubating *M. psychrotolerans* with 5 mM $CuSO_4$ for 24 hours at 20^{o}C. The medium consisted of LB_{ns} and MOPS at pH 7.5. After synthesis the CuNPs were purified using the ultracentrifugation method and resuspended in phosphate buffer at pH 7.5. Purification removed any bacterial cell debris present from the medium during CuNP synthesis and reduced noise levels when measuring CuNP zeta potential. This purified sample of nanoparticles was added to various buffers to examine their effect on the zeta potential of the nanoparticles (Figure 3.12).

CuNPs diluted tenfold with phosphate buffer at pH 7.5 measured a zeta potential of 24.66 mV over 5 cycles. However, the electrode used to measure the zeta potential turned black in colour over the course of these cycles, likely due to the copper binding to it through electron displacement, therefore the number of repeats was dropped down to 4 as this avoided excessive build-up of the copper deposits. Figure 14 shows the measurements recorded. The observed conductance parameter was 19,274 µS and electric field parameter 3.42 V/cm.

The buffer in which the CuNPs were suspended played an important role on the zeta potential of the nanoparticles. A sample resuspended in HEPES (4-(2-hydroxyethyl)-1-piperazineethanesulfonic acid) 10 mM buffer at pH 7, measured a zeta potential of -22.16 mV. In this instance no black deposits were observed on the electrode, and therefore 5 runs were performed in order to obtain a more accurate mean value. The large change in zeta potential was attributed mainly to the change in buffer, rather than the pH as it has only changed by 0.5. Measurement parameters were 5,755 µS for conductance and the electric field was at 6.09 V/cm (Figure 3.13).

The zeta potential of a third sample, prepared by a tenfold dilution of the purified nanoparticles in 50 mM sodium tartrate buffer at pH 3, was measured over five runs. Four of the values were similar, however one value was measured to be positive and

significantly different (Figure 3.13). The mean zeta potential was recorded at -7.83mV. Conductance was at 12,290 µS and electric field parameter at 4.00 V/cm.

When nanoparticles were diluted in 50 mM sodium tartrate buffer at pH 5 for a fourth sample, the mean zeta potential was -7.63 (Figure 3.13). Measurement parameters were at 17,316 µS for conductance and 3.12 V/cm for electric field. The value for pH 5 was very similar to the value found for pH 3 which was -7.83. Again one of the five runs produced a very positive zeta potential which differed significantly from the other four runs.

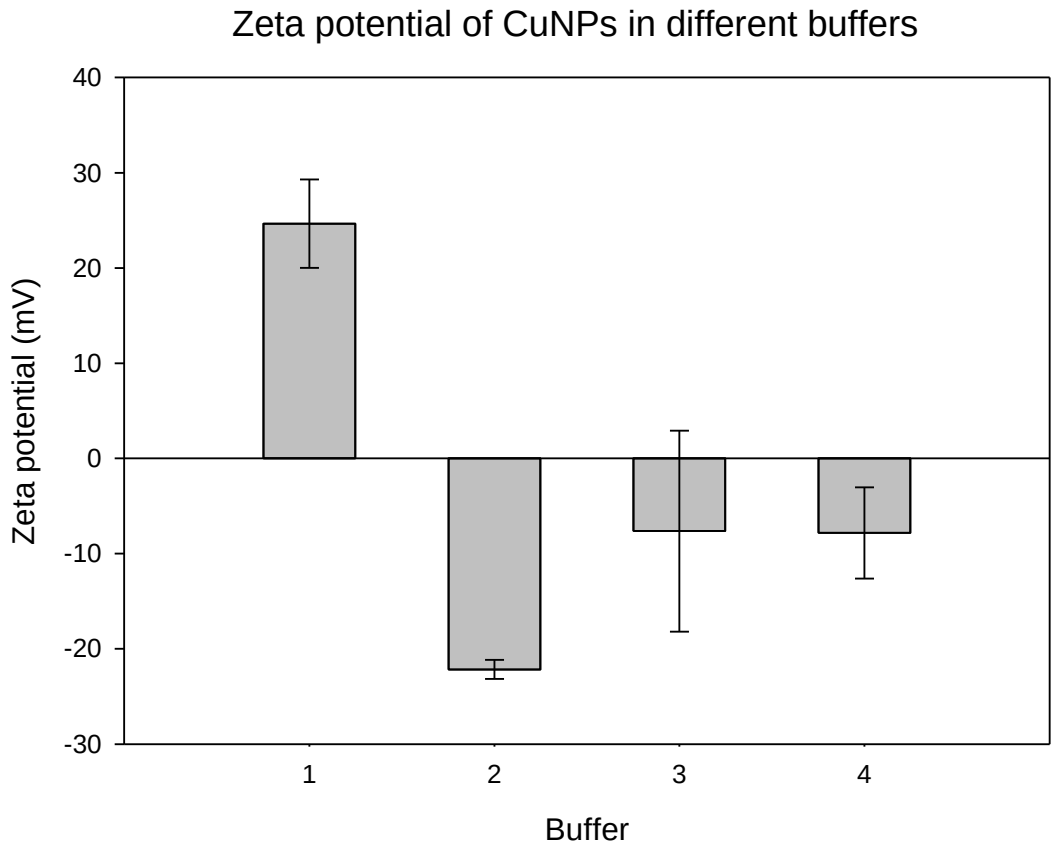

Figure 3.12: Zeta potential of CuNPs in different buffers

Bar chart illustrating the electric charge of CuNPs diluted in various buffers of different pH. The samples tested were (1) Phosphate buffer pH 7.5, (2) 10 mM HEPES buffer pH 7.5, (3) Sodium tartrate pH 5.0 and (4) Sodium tartrate pH 3.0.

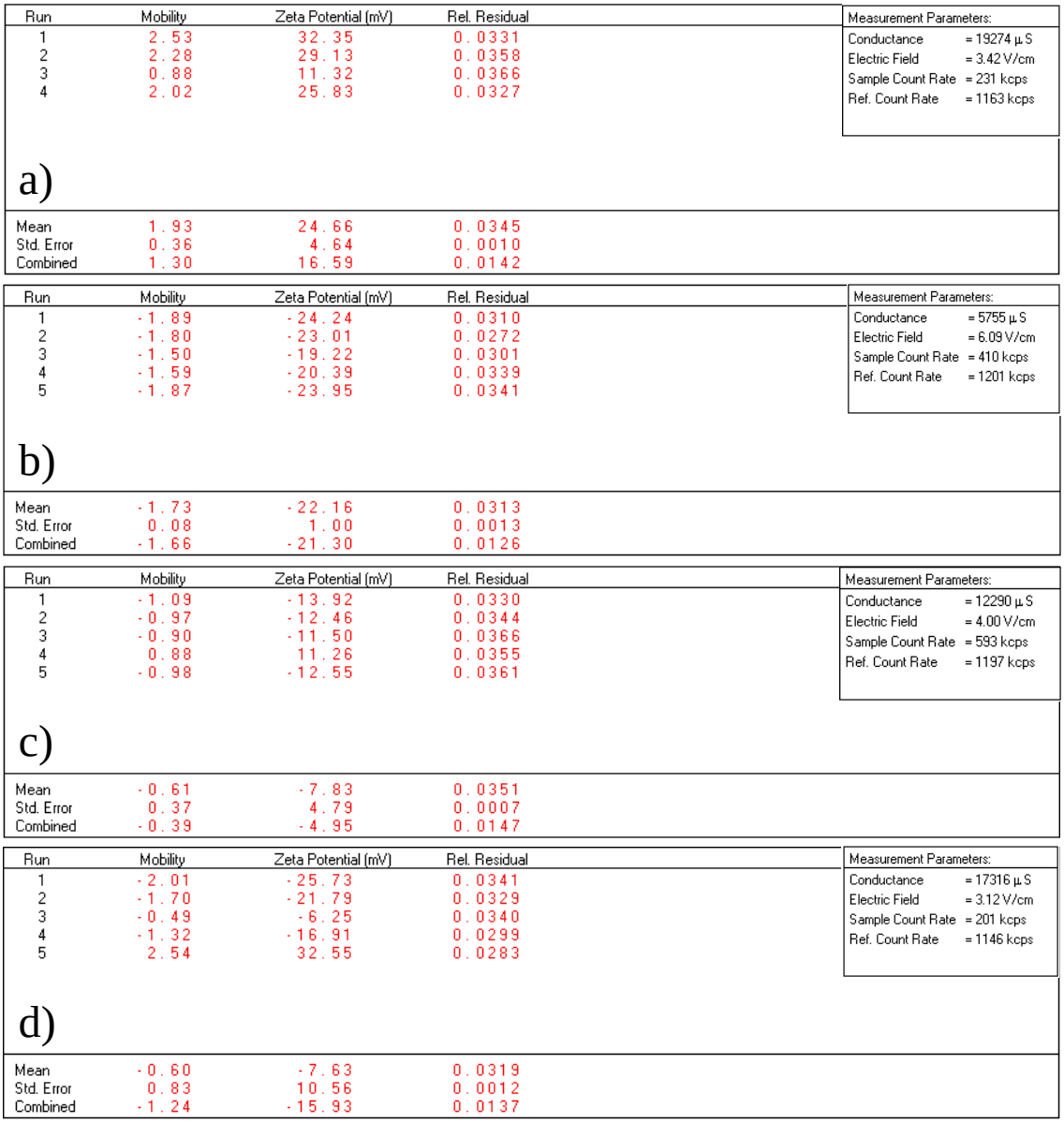

Run	Mobility	Zeta Potential (mV)	Rel. Residual
1	2.53	32.35	0.0331
2	2.28	29.13	0.0358
3	0.88	11.32	0.0366
4	2.02	25.83	0.0327

Measurement Parameters:

Conductance	= 19274 µS
Electric Field	= 3.42 V/cm
Sample Count Rate	= 231 kcps
Ref. Count Rate	= 1163 kcps

a)

Mean	1.93	24.66	0.0345
Std. Error	0.36	4.64	0.0010
Combined	1.30	16.59	0.0142

Run	Mobility	Zeta Potential (mV)	Rel. Residual
1	-1.89	-24.24	0.0310
2	-1.80	-23.01	0.0272
3	-1.50	-19.22	0.0301
4	-1.59	-20.39	0.0339
5	-1.87	-23.95	0.0341

Measurement Parameters:

Conductance	= 5755 µS
Electric Field	= 6.09 V/cm
Sample Count Rate	= 410 kcps
Ref. Count Rate	= 1201 kcps

b)

Mean	-1.73	-22.16	0.0313
Std. Error	0.08	1.00	0.0013
Combined	-1.66	-21.30	0.0126

Run	Mobility	Zeta Potential (mV)	Rel. Residual
1	-1.09	-13.92	0.0330
2	-0.97	-12.46	0.0344
3	-0.90	-11.50	0.0366
4	0.88	11.26	0.0355
5	-0.98	-12.55	0.0361

Measurement Parameters:

Conductance	= 12290 µS
Electric Field	= 4.00 V/cm
Sample Count Rate	= 593 kcps
Ref. Count Rate	= 1197 kcps

c)

Mean	-0.61	-7.83	0.0351
Std. Error	0.37	4.79	0.0007
Combined	-0.39	-4.95	0.0147

Run	Mobility	Zeta Potential (mV)	Rel. Residual
1	-2.01	-25.73	0.0341
2	-1.70	-21.79	0.0329
3	-0.49	-6.25	0.0340
4	-1.32	-16.91	0.0299
5	2.54	32.55	0.0283

Measurement Parameters:

Conductance	= 17316 µS
Electric Field	= 3.12 V/cm
Sample Count Rate	= 201 kcps
Ref. Count Rate	= 1146 kcps

d)

Mean	-0.60	-7.63	0.0319
Std. Error	0.83	10.56	0.0012
Combined	-1.24	-15.93	0.0137

Figure 3.13: Zetasizer measurements for CuNPs in buffers at different pH

Zetasizer measurements for CuNPs diluted in various buffers at different pH. a) CuNPs diluted in phosphate buffer, pH 7.5, b) CuNPs diluted in HEPES pH 7, c) CuNPs diluted in sodium tartrate pH 5 and d) CuNPs diluted in sodium tartrate pH 3.

3.9 UV-Visible Spectroscopy (UV-Vis)

After confirming that *M. psychrotolerans* synthesises CuNPs, the next step was to examine the rate of synthesis. *M. morganii* was previously shown to synthesise CuNPs over a 24 hour period, however whether the reaction reached a plateau or was still ongoing was not shown (Ramanathan, Field *et al.* 2013). The production of nanoparticles by *M. psychrotolerans* can be monitored using UV-Vis. CuNPs can be detected under UV-Vis at approximately 580 nm (Nasrollahzadeh, Sajadi *et al.* 2015), with slight variations in the wavelength of the absorption maximum caused by the size or aggregation level of the CuNPs (Cao, Tran *et al.* 2015). By monitoring the absorbance of each wavelength in the visible spectrum at different time periods, it is possible to reveal the rate of synthesis of CuNPs.

Cultures containing 350 ml of *M. psychrotolerans* were grown for 24 hours and concentrated by centrifugation at 4,500 x g for 15 min to 10 ml. After concentration, $CuSO_4$ was added to a final concentration of 5 mM. For each time point a sample was taken from the culture and the cells were removed by centrifugation followed by filtration. Following addition of $CuSO_4$, there is an immediate rise in absorbance at the wavelengths between 600 and 620 nm with a maximum absorbance at 617 nm which was caused by the presence of Cu ions (Figure 3.14). Throughout the two hours of incubation this peak in absorbance decreased to approximately half its original value. During the following 10 hours of incubation the absorbance increased gradually. However the absorbance maxima shifted to a slightly lower absorbance over that time, going from 617 nm at T=0 down to 602 nm at T=12 h. Figure 3.15 shows the absorbance over the course of the assay for the wavelength at 602 nm, which is indicative of the presence of CuNPs.

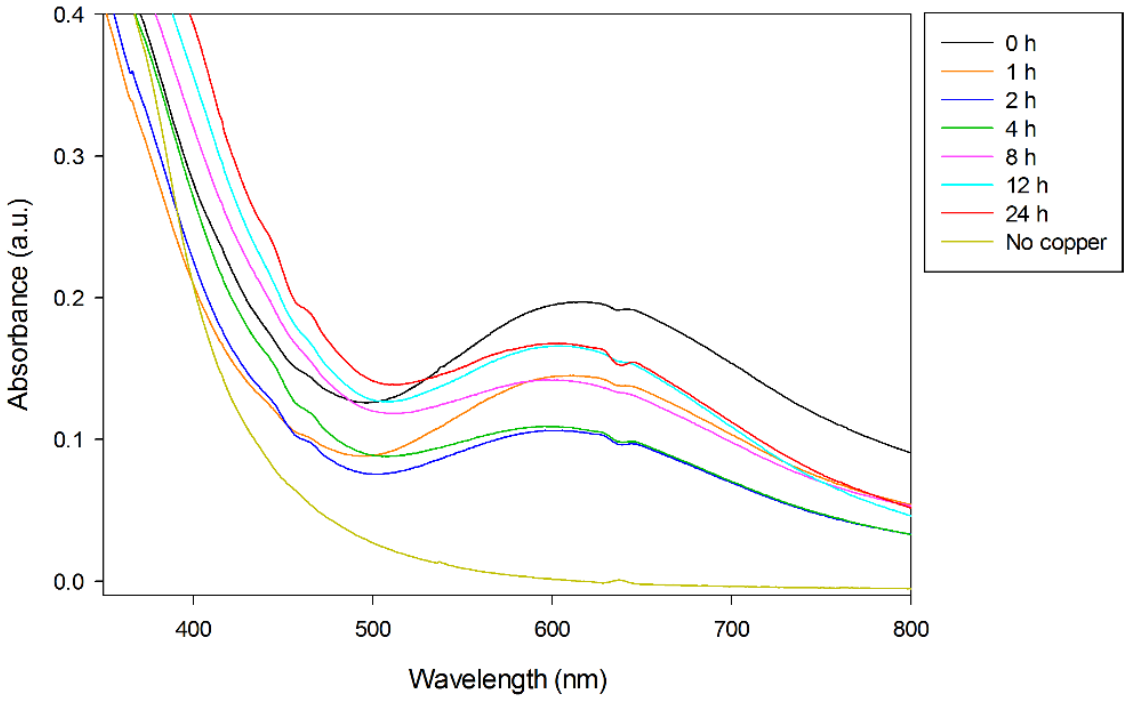

Figure 3.14: UV-Vis spectrum of CuNPs

UV-Vis spectrum of CuNPs being synthesised of a 24 hour time period.

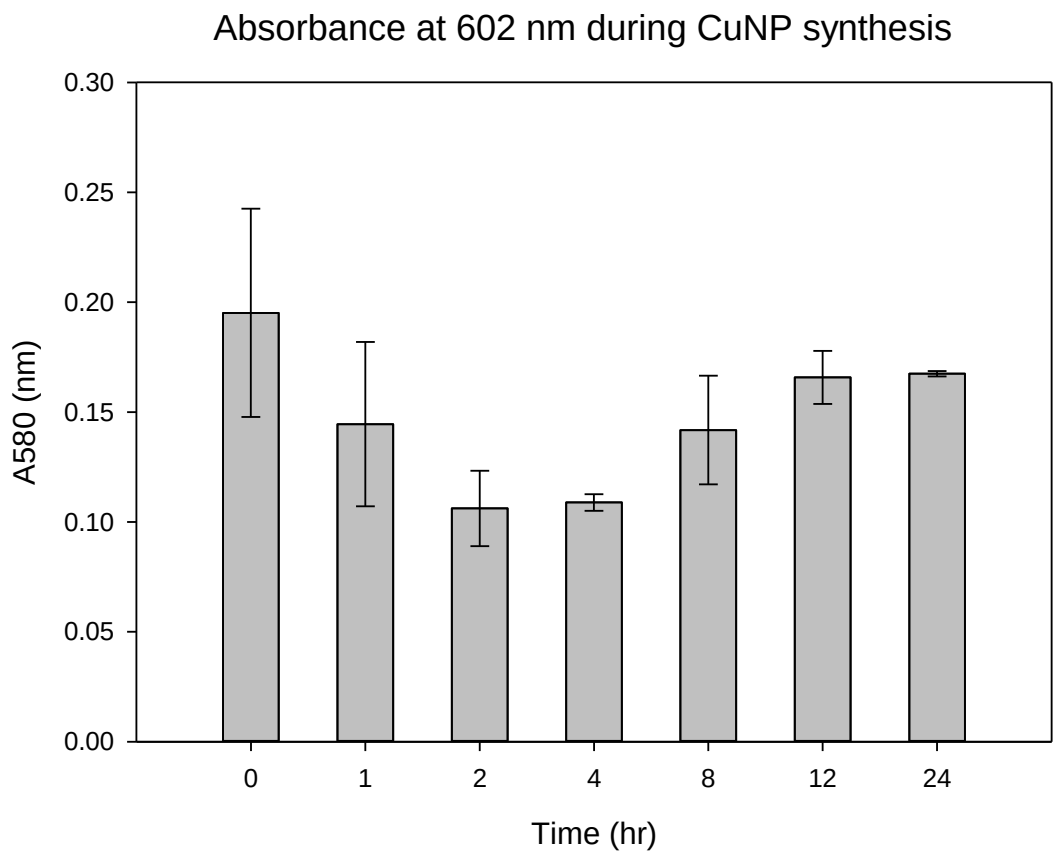

Figure 3.15: Absorbance of CuNPs at 580 nm over a 24 hour period

The absorbance value drops in the first two hours of incubation and then it rises gradually and stabilises after approximately 12 hours of incubation at 20^{o}C. The initial rise in absorbance is caused by Cu^{2+} interference which then is overcome as it is internalised into the cells and converted into CuNPs.

3.10 Aerobic vs anaerobic synthesis of CuNPs

CuNPs have the potential to be used as effective catalysts for CO_2 reduction to create hydrocarbon fuels (Alves, Silva *et al.* 2015). However they are prone to oxidation in the presence of an oxygen containing environment (Baco-Carles, Datas *et al.* 2011). Anaerobic synthesis of CuNPs may enhance the production yield and reduce oxidation or re-ionisation of newly synthesised CuNPs. Since *M. psychrotolerans* is a facultative anaerobe, the next step was to test its potential to synthesise CuNPs under anaerobic conditions.

M. psychrotolerans was grown aerobically as previously described. After 24 hours the culture was transferred into the anaerobic chamber and let to stand for one hour for the remaining oxygen dissolved in the culture to escape. A deoxygenated stock of $CuSO_4$ was used to make a final concentration of 5 mM $CuSO_4$ in the culture. The culture was mixed and incubated for 24 hours in the chamber. It was vortexed every 2 hours to ensure even mixing and prevent settling of cells to the bottom of the flask.

At the same time as the anaerobic culture was incubating with $CuSO_4$, an aerobic culture was also set up and $CuSO_4$ was added to it to a final concentration of 5 mM. The culture in this case was left to incubate in a static incubator in order to keep conditions comparable to the culture in the anaerobic chamber.

Both the anaerobic and aerobic cultures changed colour from blue to green over time. After 24 hours of incubation they were centrifuged at 4,500 x g for 15 min to remove bacterial cells and filtered to remove any remaining bacteria and large debris. The supernatant was then loaded onto a copper grid and used for TEM. In both cases nanoparticles were observed (Figure 3.16).

In aerobic conditions the nanoparticles produced were similar to those produced previously, being amorphous in shape and with sizes ranging between 7-60 nm in diameter. The average diameter of nanoparticles observed was 23 nm, similar to the diameter of 26 nm of the nanoparticles synthesised aerobically with shaking. The distribution of sizes was also similar to that of nanoparticles produced while shaking (Figure 3.17).

M. psychrotolerans also synthesised CuNPs under anaerobic conditions as seen in Figure 15b. Although synthesis occurred in both aerobic and anaerobic conditions, the nanoparticles produced have different sizes. The average size of the anaerobically synthesised nanoparticles was approximately half the size of the nanoparticles synthesised in aerobic conditions (Figure 3.17). The diameter distribution of the anaerobically synthesised nanoparticles was also smaller, 4-19 nm, compared to the aerobic ones with a range of 4-59 nm. They also had a decreased contrast when viewed by TEM (compared to the background carbon film that was coating the grid) due to their smaller size. The shape of the anaerobically synthesised nanoparticles is more amorphous than their aerobically made counterparts that have a more circular shape.

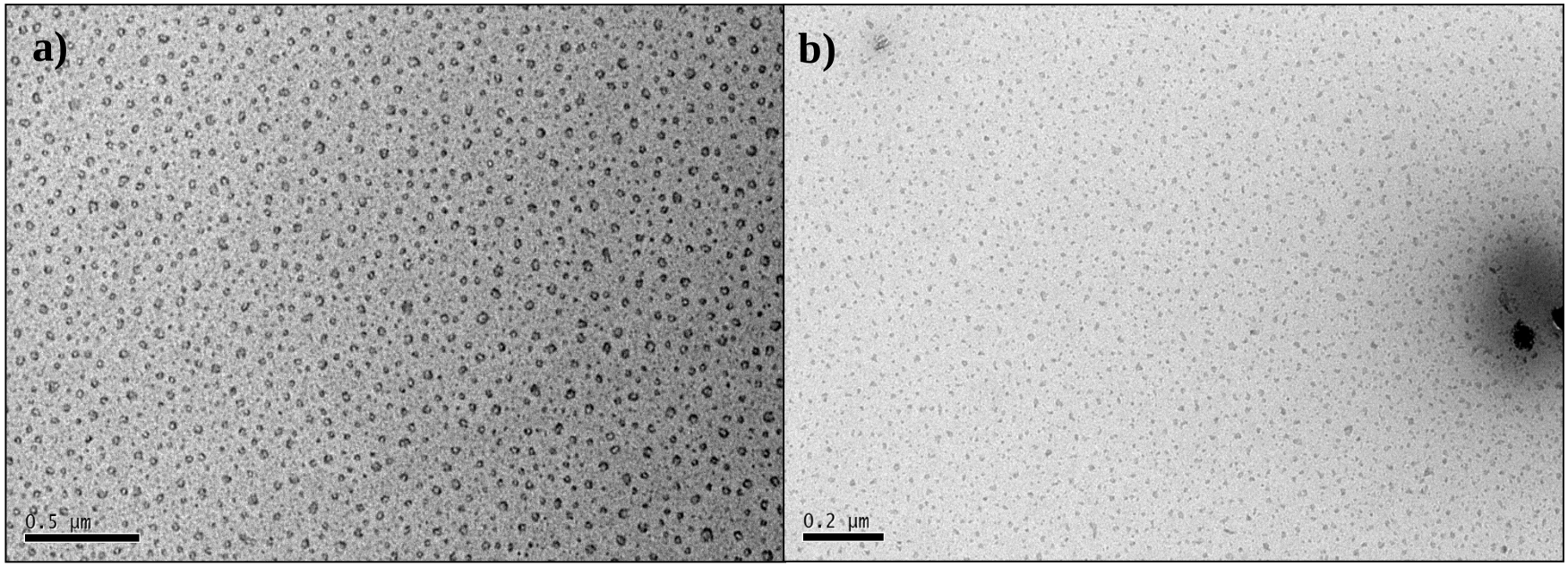

Figure 3.16: TEM of CuNPs synthesised aerobically and anaerobically

TEM pictures illustrate the presence and shape of the CuNPs synthesised after 24 hours of incubation in a) aerobic and b) anaerobic conditions.

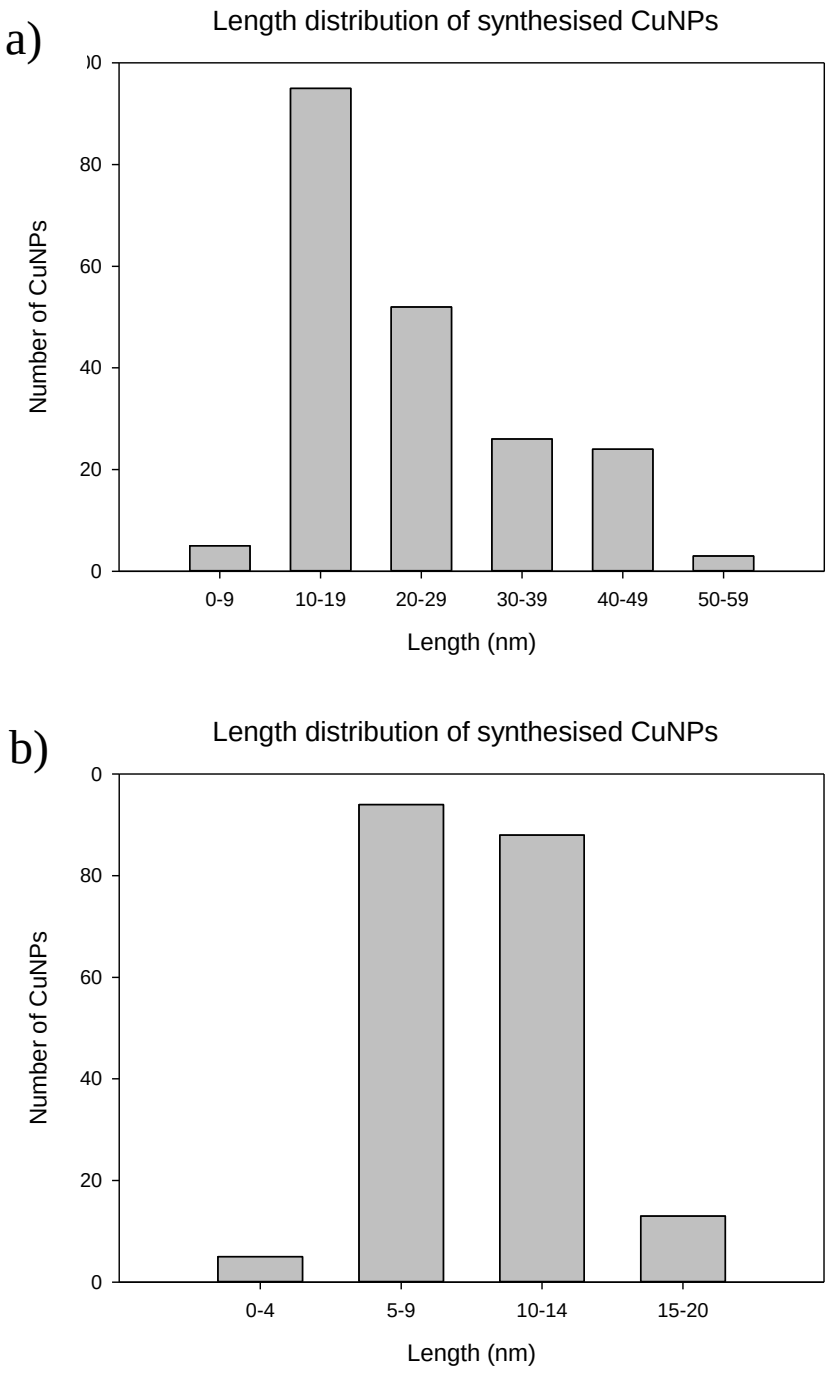

Figure 3.17: Size distribution of CuNPs synthesised in aerobic and anaerobic conditions

Histogram charts showing the diameter distribution of CuNPs synthesised in a) aerobic and b) anaerobic conditions after 24 hours.

Another run was performed to test whether anaerobic conditions for nanoparticle synthesis had a more pronounced effect on the yield of CuNPs. *M. psychrotolerans* was grown for 24 hours and divided into 24 cultures. $CuSO_4$ was added to all the tubes, 12 tubes with 1 M $CuSO_4$ and 12 with 0.5 M $CuSO_4$. Six of the falcon tubes containing 1 M $CuSO_4$ and six containing 0.5 M $CuSO_4$ were centrifuged for 10 min at 3,300 x g to form a cell pellet. Triplicate samples were then placed under 4 different incubation conditions, (i) aerobic shaking, (ii) aerobic static, (iii) anaerobic shaking and (iv) anaerobic static. A control was also made of a sample containing the bacterial growth medium with 1.0 mM $CuSO_4$ and a second control which contained 0.5 mM $CuSO_4$ for each condition. After a 24 hour incubation in their respective conditions, the samples were centrifuged for 10 min at 3,300 x g and filtered to remove the bacteria.

As seen in Figure 3.18, the anaerobic conditions for nanoparticle synthesis were more effective. Percentages were worked out by comparing the Cu ion concentrations to the controls containing 1.0 and 0.5 mM $CuSO_4$ respectively. There was a 35.4% reduction in Cu^{2+} under anaerobic shaking conditions for the 1 mM $CuSO_4$ samples compared to 3.1% reduction observed under aerobic shaking. Compared to previous results earlier in this chapter where no significant removal was observed, the Cu ion removal efficiency is much higher using this method. For the same aerobic and anaerobic conditions but with 0.5M $CuSO_4$, shaking at 200 rpm showed the most effective removal of Cu^{2+} compared to static conditions. When the initial $CuSO_4$ concentration was 0.5 mM, the removal of Cu^{2+} under anaerobic shaking conditions was 27.1%. Anaerobic conditions clearly favoured Cu^{2+} removal compared to aerobic conditions for both concentrations of $CuSO_4$ examined.

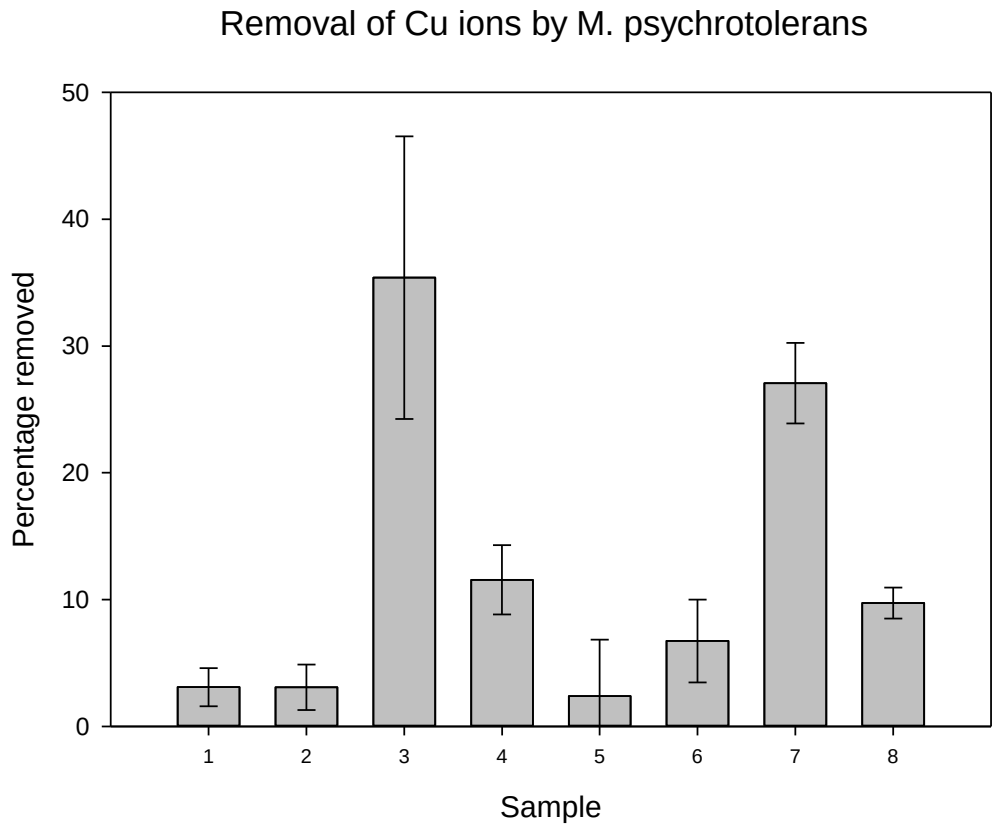

Figure 3.18: Conversion efficiency of Cu ions into CuNPs by *M. psychrotolerans* in different conditions

Bar chart showing concentrations of Cu^{2+} converted into CuNPs using *M. psychrotolerans* in various conditions. 1) aerobic shaking 1 mM, 2) aerobic static 1 mM, 3) anaerobic shaking 1 mM, 4) anaerobic static 1mM, 5) aerobic shaking 0.5 mM, 6) aerobic static 0.5 mM, 7) anaerobic shaking 0.5 mM, 8) anaerobic static 0.5 mM.

3.11 Extracellular synthesis of CuNPs

Very little was known prior to this study about the mechanism of CuNP synthesis by *M. psychrotolerans*. Ramanathan *et al.* suggested that the CuNPs are synthesised in the cytoplasm and exported outside the cell using the *Cus* efflux system (Ramanathan, Field *et al.* 2013). However this method does not account for the larger sized nanoparticles found extracellularly as the efflux pump is too small. An alternative hypothesis would be that Cu^{2+} is converted into Cu^{+} in the cytoplasm of the cells, and gets exported outside the cell where it then chemically disproportionates to form Cu^{0} and Cu^{2+} due to the lack of ligands stabilising the Cu^{+} ions. Bathocuproinedisulfonic acid (BCS) binds specifically to Cu^{+}. Therefore a BCS assay can be used to detect the presence of Cu^{+} ions in the culture supernatant after addition of Cu^{2+}.

A *M.* psychrotolerans culture grown for 24 hours was added to a 96-well plate and mixed with BCS. $CuSO_4$, at different concentrations, was added to the wells containing the cultures, mixed by shaking at 300 rpm for 10 seconds and incubated at 25ºC for 5 minutes (Figure 3.19). The absorbance was then taken at 480 nm. Immediately after the addition of the Cu ions, the colour of the wells changed to rusty red, indicating the presence of Cu^{+} ions in the medium. Rows 2-6 contained increasing concentrations of $CuSO_4$ and hence the colour of the medium appeared to be increasingly rusty red in colour due to the higher concentration of Cu^{+} present. Controls (rows 7 and 8) that contained only the medium and $CuSO_4$ or $CuCl_2$ did not show any significant change in colour, although there was still a slight absorbance rise. Wells in row 9 contained an overnight culture of *M. psychrotolerans* with no Cu ions added and it did not show a rise in absorbance after the addition of BCS. Therefore the colour change demonstrated that Cu^{+} was present in the supernatant and must have been produced by *M. psychrotolerans*. This strongly suggests that *M. psychrotolerans* converts Cu^{2+} ions into Cu^{+}, exports them into the supernatant where the Cu^{+} disproportionates to form Cu^{2+} and Cu^{0}, Cu^{0} being in the CuNP form. The reason why Cu^{+} might not disproportionate inside the cell is due to the presence of ligands that bind to it making it more stable. Outside the cell however the absence of ligands means the ions are less stable and hence disproportionate to form more stable forms.

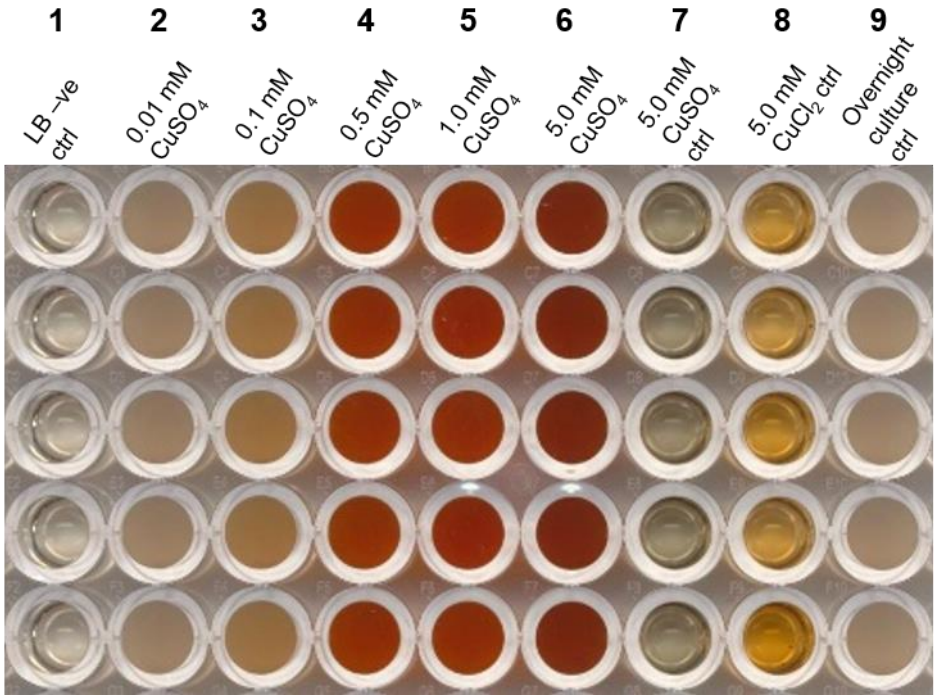

Figure 3.19: BCS assay for the detection of Cu^+

A 96-well plate assay that shows the colour change that occurred after addition of $CuSO_4$ to an overnight culture of *M. psychrotolerans*. The colour change occurred over the course of 5 minutes at 25°C.

3.12 Mass spectrometry of nanoparticles

CuNPs synthesised by *M. psychrotolerans* are stable for extended periods of time. This is important as CuNPs, due to their small size and unique chemical properties, are unstable and therefore oxidise to form CuO (Pantidos and Horsfall 2014). In some cases synthesised metallic nanoparticles have compounds added to them such as humic acids, fulvic acids, ascorbate, cysteine and oleic acid to keep them stable (Gunsolus, Mousavi *et al.* 2015; Jang, Jacobs *et al.* 2015).

The factor that keeps the CuNPs stable when synthesised by *M. psychrotolerans* is unknown, and thought to be released by the organism. Therefore matrix-assisted laser desorption/ionisation mass spectrometry (MALDI-MS) was used in order to identify it. CuNPs were synthesised and purified using the process for purified nanoparticles described previously in the materials and methods section. Since little information was known about the hypothesised stabilisation compound, a wide spectrum scan was performed using MALDI. Figure 3.20 shows the spectrum obtained from the purified CuNPs. The spectrum scan showed a distinct peak at 269 m/z which was of much higher intensity. Further analysis of the peak revealed it to be the matrix that the sample was mixed with (Figure 3.21). The matrix peak only appeared in the spectrum when copper was present and was therefore absent in the samples not containing copper nanoparticles. No other unique peak was obtained possibly due to failure to ionise the substance bound to the nanoparticles.

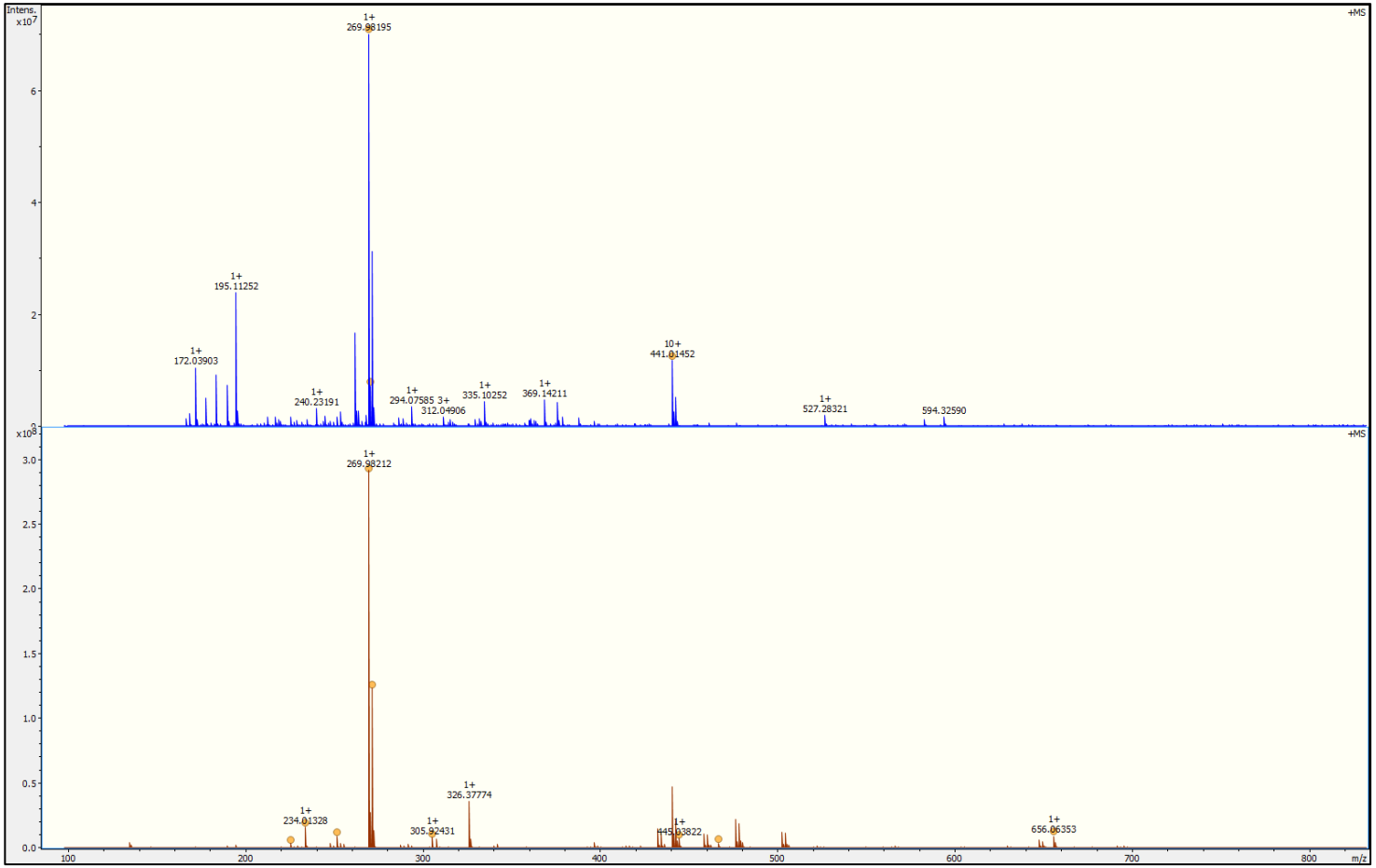

Figure 3.20: MALDI-MS wide spectrum scan of purified CuNPs

Wide spectrum scan of synthesised CuNPs. a) Run 1 and b) Run 2.

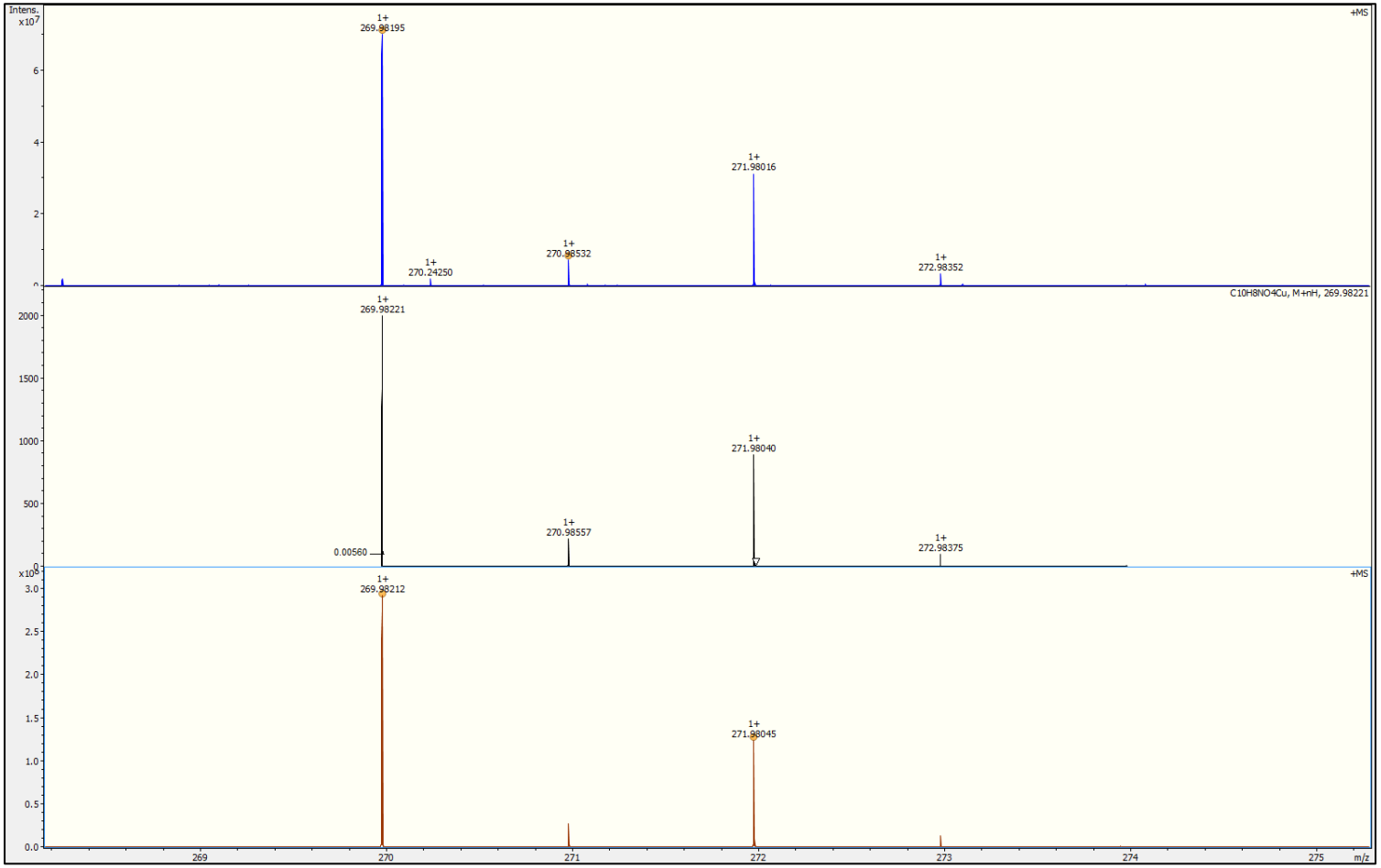

Figure 3.21: MALDI-MS narrow spectrum scan

MALDI-MS narrow spectrum scan focused close to the peak at 269 m/z. a) Run 1, b) Simulated run with the matrix

3.13 Nanoparticle printing

A potential application for the biogenic CuNPs synthesised by *M. psychrotolerans* was investigated. Microelectronics is an emerging field and CuNPs are highly sought after for this purpose. Printed electronics may have uses in flexible radio frequency identification tags, flexible organic light emitting diodes (OLEDs) and e-paper (Li, Wu *et al.* 2005; Kang, Kim *et al.* 2010). CuNPs can be used to print small electronic circuits and electrodes using an inkjet printer (Chung, Hwang *et al.* 2015).

CuNPs were synthesised using the process described previously and purified using ultracentrifugation. The resulting pellet was resuspended in 1 ml of Analar H_2O in order to keep the medium as clean as possible. The nanoparticle sample (ink) was filtered through a 0.22 µm syringe filter to remove any particulates in order to prevent clogging of the printer head.

The CuNP printing and measurements were done in collaboration with Dr Adam Stokes and Dr Gerard Cummins from the Scottish Microelectronics Centre (SMC). The nanoparticles were printed onto a glass slide to form a square pattern (Figure 3.22). Due to a low concentration of nanoparticles as well as a problem with drying, they did not form a continuous stream of CuNPs. After a conductivity measurement of the square film, no current was detected on the printed slide. AFM was used to measure the thickness of the dried deposits and look for any sign of particulates. The edge of one of the printed features was randomly selected and an AFM scan was conducted over a 50 µm square. As shown in Figure 3.23a, the height of the ridge was measured to be 0.61 µm. The raised edge appeared to be smooth with no sign of it being formed from sintered particulates. Another region within the printed area was randomly selected. In this measurement the region selected was between two raised edges. The scan was conducted over a 20 µm square. As seen from Figure 3.23b, there are signs of particulates, mainly clustered around the bottom left hand corner. The maximum height of one of these particles is 67 nm.

The experiment was repeated by synthesising more nanoparticles. This time instead of using 12 ml of supernatant containing CuNPs, 72 ml were used. The supernatant was split into 6 ultracentrifuged tubes and the nanoparticles were pelleted via centrifugation at 4,500 x g over 15 min. One of the pellets was resuspended in 500 ml

of H_2O and then transferred to all the other pellets to resuspend them in the same sample. The end sample contained 500 µl of H_2O and nanoparticles pelleted from 72 ml of supernatant, therefore 6 times concentrated. The nanoparticles were then printed again on a slide. The printing was performed 10 times and then 5 more times after rotating the slide 90 degrees. The final printed area was 1 cm^2 which was easily visible with the naked eye. Figure 3.24a shows a close-up image of the printed square where the printing lines are visible. The colour of the printed square was reddish brown, which was to be expected as it was made of CuNPs, fused together via sintering, to create this square. Compared to previous images the presence of particulates was more discernible and widespread. AFM scans of the randomly selected area were conducted over a 20 µm and 5 µm square (Figures 3.25). Electrical conductivity was checked using a multimetre, however no conductivity was detected due to insufficient sensitivity.

More accurate electrical conductivity readings were taken using an electrical probe station. Initial measurement showed resistance in the region of gigaOhms. A series of logarithmic voltage sweeps were carried out on the sample, in order to confirm that it was conducting. The voltage was initially swept up from the starting voltage and then once it reached the maximum voltage it was swept back to the original point. This double voltage sweep was done to determine whether hysteretic or any other non-linear characteristics are observable with this material. Initial sweeps were done with the probes situated close to the edge of the printed square and no hold or delay in measurements. These measurements showed hysteresis between the upward voltage sweep and downward sweep. The hold and delay times of the measurements were increased up to 1 second to see whether the hysteresis was due to some transient effect; however hysteresis could still be observed at these settings. The curves in Figure 3.26 suggest that there is a clear relationship between current and voltage and hence electrical conductivity taking place. However the relationship does not abide to Ohm's law and therefore non-Ohmic conduction is observed to take place.

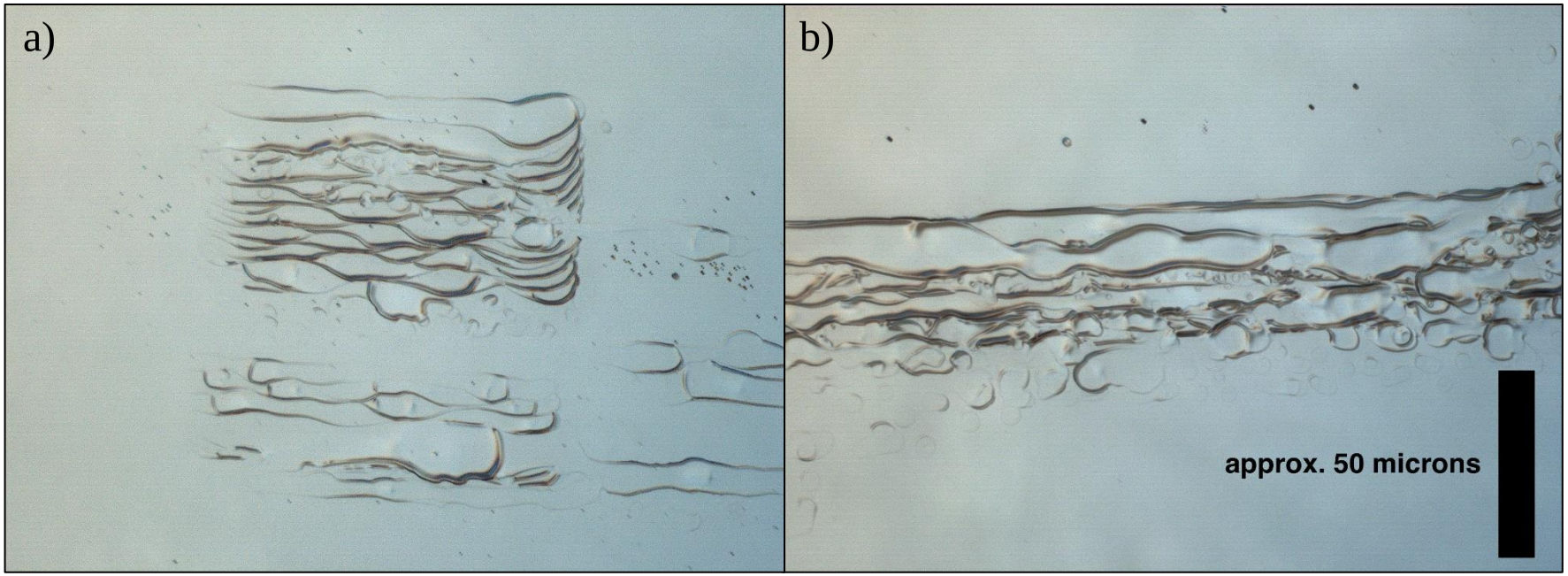

Figure 3.22: Printed CuNPs on glass microscope slides

Microscope pictures showing a) the printed CuNPs on a microscope slide at low magnification and b) at higher magnification.

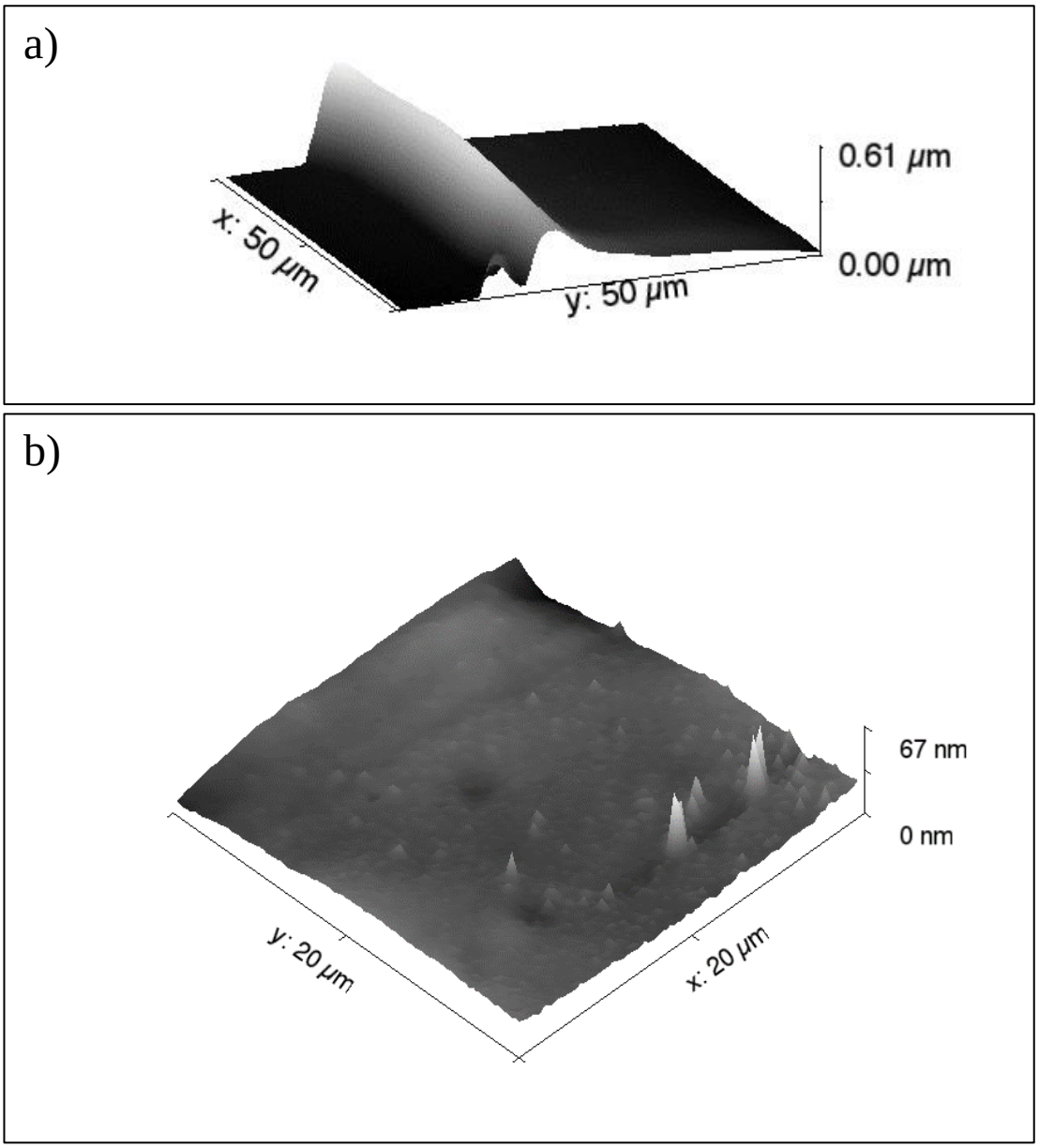

Figure 3.23: AFM scan of printed CuNPs

An AFM scan measuring the thickness of the printed nanoparticles. a) shows the first randomly scanned area with no particulates present, whilst b) another randomly chosen area contained particulates.

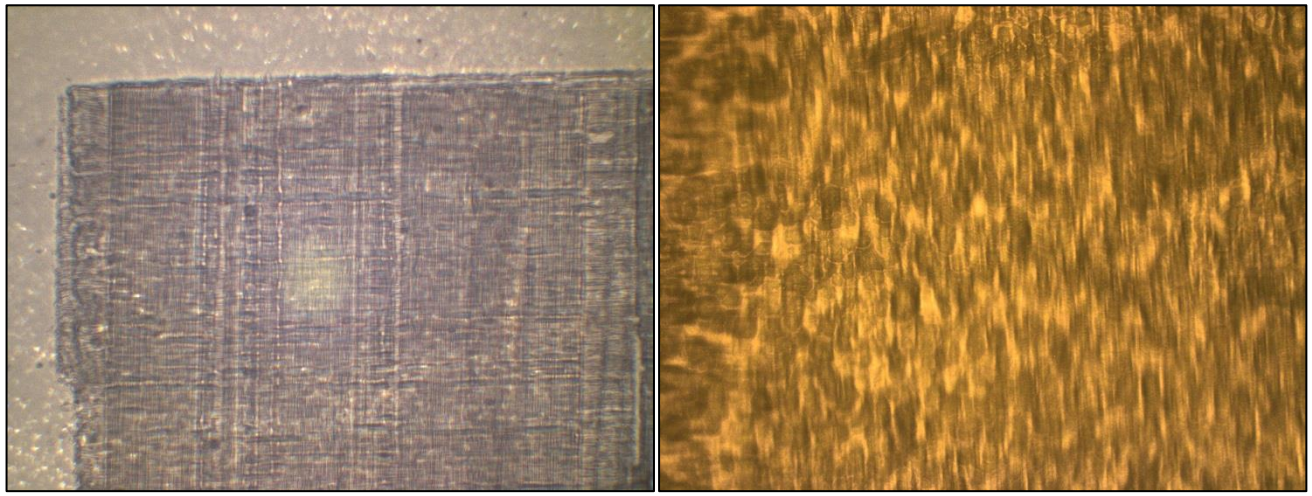

Figure 3.24: Microscope pictures of printed CuNPs post-sintering

Microscope pictures of the printed CuNP square after sintering. a) Shows a low magnification picture of the square and b) a higher magnification version of an area chosen in random within the square.

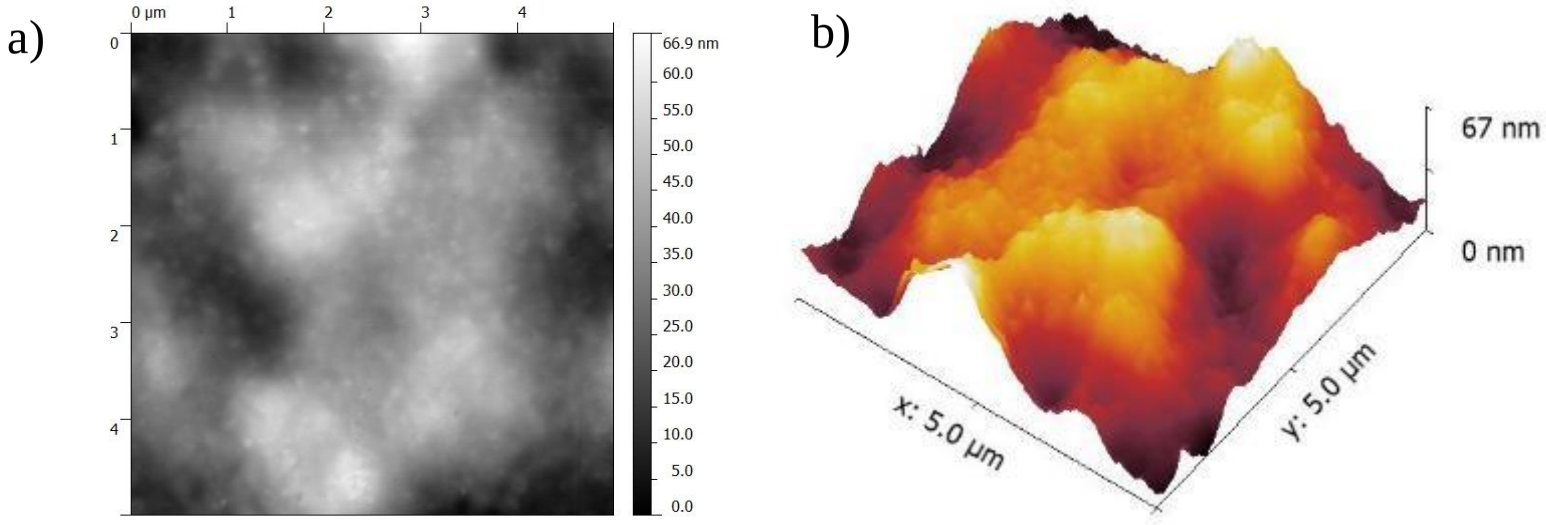

Figure 3.25: AFM scan of printed CuNPs

AFM scan of a randomly chosen area within the printed CuNP square sheet. A) shows the particulate representation of the chosen area in 2D and b) in 3D.

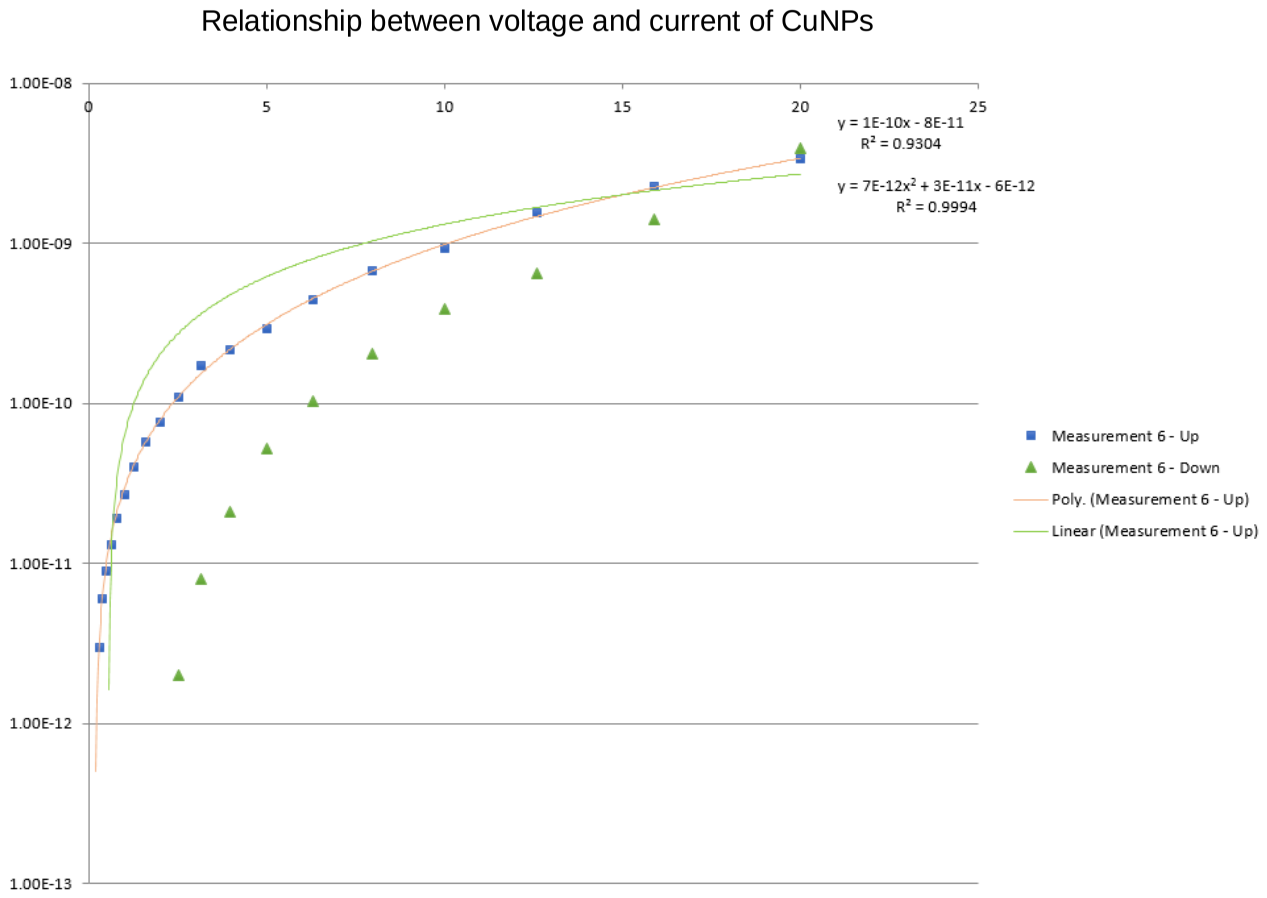

Figure 3.26: Relationship between voltage and current of CuNPs

Graph showing the relationship between the voltage and current in the slide containing the printed CuNPs.

3.14 *M. psychrotolerans* growth and CuNP synthesis in distillery co-products

The viability of *M. psychrotolerans* in whisky distillery co-products was assessed. The organism would need to be able to survive and grow in the co-products in order for it to convert Cu^{2+} into CuNPs. There have been no prior studies on this organism's viability in such media.

Pot ale (PA) and Spent Lees (SL) from the Glenkichie distillery were used as growth medium for *M. psychrotolerans*. The pH of both media was found to be very low (pH <4 on average). It was therefore raised using 5 M NaOH to pH 6.5, which is the pH of $LB_{ns,}$ in which *M. psychrotolerans* is known to grow well. Both PA and SL were inoculated with *M. psychrotolerans* and incubated for 24 hours at 20^{o}C. OD_{600} was checked after 24 hours of incubation. PA resulted in supporting a good level of growth for *M.* psychrotolerans as opposed to SL which did not show significant growth. This suggested that SL was not a good growth medium. This was expected as it consists mainly of water and impurities from the distillation process, and is therefore not sufficiently nutritious to support bacterial growth. PA on the other hand showed significant growth as it contained nutrients derived from dead yeast and unfermented carbohydrates.

SL contains the highest levels of ionic Cu which meant that *M. psychrotolerans* would preferably need to treat SL more than PA. Since the bacterium grew in PA but not SL, both media were mixed in a 1:1 ratio in order to provide the nutrients needed for growth from PA and the ionic Cu from SL that is needed to create the CuNPs. Another growth assay was performed by setting up cultures of PA, SL and PA:SL (1:1) and incubating at the same conditions as before. A measurement was taken after 24 hours and another one after 48 hours from the start of the assay. As shown in Figure 3.27, the 1:1 ratio of PA and SL showed significant growth. At the first 24 hours, growth in PA:SL was faster than PA alone. After 48 hours both PA and PA:SL had a similar $O.D._{600}$ suggesting both cultures reached stationary phase by then and were at a similar $O.D._{600}$.

Since the PA:SL medium worked well for growing *M. psychrotolerans*, a combination of ratios was made up, in order to find the optimum ratio of PA to SL for growth, in both solid and liquid versions of the media. Ratios ranging from 1:9 to 9:1 of PA:SL

were prepared and incubated at the same conditions as previously. The $O.D._{600}$ was measured after 24, 48, 72 and 96 hours as shown in Figure 3.28. The resulting graph shows that a ratio of 1:1 (PA:SL) and above for PA, does not affect the growth significantly. Growth is faster the more PA is present; further suggesting PA contains the nutrients for growth and survival of *M. psychrotolerans*.

The growth assay was then performed on the solid medium version. Agar at 3% was added to each ratio in order to solidify the medium. The pH was also corrected to 6.5 to allow for better growth conditions. Different dilutions of an overnight culture were prepared and 10 µl was spotted on the plates for each dilution. The plates were then incubated at 20^{o}C for 48 hours (Figure 3.29). No significant growth was observed after 24 hours of incubation; suggesting growth is staggered due to slower diffusion of nutrients towards the bacterium compared to the liquid medium version. A large difference was observed in the effect that PA:SL ratios had on the bacterium's growth. Optimum growth was observed at the 3:7 ratio with colonies being present even in the 10^{-6} dilution spot. The second best ratio for viability was observed at 2:8 with visible growth at a dilution factor of as low as 10^{-5}. This was in contrast to the liquid versions of the media where the lowest growth was observed at such ratios.

For nanoparticle synthesis, PA and SL were pH mixed together to make a 1:1 ratio. The pH was adjusted to match the LB_{ns} pH of 6.5 to allow for bacterial growth. *M. psychrotolerans* was inoculated in the medium and incubated for 24 hours at 20^{o}C in a shaking incubator. The bacteria and any precipitates were centrifuged down and the supernatant was filtered as mentioned in the nanoparticle synthesis protocol for non-purified CuNPs in the materials and methods. The filtrate was then spotted onto a copper grid and the nanoparticles were visualised in a Cryo-TEM. Figure 3.30 shows nanoparticles that were synthesised by *M. psychrotolerans* in distillery co-products. The nanoparticles showed different characteristics from the ones synthesised in LB_{ns}, having an irregular shape with distinct edges. The size of the nanoparticles was found to be between 3 and 6 nm wide and 9 to 22 nm in length.

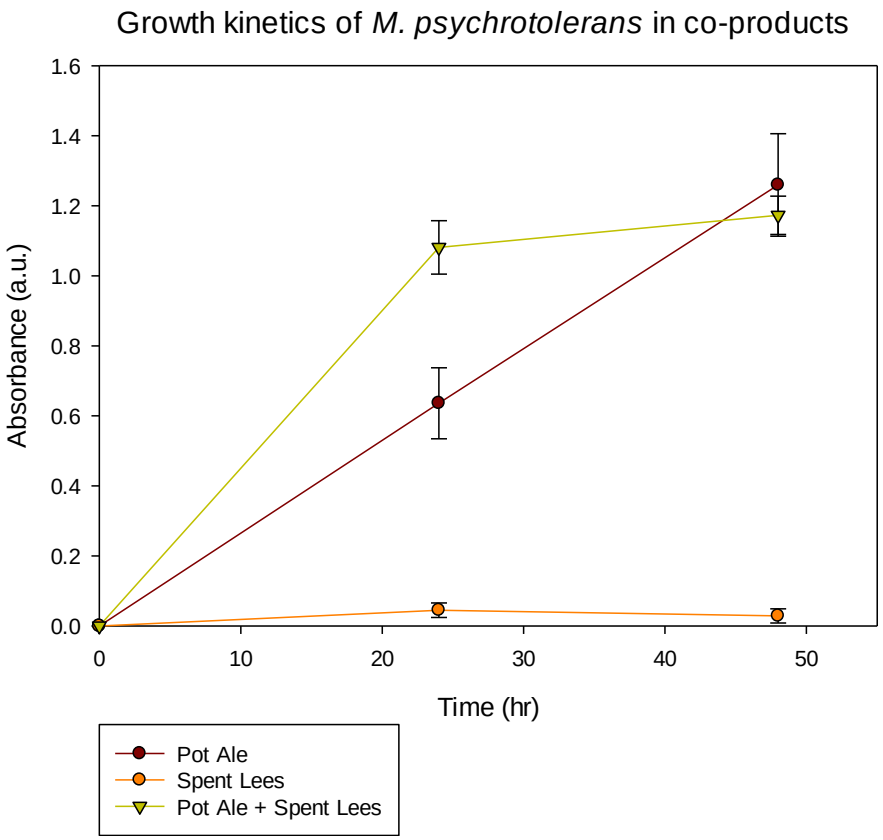

Figure 3.27: Growth kinetics of *M. psychrotolerans* in whisky distillery co-products

Growth kinetics of *M. psychrotolerans* in Pot Ale, Spent Lees and Pot Ale + Spent Lees combined in a 1:1 ratio.

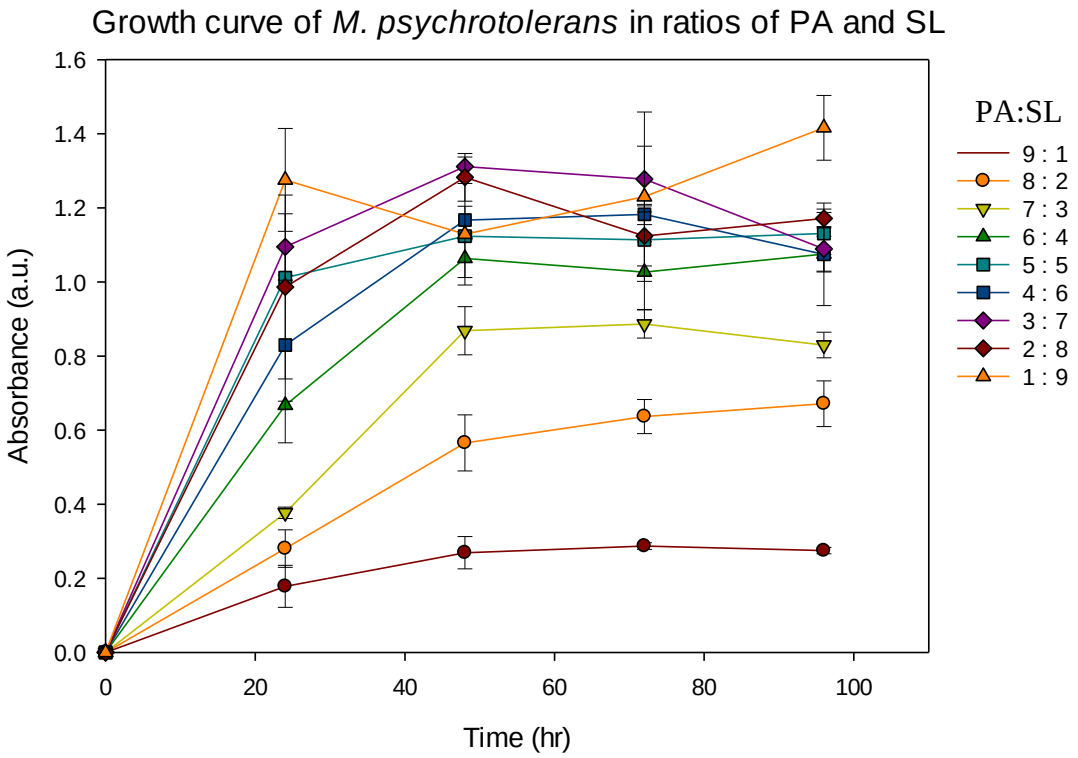

Figure 3.28: Growth curves of *M. psychrotolerans* in whisky distillery co-products

Graph showing the growth curves of *M. psychrotolerans* in Pot Ale and Spent Lees ratios. The curves were generated using a polynomial value of 2.

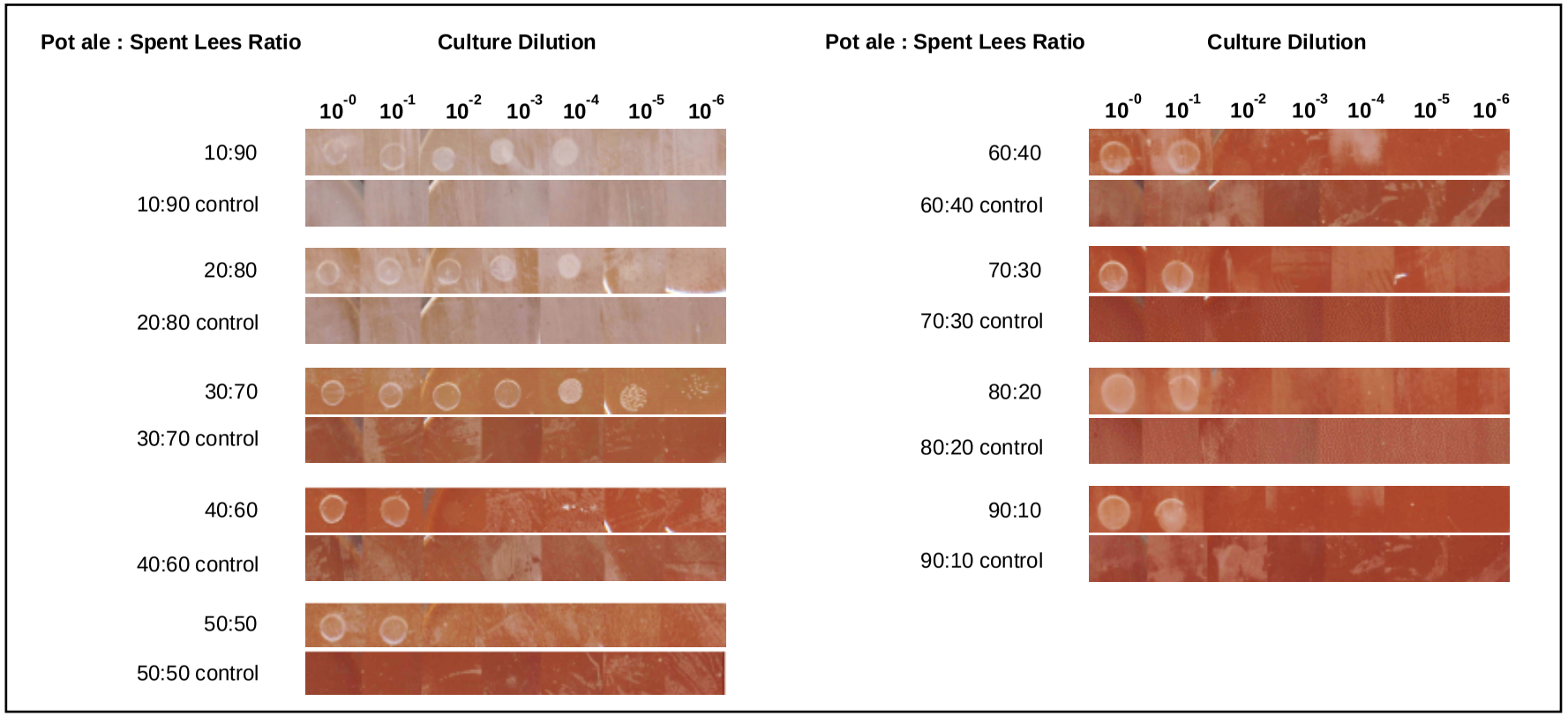

Figure 3.29: Growth assays for *M. psychrotolerans* in co-product agar media

Growth assay for *M. psychrotolerans* on different ratios of Pot Ale and Spent Lees on solid media. The controls contain no *M. psychrotolerans.*

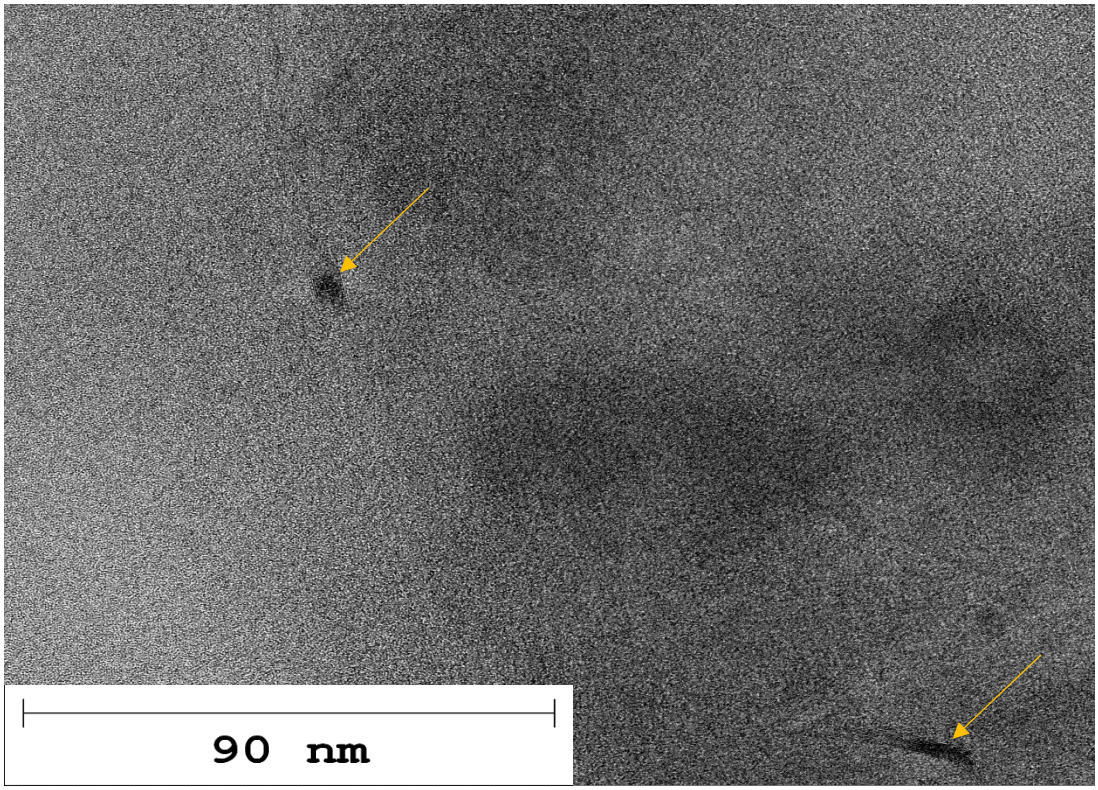

Figure 3.30: Cryo-TEM of CuNPs synthesised in whisky distillery co-products

Cryo-TEM picture illustrating two rod shaped nanoparticles synthesised by *M. psychrotolerans* in Pot Ale + Spent Lees medium.

3.15 Discussion

Synthesis of CuNPs was successfully performed by *M. psychrotolerans,* over the duration of incubation, in the presence of $CuSO_4$. It was hypothesised previously by Ramanathan *et al* (2010) that the colour change was due to the formation of CuNPs. This was shown not to be the case as the medium changes colour even without the presence of CuNPs. Adding $CuSO_4$ to a culture of *M.* psychrotolerans causes the medium to turn dark green in colour immediately after addition. This suggests that the bacterium released certain factors that affected the colour of the medium and thus is responsible for the colour change.

After CuNPs have been synthesised, there is a lot of material that needs to be removed from the solution in order to obtain a pure suspension of nanoparticles. Bacterial cells, cell debris and secondary metabolites all need to be removed. Therefore purification steps including centrifugation, filtration and subsequent ultracentrifugation were employed. The resulting suspension of CuNPs was a lot purer and more concentrated than the starting batch. The advantage of purifying is that the nanoparticles can be resuspended in any medium of our choice, such as water or a specific buffer for conducting various assays such as catalytic studies.

Very little was known about these nanoparticles prior to this study. In fact there had been only 6 studies on *M. psychrotolerans* specifically and only 3 of them focused on the production of nanoparticles using the bacterium (Emborg 2006; Emborg and Dalgaard 2008; Emborg and Dalgaard 2008; Parikh, Singh *et al.* 2008; Parikh, Ramanathan *et al.* 2011; Ramanathan, O'Mullane *et al.* 2011). Ramanathan *et al* (2010) studied the production of AgNPs by *M. psychrotolerans* and CuNPs made by *M. morganii* but neither of the studies went deep into the characterisation of the nanoparticles. An in-depth analysis of these biogenic nanoparticles revealed several characteristics of CuNPs synthesised by *M. psychrotolerans*. XPS results suggested that elemental copper was present which is similar to the findings that Ramanathan *et al.* (2013) obtained with *M. morganii.* Although the peaks observed were not at the correct binding energies due to calibration problems with the equipment, it was clear that the peak pattern corresponded to the presence of elemental copper. In order to verify this result with another experiment and ensure its validity, HR-TEM was used. By measuring the d-spacings of the nanoparticles, it was found that the nanoparticles

observed were made up of elemental copper. Similarly these results were also found with *M. morganii* (Ramanathan, Field *et al.* 2013), suggesting there is a similar nanoparticle production pathway present in both *M. psychrotolerans* and *M. morganii*. EDX spectra obtained via TEM also showed the presence of copper but no oxygen or sulphur further suggesting that elemental copper was present and it was not bound to any other element.

ICP-OES was employed to measure the conversion amount of $CuSO_4$ into CuNPs. Incubating *M. psychrotolerans* in the presence of $CuSO_4$ aerobically showed decreased nanoparticle production and therefore removal of Cu ions from the medium. When the organism was incubated in anaerobic conditions, the removal of Cu ions was more than 10x higher compared to aerobic conditions. Shaking incubation showed approximately 3x more Cu ion removal and therefore suggested that the nanoparticles were stable and not affected by physical forces. By taking these results into account the conclusion was that the process of CuNP synthesis is an anaerobic process and therefore does not require the presence of oxygen.

Zetasizer measurements were also performed to gather information on the electrical charge that the nanoparticles carry. The charge changed significantly depending on the type of buffer that they were diluted in. In all cases the charge was highly negative or positive, suggesting the nanoparticles are reactive in their respective media. A higher positive or negative charge means they can be used for applications such as antibacterials due to their reactivity (El Badawy, Silva *et al.* 2011). Although the Zetasizer can measure sizes of nanoparticles, it is not a true measurement due to the effect that the nanoparticles have on the solution immediately surrounding them. The charge may affect the hydrophobicity of the nanoparticles and the Zetasizer may measure the size of the nanoparticle including a "corona" made of solution surrounding it. Thus the size measured would be larger than the true size of the nanoparticle. Therefore TEM was used as a more effective method for measuring true particle size distributions.

A study by Sun *et al* (2014) suggested that due to their very small size, nanoparticles behave almost like a fluid rather than a solid on their surface. This gave rise to the hypothesis that nanoparticle shape might be controlled by varying the pH of the

suspension. Indeed it was found that by increasing the pH to 7.5 the CuNPs became a lot more uniform in size and shape and at pH 8.5 they formed long straight micrometre sized rods. This may make it possible to alter the shape of these nanoparticles to suit different uses in the future such as catalysts or optical devices, where one shape and size might be better suited than the other.

Oxidation of CuNPs is a major problem when they are synthesised using chemical methods (Pantidos and Horsfall 2014). This is because they are produced aerobically and copper tends to bind to oxygen fairly readily when in nanoparticle form. Although CuNPs produced by *M. psychrotolerans* are stable under aerobic conditions, the next step was to test whether it is able to synthesise them under anaerobic conditions in case oxidation becomes a problem. Nanoparticles were synthesised in this way but with some differences. The size of the anaerobically synthesised nanoparticles was half the size of their counterparts and the shape of the aerobic nanoparticles was a lot more uniform than the anaerobically made ones.

M. psychrotolerans was incubated for 24 hours in order to synthesise the CuNPs. It was unclear how long the nanoparticle synthesis process takes in the presence of Cu ions. Therefore a synthesis kinetics assay was performed which confirmed that incubation for longer than 24 hours with $CuSO_4$ present is not needed as the synthesis of nanoparticles stops after this time. UV-Vis showed a visible peak at approximately 610 nm immediately after the addition of the $CuSO_4$. This was attributed to the fact that $CuSO_4$ itself absorbs light at that wavelength which is in fact at a similar wavelength to the CuNPs. Due to surface plasmon resonance, CuNPs exhibit non-linear optical properties at therefore absorb light at around wavelength around 600 nm. During incubation time, the peak started to decrease which suggested that the $CuSO_4$ was being internalised into the bacterial cells. After 4 hours of incubation the peak shifted to a lower wavelength <600 nm which is known from the literature to correspond with the presence of CuNPs (Thi My Dung, Thi Tuyet Thu *et al.* 2011). Although not all of the $CuSO_4$ had been converted into CuNPs after a 24 hour incubation period, the experiment gave a good indication on when to stop the synthesis process and hence increase productivity of nanoparticles, which is important in industrial applications.

The study provided insight into the mechanism of production of CuNPs by *M. psychrotolerans*. A hypothesised mechanism had been suggested previously by Ramanathan *et al* (2010), however the results of this study do not support the published hypothesis and therefore we propose an alternative. The literature suggests the nanoparticles are formed intracellularly and then exported out of the cell. This however is not possible due to the size of the nanoparticles needing to be exported. A more realistic method would be that they are formed extracellularly or very near the surface of the cell membrane. *M. psychrotolerans* contains proteins that reduce Cu^{2+} into Cu^{+} - discussed in later chapters - however no proteins have been found thus far that convert Cu^{2+} or Cu^{+} into Cu^{0}. Furthermore Cu^{+} is unstable if it is not bound to a ligand, therefore it is likely that Cu^{+} is produced intracellularly and subsequently exported outside the cell. There Cu^{+} disproportionates due to its instability to form Cu^{2+} and Cu^{0} (Greenwood and Earnshaw 1997). The Cu^{2+} goes back inside the cell and gets converted again, eventually shifting the equilibrium towards the Cu^{0} side, thus reducing the levels of Cu^{2+} in the solution but increasing the Cu^{0} levels as it is stable. This hypothesis was strongly supported by this study as high levels of Cu^{+} where seen in the supernatant when incubating *M. psychrotolerans* with $CuSO_4$.

The CuNPs produced in this study by *M. psychrotolerans* are stable compared to their chemically produced counterparts that oxidise rapidly post-production (Baco-Carles, Datas *et al.* 2011). In the case of *M. morganii* there is a protective coating surrounding the nanoparticles keeping them stable (Ramanathan, Field *et al.* 2013). This theory was also considered for the nanoparticles produced by *M. psychrotolerans*. MALDI-MS was used to identify any presence of a compound associated with the biologically synthesised CuNPs. No unique compound derived from the samples containing the CuNPs was found, after numerous attempts to identify it. This may be due to the low concentrations of nanoparticles after the washing steps, or due to failure to ionise the compound capping the nanoparticles. It may also be possible that capping compounds are not be tightly bound to the nanoparticles and therefore could get easily detached through the washing steps.

CuNPs can be used in many applications such as optics, catalysts, antimicrobials and microelectronics (Pantidos and Horsfall 2014). The latter application involves the printing of electrical circuits using biologically derived nanoparticles. This study

explored the printing of CuNPs synthesised by *M. psychrotolerans* to form conductive electrodes. Stable printing was achieved along with a positive result for electrical conductance. However the resistance was relatively high which might indicate the presence of impurities or the partial oxidation of the electrode due to the sintering process after printing. Sintering is an essential part of the printing process in order to fuse the nanoparticles together to form a continuous conductive film, however it may be limited due to oxidation from the high temperatures subjected. If sintering occurs under anoxic conditions it will prevent the oxidation of the nanoparticles, however any biological stabilising capping agent will be removed, making the copper film sensitive to oxidation post-sintering. Non-ohmic conduction was observed for the printed electrode, possibly due to presence of impurities. The purification process of the nanoparticles, as well as the printing and sintering method, needs more optimisation in the future to overcome this problem. However as electrical conductance was present, it meant that the development of a cheap and efficient method for synthesising CuNPs for printing electrical circuits was one step closer.

Whisky distillery co-products including pot ale and spent lees contain relatively high levels of ionic Cu. Due to limitations in the treatment process of these co-products, greener and cheaper alternative methods are being researched to replace them or implement them in tandem with the existing ones. In this study *M. psychrotolerans* was incubated in pot ale, spent lees and a combination of both co-products. The results obtained showed good growth in pot ale and equally as good when both co-products were combined in certain ratios. This was an important finding as spent lees, which has the higher levels of ionic copper present, needs to be treated, but the bacterium does not grow in it since it is not nutritious. By combining both co-products it means that both of them are being treated simultaneously in the same batch, potentially saving time and cost. The concentration of copper present in the co-products does not inhibit its growth even at the highest levels measured. By observing the supernatant under TEM, CuNPs were observed which suggests that *M. psychrotolerans* may be used as a treatment method for such co-products.

Chapter 4. Genetic Analysis of *M. psychrotolerans*

4.1 Introduction

The availability of complete genome sequences opens up a whole new range of research possibilities. The genome of *M. psychrotolerans* however has not been sequenced prior to this study. A small number of studies on this organism have been published on its characteristics and its ability to synthesise AgNPs (Emborg 2006; Ramanathan, O'Mullane *et al.* 2011), however no information exists on CuNP synthesis by *M. psychrotolerans*. Similarly, methods for AgNP synthesis have been developed using this organism, but no methods for CuNP synthesis have been described. Any genetic analysis of this organism was not possible prior to its sequencing. Pathways, such as copper resistance gene clusters or histamine formation, were unidentified in this organism. A complete genome is crucial if gene manipulation is to take place in order to improve the CuNP synthesis potential. Native plasmids that might exist in an organism are also very important as they may carry key genes for several pathways that could be of interest towards CuNP synthesis or stability.

There are several studies on the related organism *M. morganii* which delve into its characteristics, as well as its use of CuNP synthesis (Parikh, Ramanathan *et al.* 2011; Ramanathan, Field *et al.* 2013). A bioinformatics study by Ramanathan *et al.*, suggested a pathway that *M. morganii* may use to synthesise Ag and Cu nanoparticles. However there was no experimentation performed on the described pathway to confirm the hypothesis.

In this study, the complete genome of *M. psychrotolerans* was sequenced and annotated. Analysis of the sequence revealed information that heavily contributed towards the direction of the study. Copper resistance genes and possible CuNP synthesis pathways were identified. Using the genome sequence it was possible to compare this organism to other organisms that perform similar actions under heavy metal stress. *M. psychrotolerans* was compared to *Escherichia coli*, *M. morganii* and other bacteria that also produce metallic nanoparticles in the presence of their ionic counterparts (El-Shanshoury, ElSilk *et al.* 2011; Parikh, Ramanathan *et al.* 2011).

4.2 16S rDNA sequencing of *M. psychrotolerans*

The strain *M. psychrotolerans* U2/3 was ordered from the Leibniz Institute DSMZ German Collection of Microorganisms and Cell Cultures. The organism was revived and glycerol stocks were created using the ampule delivered. Prior to performing whole genome sequencing of the organism, it was essential to ensure that the organism present was indeed the chosen organism. 16S rDNA sequencing was performed using universal primers. The primers chosen were 8F and 1391R in order to get a sequence product that resembled a large part of the gene for more accurate comparison with other organisms (Turner, Pryer *et al.* 1999). The final product size generated using these primers was 1,373 bp long. Two sequencing batches were used, each with a separate primer in order to get the 5' and the 3' sequence and join them together. The result was an assembled sequence of 1,117 bp (Figure 4.1).

The 16S sequence was entered into BLAST the bacterium confirmed as *M. psychrotolerans* U2/3. The sequence was compared to the 16S gene sequence obtained from the genome sequencing data for this organism. The 16S sequence had 100% sequence similarity to the strain U2/5. When compared to *E. coli* the percentage similarity was found to be 93% which was lower than other related organisms. This suggested that *M. psychrotolerans* is not closely related to *E. coli*.

Following the sequencing of the 16S gene and validating the strain of bacterium used, it was compared to other organisms within its genus as well as others. The bacteria chosen for comparison were based on the criteria of genus names and the environment that they are normally found in. Since *M. morganii* is in the same genus as *M. psychrotolerans* and shares a number of characteristics including heavy metal tolerance and nanoparticle formation, it was chosen for comparison. The strains *M. morganii* KT, VAR-06-2076, ZJB-09203, M11 and RP-42 were also chosen for comparison. *Proteus vulgaris* and *Providencia alcalifaciens* were also chosen due to their similar living environment as *M. morganii,* and *E. coli* was chosen as the outlier which is found in similar environments as *M. morganii*. Figure 4.2 shows the phylogenetic tree of these organisms and how related they are to each other.

The phylogenetic tree revealed the evolutionary pathway of *M. psychrotolerans* and it appeared to have evolved separately from the other *Morganella* species. It did not show a close relation to *P. vulgaris* or *E. coli* K-12 as it is shown to have evolved independently. It is worth noting that *P. vulgaris* is not very similar to *M. psychrotolerans*, however the results given later in this report in chapter 3, show that they contain the same plasmid with only minor differences in the sequence.

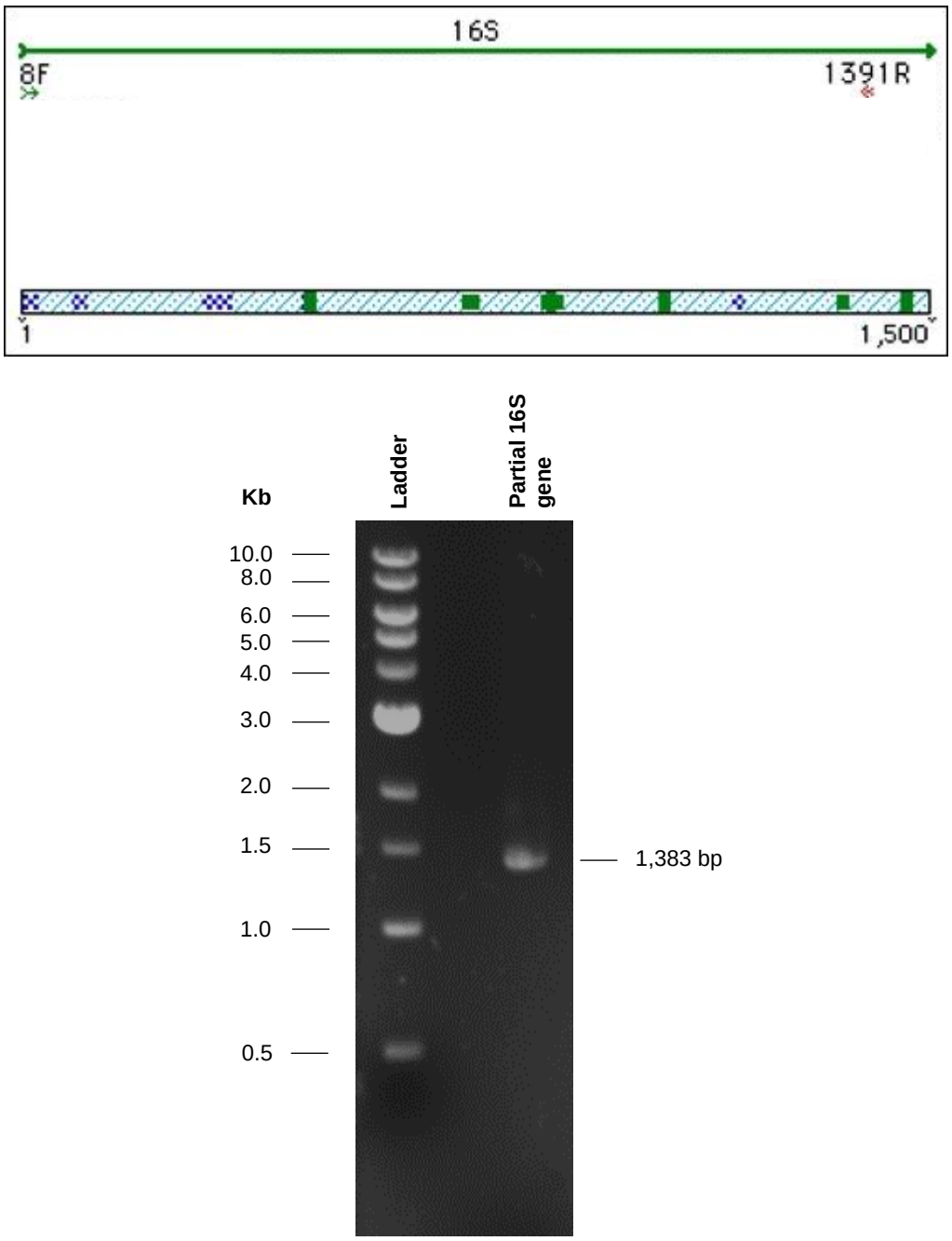

Figure 4.1: 16S sequencing primers and rDNA PCR product

The picture illustrates a) the two universal primers chosen for 16S rRNA sequencing and b) the 16S rDNA PCR product of the primers sent for sequencing.

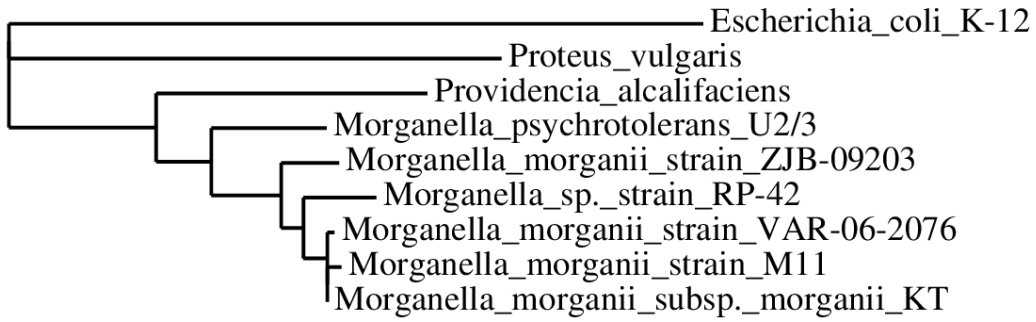

Figure 4.2: Phylogenetic tree of *M. psychrotolerans*

A Neighbour-joining phylogenetic tree of *M. psychrotolerans* and other related bacteria. *E. coli* was chosen as the outlier.

4.3 Genome extraction and sequencing

A culture of *M. psychrotolerans* U2/3 was grown overnight using the conditions described previously. The genomic DNA was extracted and quantified using a Nanodrop® in two separate procedures. The eluates containing the DNA had a concentration of 47 ng/µl and 68 ng/µl. Figure 4.3 shows a small sample of the two eluates run on an agarose gel to visualise their quality.

The genomic DNA sample containing the highest concentration of DNA was sent for Illumina sequencing. The genome sequence received was then annotated using RAST (Rapid Annotation using Subsystem Technology). The resulting file contained all the identified genes found in the genome along with their respective sequences. Although most of the genome was annotated, there were some genes left without annotation due to the lack of information about them in the literature or they were not a sufficient match to known genes. Hypothetical genes found to be in close proximity to copper resistance genes were labelled manually where sufficient information was available.

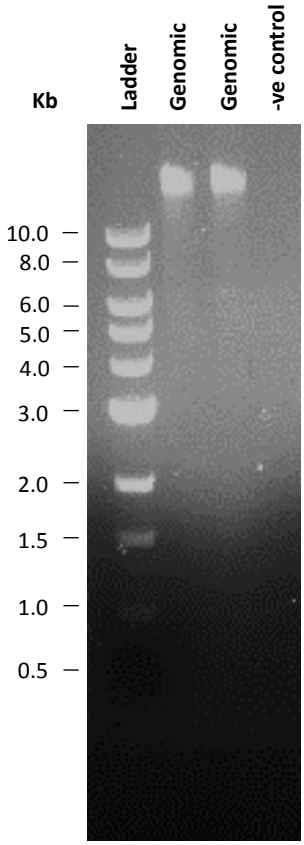

Figure 4.3: Genomic DNA of *M. psychrotolerans*

DNA agarose gel of two sets of genomic extractions (wells 2 & 3). Well 4 is the negative control not containing DNA.

4.4 Genome Characteristics

The genome sequencing data received from Edinburgh Genomics did not result in a completely assembled genome. The genome was assembled into 47 contigs as it was not possible to assemble it into a complete genome using software. Possible repetitive elements in the sequence may make it difficult to distinguish between new or already read sequence. Over 96% of the genome was assembled in the 11 largest contigs. The genome size was calculated to be 4.16 Mb and coded for a total of 4064 genes. The GC content was found to be 48% (Table 4.1). The quality of the sequence was good with only 1,900 nucleotides not accounted for and therefore replaced by N (any nucleotide) in the genome. *M. psychrotolerans* was also compared to the genome of *M. morganii* to see how related the two species are. Table 4.2 shows the main features of *M. morganii* KT strain. The genome size was 3.80 Mb and it had a GC content of 51%.

In order to get a deeper understanding of the genome of this organism, a codon bias table was created (Table 4.3). To generate this table, the 30 highest upregulated genes were chosen and their sequences compiled. The upregulated genes were chosen on the basis of the proteomics results that were obtained from the *M. psychrotolerans* proteome mass spectrometry performed with the KPF and are described later, in chapter 5. This method was chosen in order to create a codon bias table for increased gene expression and has been shown to be effective (Lanza, Curran *et al.* 2014).

Sequence Information		
Nucleotide	Count	Frequency
Adenine (A)	1,081,215	0.26
Cytosine (C)	1,001,819	0.241
Guanine (G)	1,000,581	0.24
Thymine (T)	1,077,909	0.259
C + G	2,002,400	0.481
A + T	2,159,124	0.519
Nucleotide Distribution Table		
Sequence type	DNA - Genomic	
Length		
Organism	*Morganella psychrotolerans*	
Weight (single-stranded)	1,286.229 MDa	
Weight (double-stranded)	2,572.478 MDa	
GC Content	48.10%	

Table 4.1: The table above shows the *M. psychrotolerans* genome information including size and nucleotide distribution.

Sequence Information		
Nucleotide	Count	Frequency
Adenine (A)	929,719	0.245
Cytosine (C)	972,787	0.256
Guanine (G)	970,276	0.255
Thymine (T)	926,752	0.244
C + G	1,943,063	0.511
A + T	1,856,471	0.489
Nucleotide Distribution Table		
Sequence type	DNA - Genomic	
Length	3,799,539 bp	
Organism	*Morganella morganii*	
Weight (single-stranded)	1,173.841 MDa	
Weight (double-stranded)	2,347.755 MDa	
GC Content	51.10%	

Table 4.2: The table above shows the *M. morganii* genome information including size and nucleotide distribution.

	U			C			A			G			
U	UUU	Phe	0.55	UCU	Ser	0.18	UAU	Tyr	0.60	UGU	Cys	0.50	U
	UUC	Phe	0.45	UCC	Ser	0.20	UAC	Tyr	0.40	UGC	Cys	0.50	C
	UUA	Leu	0.14	UCA	Ser	0.20	UAA	STOP	0.69	UGA	STOP	0.31	A
	UUG	Leu	0.07	UCG	Ser	0.06	UAG	STOP	0.00	UGG	Trp	1.00	G
C	CUU	Leu	0.09	CCU	Pro	0.11	CAU	His	0.57	CGU	Arg	0.43	U
	CUC	Leu	0.08	CCC	Pro	0.07	CAC	His	0.43	CGC	Arg	0.43	C
	CUA	Leu	0.01	CCA	Pro	0.09	CAA	Gln	0.22	CGA	Arg	0.01	A
	CUG	Leu	0.60	CCG	Pro	0.73	CAG	Gln	0.78	CGG	Arg	0.10	G
A	AUU	Ile	0.48	ACU	Thr	0.19	AAU	Asn	0.55	AGU	Ser	0.16	U
	AUC	Ile	0.46	ACC	Thr	0.43	AAC	Asn	0.45	AGC	Ser	0.20	C
	AUA	Ile	0.05	ACA	Thr	0.22	AAA	Lys	0.83	AGA	Arg	0.02	A
	AUG	Met	1.00	ACG	Thr	0.15	AAG	Lys	0.17	AGG	Arg	0.00	G
G	GUU	Val	0.29	GCU	Ala	0.17	GAU	Asp	0.64	GGU	Gly	0.45	U
	GUC	Val	0.25	GCC	Ala	0.24	GAC	Asp	0.36	GGC	Gly	0.30	C
	GUA	Val	0.14	GCA	Ala	0.32	GAA	Glu	0.74	GGA	Gly	0.12	A
	GUG	Val	0.32	GCG	Ala	0.27	GAG	Glu	0.26	GGG	Gly	0.13	G

Table 4.3: Codon bias of *M. psychrotolerans*. The numbers indicate the ratio of abundance of each codon in relation to all the other codons for that particular amino acid.

4.5 Copper resistance genes

It is important to note that *M. psychrotolerans* exhibits a significant resistance to Cu ions as well as converting these ions into solid CuNPs. The genes responsible for the production of these nanoparticles, as proposed in the literature, have been described previously in chapter 1. However, the results were based on an untested hypothesis. The results of this research strongly suggest that the mechanism of CuNP biosynthesis is not that which is currently described in the literature (Ramanathan, Field *et al.* 2013).

After the genome was partially assembled and annotated, all the annotated genes related to copper resistance and/or homeostasis were recorded. *M. psychrotolerans* contained 28 genes directly relating to copper regulation in the cell. The organism most closely related to the one used in this study is *M. morganii*, therefore the genes were compared to those found in that organism. 18 of these genes were found to exist in both *M. morganii* and *M. psychrotolerans*, and their similarity was compared on the protein level. There were 5 genes found in *M. psychrotolerans* but not in *M. morganii*.

The *Cus* cluster of genes was a target for study as it was reported to be involved in the production of nanoparticles in *M. morganii* (Ramanathan, Field *et al.* 2013). There are 7 genes involved in some way in this pathway, *CusA, CusB, CusC, CusF, CusR, CusS* and *SilE (*Ramanathan, Field *et al.* 2013*)*. All these genes were found to be next to each other in the *M. psychrotolerans* genome and therefore it is thought that they play a role in the synthesis pathway. These genes were compared to each of their homologues that are found in *M. morganii* to determine their relative similarity (Appendix 2). The homologues of *CusA, CusB, CusC, CusR, CusS* and *CtpA* were *SilA, SilB, SilC, SilR, SilS* and *SilP* respectively in *M. morganii*. The similarity of each gene varies widely with *CusA* and the *CtpA* showing the better sequence match of 87% and 91% respectively.

In a study by Ramanathan *et al* (2013), it was mentioned that *CusF* is a homologue of *SilE*. In this study however it was observed that *SilE* and *CusF* do not share sequence similarity in *M. psychrotolerans* and are in fact two different genes. The two genes were found to be in two separate operons.

The pathway proposed using this cluster of genes in *M. morganii* is shown in Figure 4.4. However, this pathway does not sufficiently account for the conversion of Cu^{2+}

into Cu^0 or the export of Cu^0 nanoparticles out of the cell. From the synthesis of CuNPs and proteomic results obtained and detailed in chapter 3 and 5 respectively, an alternative pathway will be proposed and discussed in chapter 5.

A deeper look into the cluster of *Cus* genes as well as the *SilE* gene revealed that the genes are located within two operons (Figure 4.5). For a promoter to be considered, a prediction confidence score cut-off of more than 0.90 was used to increase prediction accuracy. The genes *CusA, CusB, CusF* and *CusC* are all regulated by one promoter found 150 bp upstream of the *CusR* gene (5' ATCATT GAAGAT GAAAGC AAAACA GGCGAA TACCTG AAAAAA GGATTA TC 3'). The terminator for this operon was located 34 bp downstream of the *CusA* gene (5' CAATAA GAAAATC CCCGGC CTGACA GCCGGG GATCTA CTTTTT GAA 3'). The genes *CusR, CusS* and *SilE* were found to be on a separate operon that was partially overlapping with the first operon, however it was located on the opposite DNA strand. The promoter for this operon was found 34 bp upstream of the *CusR* gene (5' AAATTG TCATTT TAGGTA ACGGGC ATTGAT CTCATG ATTTTG CGCATT AA 3'). The terminator for the latter operon was located 57 bp downstream of the *SilE* gene (5' GCGTTA TTTTTGC CCCGGC TTACGG GGCTTT TTTTGT TTT 3').

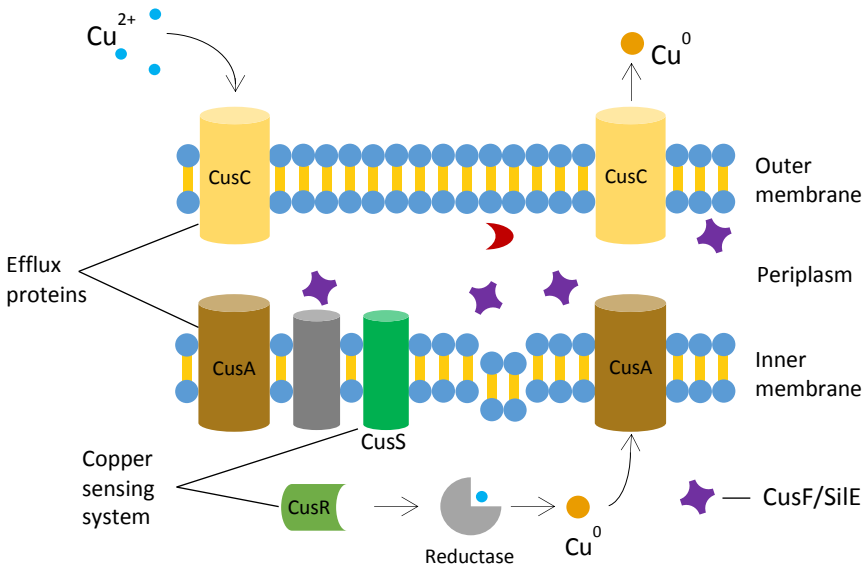

Figure 4.4: Copper ion resistance and nanoparticle synthesis pathway

Schematic diagram of the copper resistance and nanoparticle synthesis pathway as suggested in the literature.

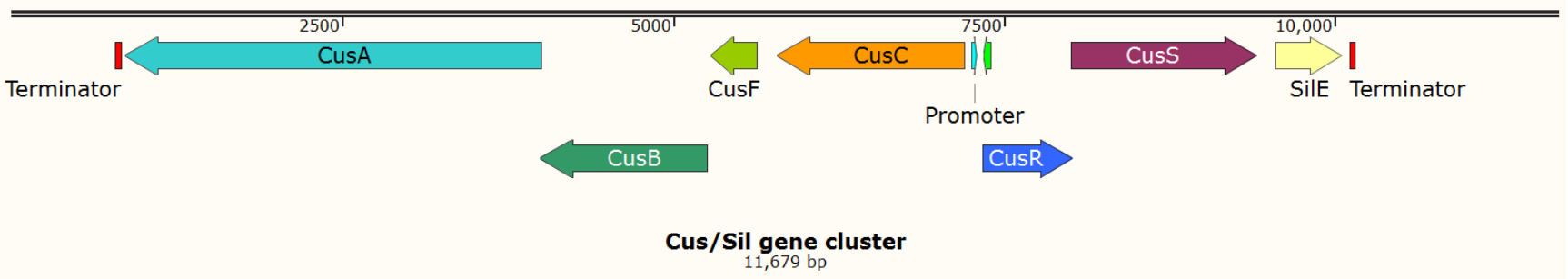

Figure 4.5: Diagram of *CusCFBA* and *CusRS/SilE* gene operons

Diagram representation of the *CusCFBA* and *CusRS/SilE* gene operons present in *M. psychrotolerans*.

Although the larger operon contained only *Cus* genes, the second and smaller operon contained a *CusS* as well as a *SilE* gene. The *SilE* gene has been previously reported to be involved with silver ion binding as well as copper ion binding in other organisms (Hao, Lüthje *et al.* 2015; Randall, Gupta *et al.* 2015). The *CusS* gene codes for one of the two proteins involved in a two-component regulatory system (the other gene being *CusR*) which is involved in silver/copper binding and silver/copper toxicity (Gudipaty and McEvoy 2014).

SilE was aligned with the copper binding protein homologue from *M. morganii* and the silver binding homologue from *E. coli* (Figure 4.6). The *M. psychrotolerans SilE* was calculated to be 41% similar to the *M. morganii* homologue and 40% similar to the *E. coli* one. Neither of the *SilE* homologues contained a sequence that coded for cysteine residues. However all three proteins were observed to contain 10 histidine molecules which are known to be involved in metal binding (Devasenathipathy, Kohilarani *et al.* 2016).

Figure 4.6: Alignment of *SilE* homologues

ClustalΩ alignment of the *SilE* homologues from *M. psychrotolerans*, *M. morganii* and *E. coli*.

4.6 Identification of native plasmid

The lack of research into *M. psychrotolerans* has limited the understanding of this bacterium. A factor never examined before, is whether or not this bacterium contains a plasmid and therefore whether a plasmid could contain any genetic information that might increase resistance to heavy metals, such as copper, as well as the production of nanoparticles.

M. psychrotolerans was grown for 24 hours as per protocol mentioned previously in chapter 2. A plasmid extraction was performed in order to isolate any potential plasmid DNA present within the bacterium. The eluate from the plasmid extraction was tested using the Nanodrop to see whether there was DNA present post-extraction. Indeed it was observed to contain 49.3 ng/µl which suggested that plasmid DNA was present. The eluate was then run in an agarose gel and the gel visualised under UV light (Figure 4.7). A number of bands of different sizes were observed to be present in the gel. The several bands were attributed to the various ways in which the circular plasmid was folded, with the brightest band seen close to 3.5 Kb accounting for the supercoiled plasmid DNA. The native *M. psychrotolerans* plasmid was named pMor.

The sequence of the plasmid was unknown, however when 2 *M. psychrotolerans* genome contigs were examined using BLAST, the plasmid pPvu1 of *Proteus vulgaris* was a significant match to a small portion of the contigs. This result showed evidence for the existence of a plasmid highly similar to pPvu1 present in *M. psychrotolerans*.

In order to explain why the 2 contigs might have contained this plasmid-like sequence, the annotated genome data was checked. A *recA* gene was identified in the chromosome which might suggest that at some point the plasmid integrated into the chromosome and was therefore picked up during genome sequencing. Since the full sequence of the plasmid was not present in the contigs, only part of the plasmid integrated into the chromosome. It is highly unlikely that the plasmid was sequenced during the genomic DNA sequencing due to the specificity of the extraction procedure.

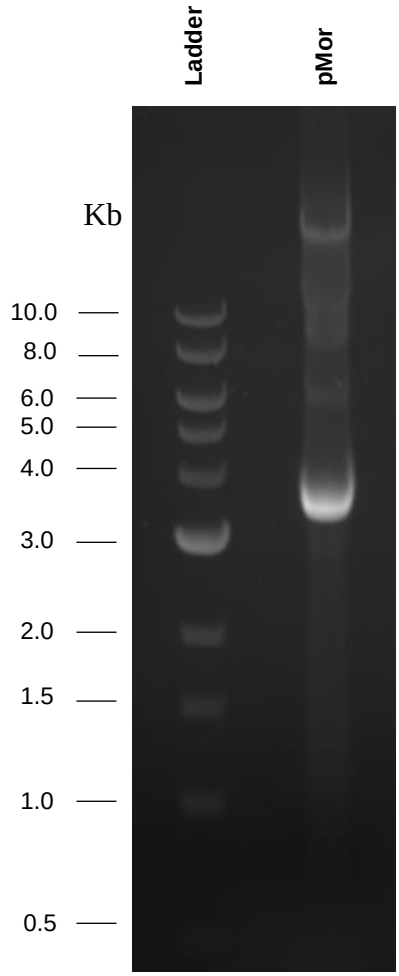

Figure 4.7: Confirmation of the presence of pMor

Agarose gel showing the presence of a plasmid after plasmid extraction from *M. psychrotolerans*.

4.7 Discussion

M. psychrotolerans is a novel organism that, as mentioned previously, was only isolated in 2006 (Emborg 2006). No published genome was available in the literature with the closest related genome to *M. psychrotolerans* being *M. morganii.* However, despite these organisms being in the same genus, they are phenotypically very different from each other.

In order to overcome the lack of prior knowledge and achieve a deeper understanding of this organism, whole genome sequencing was performed. However prior to that, the 16S rDNA of this organism was sequenced to guarantee that no contamination was present and the correct organism was being investigated.

With the help from Edinburgh Genomics at the University of Edinburgh, the genome of *M. psychrotolerans* was sequenced for the first time. It was subsequently assembled into 47 contigs with most of the genetic code being located in the 11 largest contigs. It was not possible to assemble the genome into one continuous sequence using automated software (RAST), possibly due to the presence of repetitive elements (Treangen and Salzberg 2012) or missing sequences in-between the contigs (Baker 2012).

With the genome of *M. psychrotolerans* as well as the 16S rDNA sequenced, it was possible to perform comparative studies between this organism and other related ones. Firstly the 16S rDNA gene was aligned with other organisms in the same genus, *M. morganii* strain ZJB-09203, strain RP-42, strain VAR-06-2076, strain M11 and strain KT. With the exception of *M. psychrotolerans*, these strains are all Category 2 opportunistic pathogens and they are found in human intestines as well as the environment (Falagas, Kavvadia *et al.* 2006). *P. vulgaris* and *P. alcalifaciens* are also found in the human intestines and co-exist with *M. morganii* (Sobreira, Leal *et al.* 2001; Amin 2011). *E. coli* strain K-12 was used as the outlier in the alignment as it differs more from the other species.

Once the alignments were complete, a phylogenetic tree was constructed to visualise the lineage of each organism (Figure 4.2). As expected, all the *Morganella* species were closely related with minor differences between the different strains. *M. psychrotolerans* however appeared to have evolved separately from the *morganii*

species early on in its evolutionary stages. *M. psychrotolerans* was found in cold-smoked tuna fish which was stored at low temperatures of around 0-10^{o}C, as opposed to *M. morganii* which inhabits the human intestine and has an optimum growth temperature of 37^{o}C. Such vastly different living environments of the two bacteria means that they would require many generations to evolve and adapt efficiently.

P. vulgaris was chosen for the phylogenetic analysis not only because it inhabited the same environment as *M. morganii* – a related organism to *M. psychrotolerans* – but also because they share a similar plasmid, pMor and pPvu1 in *M. psychrotolerans* and *P. vulgaris* respectively. *M. psychrotolerans* contained a plasmid that when aligned to the pPvu1 plasmid of *P. vulgaris* a very high identity was obtained. Upon closer inspection of the pMor plasmid, it was seen to contain elements that are known to help in mobilising the plasmid from one organism to another (Naderer, Brust *et al.* 2002). This would explain why both organisms might contain that part of the plasmid with such high similarity, but brings up the question of how *P. vulgaris* would be found inhabiting a space next to *M. psychrotolerans* if they live in different environments. One possibility is that since some of the mobility genes found in pMor had mutations in them rendering them inactive, it meant that the plasmid would have come from *P. vulgaris* into *M. psychrotolerans* rather than vice versa. *P. vulgaris* is able to survive and grow at 20^{o}C much like *M. psychrotolerans*. This means that at some point in their evolution, the two bacteria were most likely in close contact to one another and therefore this allowed the exchange of genetic information, i.e. pMor.

Although *M. psychrotolerans* and *M. morganii* species are found inhabiting very different environments, they do have plenty in common. The genome of *M. morganii* KT and *M. psychrotolerans* U2/3 are 85% similar on the nucleotide level. Both genomes contained similar sets of genes for heavy metal resistance. The *Cus* and *Sil* genes were found to be similar with strong homology between them. The genome size of *M. psychrotolerans* was 4.16 Mb which meant it was larger than the *M. morganii* KT genome by 0.36 Mb.

Since the work presented here focuses on the production of CuNPs using *M. psychrotolerans*, one of the main aims was to elucidate the synthesis mechanism of these nanoparticles. *Ramanathan et al.* (2013), discussed the *Cus* and *Sil* genes and

described how they work together to form a part of an efflux system to produce nanoparticles and subsequently export them outside the cell. However, there are several aspects that remain unaccounted for by the suggested mechanism. Most importantly, is the fact that there was no identified reductase to reduce the Cu^{2+} or Cu^{+} to Cu^{0}. Since the genome and proteome of *M. psychrotolerans* is now known, a search was performed in order to identify such a reductase, without success. Also, the genes involved in the pathway that *Ramanathan et al.* (2013) described, all bind to ionic forms of metals rather than zero valent elements, further reducing the possibility that the pathway is correct (Grass and Rensing 2001). Finally, it was suggested that the initial nanoparticles that are formed inside the cytoplasm of the cell, undergo growth and assembly within the cell prior to being exported outside the cell. *CusC* which is found on the outer membrane has a cylindrical shape with its central substrate transport channel having a size of ~2.5 nm (Kulathila, Kulathila *et al.* 2011). This makes the transport of the observed nanoparticles (4-60 nm) impossible as they would clog the channel due to their size.

The reasons described above, all lead to the conclusion that the suggested pathway found in the literature is not completely accurate. From the current study, a new pathway is proposed in chapter 5, using the proteomic data described in chapter 5, the genomic data presented in this chapter, the nanoparticle characterisation results in chapter 3 and also the current literature.

Chapter 5. Proteomic Analysis of *M. psychrotolerans*

5.1 Introduction

With the genome of *M. psychrotolerans* sequenced the proteins the organism produces can also be deduced. However not much was known about the proteome and its changes in the presence of a heavy metal ion such as Cu^{2+}. Proteomes change depending on the conditions that the organism is present in, whether they are favourable or extreme conditions that can be toxic (Deighton, Le Bihan *et al.* 2014). The abundance levels of proteins change when the organism is under stress and therefore this can be exploited to identify proteins that might be involved in the resistance of Cu^{2+} and nanoparticle synthesis.

The mechanism of copper nanoparticle synthesis has been reported in the literature by Ramanathan *et al.* (2008). Since both *M. morganii* and *M. psychrotolerans* contain a similar set of genes for copper resistance (See Chapter 4), it was thought that the same pathway would be utilised in the synthesis of CuNPs in both organisms. In order to validate this hypothesis, proteomics was used.

Using the genome of *M. psychrotolerans*, the predicted gene coding regions were translated into a protein sequence. The proteome had an isoelectric point of 10.01 and the aliphatic index was found to be 81.082. Each gene found using the genomic data was translated into its protein sequence and labelled using sequence similarity searches.

The aim of the work described in this chapter was to perform mass spectroscopy on *M. psychrotolerans* in the presence and absence of Cu^{2+} to identify the most abundant proteins under these conditions. This would lead to important information on how *M. psychrotolerans* defends itself from this heavy metal and how it converts the ions into metallic nanoparticles by revealing the proteins responsible. In order to verify some of the proteomic results, qRT-PCR of the predicted genes in the CuNP synthesis pathway was performed.

5.2 Liquid Chromatography Mass-Spectrometry

As mentioned previously, the proteome of an organism may change depending on the conditions that it is found in at any given time. To test the hypothesis that the *Cus/Sil* genes are responsible for the resistance of Cu^{2+} or production of CuNPs, *M.*

psychrotolerans was exposed to Cu^{2+}. The procedure is described in detail in Chapter 2. The organism was then incubated for 24 hours before washing and digestion in preparation for preparation for mass spectrometry. The peptides were fractionated during the mass spectrometry analysis in order to get a larger array of protein representation from the samples.

The mass spectrometry analysis results of the proteome of *M. psychrotolerans* exposed to Cu^{2+} and *M. psychrotolerans* without any exposure to the metal ions were compared. The analysis identified 775 proteins present in the samples. From the total proteins, 100 of them had a *p*-value lower than 0.05 of which 86 had significantly different abundance.

From the total pool of proteins identified using LC-MS, only a small number of them showed an abundance of any significant difference. The criteria chosen for selecting significant hits were an increased or decreased abundance ratio of >1.5 or <0.67 respectively, a peptide number quantification of ≥2 and a *p*-value of <0.05 (Figure 5.1). From the identified proteins, 62 unique proteins were more abundant in the samples containing *M. psychrotolerans* exposed to Cu^{2+} (8.0% of the proteins were more abundant). Of the more abundant proteins, 35 were identified by 2 or more peptides. Twenty-four unique proteins were less abundant in the same samples. Of the less abundant proteins, 13 of them were identified by 2 or more peptides and 6 of those were less abundant with a max fold change of <0.67 (3.1% of proteins were less abundant) (Figure 5.2). A logarithmic association of the 96 protein abundance levels emphasises the fact that multiple proteins were affected by the presence of Cu^{2+} (Figure 5.3).

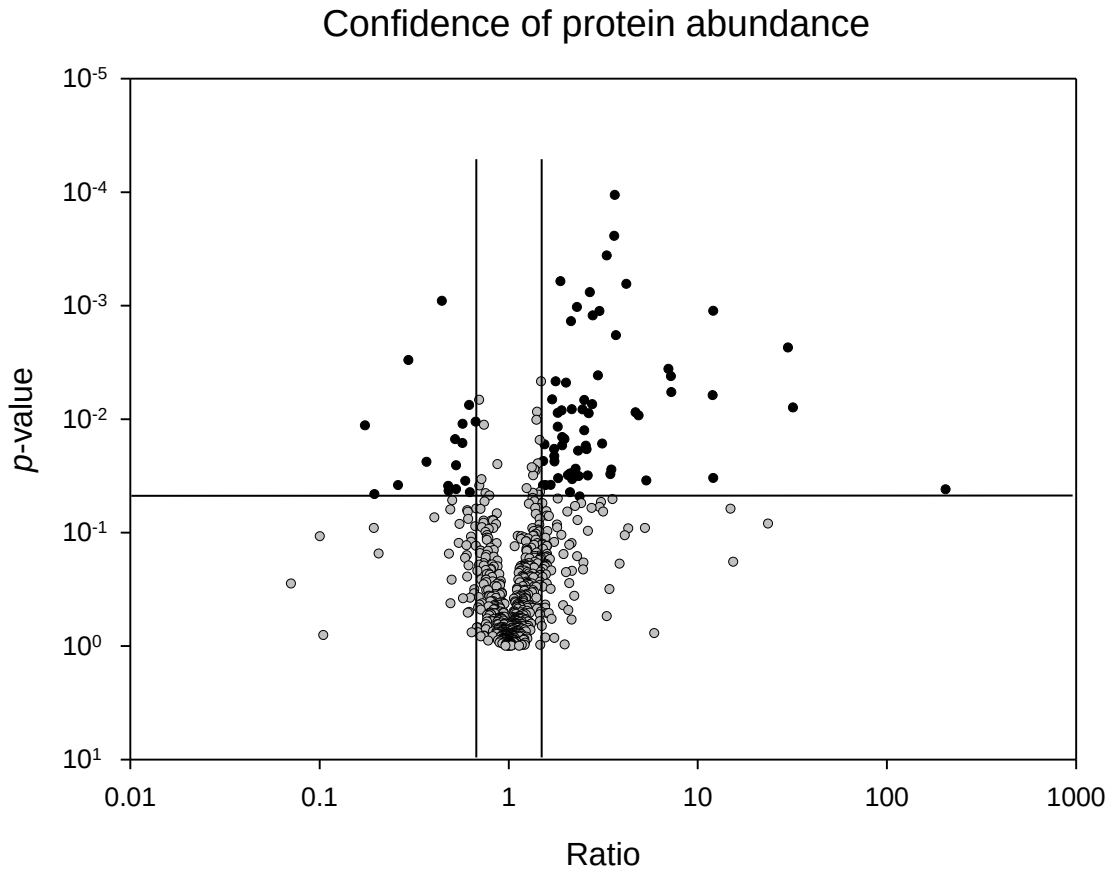

Figure 5.1: Confidence of protein abundance

Volcano plot showing the relationship of identified proteins through LC-MS and their relative differential abundance based on their individual *p*-value. Grey dots indicate proteins that have not passed the three selection criteria for significant differential abundance (increased or decreased abundance ratio of >1.5 or <0.67 respectively, a peptide number quantification of ≥2 and a *p*-value of <0.05). Black dots indicate significantly less abundant proteins (left side of the lines) and significantly more abundant proteins (right side of the lines) in the presence of 5 mM $CuSO_4$.

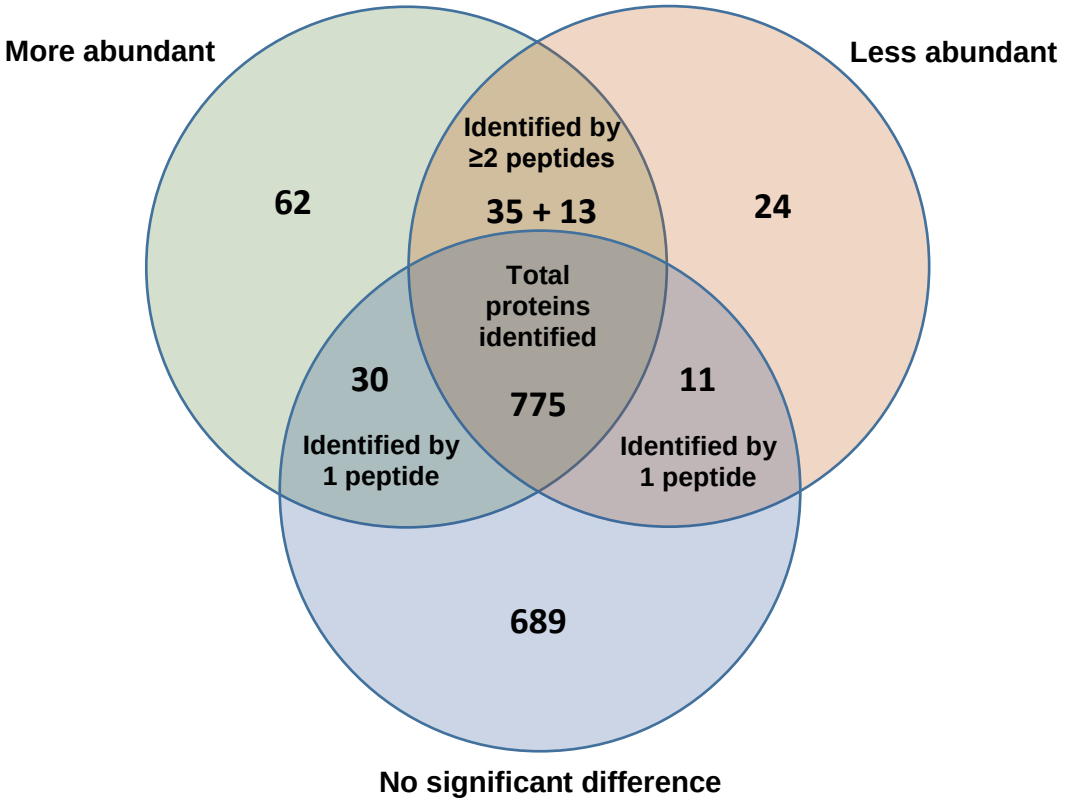

Figure 5.2: Distribution of proteins identified by LC-MS

Venn diagram illustrating the numbers of differentially abundant proteins identified using LC-MS on *M. psychrotolerans* exposed to Cu^{2+}.

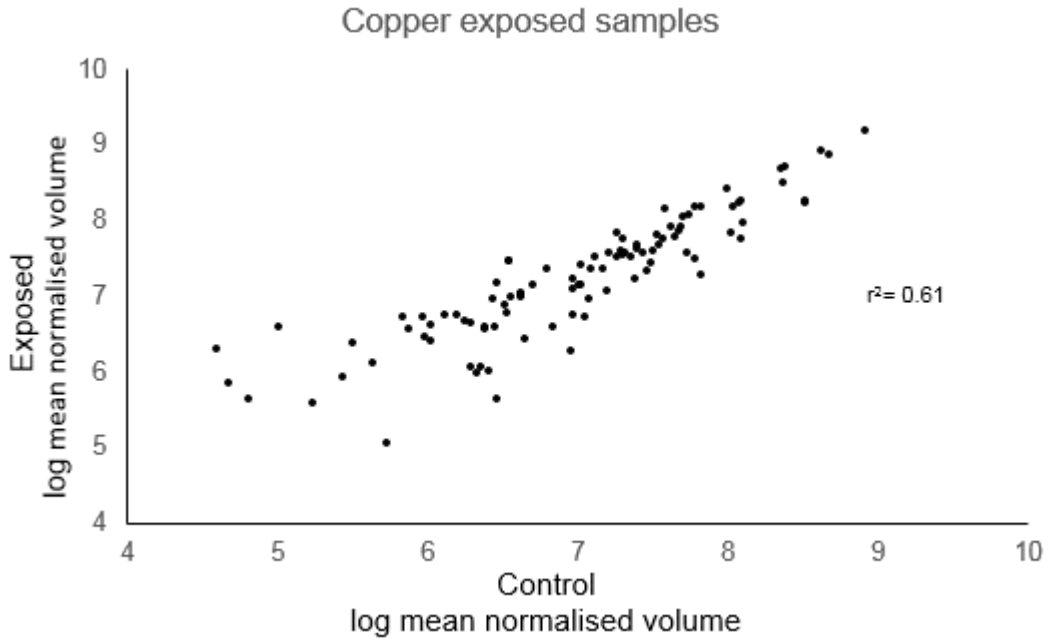

Figure 5.3: Protein abundance change under $Cu2^{+}$ presence

The normalised volume results represent the relative protein amounts in each dot. Each dot equates to each of the 96 proteins identified with a high confidence level. The graph emphasizes that abundance levels of these proteins are altered significantly when the organism is under the presence of Cu^{2+}. There was a good correlation between the Cu^{2+} exposed samples and the control samples (r^2= 0.61) and 8.65% of the dots were significantly different.

Three of the proteins identified through LC-MS were a P-Type ATPase, SilE and Glutathione reductase (GR) (Huang, Deng *et al.* 2016; Ilyas, Rehman *et al.* 2016; Staehlin, Gibbons *et al.* 2016). All three proteins have been associated with heavy metal ion resistance in different ways. The ATPase was more abundant by 12.1 fold and it was also the most abundant protein identified in the dataset. SilE was also the most abundant protein observed (max fold change of 204.5) however it only being identified by 1 peptide count, meant it required supporting information. GR was more abundant by 1.9 fold and was identified by 3 peptides.

5.3 Copper Nanoparticle Synthesis Pathway

With the LC-MS results and the genomic results in place, a clearer picture emerged involving the CuNP synthesis pathway. It has been suggested before that a P-Type ATPase and SilE might be involved in this pathway. However the protein responsible for reducing Cu^{2+} into a lower oxidation state had not been identified. The results described in the previous section showed the greater abundance of GR that is directly involved in the reduction of glutathione (GSH). With this in mind, the reductase was hypothesised to be GSH as it is responsible for heavy metal ion binding and resistance (Ilyas, Rehman *et al.* 2016).

The pathway suggested in the literature does not include the name of a reductase (Figure 5.4a). By looking at the LC-MS results, GR was more abundant which suggests that GSH is oxidised in the presence of Cu^{2+}. Revised versions of the CuNP synthesis pathway were developed and are shown in Figure 5.4b-g.

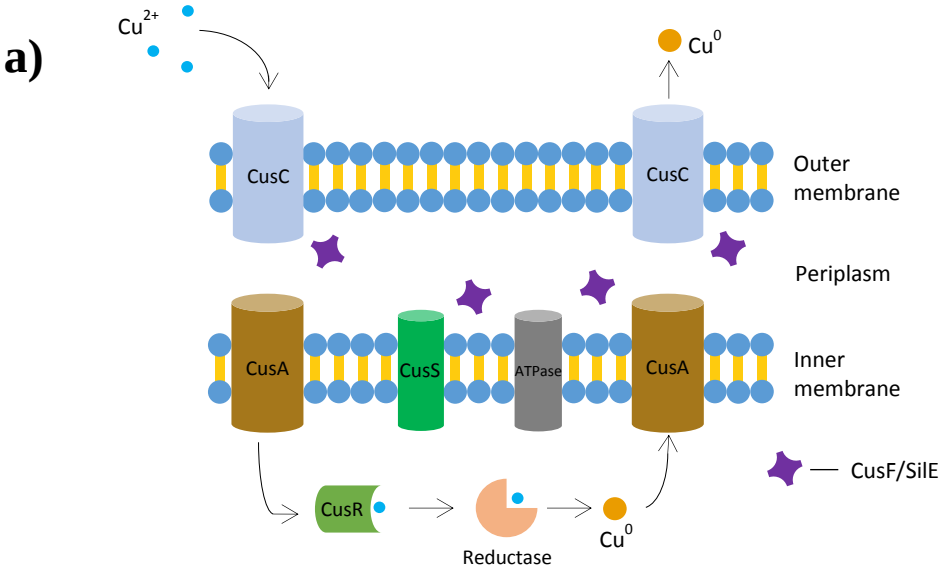
a)
Cu2+
Cu0
CusC
CusC
Outer membrane
Periplasm
CusA
CusS
ATPase
CusA
Inner membrane
CusF/SilE
CusR
Cu0
Reductase

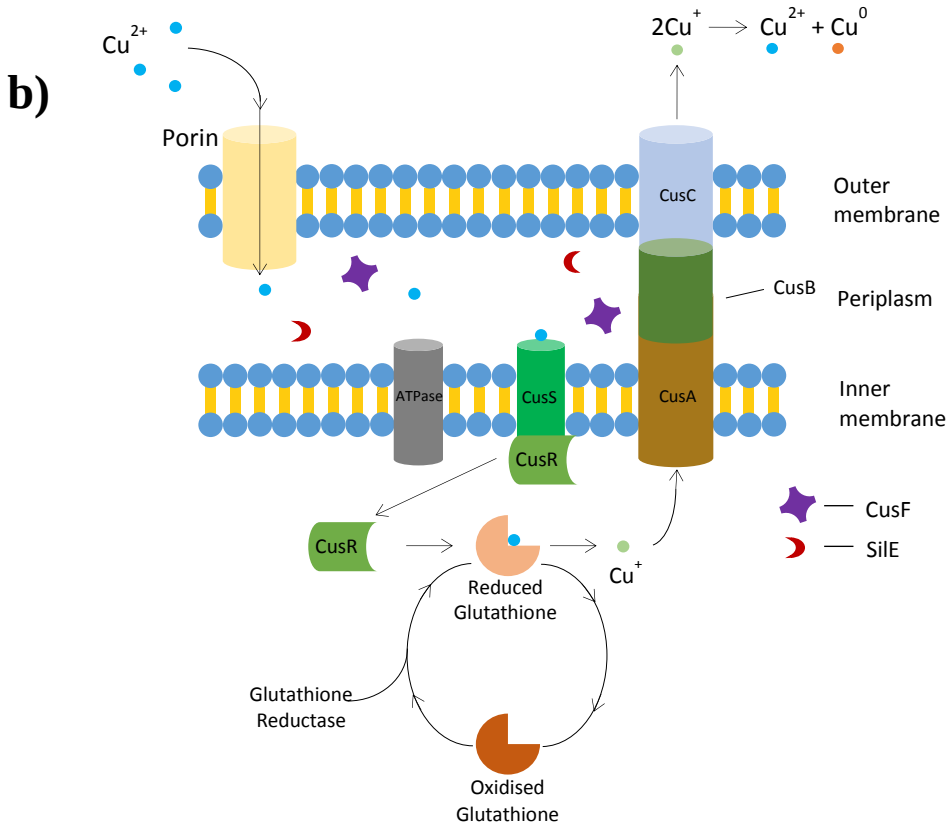
b)
Cu2+
2Cu+ → Cu2+ + Cu0
Porin
CusC
Outer membrane
CusB
Periplasm
ATPase
CusS
CusA
Inner membrane
CusR
CusR
CusF
SilE
Cu+
Reduced Glutathione
Glutathione Reductase
Oxidised Glutathione

c)

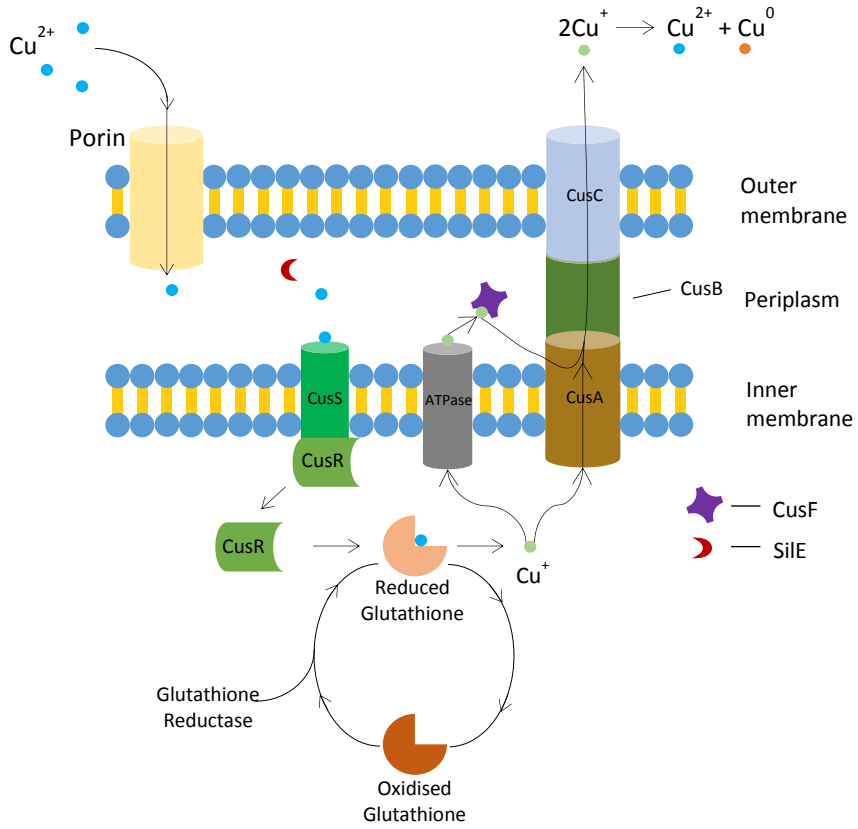
Cu2+
Porin
2Cu+ → Cu2+ + Cu0
CusC
Outer membrane
CusB
Periplasm
CusS
ATPase
CusA
CusR
Inner membrane
CusR
CusF
SilE
Cu+
Reduced Glutathione
Glutathione Reductase
Oxidised Glutathione

d)

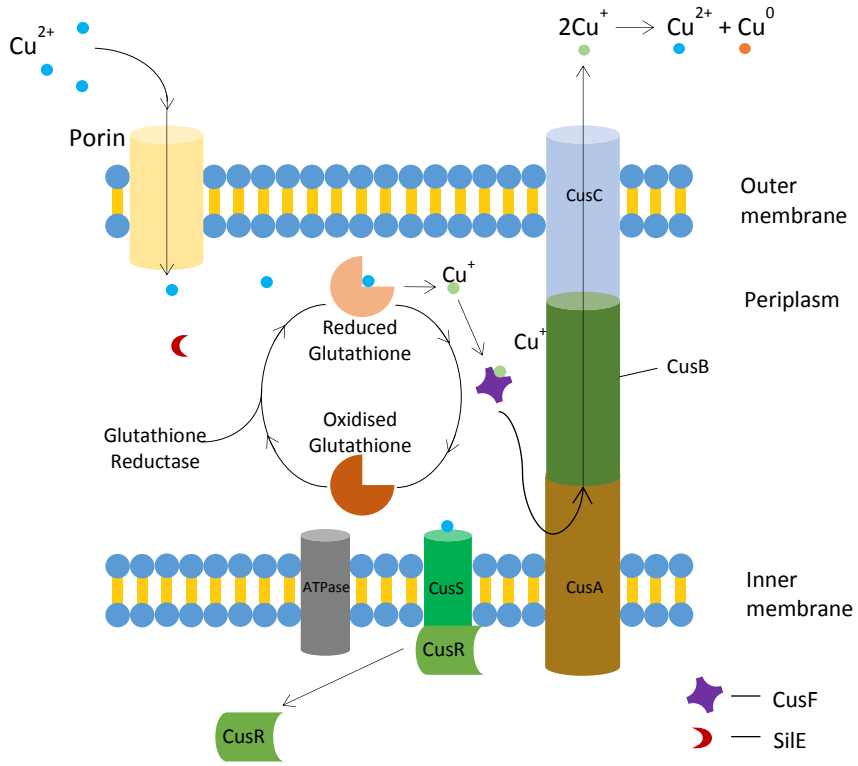
Cu2+
Porin
2Cu+ → Cu2+ + Cu0
CusC
Outer membrane
Cu+
Periplasm
Reduced Glutathione
Cu+
CusB
Glutathione Reductase
Oxidised Glutathione
ATPase
CusS
CusA
Inner membrane
CusR
CusR
CusF
SilE

e)

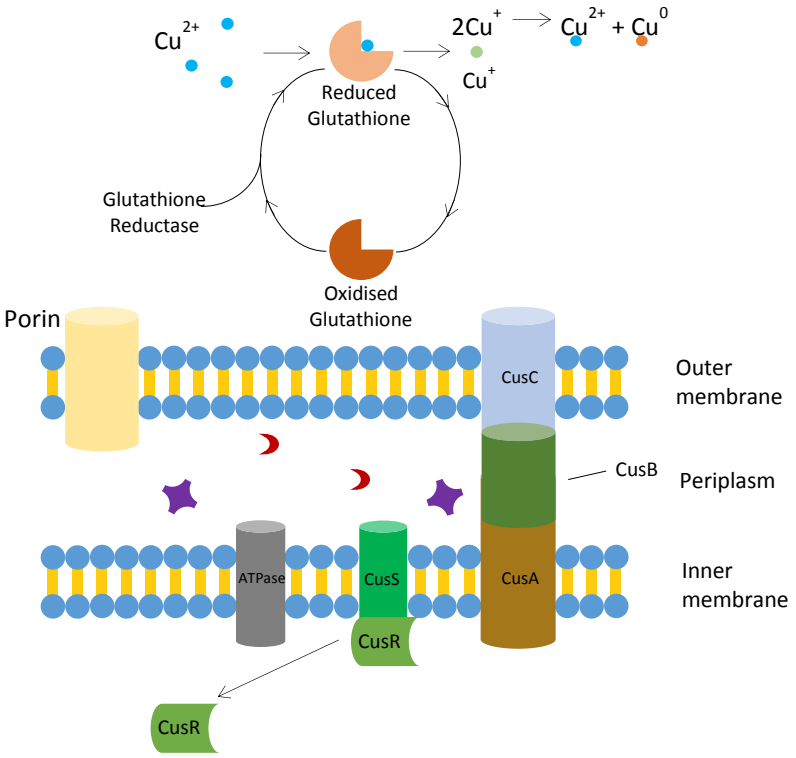
Cu2+
Reduced Glutathione
2Cu+
Cu2+ + Cu0
Cu+
Glutathione Reductase
Oxidised Glutathione
Porin
CusC
Outer membrane
CusB
Periplasm
ATPase
CusS
CusA
Inner membrane
CusR
CusR

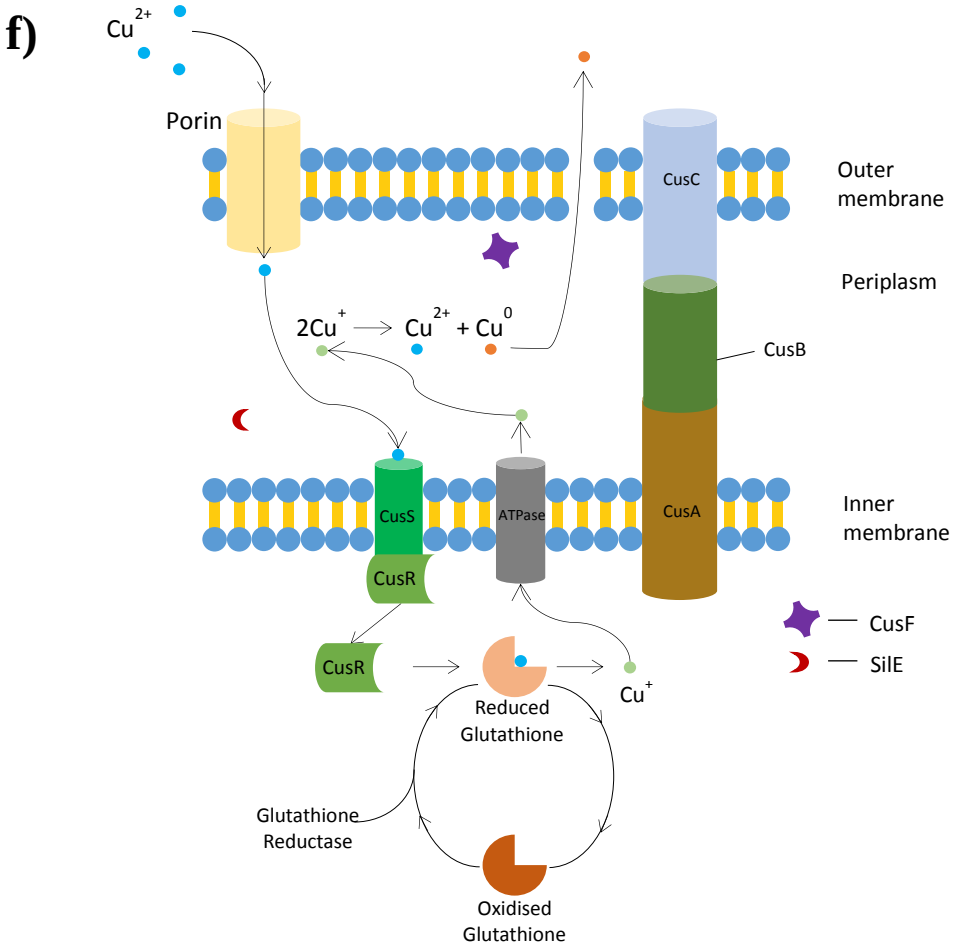

Figure 5.4: Proposed CuNP synthesis pathway by *M. psychrotolerans*

The diagrams illustrate the suggested CuNP synthesis pathway a) described in the literature by Ramanathan *et al* (2008) and b-g) possible pathways suggested by the work carried out and described in this project.

This new proposed pathway involves the entry of Cu^{2+} into the periplasmic space through porins, and subsequently into the cytoplasm. In the cytoplasm it is then converted from Cu^{2+} into Cu^{+} by GSH leading to the oxidation of GSH. The GSH is then converted back into its reduced state by GR. Meanwhile the Cu^{+} is sensed by CusS and subsequently activates CusR by phosphoryl transfer, the transcription factor that regulates the CusCFBA genes. The Cu^{+} then gets transferred into the periplasm and then extracellularly via the CusCBA proton-metal antiport system through a chemiosmosis process (Tseng, Gratwick *et al.* 1999; Nies 2003). Since Cu^{+} is unstable if it is not bound to a ligand, it disproportionates chemically to form Cu^{0} and Cu^{2+}. The Cu^{0} becomes the nanoparticle or seed nanoparticle to which more Cu^{0} binds to in order to grow in size and the Cu^{2+} gets recycled again in the CuNP synthesis process. The export of Cu^{+} to the extracellular space was tested, confirmed and is described in detail in Chapter 3. The pathway depicted n Figure 5.4c is similar to Figure 5.4b but shows the Cu^{+} also being transported to the periplasm via the P-Type ATPase and then CusF transports it CusA where it is then transported extracellularly by CusABC. Another pathway could be hypothesised where GSH was localised in the periplasm and the reduction of Cu^{2+} to Cu^{+} occurred there, prior to transporting Cu^{+} outside the cell (Figure 5.4d). It has been also hypothesised that GSH might also be released extracellularly and hence this reduction process occurs outside the cell without using the Cus pathway (Figure 5.4e). Finally, reduction of Cu^{+} could also occur in the periplasm, hence synthesised nanoparticles could be released into the supernatant via damaged parts of the outer membrane (Figure 5.4.f).

5.4 Quantitative Real-Time Polymerase Chain Reaction (qRT-PCR)

The proteomics results provided a good indication that the presence of $CuSO_4$ caused an increased abundance of several proteins related to Cu tolerance. Moreover all three proteins in question were found to be related to the CuNP pathway suggested in the literature (Ramanathan, Field *et al.* 2013). For proteome LC-MS data to be considered accurate, the proteins need to be identified by more than 1 peptide. Also, not all proteins can be identified due to method limitations and therefore additional data is required in some cases in order to provide sufficient supporting evidence.

In this study, only 3 proteins were identified to be related with Cu resistance using LC-MS, Glutathione reductase, *SilE* and a P-Type ATPase. In Chapter 4 it was observed

that the gene *SilE* is located downstream of *CusR* and is regulated under the same promoter. This gave rise to the hypothesis that if the protein SilE is more abundant, it may indicate that CusS and CusR are also more abundant caused by their respective gene overexpression. Moreover, since CusS and CusR are involved in the same defence mechanism pathway as CusCFBA, then their genes may also be overexpressed (Gudipaty, Larsen *et al.* 2012). In order to investigate this hypothesis, qRT-PCR was used targeting the *Cus* efflux pump genes and Glutathione reductase. A housekeeping gene was used in order to establish a baseline to compare the overexpression ratios, and in this case *DnaK* was chosen, due to its protein not being found to be differentially abundant in the presence of $CuSO_4$ in the LC-MS experiments.

The results were normalised and referenced to *DnaK*, prior to studying the outcomes. qRT-PCR revealed that *CusS* and *CusR* were not significantly overexpressed, even though they are located under the same promoter as *SilE* and the protein SilE was more abundant in the LC-MS results. On the other hand, the genes *CusC*, *CusF*, *CusB* and *CusA* were all overexpressed in the presence of $CuSO_4$ (Table 5.1).

Target Gene	Before/After Ratio	Normalised Ratio	Fold Change
Glutathione Reductase	0.75	4.65	0.04
CusC	2700.00	-7.17	143.57
CusF	580.70	-4.95	30.87
CusB	199.30	-3.41	10.59
CusA	28.21	-0.58	1.50
CusS	6.57	1.52	0.35
CusR	15.70	0.26	0.83

Table 5.1: qRT-PCR results of *M. psychrotolerans* in the presence of $CuSO_4$. The results show 7 genes related in Cu tolerance followed by their fold change over the course of the experiment. Fold change was referenced to *DnaK* which was used as the housekeeping gene.

5.5 Discussion

With the genetic information of *M. psychrotolerans* known, it was important to understand the proteome of this organism under Cu^{2+} stress. The importance of this study was to shed light into the mechanism of Cu resistance and CuNP synthesis by *M. psychrotolerans*. In order to do this the proteomic results were cross-referenced with the genome data gathered previously to provide a clearer picture of the process. Supporting data from qRT-PCR assays were also used to form a stronger view of the CuNP synthesis pathway.

Whole cell LC-MS is an extremely helpful tool for investigating pathways of interest. In the case of this study, LC-MS on the proteome of *M. psychrotolerans* was used to test whether the CuNP synthesis pathway suggested in the literature was valid (Ramanathan, Field *et al.* 2013). The focus was the proteins suggested in the pathway by Ramanathan *et al.*, as well as other proteins that might be involved in some way and have not been mentioned before.

The LC-MS results showed a clear effect of $CuSO_4$ presence on *M. psychrotolerans* with a large number of proteins being affected (8.65%). When a protein was affected, its relative abundance changed in either of two ways, increased or decreased. The main focus was drawn towards the more abundant proteins in order to find proteins that might be involved in Cu^{2+} tolerance or CuNP nanoparticle synthesis. Indeed 3 proteins were found that are directly and indirectly involved in Cu ion resistance. Glutathione reductase, SilE and a P-Type ATPase were found to be more abundant in the presence of Cu^{2+}.

A pathway was suggested (Figure 5.4) using these results as well as using previously published research. The pathway was strongly supported by the extracellular Cu^{+} presence assay described in Chapter 3, which confirmed the presence of Cu^{+} outside the cells in the presence of $CuSO_4$ in the growth medium.

Three of the proteins shown in the proposed pathway were present in the LC-MS results. However as mentioned previously in Chapter 4, the *Cus* and *Sil* genes were located in two operons and regulated by two promoters. Since SilE was found to be more abundant, this suggested that both CusR and CusS would be present, as their respective genes would also be transcribed in the process due to all three of them being

regulated under the same promoter. Under increased Cu ion presence, the presence of CusR and CusS cause the transcription of the *CusCFBA* genes which means that that they may also be involved in the pathway of CuNP synthesis (Delmar, Su *et al.* 2015). The increased abundance of the P-Type ATPase suggested that it is also involved in Cu ion defence. The increased abundance of GR suggests that GSH is also involved in the process in which it binds to Cu^{2+}, converting it to Cu^{+} and therefore altering itself into the oxidised form of GSH. GR therefore acts as a reducer for GSH (Muller 2015) in order to keep it in an active (reduced) state to control the Cu^{2+} presence within the cell.

In order to confirm the aforementioned results from LC-MS, qRT-PCR was performed. The GR, *CusC, CusF, CusB, CusA, CusS and CusR* genes were targeted to investigate whether they were upregulated in the presence of $CuSO_4$. The *CusCFBA* operon was significantly upregulated in the presence of $CuSO_4$. This was anticipated as the presence of $CuSO_4$ causes the activation of CusS and CusR which subsequently bind to the promoter that regulates expression of the *CusCFBA* operon (Munson, Lam *et al.* 2000). On the other hand the genes *CusS* and *CusR* were not upregulated in the presence of $CuSO_4$. This may be because the CusS and CusR proteins act as a two-component sensory kinase molecule that is constitutively expressed for the constant "monitoring" of Cu^{2+} presence. Upon Cu^{2+} detection, the CusS and CusR activate expression of the *CusCFBA* operon, hence why the genes on this operon are found to be overexpressed (Gudipaty, Larsen *et al.* 2012). Moreover, GR was not overexpressed at the gene level in the presence of $CuSO_4$. This was in contrast with the LC-MS results that showed the overabundance of GR in *M. psychrotolerans* when $CuSO_4$ was added to the growth medium. This may be because GR has a longer half-life and therefore does not need to be produced in high quantities when needed, as there is already enough to keep GSH in the reduced state. It may also mean that GR is very efficient at reducing GSH to the reduced state and therefore overexpression of GR is not required by the cell. The observed increased abundance of SilE protein in the LC-MS results may be because it was only identified using one peptide. qRT-PCR data did not support the LC-MS results which showed increased abundance of SilE. However, as mentioned previously, this could be due to a number of reasons such as protein degradation rate or inaccurate reading from the LC-MS as it was identified using 1

peptide count. It is worth noting that all the genes and proteins studied here and their functions in copper nanoparticle synthesis are putative. Further research is needed to provide sufficient evidence that these genes and proteins are indeed involved in CuNP synthesis such as deletion/knockout, or overexpression studies.

Chapter 6. Genetic Engineering of *M. psychrotolerans*

6.1 Introduction

Having the protocols for CuNP synthesis established as well as the genes responsible for their synthesis, the next step was to improve upon the synthesis rate and yield of CuNPs by genetic modification. No previous genetic modification techniques had been developed for *M. psychrotolerans* since its genome had not been sequenced prior to this project. It has been reported that genes from *M. morganii* have been cloned into *E. coli* (Verdet, Benzerara *et al.* 2006). However the opposite is not true as there is no literature on the insertion of recombinant genes into *M. morganii* and similarly no methods exist for *M. psychrotolerans* either.

Prior to attempting genetic modification of *M. psychrotolerans*, the antibiotic resistance profile of *M. psychrotolerans* was studied. According to Emborg *et al* (2006), it is sensitive to apramycin, ceftiofur, chloramphenicol, neomycin, ciprofloxacin, florfenicol, gentamicin, nalidixic acid, spectinomycin, streptomycin, sulfamethoxazole and trimethoprim. Antibiotic assays described in this chapter did not show the same result for chloramphenicol as it was found to be resistant.

There were no known plasmids that replicated in *M. psychrotolerans* which added to the challenge of genetic modification. As described in Chapter 4, a native plasmid was discovered that was closely related to the pPvu1 plasmid of *P. vulgaris*. However the plasmid was not fully sequenced at the time and therefore it could not be used for bacterial transformations. Instead, a series of plasmids derived from various sources were used to identify which ones are able to replicate within *M. psychrotolerans*. The plasmids tested along with their characteristics are mentioned in Chapter 2.

The successful genetic modification of *M. psychrotolerans* is a key step for a non-conventional organism to become a model organism for industrial applications. *E. coli* is currently a model organism for a vast number of research areas such as antibiotics, protein production and biofuel production (Miroux and Walker 1996; Sondi and Salopek-Sondi 2004; Bokinsky, Peralta-Yahya *et al.* 2011). However *E. coli* requires higher temperatures for growth compared to *M. psychrotolerans* which would negatively impact on industrial costs. In projects where the bacterium used requires growth and maintenance in industrial volumes, an organism such as *M.*

psychrotolerans could work best as it is fast growing, does not require heating as well as being a Class I organism compared to the other species in the *Morganella* genus (Emborg 2006). The organism's innate ability to withstand high concentrations of various heavy metals also make it ideal for use in bioremediation of heavy metal contaminated industrial waste.

M. psychrotolerans is known to be a food contaminant as it survives cold temperatures and produces relatively high levels of histamine potentially causing food poisoning (Emborg 2006). Due to this problem the gene responsible for the conversion of histidine into histamine (*hdc*) needed to be removed. This is an important step towards creating an organism that is suitable for use in industry, as it would prevent the organism from producing histamine and therefore make it safer for use. The *hdc* gene is responsible for catalysing the conversion of histidine into histamine (Rosenthaler, Guirard *et al.* 1965).

Work detailed in this chapter assesses the antibiotic resistance of *M. psychrotolerans* and develop protocols for genetic manipulation. Bacterial transformations were performed with various plasmids described in Chapter 2. Finally a method for markerless deletions of chromosomal genes was also developed using the suicide plasmid pK18mobSacB.

6.2 Antibiotic Resistance

Antibiotic susceptibility of *M. psychrotolerans* was assessed with antibiotics commonly used in bacterial selection. As described in the method in chapter 2, the antibiotics were ampicillin, chloramphenicol, kanamycin, tetracycline and nalidixic acid. Concentrations of antibiotics ranged from 0 to 80 µg/ml. Cultures of the bacterium were grown for 24 hours prior to plating on agar with the respective antibiotics. The cultures were also serially diluted to 10^{-5}.

After 10 µl of each culture dilution was spotted on the plates, they were grown for 48 hours in order to allow enough time for colony formation. Growth was observed on agar plates containing ampicillin, chloramphenicol and kanamycin (Table 6.1). The presence of ampicillin at a concentration of 50 µg/ml did not inhibit the growth of the bacterium as it appeared to have similar growth as the positive control not containing antibiotics. Chloramphenicol showed improved antibiotic effect compared to

ampicillin by inhibiting growth at concentrations as low as 10 µg/ml. Although the growth inhibition was clearly visible at concentrations above 10 µg/ml, growth was still observed up to concentrations of 80 µg/ml. For kanamycin, the organism was only able to grow at concentrations of up to 5 µg/ml and was shown to be susceptible to any higher concentrations. No growth was observed on agar plates containing tetracycline or nalidixic acid at any concentrations.

Antibiotic tested	Antibiotic concentration (µg/ml)	*Morganella psychrotolerans* U2/3 culture dilution rate					
		10^0	10^{-1}	10^{-2}	10^{-3}	10^{-4}	10^{-5}
No antibiotic (+ve control)	–						
Ampicillin	50						
Chloramphenicol	5						
	10			No growth			
	20						
	40		No growth				
	60						
	80						
Kanamycin	5						
	10	No growth					
	20						
	40						
	60						
	80						
Tetracycline	5	No growth					
	10						
	20						
	50						
Nalidixic acid	50	No growth					

Table 6.1: Antibiotic assay performed on *M. psychrotolerans* with a series of antibiotics. Growth is shown in pictures for each dilution. No picture is shown in case of growth absence.

6.3 Transformations of *M. psychrotolerans*

Following the antibiotic assays to determine a suitable selection marker, seven plasmids were used to perform transformations of *M. psychrotolerans*. The antibiotics suitable for use as selection markers were nalidixic acid, tetracycline and kanamycin concentrations higher than 5 µg/ml. The plasmids chosen in this study were *E. coli* and broad host range plasmids as described in Chapter 2.

Both chemically competent and electrocompetent *M. psychrotolerans* was used for transformations. Both types of transformations were performed with all seven aforementioned plasmids. Electrotransformation was successful for only one plasmid; pSUP404.2. The antibiotic selection used for this plasmid was 50 µg/ml kanamycin. No colonies were observed in the negative control that contained non-transformed electrocompetent *M. psychrotolerans*. The efficiency of the transformation was low, with colonies forming in the numbers of 5-20 for each transformation repeat. Electroporation with the other 6 plasmids were unsuccessful after repeated attempts with various conditions suggesting that the plasmids do not replicate within *M. psychrotolerans*. Transformants were picked, grown in LB_{ns} overnight, plasmid extracted and digested using *MfeI* to confirm the presence of the pSUP404.2 vector (Figure 6.1). Chemical transformations with all 7 plasmids were unsuccessful as no colonies were obtained following incubation of the transformed cultures on their respective antibiotic selection plates.

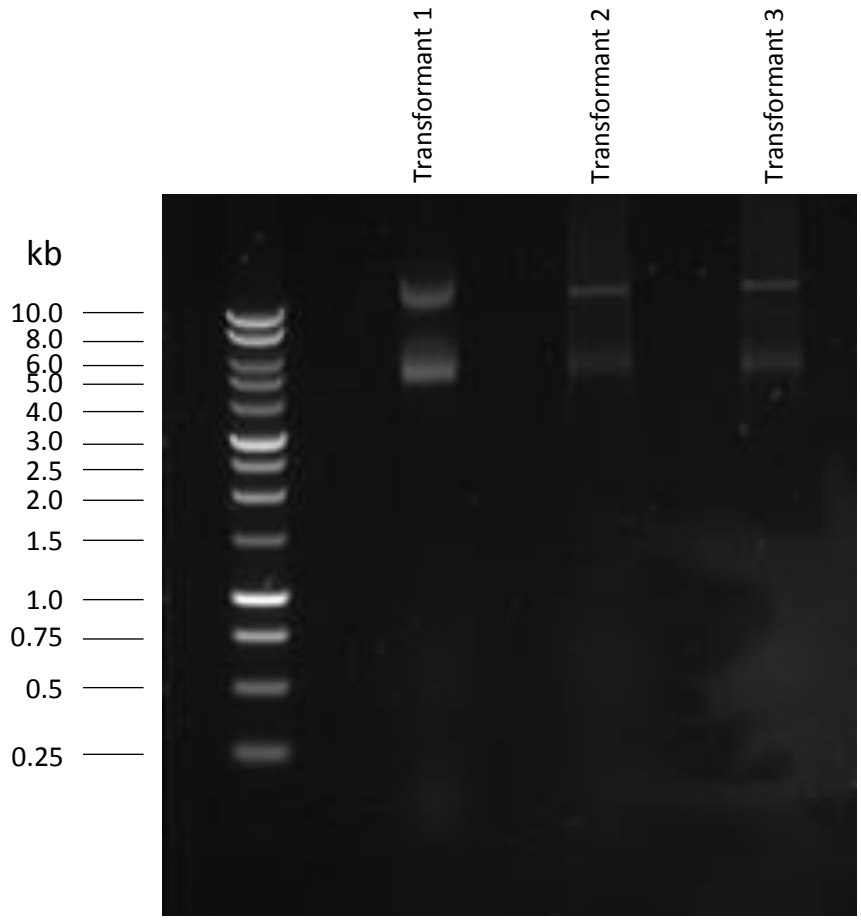

Figure 6.1: Restriction digest of pSUP404.2 using *MfeI* extracted from *M. psychrotolerans* transformants.

6.4 Generating an Inducible Expression System in *M. psychrotolerans*

After finding a plasmid that was able to replicate in *M. psychrotolerans*, the next step was to create an inducible expression system. No expression vectors have been developed for this organism prior to this study.

An inducible expression system was adapted from the plasmid pMind which contained a tetracycline inducible promoter originally developed for mycobacteria (Blokpoel, Murphy *et al.* 2005). Common inducible expression systems such as the ones based on *lacZ* regulation by Isopropyl β-D-1-thiogalactopyranoside (IPTG), are "leaky" and therefore do not completely stop expression when they are inactive. The system developed by Blokpoel *et al.*, was designed to be tightly controlled preventing the regulated genes from being expressed when the promoter is inactive.

The system works by constant expression of the *TetR* gene which produces the protein TetR. TetR then binds to the promoter region upstream of the *TetR* gene and causes repression of the two promoters present in the region (Figure 6.2). This prevents the expression of any gene present in the cloning site. When tetracycline is added to the medium, it binds to TetR and hence prevents it from binding onto the promoter region, allowing for transcription of any gene present in the cloning region to take place.

This expression system was adapted for *M. psychrotolerans* by adding two restriction sites *Mfe*I and *Sal*I in the cloning site, in order to allow for insertion of genes. After designing the sequence, it was sent to Genewiz to synthesise it and insert it into pSUP404.2.

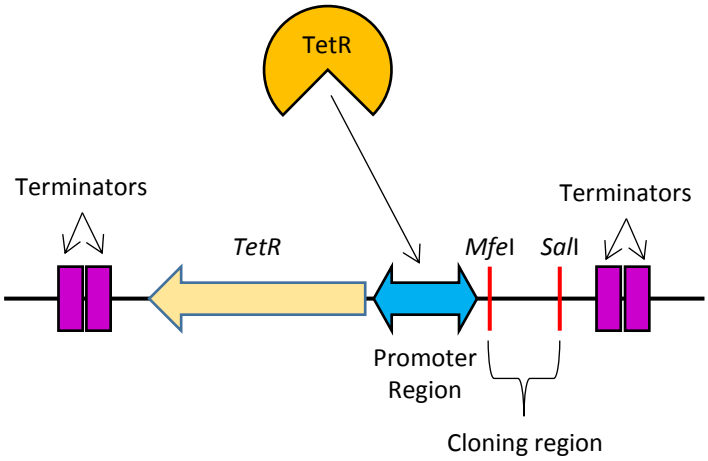

Figure 6.2: Tetracycline inducible expression system

Diagram illustrating the tetracycline inducible expression system. The promoter region contains two promoters each facing a different direction. When *TetR* is expressed, TetR binds on the promoter region silencing both promoters and hence not allowing the transcription of any gene present in the cloning region. When tetracycline is present, it binds competitively to TetR and thus allows the promoters to stay active.

6.5 Markerless Chromosomal Gene Deletions in *M. Psychrotolerans*

As mentioned previously, *M. psychrotolerans* contained a histidine decarboxylase gene that was responsible for producing histamine from histidine. Since this gene is responsible for potential toxicity, it was used as the target for chromosomal gene deletion using the method described in Chapter 2.

The flanking chromosomal regions of histidine decarboxylase were used as regions of complementarity for recombination. Two fragments were successfully created using PCR which constituted to 612 bp upstream and 572 bp downstream of the gene (Figure 6.3). The two flanking regions were then used as a template in a subsequent PCR which yielded a 1,152 bp insert sequence (Figure 6.4a). This contained the two flanking regions of the histidine decarboxylase gene which were complementary to the flanking regions of the chromosome next to either side of the wild type gene. The insert sequence also contained 6 bp of the wild type gene (6 from the 5' end of the gene and 6 from the 3' end) which equated to a deleted version of histidine decarboxylase. Figure 3b shows the insert sequence containing the *Eco*RI restriction sites for incorporation into pK18mobSacB in subsequent stages.

Since the insert sequence was ready for incorporation into the suicide vector, a Gibson Assembly was performed. The primers HisDecFlt-F and HisDecFlt-R were used in the reaction (described in detail in Chapter 2). Electrophoresis of the assembly product shown in figure 3 shows the size of the resulting pK18mobSacB+Ins. The original size of the plasmid was 4.7 kb, however this result showed the presence of a band between 5.0 and 6.0 kb and closer to the 6.0 marker (Figure 6.5). This strongly suggested that the insert was integrated into the plasmid. To further verify the presence of the insert inside pK18mobSacB, primers that bind upstream and downstream of the insert on the plasmid were used in a PCR. The agarose gel electrophoresis of the PCR product revealed the presence of a band of approximately 1.5 kb (Figure 6.6). This suggested that the full insert was incorporated into the plasmid. Sequencing results obtained using the same primers confirmed the correct sequence of the insert present inside the vector. With the suicide vector construction being complete, transformations of *M. psychrotolerans* were performed.

Using the Gibson Assembly product which contained the pK18mobSacB+ins product, a transformation of electrocompetent *M. psychrotolerans* was performed as per protocol in Chapter 2. The antibiotic screening post-transformation yielded only 2 colonies when 2µl of Gibson Assembly mix was used for the transformation. However after diluting the mix 1in 4, the number of colonies after transformation observed were 5, suggesting that a lower concentration of the mix works better due to compounds present in the mix that might affect transformation yields.

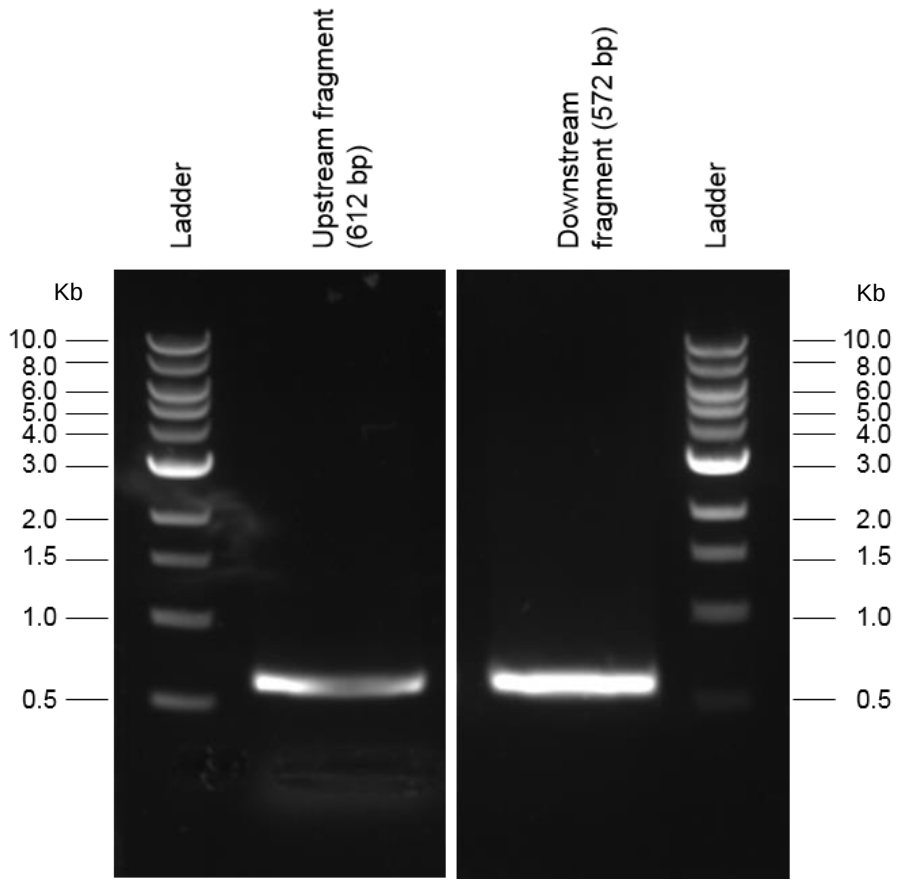

Figure 6.3: Flanking PCR products for the assembly of the faulty *hdc* gene

Agarose gels (0.8% agarose) showing the PCR products made up of the upstream fragment (left) and downstream fragment (right) of the wild-type histidine decarboxylase.

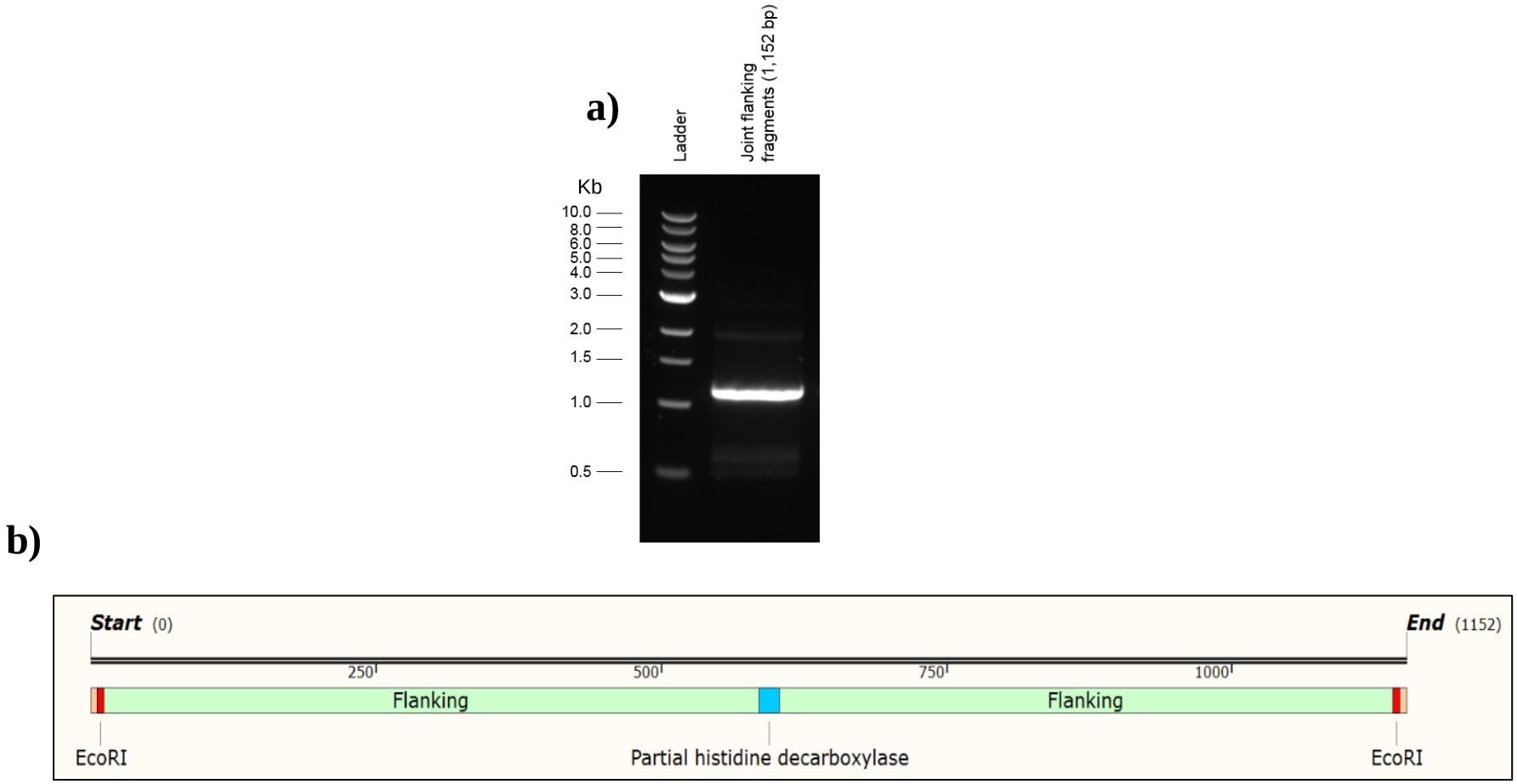

Figure 6.4: Assembly of PCR flanking products

a) Agarose gel showing a clear band at approximately 1.1 kb which suggested that the two flanking fragments had joined through PCR and b) the sequence representation that the band equates to.

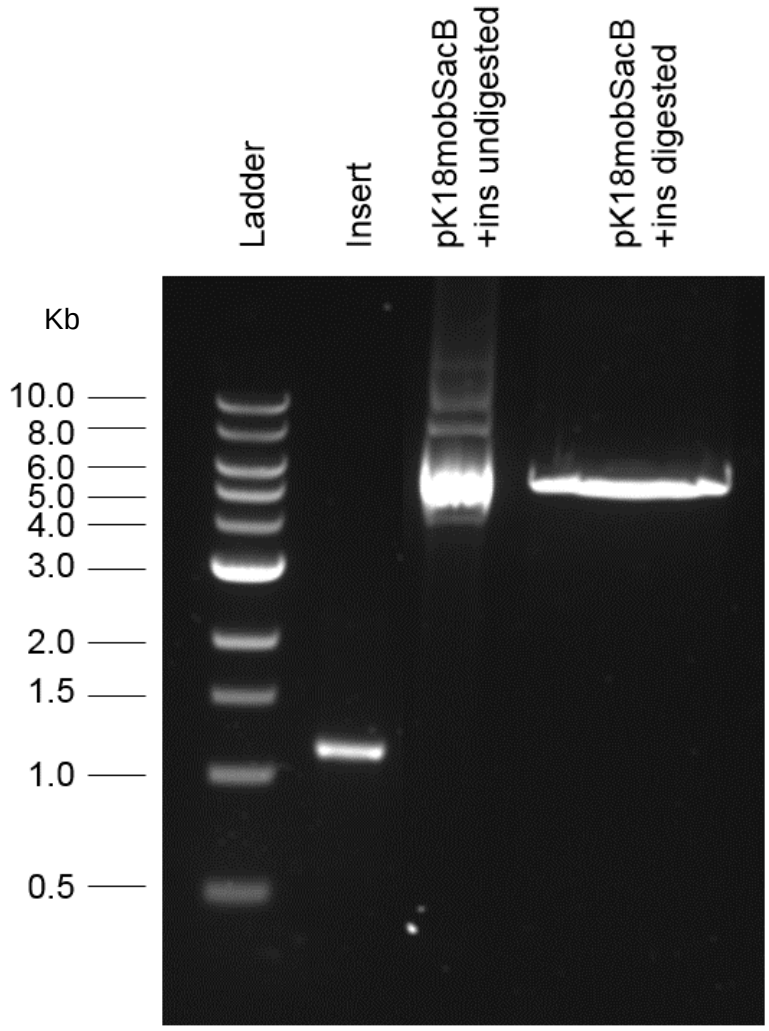

Figure 6.5: Confirmation of pK18mobsacB size with the faulty gene insert

Agarose gel (0.8% agarose) showing the size of the plasmid after the insert was integrated into it.

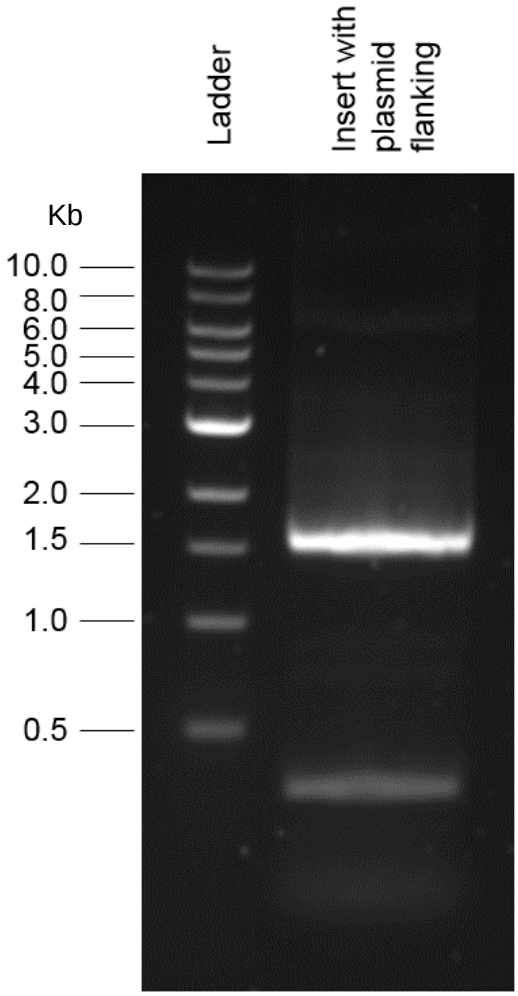

Figure 6.6: Confirmation of the presence of the faulty gene inside pK18mobsacB

Agarose gel (0.8% agarose) showing the presence of the insert inside pK18mobSacB. The increased size of the band is caused by the sequencing primers binding approximately 200 bp upstream and downstream of the insert giving rise to a band of approximately 1.5 kb.

Following the transformations of *M. psychrotolerans* with the modified pK18mobSacB+ins vector, colonies were subcultured in liquid LB_{ns} for 24 hours at 20^{o}C. The next step was to spread the grown cultures on agar plates containing 10% sucrose to select for clones that do not contain the vector but that might have recombined to form a deletion mutant. The plates showed a high level of growth after incubation which suggested that 10% sucrose was not very efficient in killing all the clones containing the vector. All the single colonies that were obtained were replica plated onto no selection and kanamycin containing agar plates to see which clones had grown without the presence of the suicide plasmid. Nevertheless, single colonies were picked and streaked on a no selection plate as well as a kanamycin selection agar plate.

Incubation of the no selection plate and the kanamycin plate at 20^{o}C for 48 hours resulted in all clones failing to grow in kanamycin but all showed growth in the no selection plate. The total number of clones tested this way was 64. All 64 clones from the no selection plate were used for a colony PCR using primers HisDecFF and HisDecRF which bind approximately 500 bp upstream and downstream of the *hdc* gene. Figure 6.7 shows the presence of 5 clones that contained a band close to 1.1 kb which was the expected sized band corresponding to the deleted gene size. The rest of the clones showed either the wild-type gene being present or both sizes which suggested they were merodiploid.

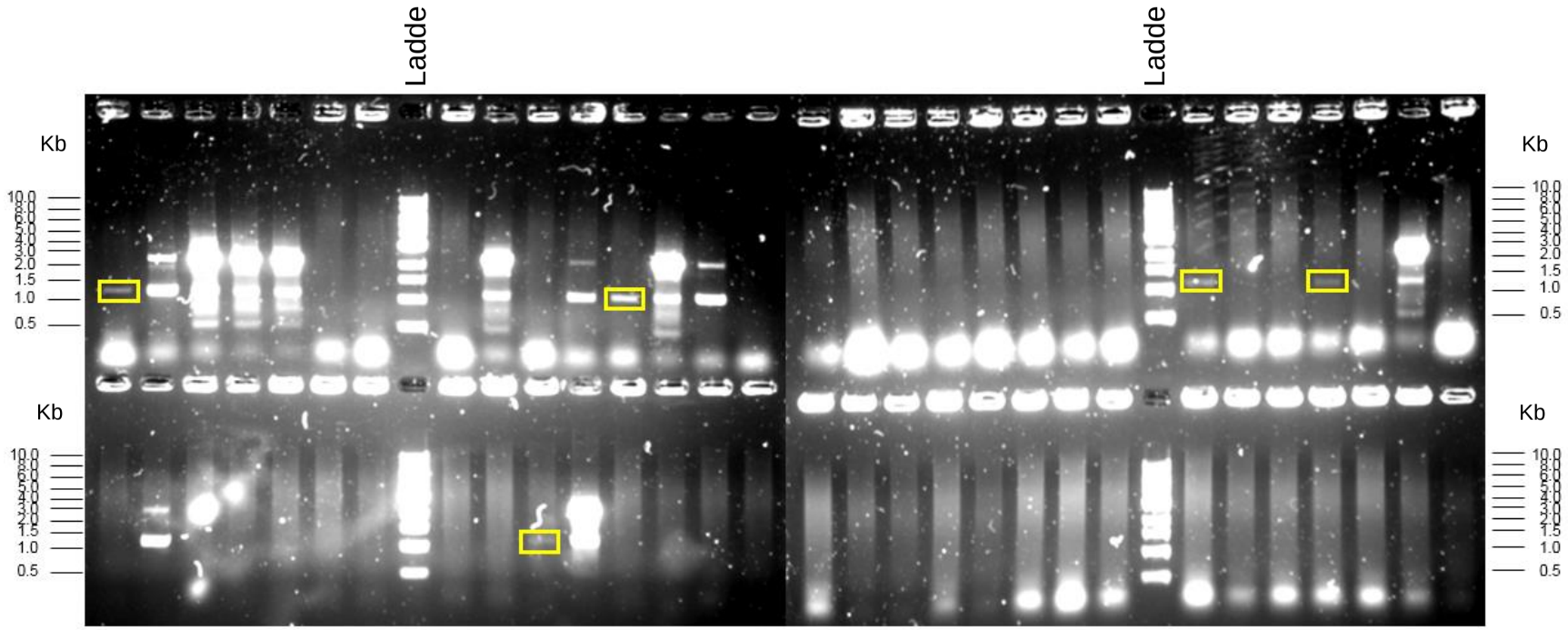

Figure 6.7: Screening of deletion mutants by PCR

Colony PCR samples from the 64 colonies samples from the no selection plates. Colonies were screened for the presence of the 1,152 bp band and absence of the 2,271 bp band indicating the presence of the modified histidine decarboxylase and the absence of the wild-type gene. The yellow boxes highlight the presence of the 1,152 bp DNA fragment potentially indicating the successful deletion of the *hdc* gene.

The colony PCR suggested that 5 clones may potentially be deletion mutants. A subsequent PCR was also performed on specifically those 5 clones in order to verify the absence of the wild-type gene. The PCR primers used were HisDecFF, HisDecRF and 291R. Figure 6.8a shows which position each primer binds to as well as the possible fragment sizes expected from each primer combination. Figure 6.8b shows the agarose gel of those 5 clones. Each clone was used in a PCR reaction with primers HisDecFF and HisDecRF as well as a separate PCR including HisDecFF and 291R. Clone 1 revealed the presence of a wild-type gene size (well 3 and 4). Clones 2, 3, 4 and 5 also were shown to contain the wild-type gene, although they also contained the 1,152 bp fragment which suggested these clones were merodiploid containing both the wild-type histidine decarboxylase as well as the deleted version.

A deletion mutant was not obtained thus far, therefore further transformations were performed, using the suicide vector pK18mobSacB+Ins, and the screening process was repeated. A total of 364 colonies were screened for the absence of the *hdc* gene. In all cases the gene was still present and a deletion did not occur. More transformations and screening will need to be performed in order to thoroughly test the effectiveness of this method in deleting chromosomal genes in *M. psychrotolerans*.

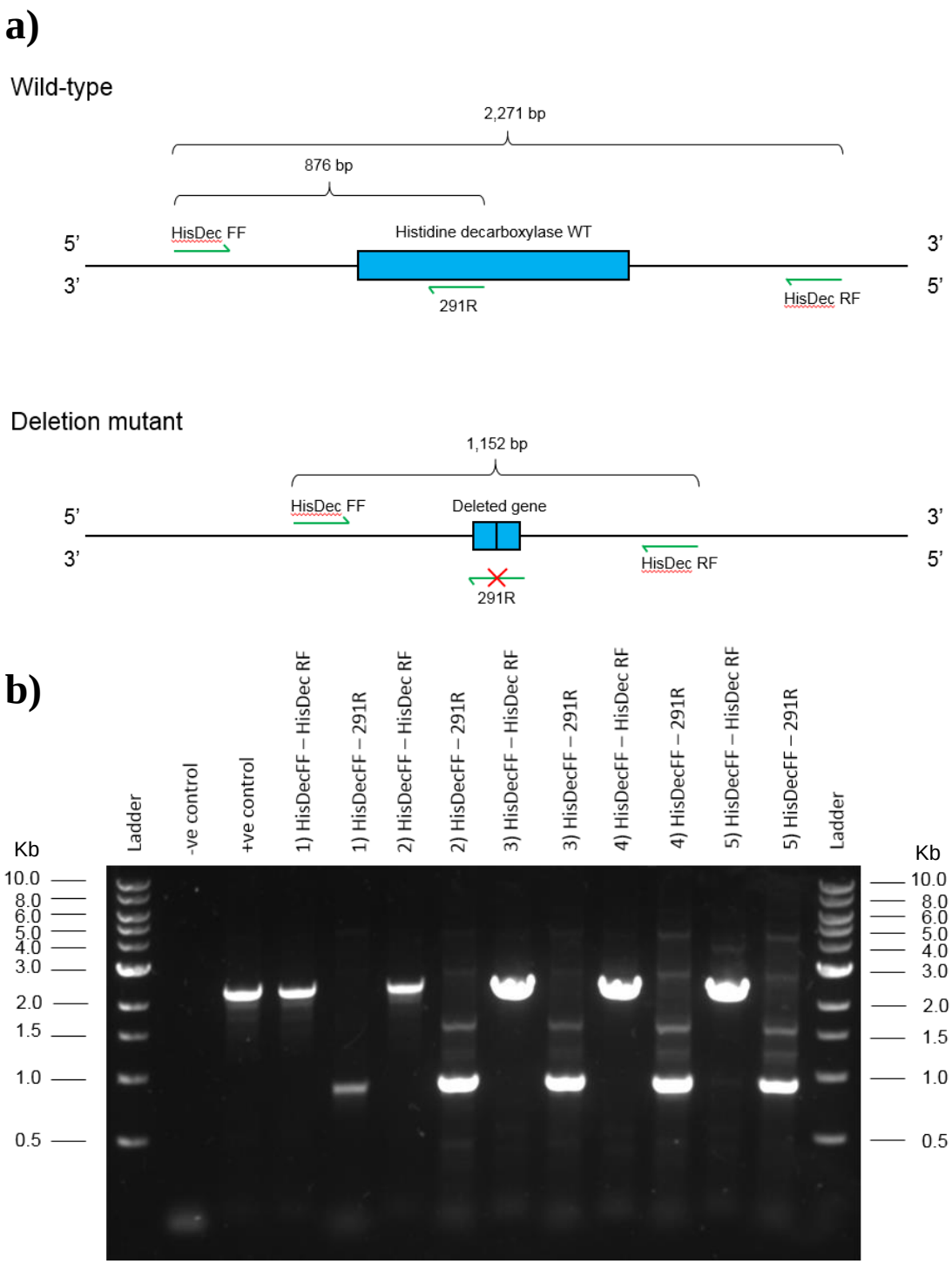

Figure 6.8: Expected sizes of PCR products and screening for mutants

a) Expected sizes for products arising from PCR with HisDecFF, HisDecRF and 291R. b) Screening of 5 potential deletion mutants for histidine decarboxylase using HisDecFF, HisDecRF primers.

6.6 Discussion

M. psychrotolerans, as described previously, is a relatively newly identified species (Emborg 2006). This meant that there is a lack of scientific studies on this organism. Prior to this study there was no genetic or proteomic information available on this organism and targeted genetic modifications were impossible due to this reason. Moreover, the mechanism of nanoparticle synthesis was not identified due to the lack of genetic sequence. This thesis went ahead to study *M. psychrotolerans* U2/3 in much deeper detail than before by revealing its genetic and proteomic makeup.

The antibiotic susceptibility results according to Emborg *et al.*, described *M. psychrotolerans* as being sensitive to apramycin, ceftiofur, chloramphenicol, ciprofloxacin, florfenicol, gentamicin, nalidixic acid, neomycin, spectinomycin, streptomycin, sulfamethoxazole and trimethoprim. However the results obtained in this study were in contrast with the literature. The antibiotic assay revealed that *M. psychrotolerans* was actually resistant to chloramphenicol even at concentrations of 80 µg/ml. This meant that it was not possible to use plasmids with chloramphenicol resistance markers for transformations of *M. psychrotolerans*.

With the antibiotic sensitivity profile established, a range of vectors were selected for transformations. The only vector that was able to replicate in *M. psychrotolerans* was found to be pSUP404.2 which is a broad host range plasmid with chloramphenicol and kanamycin resistance cassettes (detailed in Chapter 2). The rest of the vectors did not yield any successful transformants for a number of possible reasons such as not offering a competitive advantage or the transformation protocol needed further optimisation to increase efficiency. *M. psychrotolerans* contains a Type I restriction modification system which might have been responsible for degrading the plasmids upon entering the cell. The organism also contains an active *recA* gene which could be responsible for causing the plasmids to integrate into the chromosome with loss of function of the antibiotic resistance cassette. Another possibility is that the origins of replication of the plasmids might have been incompatible with the genetic makeup of *M. psychrotolerans*. Despite plasmids having the ability to replicate autonomously, they often use the host's replication mechanism to propagate, therefore having similar origins of replication with the host would be beneficial (del Solar, Giraldo *et al.* 1998).

Of all the plasmids tested for their ability to replicate in *M. psychrotolerans*, only the vector pSUP404.2 was able to do so and was maintained within the cell after several generations of growth, suggesting that it was stable enough to survive in the cell as well as provide resistance to *M. psychrotolerans* from kanamycin. In the case of chemical transformations of this organism with the same vector, no transformants were obtained. This suggested that the heat shock during the transformation was not enough to induce uptake of extracellular DNA, or that the method for preparing competent *M. psychrotolerans* cells was not optimised. Several attempts were performed to increase competency by varying the heat shock temperature and incubation times, however without success. *M. psychrotolerans* had not had its viability affected during the chemical transformation method as it was still able to grow in media without a selection marker. It has been reported that kanamycin chelates Cu^{2+} and therefore this might cause problems when performing Cu resistance assays using transformants that contain plasmid expressing kanamycin cassettes (Szczepanik, Kaczmarek et al. 2002). Therefore the kanamycin cassette would need to be swapped for a different antibiotic such as tetracycline or nalidixic acid.

Analysis of pSUP404.2 was performed in an attempt to find the unique properties that allowed the vector to successfully replicate and survive inside *M. psychrotolerans*. The main backbone of the plasmid was taken from *E. coli* pACYC177 which contained the ampicillin and kanamycin antibiotic cassettes. The backbone was joined with a 6.0 kb fragment RSF1010 which contained the determinants essential for mobilisation (*mob B, C*) and also replication (*repB, D, F, A, C*). Since the mobilisation factors are essential for bacterial conjugation, it was hypothesised that conjugation may also be used for bacterial transformation of *M. psychrotolerans,* however this was not tested. The ampicillin resistance cassette was also replaced with a chloramphenicol resistance cassette derived from phage P1. The presence of the RSF1010 fragment was important for the vector's replication in the organism and therefore is the reason for its stability. Although pSUP404.2 replicated in *M. psychrotolerans*, it is a large low copy plasmid with no suitable restriction sites for inserting genes.

After selecting the vector for transformations of *M. psychrotolerans*, pSUP404.2 was modified by inserting two restriction sites *Sal*I and *Mfe*I, in order to allow for directed gene insertions. An inducible expression system was designed for *M. psychrotolerans*

using the pSUP404.2 vector and the *tetR* inducible system from pMIND (Blokpoel, Murphy *et al.* 2005). The method of induction is described by (Blokpoel, Murphy *et al.* 2005). Tetracycline presence in the growth medium inhibits the binding of TetR to the promoter region which then in turn activates the transcription of the gene present in the cloning region. The vector was designed in such a way that the gene to be induced could be easily replaced with any other gene or series of genes using the restriction enzymes *Mfe*I and *Sal*I. The vector designed for synthesis by Genewiz contained the sequence coding for RFP which would be used as a reporter for the successful expression of the gene by tetracycline induction. Due to the size of the plasmid and the problems the company had with the gene synthesis, it was not possible to perform the experiments needed to validate the expression of the reporter.

M. psychrotolerans was first isolated by Emborg *et al.* (2006) from cold-smoked tuna associated with food poisoning. It was found to be a producer of high levels of histamine as it utilised the proteins from the tuna to convert it into histamine. Using the genome sequence revealed in this study, a gene involved in the histamine production pathway was identified; histidine decarboxylase (*hdc)*. This gene is responsible for the production of the protein involved in the catalysis of histidine into histamine (Podeur, Dalgaard *et al.* 2015). It is not fully understood why bacteria produce histamine from histidine (Emborg, Laursen *et al.* 2005), however *hdc* is not an essential gene for growth and therefore deleting the gene should not affect survival rates. In order for *M. psychrotolerans* to be industrially relevant, this gene would have to be deleted to make it safer for use. Since a method for chromosomal deletions was being developed, histidine decarboxylase was chosen to be the target gene for deletion.

The method chosen for creating the deletion mutant was adapted from a method for creating markerless chromosomal deletions in *Bdellovibrio bacteriovorus* (Steyert and Pineiro 2007). The protocol was improved through several attempts to create the correct insert for making the deletion. The method involved making a deleted version of histidine decarboxylase which would subsequently replace the wild-type version through recombination with a suicide plasmid (See Chapter 2). The reasons for the chosen method of gene deletion were based on the lack of stable plasmids that replicate efficiently in *M. psychrotolerans* and the benefit of generating mutants without adding antibiotic cassettes increasing its resistance to more antibiotics which is unsuitable for

industrial purposes. The construction of the insert was successful and it was then inserted into pK18mobSacB suicide plasmid, which was then also successfully inserted into *M. psychrotolerans*.

Transformations with pK18mobSacB in this study were not successful as the plasmid was not able to replicate in *M. psychrotolerans*. However the method for chromosomal gene deletions requires the plasmid to integrate into the region of homology. The plasmid pK18mobSacB+ins contained the faulty gene as well as flanking regions of homology that correspond to the flanking regions of the wild-type gene. It was inserted and recombined effectively as growth on kanamycin selection was observed after transformation. Screening of the transformants for the deletion mutant did not show any clones without the wild-type fragment. This might be due to a low double recombination rate, low sucrose induction and effectiveness or the presence of revertants. The screening was performed using PCR annealing on DNA flanking the *hdc* gene. The false positives observed in the first round of screening could be due to possible cross-contamination of DNA. This could be avoided in the future by designing primers that anneal at a different part of the flanking DNA sequence that has not been amplified in the lab before. Another possible method for screening for the correct mutants would be by performing a Southern Blot, albeit with a lower throughput.

Although 384 clones were tested using this chromosomal gene deletion method, it is still too early to tell whether this method does not work. More clones will need to be screened for the deletion of the gene to establish whether the method is effective. In case the method does not yield a deletion mutant after enough screenings, the method will need to be optimised by adding varying concentrations of sucrose to test for their effect on selecting the correct clones. Growing *M. psychrotolerans* in liquid media containing sucrose may prove more effective in selecting the correct clones rather than on agar plates. An alternative method to make a chromosomal deletion would involve the use of a λ prophage that would provide the function to protect and recombine linear pieces of DNA substrates inside the cell. This method has proved successful in *E. coli* and uses recombination to alter chromosomal DNA in a similar way to the current method being tested (Mosberg, Lajoie *et al.* 2010). Another method that can be used is the CRISPR/Cas9 system which has shown very promising results with very high

efficiencies in deleting single and multiple chromosomal genes (Jiang, Chen *et al.* 2015).

Chapter 7. Discussion

The main aim of this doctorate study was to develop a biological method of removing toxic concentrations of Cu ions from whisky distillery waste and to convert them into a form that is of further use. In my findings in chapter 2, I showed that it is possible to synthesise CuNPs using *M. psychrotolerans*. The nanoparticles showed long-term (over 6 weeks) stability and resistance against oxidation and retained their pure zero valent form over the course of the experiments. Although the majority of research was performed in media prepared in the laboratory rather than co-products from whisky distilleries, the research showed the potential of using *M. psychrotolerans* as a means for bioremediating whisky distillery waste. The organism not only survived, but thrived in distillery co-products and produced nanoparticles.

Prior to this study, there was little knowledge of *M. psychrotolerans* as a nanoparticle producing organism. *M. psychrotolerans* had only been used for the production of AgNPs (Parikh, Singh *et al.* 2008). Although it was known that it was possible to synthesise AgNPs using this organism, the synthesis mechanism had not been proved.

By sequencing its genome and performing proteomics, it was possible to shed more light into the characteristics of the organism as well as gain a better understanding of the CuNP synthesis pathway. As mentioned previously, the exact method of Cu ion reduction as well as the capping compound stabilising the nanoparticles were not known. Through this study, a revised pathway for CuNP synthesis was suggested based on the previous literature, genomics, proteomics and gene transcript analysis. It is worth noting however that this newly suggested pathway would need more work in order to verify it, in the form of chromosomal gene deletion mutants specific to the genes involved in the suggested pathway. Nevertheless, this work was able to improve upon the existing pathway for CuNP synthesis present in the current literature.

Significant strides were also made in identifying the stabilising compound surrounding the CuNPs. It is widely known that many biologically synthesised metallic nanoparticles contain a capping compound found on their surface that provides stability and protection from oxidation (Brun and Sicard – Roselli 2014). Besides the studies in which known compounds have been added manually in order to induce nanoparticle stabilisation, there is very little knowledge on biologically made capping

compounds. Moreover, a study on *M. morganii* also discussed a possible capping compound on the surface of CuNPs produced by this organism (Ramanathan, Field *et al.* 2013). In the study presented here, the stability of the CuNPs produced by *M. psychrotolerans* was also thought to be attributed to the presence of a capping compound on their surface. By using MALDI, it was not possible to identify a compound bound to the nanoparticles. This may have been due to "masking" of the compound's peak by the presence of another compound at a similar molecular weight or the fact that it may have been too small to detect using the instrument. To identify the presence of the compound, a mass spectrometer that is able to detect smaller molecular weight compounds would need to be used.

After synthesising the CuNPs using *M. psychrotolerans* and verifying their purity, the next step was to use them in an application. In collaboration with the SMC, it was possible to print the CuNPs using an inket printer and form a continuous electrode. The resulting electrode was verified to be conductive, despite having a relatively high resistance, possibly caused by impurities or partial oxidation due to the electrode been stored under oxic conditions for prolonged periods of time. With some further optimisation, CuNPs synthesised in this study have a great potential to be used as "ink" for printing microcircuits and electrodes for microelectronics. Further work will need to be carried out involving optimisation of the purification process of CuNPs, handling and post-printing coatings to prevent oxidation and degradation.

At the start of the study, *M. psychrotolerans* was a relatively new organism and therefore no previous genetic modification studies had been performed. One of the objectives of this study was to develop a biological chassis for metallic nanoparticle synthesis. In order to accomplish this task, genetic modification tools had to be developed. A broad host range plasmid pSUP404.2, was successfully integrated into *M. psychrotolerans* and screened using antibiotic selection. Subsequently the plasmid was modified (pSUP404.3) to allow for insertion of genes in a directional manner. *M. psychrotolerans* transformations were therefore possible using the vector pSUP404.3 with good yields.

With the success of plasmid insertions into *M. psychrotolerans*, the next step was to develop a method for chromosomal gene deletions. Since *M. psychrotolerans* contains

the *hdc* gene which is responsible for producing histamine, it was used as the target for deletion. The method that had been successfully used in *B. bacteriovorus* for chromosomal gene deletions was modified for *M. psychrotolerans* (Steyert and Pineiro 2007). Over 350 clones were screened for the absence of the *hdc* gene, however no deletion mutants were obtained. Nevertheless, this research developed the basis for genetic modification of *M. psychrotolerans*, where other gene deletion protocols may be based on the suicide vector used in this method. A different method will need to be developed in order to delete the *hdc* gene from the *M. psychrotolerans* chromosome.

Ultimately the main interest of this study was to identify, investigate and improve an organism that has the potential to bioremediate whisky distillery co-products whilst also converting the contaminant into a useful material. Despite no previous studies in the area, this doctoral work provides a significant amount of knowledge and techniques developed in order to get closer to that goal. Future work could address the implementation of this technique with whisky distillery co-products in small and large scale and attempt to purify the synthesised CuNPs for further use. One could research another method of performing chromosomal gene deletions in *M. psychrotolerans* in order to further the genetic modification protocols and make this organism a unique chassis for the environmentally friendly and economical synthesis of metallic nanoparticles for a range of different metals.

Bibliography

Ahmad, A., P. Mukherjee, et al. (2002). "Enzyme mediated extracellular synthesis of CdS nanoparticles by the fungus, Fusarium oxysporum." J Am Chem Soc **124**(41): 12108-12109.

Ahmad, A., P. Mukherjee, et al. (2003). "Extracellular biosynthesis of silver nanoparticles using the fungus Fusarium oxysporum." Colloids and Surfaces B: Biointerfaces **28**(4): 313-318.

Alves, D. B., R. Silva, et al. (2015). "Copper nanoparticles stabilized by reduced graphene oxide for CO2 reduction reaction." Materials for Renewable and Sustainable Energy **4**(1): 1-7.

Amin, O. M. (2011). "The Contribution of Pathogenic Bacteria to GI Symptoms in Parasite-Free Patients." J Bacteriol Parasitol **2**(109).

Baco-Carles, V., L. Datas, et al. (2011). "Copper Nanoparticles Prepared from Oxalic Precursors." ISRN Nanotechnology **2011**: 1-7.

Baker, M. (2012). "De novo genome assembly: what every biologist should know." Nat Meth **9**(4): 333-337.

Bar, H., D. K. Bhui, et al. (2009). "Green synthesis of silver nanoparticles using latex of Jatropha curcas." Colloids and Surfaces A: Physicochemical and Engineering Aspects **339**(1–3): 134-139.

Bharde, A., D. Rautaray, et al. (2006). "Extracellular biosynthesis of magnetite using fungi." Small **2**(1): 135-141.

Blokpoel, M. C. J., H. N. Murphy, et al. (2005). "Tetracycline-inducible gene regulation in mycobacteria." Nucleic Acids Research **33**(2): e22-e22.

Bokinsky, G., P. P. Peralta-Yahya, et al. (2011). "Synthesis of three advanced biofuels from ionic liquid-pretreated switchgrass using engineered Escherichia coli." Proceedings of the National Academy of Sciences **108**(50): 19949-19954.

Bratlie, K. M., H. Lee, et al. (2007). "Platinum Nanoparticle Shape Effects on Benzene Hydrogenation Selectivity." Nano Letters **7**(10): 3097-3101.

Brun, E. and C. Sicard – Roselli (2014). "Could nanoparticle corona characterization help for biological consequence prediction?" Cancer Nanotechnology **5**(1): 7.

Cai, J., S. Kimura, et al. (2008). "Nanoporous Cellulose as Metal Nanoparticles Support." Biomacromolecules **10**(1): 87-94.

Cao, V. D., N. Q. Tran, et al. (2015). "Synergistic effect of citrate dispersant and capping polymers on controlling size growth of ultrafine copper nanoparticles." Journal of Experimental Nanoscience **10**(8): 576-587.

Capeness, M. J., M. C. Edmundson, et al. (2015). "Nickel and platinum group metal nanoparticle production by Desulfovibrio alaskensis G20." New Biotechnology **32**(6): 727-731.

Castro-Longoria, E., S. D. Moreno-Velazquez, et al. (2012). "Production of platinum nanoparticles and nanoaggregates using Neurospora crassa." J Microbiol Biotechnol **22**(7): 1000-1004.

Chen, J., B. Lim, et al. (2009). "Shape-controlled synthesis of platinum nanocrystals for catalytic and electrocatalytic applications." Nano Today **4**(1): 81-95.

Chung, W.-H., H.-J. Hwang, et al. (2015). "Flash light sintered copper precursor/nanoparticle pattern with high electrical conductivity and low porosity for printed electronics." Thin Solid Films **580**: 61-70.

Daniel, H., L. Frank, et al. (2003). "Plastic-Compatible Low Resistance Printable Gold Nanoparticle Conductors for Flexible Electronics." Journal of The Electrochemical Society **150**(7).

Das, V., R. Thomas, et al. (2014). "Extracellular synthesis of silver nanoparticles by the Bacillus strain CS 11 isolated from industrialized area." 3 Biotech **4**(2): 121-126.

Deighton, R., T. Le Bihan, et al. (2014). "The proteomic response in glioblastoma in young patients." Journal of Neuro-Oncology **119**(1): 79-89.

del Solar, G., R. Giraldo, et al. (1998). "Replication and Control of Circular Bacterial Plasmids." Microbiology and Molecular Biology Reviews **62**(2): 434-464.

Delmar, J. A., C.-C. Su, et al. (2015). "Heavy metal transport by the CusCFBA efflux system." Protein Science **24**(11): 1720-1736.

Deplanche, K., I. Caldelari, et al. (2010). "Involvement of hydrogenases in the formation of highly catalytic Pd(0) nanoparticles by bioreduction of Pd(II) using Escherichia coli mutant strains." Microbiology **156**(Pt 9): 2630-2640.

Devasenathipathy, R., K. Kohilarani, et al. (2016). "Electrochemical preparation of biomolecule stabilized copper nanoparticles decorated reduced graphene oxide for the sensitive and selective determination of hydrogen peroxide." Electrochimica Acta **191**: 55-61.

Dos Santos, C. A., M. M. Seckler, et al. (2014). "Silver Nanoparticles: Therapeutical Uses, Toxicity, and Safety Issues." Journal of Pharmaceutical Sciences **103**(7): 1931-1944.

Durán, N., P. D. Marcato, et al. (2007). "Antibacterial Effect of Silver Nanoparticles Produced by Fungal Process on Textile Fabrics and Their Effluent Treatment." Journal of Biomedical Nanotechnology **3**(2): 203-208.

Edmundson, M. C., M. Capeness, et al. (2014). "Exploring the potential of metallic nanoparticles within synthetic biology." N Biotechnol.

Edmundson, M. C. and L. Horsfall (2015). "Construction of a Modular Arsenic-Resistance Operon in E. coli and the Production of Arsenic Nanoparticles." Frontiers in Bioengineering and Biotechnology **3**(160).

El-Shanshoury, A. E.-R. R., S. E. ElSilk, et al. (2011). "Extracellular Biosynthesis of Silver Nanoparticles Using Escherichia coli ATCC 8739, Bacillus subtilis ATCC 6633, and Streptococcus thermophilus ESh1 and Their Antimicrobial Activities." ISRN Nanotechnology **2011**: 7.

El Badawy, A. M., R. G. Silva, et al. (2011). "Surface Charge-Dependent Toxicity of Silver Nanoparticles." Environmental Science & Technology **45**(1): 283-287.

Emborg, J. (2006). "Morganella psychrotolerans sp. nov., a histamine-producing bacterium isolated from various seafoods." International Journal of Systematic and Evolutionary Microbiology **56**(10): 2473-2479.

Emborg, J. and P. Dalgaard (2008). "Growth, inactivation and hsitamine formation of Morganella psychrotolerans and Morgaella morganii - development and evaluation of predicive models." International Journal of Food Microbiology **128**: 234-243.

Emborg, J. and P. Dalgaard (2008). "Modelling the effect of temperature, carbon dioxide, water activity and pH on growth and histamine formation by Morganella psychrotolerans." International Journal of Food Microbiology **128**(2): 226-233.

Emborg, J., B. G. Laursen, et al. (2005). "Significant histamine formation in tuna (Thunnus albacares) at 2 °C — effect of vacuum- and modified atmosphere-packaging on psychrotolerant bacteria." International Journal of Food Microbiology **101**(3): 263-279.

Evans, G. A. (2001). "Molecular cloning: A laboratory manual. Third edition. Volumes 1, 2, and 3. Current protocols in molecular biology. Volumes 1 and 2." Cell **61**(1): 17-18.

Falagas, M. E., P. K. Kavvadia, et al. (2006). "Morganella morganii Infections in a General Tertiary Hospital." Infection **34**(6): 315-321.

Gardea-Torresdey, J. L., J. G. Parsons, et al. (2002). "Formation and Growth of Au Nanoparticles inside Live Alfalfa Plants." Nano Letters **2**(4): 397-401.

Grass, G. and C. Rensing (2001). "Genes Involved in Copper Homeostasis in Escherichia coli." Journal of Bacteriology **183**(6): 2145-2147.

Greenwood, N., N. and A. Earnshaw (1997). *Chemistry of the Elements*, Butterworth-Heinemann.

Gudipaty, S. A., A. S. Larsen, et al. (2012). "Regulation of Cu(I)/Ag(I) efflux genes in Escherichia coli by the sensor kinase CusS." FEMS Microbiology Letters **330**(1): 30-37.

Gudipaty, S. A. and M. M. McEvoy (2014). "The histidine kinase CusS senses silver ions through direct binding by its sensor domain." Biochimica et biophysica acta **1844**(9): 1656-1661.

Gunsolus, I. L., M. P. S. Mousavi, et al. (2015). "Effects of Humic and Fulvic Acids on Silver Nanoparticle Stability, Dissolution, and Toxicity." Environmental Science & Technology **49**(13): 8078-8086.

Guzmán, M., G. D. Jean, et al. (2009). "Synthesis of silver nanoparticles by chemical reduction method and their antibacterial activity." International Journal of Chemical and Biomolecular Engineering **2**(3): 104-111.

Hanaor, D., M. Michelazzi, et al. (2012). "The effects of carboxylic acids on the aqueous dispersion and electrophoretic deposition of ZrO2." Journal of the European Ceramic Society **32**(1): 235-244.

Hao, X., F. L. Lüthje, et al. (2015). "Survival in amoeba—a major selection pressure on the presence of bacterial copper and zinc resistance determinants? Identification of a “copper pathogenicity island”." Applied Microbiology and Biotechnology **99**(14): 5817-5824.

He, S., Z. Guo, et al. (2007). "Biosynthesis of gold nanoparticles using the bacteria Rhodopseudomonas capsulata." Materials Letters **61**(18): 3984-3987.

Huang, H. H., F. Q. Yan, et al. (1997). "Synthesis, Characterization, and Nonlinear Optical Properties of Copper Nanoparticles." Langmuir **13**(2): 172-175.

Huang, X.-Y., F. Deng, et al. (2016). "A heavy metal P-type ATPase OsHMA4 prevents copper accumulation in rice grain." Nat Commun **7**.

Husseiny, M. I., M. A. El-Aziz, et al. (2007). "Biosynthesis of gold nanoparticles using Pseudomonas aeruginosa." Spectrochimica Acta Part A: Molecular and Biomolecular Spectroscopy **67**(3-4): 1003-1006.

Ilyas, S., A. Rehman, et al. (2016). "Proteomic analysis of an environmental isolate of Rhodotorula mucilaginosa after arsenic and cadmium challenge: Identification of a protein expression signature for heavy metal exposure." J Proteomics **141**: 47-56.

Institute, A. N. S. (2000). Standard Practice for Calibration of the Electron Binding-Energy Scale of an X-Ray Photoelectron Spectrometer, Annual Book of ASTM Standards**:** 1-16.

Iravani, S. (2014). "Bacteria in Nanoparticle Synthesis: Current Status and Future Prospects." International Scholarly Research Notices **2014**: 18.

Jang, G. G., C. B. Jacobs, et al. (2015). "Size tunable elemental copper nanoparticles: extracellular synthesis by thermoanaerobic bacteria and capping molecules." Journal of Materials Chemistry C **3**(3): 644-650.

Jiang, Y., B. Chen, et al. (2015). "Multigene Editing in the Escherichia coli Genome via the CRISPR-Cas9 System." Applied and Environmental Microbiology **81**(7): 2506-2514.

Johnston, C. W., M. A. Wyatt, et al. (2013). "Gold biomineralization by a metallophore from a gold-associated microbe." Nat Chem Biol **9**(4): 241-243.

Kalimuthu, K., R. Suresh Babu, et al. (2008). "Biosynthesis of silver nanocrystals by Bacillus licheniformis." Colloids Surf B Biointerfaces **65**(1): 150-153.

Kang, J., H. Kim, et al. (2010). "Inkjet printed electronics using copper nanoparticle ink." Journal of Materials Science: Materials in Electronics **21**(11): 1213-1220.

Kasthuri, J., K. Kathiravan, et al. (2009). "Phyllanthin-assisted biosynthesis of silver and gold nanoparticles: a novel biological approach." Journal of Nanoparticle Research **11**(5): 1075-1085.

Katz, A., A. Alimova, et al. (2003). "Bacteria size determination by elastic light scattering." Selected Topics in Quantum Electronics, IEEE Journal of **9**(2): 277-287.

Keen, N. T., S. Tamaki, et al. (1988). "Improved broad-host-range plasmids for DNA cloning in gram-negative bacteria." Gene **70**(1): 191-197.

Kemp, M. M., A. Kumar, et al. (2009). "Synthesis of Gold and Silver Nanoparticles Stabilized with Glycosaminoglycans Having Distinctive Biological Activities." Biomacromolecules **10**(3): 589-595.

Krishnaraj, C., E. G. Jagan, et al. (2010). "Synthesis of silver nanoparticles using Acalypha indica leaf extracts and its antibacterial activity against water borne pathogens." Colloids and Surfaces B: Biointerfaces **76**(1): 50-56.

Kulathila, R., R. Kulathila, et al. (2011). "Crystal Structure of Escherichia coli CusC, the Outer Membrane Component of a Heavy Metal Efflux Pump." PLoS ONE **6**(1): e15610.

Kuzma, A., M. Weis, et al. (2012). "Influence of surface oxidation on plasmon resonance in monolayer of gold and silver nanoparticles." Journal of Applied Physics **112**(10): 103531.

Lanza, A. M., K. A. Curran, et al. (2014). "A condition-specific codon optimization approach for improved heterologous gene expression in Saccharomyces cerevisiae." BMC Systems Biology **8**(1): 1-10.

Laudenslager, M. J., J. D. Schiffman, et al. (2008). "Carboxymethyl Chitosan as a Matrix Material for Platinum, Gold, and Silver Nanoparticles." Biomacromolecules **9**(10): 2682-2685.

Li, X., H. Xu, et al. (2011). "Biosynthesis of Nanoparticles by Microorganisms and Their Applications." Journal of Nanomaterials **2011**: 16.

Li, Y., Y. Wu, et al. (2005). "Facile Synthesis of Silver Nanoparticles Useful for Fabrication of High-Conductivity Elements for Printed Electronics." Journal of the American Chemical Society **127**(10): 3266-3267.

Lima, E., R. Guerra, et al. (2013). "Gold nanoparticles as efficient antimicrobial agents for Escherichia coli and Salmonella typhi." Chem Cent J **7**(1): 11.

Lloyd, J. R., P. Yong, et al. (1998). "Enzymatic recovery of elemental palladium by using sulfate-reducing bacteria." Appl Environ Microbiol **64**(11): 4607-4609.

Lukman, A. I., B. Gong, et al. (2011). "Facile synthesis, stabilization, and anti-bacterial performance of discrete Ag nanoparticles using Medicago sativa seed exudates." J Colloid Interface Sci **353**(2): 433-444.

Lyubchenko, Y. L. and L. S. Shlyakhtenko (1997). "Visualization of supercoiled DNA with atomic force microscopy in situ." Proceedings of the National Academy of Sciences of the United States of America **94**(2): 496-501.

Ma, Y., N. Li, et al. (2005). "One-step synthesis of amino-dextran-protected gold and silver nanoparticles and its application in biosensors." Analytical and Bioanalytical Chemistry **382**(4): 1044-1048.

Mafuné, F., J.-y. Kohno, et al. (2003). "Formation of Stable Platinum Nanoparticles by Laser Ablation in Water." The Journal of Physical Chemistry B **107**(18): 4218-4223.

McFarland, A. D. and R. P. Van Duyne (2003). "Single Silver Nanoparticles as Real-Time Optical Sensors with Zeptomole Sensitivity." Nano Letters **3**(8): 1057-1062.

Merson, S. and P. Evans (2003). "A high accuracy reference method for the determination of minor elements in steel by ICP-OES." Journal of Analytical Atomic Spectrometry **18**(4): 372-375.

Miroux, B. and J. E. Walker (1996). "Over-production of Proteins inEscherichia coli: Mutant Hosts that Allow Synthesis of some Membrane Proteins and Globular Proteins at High Levels." Journal of Molecular Biology **260**(3): 289-298.

Mohanraj, V. J. and Y. Chen (2006). "Nanoparticles – A Review." Tropical Journal of Pharmaceutical Research **5**(1): 561-573.

Montazer, M., A. Shamei, et al. (2014). "Synthesis of nanosilver on polyamide fabric using silver/ammonia complex." Mater Sci Eng C Mater Biol Appl **38**: 170-176.

Mosberg, J. A., M. J. Lajoie, et al. (2010). "Lambda Red Recombineering in Escherichia coli Occurs Through a Fully Single-Stranded Intermediate." Genetics **186**(3): 791-799.

Mukherjee, P., M. Roy, et al. (2008). "Green synthesis of highly stabilized nanocrystalline silver particles by a non-pathogenic and agriculturally important fungus T. asperellum." Nanotechnology **19**(7): 075103.

Muller, S. (2015). "Role and Regulation of Glutathione Metabolism in Plasmodium falciparum." Molecules **20**(6): 10511-10534.

Munson, G. P., D. L. Lam, et al. (2000). "Identification of a copper-responsive two-component system on the chromosome of Escherichia coli K-12." J Bacteriol **182**(20): 5864-5871.

Naderer, M., J. R. Brust, et al. (2002). "Mobility of a Restriction-Modification System Revealed by Its Genetic Contexts in Three Hosts." Journal of Bacteriology **184**(9): 2411-2419.

Naila, A., D. Nadia, et al. (2014). Stable Silver Nanoparticles Synthesis by Citrus Sinensis (Orange) and Assessing Activity Against Food Poisoning Microbes, Biomed Environ Sci. 2014 Oct;27(10):815-8. doi: 10.3967/bes2014.118.

Narayanan, K. B. and N. Sakthivel (2010). "Biological synthesis of metal nanoparticles by microbes." Advances in Colloid and Interface Science **156**(1-2): 1-13.

Nasrollahzadeh, M., S. M. Sajadi, et al. (2015). "Immobilization of copper nanoparticles on perlite: Green synthesis, characterization and catalytic activity on aqueous reduction of 4-nitrophenol." Journal of Molecular Catalysis A: Chemical **400**: 22-30.

Nevalainen, H., P. Suominen, et al. (1994). "On the safety of Trichoderma reesei." J Biotechnol **37**(3): 193-200.

Nies, D. H. (2003). "Efflux-mediated heavy metal resistance in prokaryotes." FEMS Microbiol Rev **27**(2-3): 313-339.

Pantidos, N. and E. L. Horsfall (2014). "Biological synthesis of metallic nanoparticles by bacteria, fungi and plants." Nanomedicine & Nanotechnology **5**(233).

Parikh, R. Y., R. Ramanathan, et al. (2011). "Genus-Wide Physicochemical Evidence of Extracellular Crystalline Silver Nanoparticles Biosynthesis by Morganella spp." PLoS ONE **6**(6): e21401.

Parikh, R. Y., S. Singh, et al. (2008). "Extracellular synthesis of crystalline silver nanoparticles and molecular evidence of silver resistance from Morganella sp.: towards understanding biochemical synthesis mechanism." Chembiochem **9**(9): 1415-1422.

Parikh, R. Y., S. Singh, et al. (2008). "Extracellular Synthesis of Crystalline Silver Nanoparticles and Molecular Evidence of Silver Resistance fromMorganellasp.: Towards Understanding Biochemical Synthesis Mechanism." ChemBioChem **9**(9): 1415-1422.

Park, Y., Y. N. Hong, et al. (2011). "Polysaccharides and phytochemicals: a natural reservoir for the green synthesis of gold and silver nanoparticles." Nanobiotechnology, IET **5**(3): 69-78.

Parker, H. L., E. L. Rylott, et al. (2014). "Supported Palladium Nanoparticles Synthesized by Living Plants as a Catalyst for Suzuki-Miyaura Reactions." PLoS ONE **9**(1): e87192.

Podeur, G., P. Dalgaard, et al. (2015). "Development of a real-time PCR method coupled with a selective pre-enrichment step for quantification of Morganella morganii and Morganella psychrotolerans in fish products." International Journal of Food Microbiology **203**: 55-62.

Pollmann, K., J. Raff, et al. (2006). "Metal binding by bacteria from uranium mining waste piles and its technological applications." Biotechnol Adv **24**(1): 58-68.

Priefer, U. B., R. Simon, et al. (1985). "Extension of the host range of Escherichia coli vectors by incorporation of RSF1010 replication and mobilization functions." J Bacteriol **163**(1): 324-330.

Pugazhenthiran, N., S. Anandan, et al. (2009). "Microbial synthesis of silver nanoparticles by Bacillus sp." Journal of Nanoparticle Research **11**(7): 1811-1815.

Rai, M., A. Yadav, et al. (2009). "Silver nanoparticles as a new generation of antimicrobials." Biotechnol Adv **27**(1): 76-83.

Ramanathan, R., M. R. Field, et al. (2013). "Aqueous phase synthesis of copper nanoparticles: a link between heavy metal resistance and nanoparticle synthesis ability in bacterial systems." Nanoscale **5**(6): 2300-2306.

Ramanathan, R., A. P. O'Mullane, et al. (2011). "Bacterial Kinetics-Controlled Shape-Directed Biosynthesis of Silver Nanoplates UsingMorganella psychrotolerans." Langmuir **27**(2): 714-719.
Randall, C. P., A. Gupta, et al. (2015). "Silver resistance in Gram-negative bacteria: a dissection of endogenous and exogenous mechanisms." Journal of Antimicrobial Chemotherapy.
Raveendran, P., J. Fu, et al. (2003). "Completely "Green" Synthesis and Stabilization of Metal Nanoparticles." Journal of the American Chemical Society **125**(46): 13940-13941.
Ren, L., J. Chong, et al. (2015). "Determination of Cu2+ ions release rate from antimicrobial copper bearing stainless steel by joint analysis using ICP-OES and XPS." Materials Technology **30**(sup3): B86-B89.
Riddin, T. L., M. Gericke, et al. (2006). "Analysis of the inter- and extracellular formation of platinum nanoparticles by Fusarium oxysporum f. sp. lycopersici using response surface methodology." Nanotechnology **17**(14): 3482-3489.
Rosenthaler, J., B. M. Guirard, et al. (1965). "Purification and properties of histidine decarboxylase from Lactobacillus 30a." Proceedings of the National Academy of Sciences of the United States of America **54**(1): 152-158.
Saha, S., A. Pal, et al. (2009). "Photochemical Green Synthesis of Calcium-Alginate-Stabilized Ag and Au Nanoparticles and Their Catalytic Application to 4-Nitrophenol Reduction." Langmuir **26**(4): 2885-2893.
Sanghi, R. and P. Verma (2009). "Biomimetic synthesis and characterisation of protein capped silver nanoparticles." Bioresour Technol **100**(1): 501-504.
Schäfer, A., A. Tauch, et al. (1994). "Small mobilizable multi-purpose cloning vectors derived from the Escherichia coli plasmids pK18 and pK19: selection of defined deletions in the chromosome of Corynebacterium glutamicum." Gene **145**(1): 69-73.
Schluter, M., T. Hentzel, et al. (2014). "Synthesis of novel palladium(0) nanocatalysts by microorganisms from heavy-metal-influenced high-alpine sites for dehalogenation of polychlorinated dioxins." Chemosphere **11**: 462-470.
Shankar, S. S., A. Rai, et al. (2004). "Rapid synthesis of Au, Ag, and bimetallic Au core–Ag shell nanoparticles using Neem (Azadirachta indica) leaf broth." Journal of Colloid and Interface Science **275**(2): 496-502.
Shankar, S. S., A. Rai, et al. (2004). "Biological synthesis of triangular gold nanoprisms." Nat Mater **3**(7): 482-488.
Simon, R., U. Priefer, et al. (1983). "A Broad Host Range Mobilization System for In Vivo Genetic Engineering: Transposon Mutagenesis in Gram Negative Bacteria." Nat Biotech **1**(9): 784-791.
Singla, N., N. Kaistha, et al. (2010). "Morganella morganii could be an important Intensive Care Unit pathogen." Indian Journal of Critical Care Medicine : Peer-reviewed, Official Publication of Indian Society of Critical Care Medicine **14**(3): 154-155.
Sintubin, L., W. De Windt, et al. (2009). "Lactic acid bacteria as reducing and capping agent for the fast and efficient production of silver nanoparticles." Appl Microbiol Biotechnol **84**(4): 741-749.
Sleytr, U. B., P. Messner, et al. (1993). "Crystalline bacterial cell surface layers." Mol Microbiol **10**(5): 911-916.

Sobreira, M., N. C. Leal, et al. (2001). "Molecular analysis of clinical isolates of Providencia alcalifaciens." Journal of Medical Microbiology **50**(1): 29-34.
Sondi, I. and B. Salopek-Sondi (2004). "Silver nanoparticles as antimicrobial agent: a case study on E. coli as a model for Gram-negative bacteria." Journal of Colloid and Interface Science **275**(1): 177-182.
Song, J. Y. and B. S. Kim (2009). "Rapid biological synthesis of silver nanoparticles using plant leaf extracts." Bioprocess Biosyst Eng **32**(1): 79-84.
Song, J. Y., E. Y. Kwon, et al. (2010). "Biological synthesis of platinum nanoparticles using Diopyros kaki leaf extract." Bioprocess Biosyst Eng **33**(1): 159-164.
Spadaro, D. and M. L. Gullino (2005). "Improving the efficacy of biocontrol agents against soilborne pathogens." Crop Protection **24**(7): 601-613.
Staehlin, B. M., J. G. Gibbons, et al. (2016). "Evolution of a Heavy Metal Homeostasis/Resistance Island Reflects Increasing Copper Stress in Enterobacteria." Genome Biology and Evolution **8**(3): 811-826.
Steyert, S. R. and S. A. Pineiro (2007). "Development of a Novel Genetic System To Create Markerless Deletion Mutants of Bdellovibrio bacteriovorus." Applied and Environmental Microbiology **73**(15): 4717-4724.
Steyert, S. R. and S. A. Pineiro (2007). "Development of a novel genetic system to create markerless deletion mutants of Bdellovibrio bacteriovorus." Appl Environ Microbiol **73**(15): 4717-4724.
Stuchinskaya, T., M. Moreno, et al. (2011). "Targeted photodynamic therapy of breast cancer cells using antibody-phthalocyanine-gold nanoparticle conjugates." Photochemical & Photobiological Sciences **10**(5): 822-831.
Sun, S. and H. Zeng (2002). "Size-controlled synthesis of magnetite nanoparticles." J Am Chem Soc **124**(28): 8204-8205.
Suresh, K., S. R. Prabagaran, et al. (2004). "Bacillus indicus sp. nov., an arsenic-resistant bacterium isolated from an aquifer in West Bengal, India." Int J Syst Evol Microbiol **54**(Pt 4): 1369-1375.
Szczepanik, W., P. Kaczmarek, et al. (2002). "Copper(ii) binding by kanamycin A and hydrogen peroxide activation by resulting complexes." New Journal of Chemistry **26**(10): 1507-1514.
Taylor, L. A. and R. E. Rose (1988). "A correction in the nucleotide sequence of the Tn903 kanamycin resistance determinant in pUC4K." Nucleic Acids Research **16**(1): 358.
Thakkar, K. N., S. S. Mhatre, et al. (2010). "Biological synthesis of metallic nanoparticles." Nanomedicine: Nanotechnology, Biology and Medicine **6**(2): 257-262.
Thapa, D., V. R. Palkar, et al. (2004). "Properties of magnetite nanoparticles synthesized through a novel chemical route." Materials Letters **58**(21): 2692-2694.
Thi My Dung, D., L. Thi Tuyet Thu, et al. (2011). "Synthesis and optical properties of copper nanoparticles prepared by a chemical reduction method." Advances in Natural Sciences: Nanoscience and Nanotechnology **2**(1): 015009.
Treangen, T. J. and S. L. Salzberg (2012). "Repetitive DNA and next-generation sequencing: computational challenges and solutions." Nat Rev Genet **13**(1): 36-46.

Tseng, T. T., K. S. Gratwick, et al. (1999). "The RND permease superfamily: an ancient, ubiquitous and diverse family that includes human disease and development proteins." J Mol Microbiol Biotechnol **1**(1): 107-125.

Turner, S., K. M. Pryer, et al. (1999). "Investigating Deep Phylogenetic Relationships among Cyanobacteria and Plastids by Small Subunit rRNA Sequence Analysis1." Journal of Eukaryotic Microbiology **46**(4): 327-338.

Ummartyotin, S., N. Bunnak, et al. (2012). "Synthesis of colloidal silver nanoparticles for printed electronics." Comptes Rendus Chimie **15**(6): 539-544.

Vahabi, K., G. A. Mansoori, et al. (2011). "Biosynthesis of Silver Nanoparticles by Fungus *Trichoderma Reesei* (A Route for Large-Scale Production of AgNPs)." Insciences J. **1**(1): 65-79.

Verdet, C., Y. Benzerara, et al. (2006). "Emergence of DHA-1-Producing Klebsiella spp. in the Parisian Region: Genetic Organization of the ampC and ampR Genes Originating from Morganella morganii." Antimicrobial Agents and Chemotherapy **50**(2): 607-617.

Wagner, E., C. Plank, et al. (1992). "Influenza virus hemagglutinin HA-2 N-terminal fusogenic peptides augment gene transfer by transferrin-polylysine-DNA complexes: toward a synthetic virus-like gene-transfer vehicle." Proceedings of the National Academy of Sciences **89**(17): 7934-7938.

Waszczuk, P., T. M. Barnard, et al. (2002). "A nanoparticle catalyst with superior activity for electrooxidation of formic acid." Electrochemistry Communications **4**(7): 599-603.

Wiley, B., T. Herricks, et al. (2004). "Polyol Synthesis of Silver Nanoparticles: Use of Chloride and Oxygen to Promote the Formation of Single-Crystal, Truncated Cubes and Tetrahedrons." Nano Letters **4**(9): 1733-1739.

Yan, J.-K., J.-L. Liu, et al. (2015). "Green synthesis of biocompatible carboxylic curdlan-capped gold nanoparticles and its interaction with protein." Carbohydrate Polymers **117**: 771-777.

Zain, N. M., A. G. F. Stapley, et al. (2014). "Green synthesis of silver and copper nanoparticles using ascorbic acid and chitosan for antimicrobial applications." Carbohydrate Polymers **112**(0): 195-202.

Appendix

Appendix 1: List of overabundant (green coloured) and underabundant proteins (red coloured) identified by LC-MS in presence of $CuSO_4$.

Protein name	Fold change	*p*-value
P-Type ATPase	12.08	0.03
LSU ribosomal protein L18p	4.22	0.00
Cysteine synthase	3.70	0.00
LSU ribosomal protein L32p	3.64	0.00
Peptide chain release factor 2	2.78	0.00
GTP cyclohydrolase II	2.76	0.01
Phage shock protein A	2.62	0.03
SSU ribosomal protein S17p	2.58	0.02
LSU ribosomal protein L27p	2.51	0.01
Agmatinase	2.51	0.01
Tyrosyl-tRNA synthetase	2.46	0.01
CDP-diacylglycerol--serine O-phosphatidyltransferase	2.37	0.05
Alanyl-tRNA synthetase	2.34	0.03
SSU ribosomal protein S16p	2.33	0.02
UDP-4-amino-4-deoxy-L-arabinose--oxoglutarate aminotransferase	2.16	0.03
LSU ribosomal protein L24p	2.15	0.01
LSU ribosomal protein L22p	2.13	0.00
LSU ribosomal protein L30p	2.11	0.04
Na(+)-translocating NADH-quinone reductase subunit E	2.06	0.03
3-oxoacyl-[acyl-carrier-protein] synthase, KASIII	2.01	0.00
Glutathione reductase	1.92	0.01
ClpB protein	1.92	0.02
LSU ribosomal protein L6p	1.90	0.01
Hypothetical protein	1.88	0.00
5'-methylthioadenosine nucleosidase	1.83	0.03
Biosynthetic arginine decarboxylase	1.82	0.01
Glutamate-1-semialdehyde aminotransferase	1.82	0.01
High-affinity branched-chain amino acid transport system permease protein LivH	1.77	0.00
L-arabinose 1-dehydrogenase	1.74	0.02
GTP-binding protein EngB	1.74	0.02
Iojap protein	1.74	0.02
Biotin carboxylase of acetyl-CoA carboxylase	1.70	0.01
Rod shape-determining protein MreB	1.55	0.02
Inosine-5'-monophosphate dehydrogenase	1.52	0.02
Phage major capsid protein	1.52	0.04
SilE	204.53	0.04

Dihydroneopterin aldolase	31.90	0.01
Pyridoxal kinase	30.01	0.00
Uptake hydrogenase small subunit precursor	12.00	0.01
Predicted P-loop-containing kinase	7.26	0.01
Peptide chain release factor 1	7.21	0.00
Putative glycosyltransferase	7.01	0.00
Cell division protein FtsA	5.35	0.03
Pyruvate formate-lyase activating enzyme	4.87	0.01
tRNA-guanine transglycosylase	4.70	0.01
tRNA pseudouridine synthase B	4.20	0.00
Putative phosphatase	3.62	0.00
Osmosensitive K+ channel histidine kinase KdpD	3.50	0.03
Anaerobic glycerol-3-phosphate dehydrogenase subunit A	3.46	0.03
LSU ribosomal protein L25p	3.31	0.00
Hypothetical protein	3.12	0.02
Hypothetical protein	3.01	0.00
NAD(P) transhydrogenase alpha subunit	2.96	0.00
Homolog of E. coli HemY protein	2.69	0.00
1-acyl-sn-glycerol-3-phosphate acyltransferase	2.64	0.01
3'(2'),5'-bisphosphate nucleotidase	2.56	0.02
ATP synthase epsilon chain	2.30	0.00
D-alanyl-D-alanine carboxypeptidase	2.26	0.03
Hypoxanthine-guanine phosphoribosyltransferase	2.11	0.03
Cytidine deaminase	1.97	0.01
Na(+)-translocating NADH-quinone reductase subunit	1.67	0.04
Protein YicC	1.56	0.04

Appendix 2: Protein sequence alignments of Cus and Sil homologues from *M. psychrotolerans* and *M. morganii* sp. RP-42

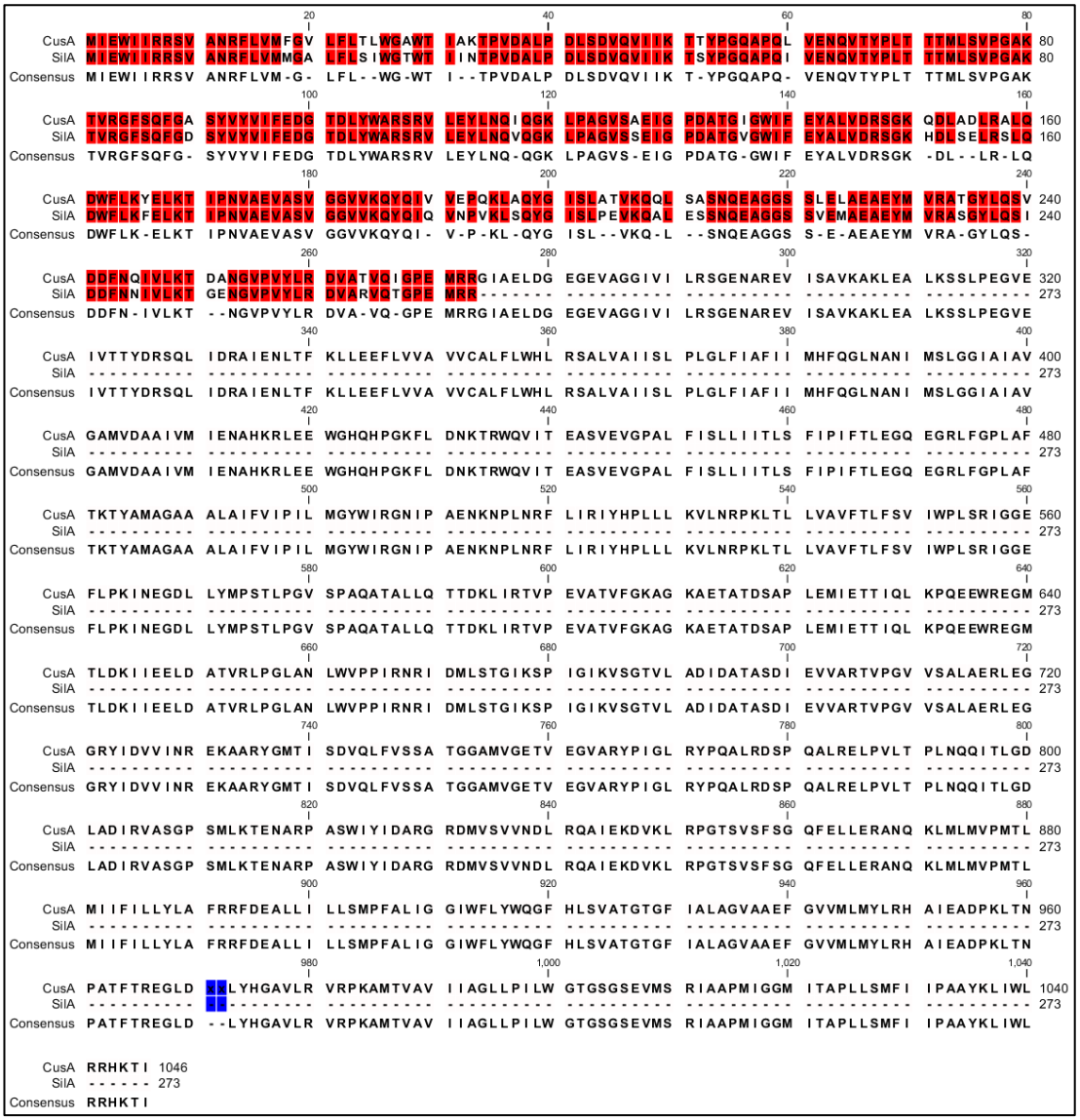

a) Alignment of CusA and SilE.

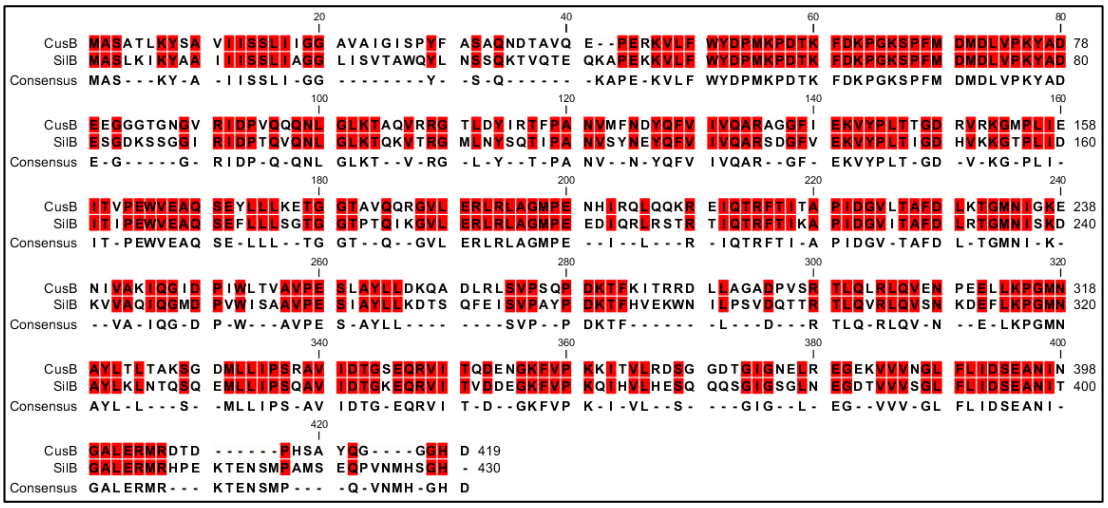

b) Alignment of CusB and SilB.

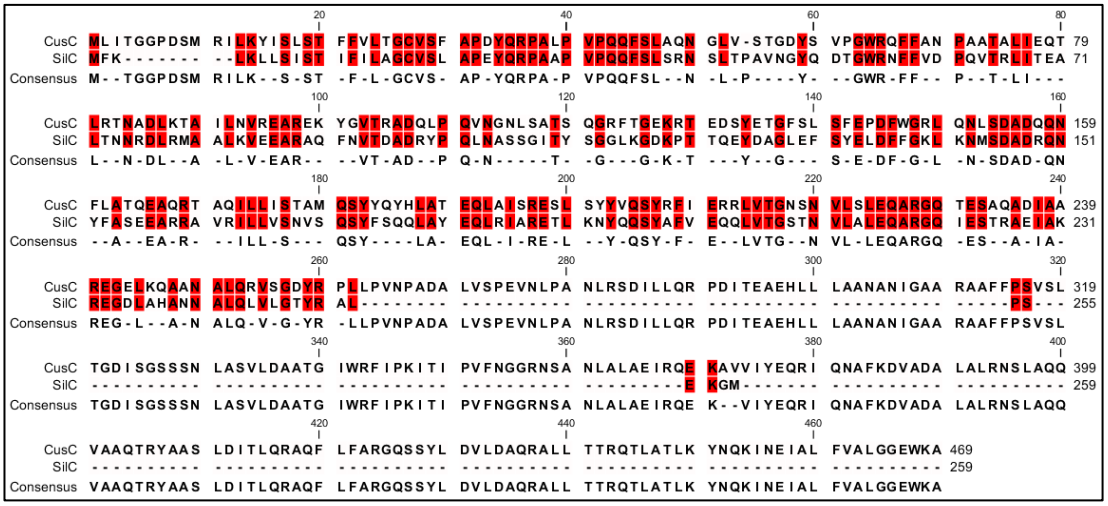

c) Alignment of CusC and SilC.

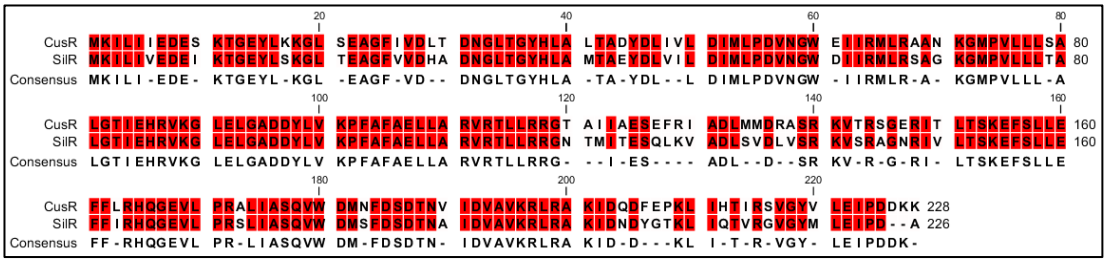

d) Alignment of CusR and SilR.

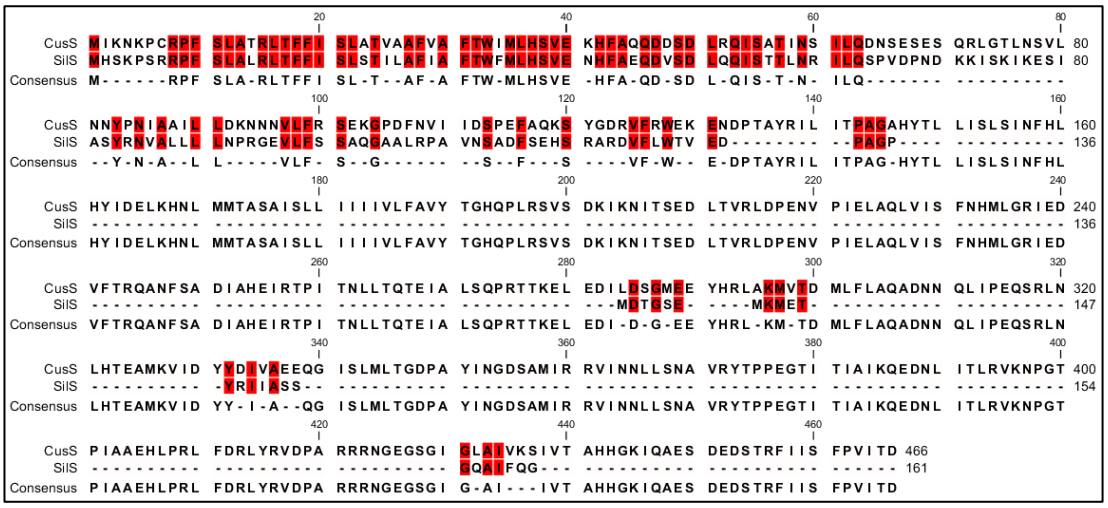

e) Alignment of CusS and SilS.

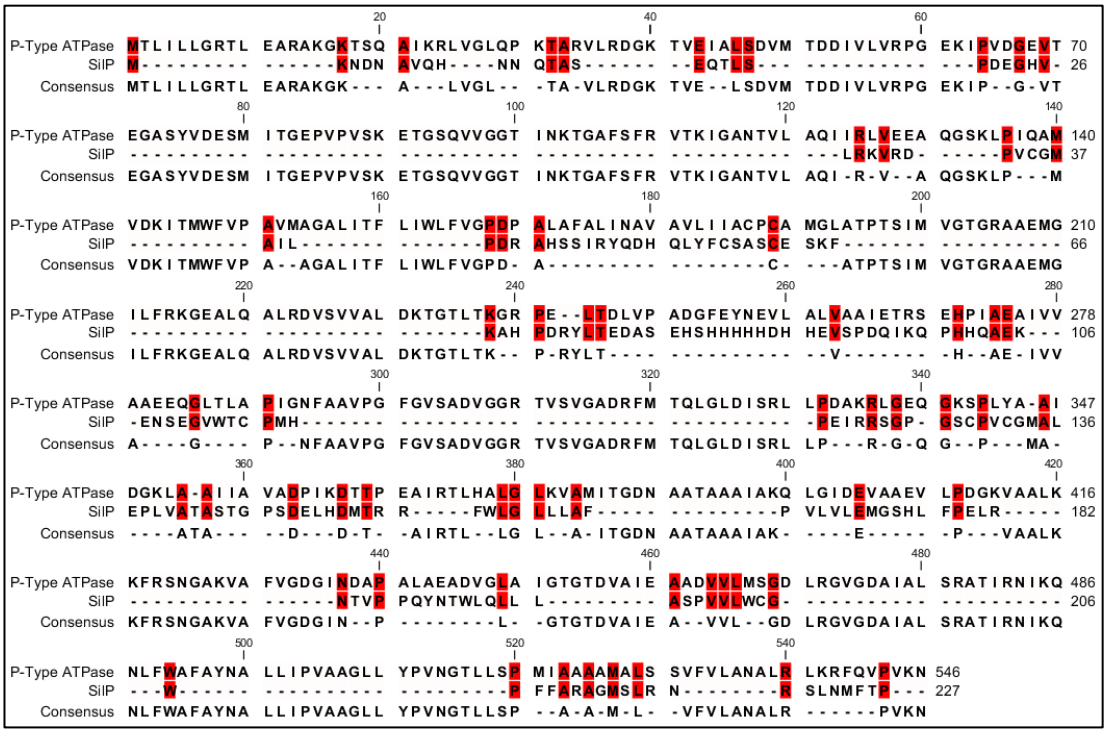

f) Alignment of P-Type ATPase and SilP.

Nanomedicine & Nanotechnology

Pantidos and Horsfall, J Nanomed Nanotechnol 2014, 5:5
http://dx.doi.org/10.4172/2157-7439.1000233

Review Article Open Access

Biological Synthesis of Metallic Nanoparticles by Bacteria, Fungi and Plants

Nikolaos Pantidos and Louise E Horsfall*

School of Biological Sciences, University of Edinburgh, Edinburgh, UK

Abstract

Over the past few decades interest in metallic nanoparticles and their synthesis has greatly increased. This has resulted in the development of numerous ways of producing metallic nanoparticles using chemical and physical methods. However, drawbacks such as the involvement of toxic chemicals and the high-energy requirements of production make it difficult for them to be widely implemented. An alternative way of synthesising metallic nanoparticles is by using living organisms such as bacteria, fungi and plants. This "green" method of biological nanoparticle production is a promising approach that allows synthesis in aqueous conditions, with low energy requirements and low-costs. This review gives an overview of some of these environmentally friendly methods of biological metallic nanoparticle synthesis. It also highlights the potential importance of these methods in assessing nanoparticle risk to both health and the environment.

Keywords: Biogenic nanoparticles; Biological nanoparticles; Green nanoparticle synthesis

Introduction

In recent years the topic of nanoparticles has received particular interest in a wide range of fields. The term "*nano*" comes from the Greek word "*nanos*" meaning dwarf and denotes a measurement on the scale of one-billionth (10^9) of a metre in size [1,2]. A strand of DNA is 2.5 nm in diameter [3], a typical virus is around 100 nm wide [4] and a typical bacterium is around 1-3 μm wide [5]. Nanoparticles are defined as particulate dispersions of solid particles with at least one dimension at a size range of 10-1000 nm [2,6]. The most important feature of nanoparticles is their surface area to volume aspect ratio, allowing them to interact with other particles easier [1,2].

In order to survive in environments containing high levels of metals, organisms have adapted by evolving mechanisms to cope with them. These mechanisms may involve altering the chemical nature of the toxic metal so that it no longer causes toxicity, resulting in the formation of nanoparticles of the metal concerned. Thus nanoparticle formation is the "by-product" of a resistance mechanism against a specific metal, and this can be used as an alternative way of producing them. Nanoparticles have unique thermal, optical, physical, chemical, magnetic and electrical properties compared to their bulk material counterparts [7,8]. These features can be exploited for next generation biosensors, electronics, catalysts and antimicrobials [1,8]. Metallic nanoparticles are one important and widely studied group of materials, showing great diversity and many different uses. This review will focus on how material science and biology can work together to create a "green" way of synthesising metal nanoparticles for a wide range of uses.

There are important links between the way nanoparticles are synthesised and their potential uses. Silver nanoparticles (AgNPs) have been shown in numerous studies to display antibacterial properties [8-11]. For instance, nanoparticles such as silver and gold have been shown to be effective in inhibiting growth of both Gram-positive and Gram-negative bacteria [10,12]. With the rise in antibiotic resistance in recent years and the development of fewer new antibiotics, research has begun to focus on these antibacterial nanoparticles as potential new medical tools. Silver nanoparticles have also been used as optical sensors for the formation of small molecule adsorbates [13]. Whereas catalysts based on Pt nanoparticles have been shown to exhibit high activity for the electrooxidation of formic acid [14]. The most common methods for preparing all of these nanoparticles are wet-chemical techniques, which are generally low-cost and high-volume. However, the need for toxic solvents and the contamination from chemicals used in nanoparticle production limit their potential use in biomedical applications [15]. Therefore a "green", non-toxic way of synthesising metallic nanoparticles is needed in order to allow them to be used in a wider range of industries. This could potentially be achieved by using biological methods.

Many bacteria, fungi and plants have shown the ability to synthesise metallic nanoparticles and all have their own advantages and disadvantages (Table 1) [16-18]. Intracellular or extracellular synthesis, growth temperature, synthesis time, ease of extraction and percentage synthesised versus percentage removed from sample ratio, all play an important role in biological nanoparticle production. Finding the right biological method can depend upon a number of variables. Most importantly, the type of metal nanoparticle under investigation is of vital consideration, as in general organisms have developed resistance against a small number of metals, potentially limiting the choice of organism. However synthetic biology; a nascent field of science, is starting to address these issues in order to create more generalised chassis, able to synthesise more than one type of metallic nanoparticle using the same organism [19].

"Natural" biogenic metallic nanoparticle synthesis can be split into two categories. The first is bioreduction, in which metal ions are chemically reduced into more stable forms biologically. Many organisms have the ability to utilise dissimilatory metal reduction, in which the reduction of a metal ion is coupled with the oxidation of an enzyme [20]. This results in stable and inert metallic nanoparticles that can then be safely removed from a contaminated sample. The second category is biosorption. This involves the binding of metal ions from

***Corresponding author:** Louise E Horsfall, 505 Darwin Building, School of Biological Sciences, The King's Buildings, University of Edinburgh, Edinburgh, UK, Tel: 0131-650-5363; E-mail: louise.horsfall@ed.ac.uk

Received July 30, 2014; **Accepted** September 29, 2014; **Published** October 09, 2014

Citation: Pantidos N, Horsfall LE (2014) Biological Synthesis of Metallic Nanoparticles by Bacteria, Fungi and Plants. J Nanomed Nanotechnol 5: 233. doi: 10.4172/2157-7439.1000233

Copyright: © 2014 Pantidos N, et al. This is an open-access article distributed under the terms of the Creative Commons Attribution License, which permits unrestricted use, distribution, and reproduction in any medium, provided the original author and source are credited.

Name of organism	Nanoparticles Produced	Synthesis Location	Method	References
A) Bacteria				
Thermomonospora sp.	Au	Extracellular	Reduction	[62]
Rhodococcus sp.	Au	Intracellular	Reduction	[63]
Escherichia coli	Pd, Pt	Extracellular	Reduction	[20]
Rhodopseudomonas capsulata	Au	Extracellular	Reduction	[25]
Pseudomonas aeruginosa	Au	Extracellular	Reduction	[1]
Delftia acidovorans	Au	Extracellular	Reduction	[26]
Bacillus licheniformis	Ag	Intracellular	Reduction	[28]
Shewanella sp.	AsS	Extracellular	Reduction	[64]
	Se	Extracellular	Reduction	[65]
Desulfovibrio desulfuricans	Pd	Extracellular	Reduction	[66]
Bacillus sphaericus JG-A12	U, Cu, Pb, Al, Cd	Extracellular	Biosorption and Reduction	[33]
Bacillus sp.	Ag	Intracellular	Reduction	[29]
Klebsiella pneumonia	Ag	Extracellular	Reduction	[30]
Escherichia coli	Ag	Extracellular	Reduction	[30]
Enterobacter cloacae	Ag	Extracellular	Reduction	[30]
Lactobacillus sp.	Ag	Extracellular	Biosorption and Reduction	[32]
Enterococcus faecium	Ag	Extracellular	Biosorption and Reduction	[32]
Lactococcus garvieae	Ag	Extracellular	Biosorption and Reduction	[32]
B) Fungi				
Pediococcus pentosaceus	Ag	Extracellular	Biosorption and Reduction	[32]
Fusarium oxysporum	CdS	Extracellular	Enzyme Mediated	[41]
	Ag	Extracellular	Reduction	[27]
	Pt			
	Au	Intracellular	Reduction	[67]
Aspergillus fumigatus	Ag	Extracellular	Reduction	[17]
Neurospora crassa	Pt	Intracellular & Extracellular	Reduction	[45]
Verticillium sp.	Au	Intracellular	Reduction	[38]
C) Plants & Extracts				
Coriolus versicolor	Ag	Intracellular & Extracellular	Reduction	[43]
Aspergillus flavus	Ag	Extracellular	Reduction	[68]
Jatropha curcas latex	Ag	Extracellular	Latex Mediated Reduction	[52]
Acalypha indica leaf extract	Ag	Extracellular	Reduction	[11]
Medicago sativa seed exudate	Ag	Extracellular	Reduction	[53]
Cymbopogon flexuosus extract	Au	Extracellular	Reduction	[57]
Live Alfalfa plants	Au	Intracellular	-	[61]
Magnolia kobus leaf broth	Ag	Extracellular	Reduction	[18]

Table 1: Metallic nanoparticles formed by different organisms. The table also illustrates the location of the nanoparticles in relation to the cells and the suggested method of synthesis.

an aqueous or soil sample onto the organism itself, such as on the cell wall, and does not require the input of energy. Certain bacteria, fungi and plants express peptides or have a modified cell wall which binds to metal ions, and these are able to form stable complexes in the form of nanoparticles [21].

Metallic nanoparticles are becoming increasingly important due to their potential application in many fields. The development of an environmentally friendly and inexpensive way of synthesising them is therefore crucial. There are numerous organisms possessing the ability to synthesise nanoparticles and which therefore have the potential to be exploited and modified to optimise them to fulfil this purpose. The following sections will focus on providing an overview and a discussion of metallic nanoparticle synthesis by various biological and non-biological ways.

Chemical and Physical Methods of Nanoparticle Synthesis

Metallic nanoparticles can be synthesised in many different ways. In order to study the biological methods of synthesising nanoparticles (NPs), a clear understanding of the current chemical and physical methods is needed to allow comparisons to be made and a basis for improvement to become evident. There is an abundant volume of research on the synthesis of metallic nanoparticles available in the literature. Here a number of studies will be discussed in order to gain insight into the "non-green" methods of NP synthesis.

Wiley et al. were able to produce silver nanoparticles (AgNPs) of cube and tetrahedron shape. They achieved this by heating $AgNO_3$ and Ethylene glycol to 148°C. The resulting nanoparticles were single crystals and had a size range of 20-80 nm in diameter. The AgNPs were relatively monodispersed and the reaction time was only 10 minutes [22]. However the temperature needed for the reaction to occur was relatively high therefore requiring a significant amount of energy if commercial volumes were to be made.

A method using polyamide fabrics developed by Montazer et al. successfully formed AgNPs. The NPs were observed under SEM and were found to be between 20 and 150 nm across with an average size of 90 nm. A small number of aggregates was seen which were attributed to the boiling point temperature during the reaction. The polyamide

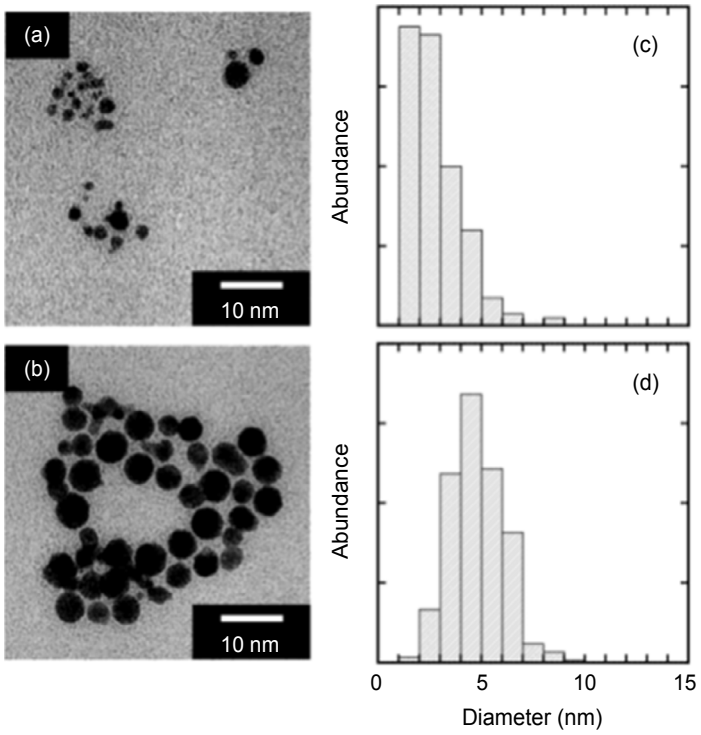

Figure 1: TEM micrograph of PtNP synthesis via laser ablation. The histograms show the size distribution of the synthesised nanoparticles. a) Formation of PtNPs in 0.01 M SDS aqueous solution and b) PtNPs produced in pure water. c) and d) display the measured length of PtNPs from a) and b) respectively. Reprinted with permission from Mafuné et al., Copyright 2003 American Chemical Society [24].

fabric itself was used as the reducing agent for the Ag^+ and was found to stabilise the synthesised NPs. This important result meant that the use of extra stabilising agents was redundant. The fabric was subsequently tested for its antibacterial activity which showed high bactericidal effects even after 30 washing cycles [23].

Stable platinum nanoparticles (PtNPs) have been produced using a physical method, which does not require the reducing agents that cause contamination in the nanoparticles produced [24]. Mafuné et al. used laser ablation that creates nanoparticles by heating up bulk material using a laser beam. Mafuné and group performed this method in both SDS and pure water and found in both cases that stable PtNPs were produced (Figure 1). Subsequently the size distribution of the PtNPs was measured under TEM and was found to be 1-7 nm, which proved to be too small for isolating them using centrifugation [24].

Nanoparticle Synthesis by Bacteria

Research has focused heavily on prokaryotes as a means of synthesising metallic nanoparticles. Due to their abundance in the environment and their ability to adapt to extreme conditions, bacteria are a good choice for study. They are also fast growing, inexpensive to cultivate and easy to manipulate. Growth conditions such as temperature, oxygenation and incubation time can be easily controlled. In a study by He et al. it was discovered that changing the pH of the growth medium during incubation results in the production of nanoparticles of differing size and shape [25] Controlling such properties is important, as varying sizes of nanoparticles are required for different applications such as optics, catalysts or anti-microbials.

In a recent study, Johnston et al. illustrated the production of pure gold nanoparticles by the bacterium *Delftia acidovorans*. Reporting the production of a small non-ribosomal peptide, delftibactin, to be responsible for generating the gold nanoparticles [26]. Johnston et al. believed the production of delftibactin was associated with the resistance mechanism of *D. acidovorans* to toxic gold ions. By producing inert gold nanoparticles bound to delftibactin, the gold no longer posed any toxicity problem for the cells. The Johnston group was first to report the mechanism that is responsible for the formation of metallic nanoparticles and how it can vary in different bacteria. Another group suggested an alternative method for gold nanoparticle synthesis by bacteria. He et al. observed the extracellular formation of gold nanoparticles of 10-20 nm by the bacterium *Rhodopseudomonas capsulata* and suggested that these nanoparticles were synthesised via an NADH-Dependant Reductase [25], an enzyme that has been shown in the past to be important in metal biosynthesis (Figure 2) [27].

Pd is a member of the Platinum Group Metals (PGM) which is a collection of highly catalytically active metals and are currently being primarily used as catalysts for dehalogenation and hydrogenation reactions [28]. Recently it has been shown that zero valent palladium (Pd^0) nanoparticles can be synthesised using bacteria found at Alpine sites heavily contaminated with heavy metals [28]. Of all the variety of heavy metal resistant bacteria that they have found in that environment, they found that *Pseudomonas* cells were involved in producing catalytically active nanoparticles which were successfully used in reductive dehalogenation of tri and tetra-chlorinated dioxin congeners [28]. Macaskie et al. suggested that *Escherichia coli,* can also synthesise Pd^0 nanoparticles with the help of hydrogenases found in the bacterium [29]. In both studies mentioned, the Pd nanoparticles were found to be formed on the cell envelope of the bacteria which makes them attractive as they are easily accessible.

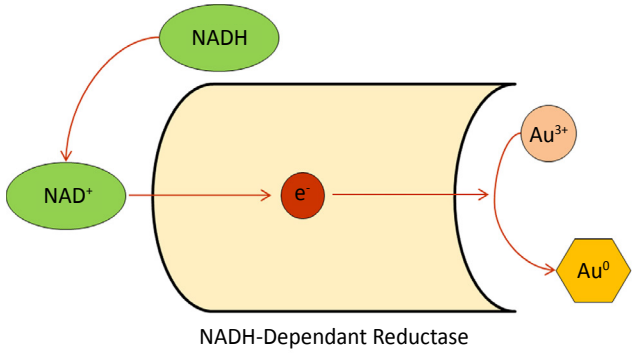

Figure 2: A suggested mechanism for the reduction of gold ions into AuNPs. The bioreduction is initiates by the electron transfer from NADH by NADH-Dependant Reductase as an electron carrier to form NAD+. The resulting electrons are obtained by gold ions which get reduced to elemental AuNPs. Figure adapted from [25].

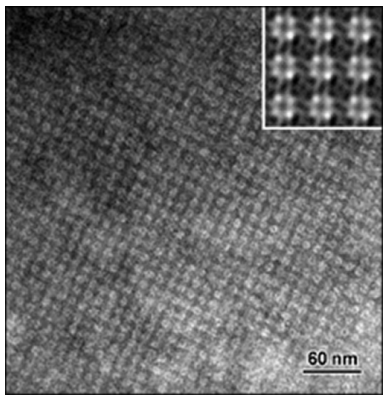

Figure 3: Bacterial S-layer of *Bacillus sphaericus* JG-A12 shown under Transmission Electron Microscopy. The picture illustrates the symmetry of S-layers and allows the visualisation of the pores where metallic nanoparticles are localised. Reprinted from Pollman et al., with permission from Elsevier: Biotechnology Advances, copyright 2005 [36].

The bacterium *Bacillus licheniformis* was observed to produce intracellular AgNPs [30]. The colour of the culture after addition of silver ions turned a dark brown indicating the presence of AgNPs [30]. Kalimuthu and group illustrated that the nanoparticles were indeed made of Ag and also that they were quite dispersed in solution. However the nanoparticles were synthesised intracellularly, therefore Kalimuthu et al. had to add an additional extraction step. Pugazhenthiran et al. observed a similar result when they attempted to create biological AgNPs. It was found that intracellular AgNPs were created when members of the *Bacillus sp.* were sub-cultured into media containing $AgNO_3$. The reaction was slow and the incubation time was 7 days [31]. This is not suitable for industrial purposes due to the lengthy production time. Whereas, despite the additional extraction step, the method proposed by Kalimuthu et al. was more industrially significant as it took only 24 hours for *Bacillus licheniformis* to create AgNPs. However, the approach with the greatest potential for the industrial bio-production of AgNPs was reported by Shaverdi et al. Instead of adding metal ions to a live culture, the cultures were centrifuged and the supernatant was tested for the ability to create metallic nanoparticles [32]. Therefore Shaverdi et al. were able to create AgNPs in 5 minutes, without the need for a cell lysis step by the use of culture supernatant. This extracellular type of formation is a more desirable not only because of the simplicity of purification but also due to the observed increased production rate [33].

An interesting study by Sintubin et al. focused on the production of AgNPs by lactic acid bacteria. Many bacterial species were tested but only four were found to synthesise AgNPs: *Lactobacillus spp., Pediococcus pentosaceus, Enterococcus faecium* and *Lactococcus garvieae* [34]. A two-step process of AgNP formation was proposed. First, the Ag ions were accumulated at the cell wall via biosorption and then subsequent reduction of those ions formed the metallic nanoparticles [34]. Sintubin et al. also suggest that the cell wall may act as a capping agent for the nanoparticles, which keeps them stable by preventing aggregation and showed that by increasing the pH of the medium, the reduction rate of the nanoparticles increased [34]. The effect of pH on nanoparticle synthesis was also observed by He et al. By varying the pH levels, nanoparticles of differing size and shape were formed [25]. He et al. illustrated that by increasing the pH, AgNPs of around 10-20 nm were formed and by lowering the pH to 4, nanoplate formation was observed.

Although Ag and AuNPs are important due to their antimicrobial abilities, many studies have been done on other metals such as uranium (U). A significant amount of research has been done on *Bacillus* species due to their metal bioaccumulation abilities [30,31,35]. Pollmann and group studied the ability of *Bacillus sphaericus* JG-A12 to accumulate high concentrations of toxic metals such as Cu, Pb, Al, Cd and U. They found that the S-layer proteins of *B. sphaericus* are responsible for the bioremediation of uranium from aqueous environments. The S-layer is a porous layer consisting of identical proteins which surround the bacterial cell and can contribute up to 15% of the total cell protein content (Figure 3) [36]. Sleytr et al. found that S-layers are approximately 5-15 nm thick and consist of pores with a size range of 2-6 nm [36]. It is this layer that was proposed by Pollman et al. to be responsible for the binding of heavy metals, such as U at up to 20 mg of U per gram of protein, and they suggested that binding was via the carboxyl and phosphate groups of the S-layer resulting in bioaccumulation.

The synthesis of copper nanoparticles (CuNPs) has proven to be a difficult feat in the past, by any available method. Cu is not stable at the nanometre scale and oxidises fairly rapidly to form copper oxide (CuO) [37]. Therefore, if Cu nanoparticles are to be used in an application after their synthesis, they need to be stabilised. In 2013 a study suggested the production of pure elemental Cu nanoparticles by biological means, using *Morganella morganii* was possible [38]. Ramanathan and group state that *M. morganii* synthesises the Cu nanoparticles intracellularly by uptake of the Cu ions and subsequent binding of the ions to either a metal ion reductase or similar protein. This results in the reduction of the ion to metallic Cu^0 which then accumulates extracellularly as nanoparticles once effluxed out of the cell [38], however this has not been confirmed. Another study based on *Morganella sp.* showed the extracellular synthesis of AgNPs [39]. Parikh et al. suggested the pathway of Ag resistance is also responsible for the formation of the AgNPs. Bioinformatics analysis of the *silE* gene from *Morganella sp.* showed 99% similarity with previously reported silver-binding proteins. Further results showed the similarity of the *silE* homologue to copper binding proteins from other microorganisms [38]. Using this result, Ramanathan and group suggested that *M. morganii* may use the Ag resistance mechanism to produce elemental Cu nanoparticles.

Nanoparticle Synthesis by Fungi

The use of fungi in producing metallic nanoparticles has received significant interest as they offer certain advantages over the use of

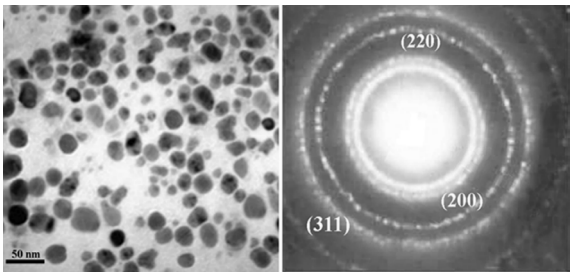

Figure 4: a) TEM micrograph of AgNPs on a drop-coated carbon grid after 72 hours of synthesis by *Trichoderma reesei*. b) SAED pattern from a AgNP shown in the left picture. The diffraction rings correlate to the fcc silver [82,83].

bacteria for the synthesis of nanoparticles. The ease of scaling up and downstream processing, the economic feasibility and the presence of mycelia offering an increased surface area, are important advantages to consider [40]. Mukherjee et al. also suggested that because fungi secrete significantly higher amounts of proteins than bacteria, this would amplify the nanoparticle synthesis productivity.

Silver nanoparticle production has been the focus of research by the scientific community, and rightly so. AgNPs have great potential in a number of industries such as antimicrobials and electronics [41,42]. The fungus *Fusarium oxysporum* has been used in a large number of studies attempting to create metallic nanoparticles, especially those made of silver. Pure AgNPs were synthesised at a size range of 5-15 nm and it was suggested that they were capped in order to stable them by proteins secreted by the fungus [27]. Although the most important advance in the fungal synthesis of metal nanoparticles was that *F. oxysporum* produced these nanoparticles extracellularly, in contrast to all previous research which reported only the intracellular production of Ag and AuNPs [27]. *Fusarium oxysporum* has also been shown to produce Cadmium sulphide (CdS), lead sulphide (PbS), zinc sulphide (ZnS) and molybdenum sulphide (MoS) nanoparticles, when the appropriate salt is added to the growth medium [43].

A later study on the production of AgNPs was done by Bhainsa et al., in which they used *Aspergillus fumigatus* to synthesise extracellular silver nanoparticles in the size range of 5-25 nm [17]. This range in size was larger than previously reported by *F. oxysporum* [27], which might cause a disadvantage when application predictability comes into play, as it would be difficult to predict the catalytic activity of the nanoparticles produced if their sizes are different in every batch. However bio-production by *A. fumigatus* is a very attractive prospect as the organism was able to reduce Ag ions into nanoparticles within 10 minutes of exposure [17], in contrastto the research by Ahmad et al. which showed AgNP production by *F. oxysporum* within an hour [27]. The results of the Bhainsa group present the biological synthesis of metallic nanoparticles as comparable to the chemical and physical processes that exist to create them [22]. The fungus *Trichoderma reesei* has also been shown to produce extracellular AgNPs (Figure 4) [44]. Bahabi et al. were able to produce AgNPs using this fungus after 72 hours, which was significantly slower than *A. fumigatus* and *Fusarium oxysporum* [17,27]. However the use of *T. reesei* does have an advantage over the use of other fungi for the production of metallic nanoparticles. As a comparatively well studied organism it can be manipulated to produce high quantities of enzymes, up to 100 g/L [44], which may help increase the nanoparticle production rate in the future. The size range of the AgNPs reportedly produced by *T. reesei* was 5-50 nm [44], which were not as homogenous as those produced by either *A. fumigatus* [17] or *F. oxysporum* [27].

Although extracellular formation has its advantages, such as lower-cost, simpler downstream processing [33], intracellular formation can also be of great importance. In the case of bioremediation, heavy metals such as Cu and Pt need to be removed from contaminated environments. By using fungi that have the ability to produce intracellular nanoparticles, it would be far easier to remove the fungus and its accumulated metal contaminant from the contaminated sample. A noteworthy study was done on the white rot fungus *Coriolus versicolor* by Sanghi et al. into the production and accumulation of intracellular AgNPs [45]. The group manipulated the reaction conditions and observed that *C. versicolor* had the ability to produce AgNPs intracellularly and extracellularly. Therefore the production process is not fixed and can be adapted according to specific requirements.

Gold nanoparticles have been increasing in their importance over recent years but, despite this, there are fewer examples of their synthesis by fungi than those composed of silver. Their small size makes them reactive, unlike the bulk form of gold, which makes AuNPs ideal for use as catalysts and as precursors for electronics applications [40,46]. Mukherjee et al. reported the synthesis of AuNPs using the fungus *Verticillium sp.* whereby intracellular AuNPs were observed localised on the surface of the mycelia via the biological reduction of $AuCl_4^-$ [47].

Unlike the most commonly researched metallic nanoparticles, such as AgNPs and AuNPs, very little is known about the biological synthesis of Platinum nanoparticles (PtNPs). An enlightening study by Castro-Longoria et al. showed the synthesis of PtNPs using the fungus *Neurospora crassa*. This fungus was reported to produce intracellular single PtNPs of 4-35 nm in diameter and spherical nano-agglomerates of 20-110 nm in diameter [48]. What is interesting about this study is that they attempted to create PtNPs using *N. crassa* extract and then compared the results with the PtNPs produced from the *N. crassa* biomass. They noticed that after the reaction, the sample from the extract contained almost exclusively single-crystal nanoagglomerates [48]. An additional study by Riddin et al. on the previously mentioned fungus *F. oxysporum*, also confirmed the production of PtNPs. In this case the PtNPs were formed both intracellularly and extracellularly, however the amount synthesised intracellularly was deemed to be statistically insignificant. The amount of extracellularly produced PtNPs was reported to be 5.66 mg l^{-1} [49], with temperature variation effecting production rates of the PtNPs and even slight pH variation away from the standard inhibiting the formation of PtNPs [49]. Knowledge of such results is crucial in order to understand the effects of environmental factors on NP synthesis as they can help us optimise the biological synthesis of metallic NPs.

Not all metallic nanoparticles are made of elemental metals in their zero-valent form. Magnetite (Fe_3O_4) is a common iron oxide that possesses magnetic properties and magnetite NPs (MaNPs) have been shown to be produced by the pathogenic fungus *F. oxysporum* and the endophytic fungus *Verticillium* sp [50]. The use of magnetite nanoparticles has been talked about extensively for use in biomedical applications such as magnetic resonance imaging [51] and for oscillation damping and position sensing [52], in addition to non-medical applications, such as in magnetic recording devices. The synthesised MaNPs described by Bharde and group were formed intracellularly, which again means an extra step in the purification of MaNPs if they are intended to be of commercially such as use.

Similar to bacteria, fungi also have an important disadvantage

when it comes to safety. Many well studied fungi such as *F. oxysporum* are pathogenic and therefore might pose a safety risk [53]. *Trichoderma asperellum* and *Trichoderma reesei* are both fungi that produce AgNPs when exposed to silver salts [44,54] and have been proven to be non-pathogenic which makes them ideal for use commercially [54,55]. In fact, *T. reesei* has already been used widely in sectors such as food, animal feed, pharmaceuticals, paper and textile industries [55].

Nanoparticle Synthesis by Plants

Bacteria and fungi have been studied extensively in the past few decades for their ability to synthesise metallic nanoparticles, however there has been less of a focus on plants in this matter. In the past decade an increasing amount of research is being performed on the green synthesis of metallic nanoparticles using plants or plant extracts [56-58]. This area is relatively underexplored and offers promising results

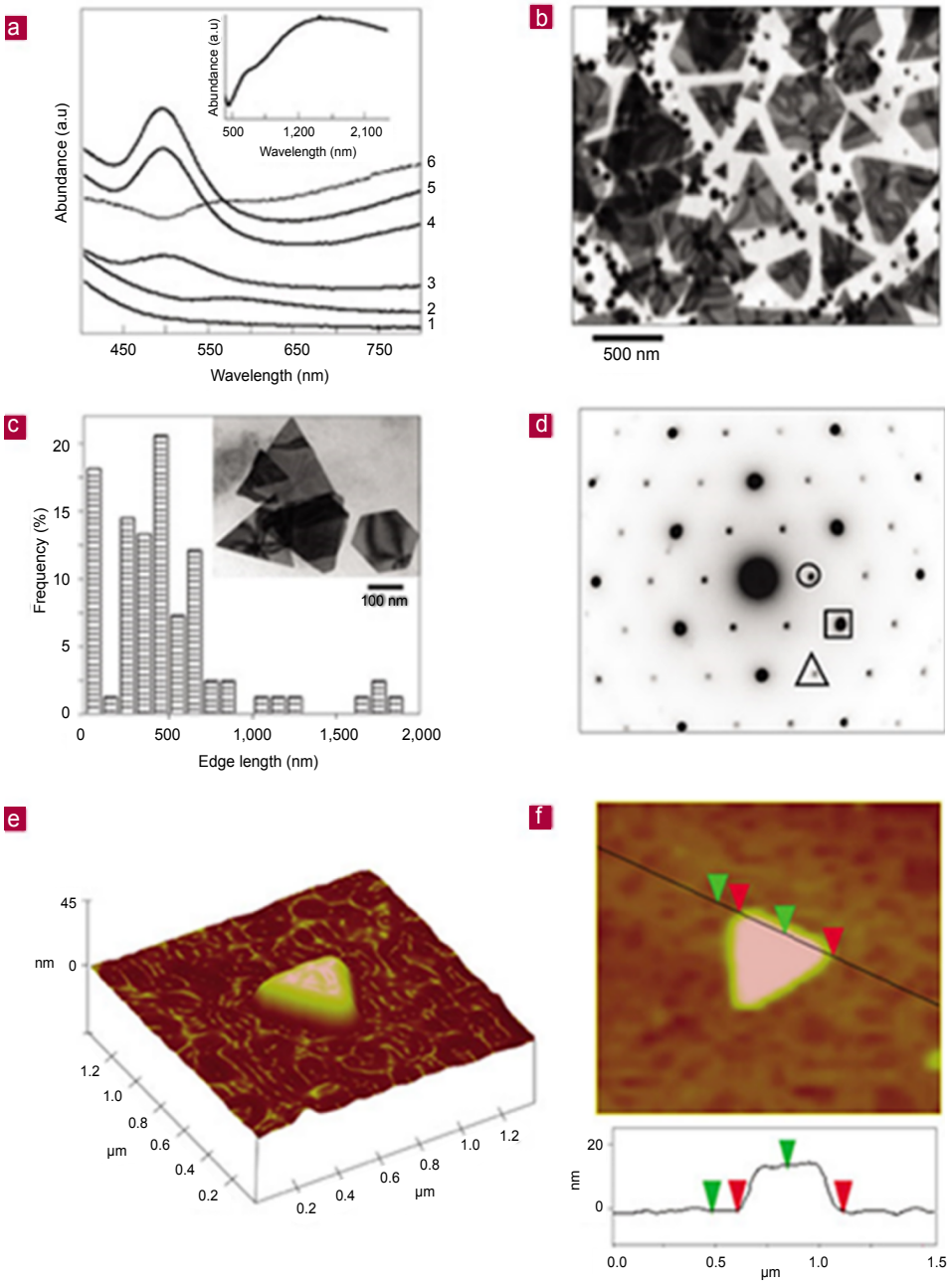

Figure 5: UV-vis-NIR kinetics, TEM and Atomic Force Microscopy (AFM) images of AuNPs produced by lemongrass. a) UV-vis spectra illustrating the time of reaction assay with gold ions over time. Curve 6 shows the spectrum obtained from a purified AuNP solution; inset shows the UV-Vis-NIR spectrum of a drop-cast film of purified gold nanotriangles attained from the reaction of $AuCl_4^-$ and lemongrass extract. b) TEM micrograph of synthesised circular and nanotriangular AuNPs by lemongrass extract. c) Histograph representing the size of triangular AuNPs; inset demonstrates purified gold nanotriangles. d) Selected Area Electron Diffraction (SAED) pattern of a gold nanotriangle. The highlighted spots correspond to the 1/3{422},{220} and {311} Bragg reflections with lattice spacings found to be 2.5, 1.44 and 1.23 Å respectively. e) AFM image of a gold nanotriangle and f) its dimensional profile. Reprinted by permission from Macmillan Publishers Ltd: Nature Materials [71], copyright 2004.

for the field. A very important aspect of using plants instead of bacteria or fungi for NP production is the lack of pathogenicity.

An interesting study by Bar et al. illustrated a simple green synthesis route for AgNPs from $AgNO_3$ salts using the extract from *Jatropha curcas*. The result was the production of fairly homogenous (10-20 nm) AgNPs in 4 hours [59]. Most bacteria and fungi produce nanoparticles of a much wider size range as described earlier. However, for the synthesis process to occur the sample needs to be heated to a temperature of 85°C, which would be fairly costly if high volumes are required. Another study, using *Acalypha indica* leaf extracts showed that AgNP synthesis using plants is possible [11]. The size of the AgNPs was 20-30 nm, which is again significantly homogenous. Krishnaraj and group went on to test the synthesised AgNPs' antimicrobial capacity on *Escherichia coli* and *Vibrio cholera*. They observed that the AgNPs inhibited bacterial growth at a concentration as low as 10 µg/ml [11]. Lukman et al. reported the production of AgNPs using *Medicago sativa* seed exudates. Ag^+ reduction occurred almost instantly as AgNPs were observed within 1 minute of exposure to the silver salt. In less than 50 minutes 90% Ag^+ reduction occurred when the reaction was carried out at 30°C [60] which is significantly lower than the temperature used for *J. curcas*. The nanoparticles produced were spherical, flower-like and/or triangular in shape with a size range of 5-108 nm [60]. In contrast to Krishnaraj et al.'s study, not only were the purified AgNPs from *M. sativa* heterogenous in size, they did not show significant inhibition of bacterial growth. However, it was suggested that they could act synergistically with the seed exudate in order to eliminate bacteria [60]. Another plant that has the potential to reduce Ag^+ is *Ocimum sanctum* [61]. Its leaf extract was mixed with 1 mM $AgNO_3$ and the production of AgNPs of 3-20 nm in size was observed. The particles were spherical in shape and it was suggested that they may be stabilised by a component of the leaf broth [61].

In a study by Kasthuri et al., phyllanthin was extracted from the plant *Phyllanthus amarus* and subsequently used for the production of Ag and AuNPs. This is a unique study as only a single constituent of a plant extract was used for the synthesis of metallic nanoparticles, contrasting other studies mentioned earlier in which whole plants or extracts were used. Phyllanthin concentrations played a key role in the size and shape of the nanoparticle produced. Low concentrations resulted in the slow formation of triangular and hexagonal AuNPs and higher concentrations of phyllanthin gave rise to greater levels of spherical NPs which was confirmed by UV-Visible and TEM analysis [62].

Park et al. talked about the use of plant derived polysaccharides and phytochemicals which can be used for the synthesis of gold and silver nanoparticles. The use of such compounds for nanoparticle synthesis offers advantages such as decreased use of toxic chemicals and the ability of creating nanocomposites with different metals [63]. Soluble starch [64], chitosan [65], cellulose [66], dextran [67], alginic acid [68] and hyaluronic acid [69] have been used for the production of silver and gold nanoparticles successfully [63].

An extensive study was done by Song et al. on the production of AgNPs from a number of different plant leaf extracts. They examined the use of Pine, Persimmon, Ginkgo, Magnolia and Platanus extracts and compared their ability to produce AgNPs. The Magnolia leaf broth was found to be the best Ag^+ reducer as it took only 11 minutes to reduce 90% of the Ag^+ present in the sample [70]. In this example, once again, reaction conditions such as temperature needed to be controlled closely during the synthesis stage as they affected the rate, size and shape of the NPs. Song et al. tested the effect of different reaction temperatures and found that at 95°C Ag^+ conversion was much higher than at 25°C. However the size of the nanoparticles decreased at higher temperatures. It was hypothesised this was caused by the increased turnover of the nanoparticles by the reducing agent, as it has less time to build upon the presynthesised nanoparticles before starting to synthesise new ones [70].

Extracellular synthesis of AuNPs was illustrated using extracts from a lemongrass plant, *Cymbopogon flexuosus* [71]. Liquid-like nanotriangles formed by aggregates of spherical AuNPs were obtained when the extract was incubated with gold tetrachloride ($AuCl_4^-$) (Figure 5). This fluidity was attributed to the nanoparticle surface complexation of aldehydes and/or ketones that were present in the plant extract [71]. An additional study showed the synthesis of Au, Ag and bimetallic Au-AgNPs. The leaf broth of a Neem plant, *Azadirachta indica* was mixed with the salts of Au, Ag and then both metal ions simultaneously. The production was rapid with the synthesis rate starting to plateau at approximately 2 hours. It is believed that the terpenoid and flavanone components of the leaf broth may keep the NPs stable [72].

The production of PtNPs by bacteria and fungi has been researched in the past but not to a great extent and research on PtNP production by plants is even scarcer. Song et al. attempted to create PtNPs using the leaf extract of *Diopyros kaki*. A greater than 90% reduction of Pt ions into nanoparticles was illustrated in approximately 2.5 hours [73]. Song and group suggested that the reduction of the Pt ions was due to the presence of functional groups within the leaf extract such as amines, alcohols, ketones and carboxylic acids; as opposed to an enzyme mediated process. This was based on the fact that the reaction temperature was 95°C and no protein peaks were found in their FTIR analysis [73].

All the aforementioned studies on the synthesis of metallic NPs by plants involved using part or whole plant extracts, though it is also possible to synthesise metallic nanoparticles inside live growing plants. However there were no reports where plants have been used as the biological producers of PdNPs until Parker et al. presented a method of creating such nanoparticles using the plant, *Arabidopsis thaliana*. After growing Arabidopsis, its medium was then replaced with potassium tetrachloropalladate (K_2PdCl_4) and incubated for 24 hours in the salt solution. Subsequent TEM results visualised the PdNPs produced were at 2-4 nm size range. The produced PdNPs were subsequently used in Suzuki-Miyaura coupling reactions where the biogenic PdNPs were shown to convey a higher catalytic activity that commercially available PdNPs [74].

Moreover, Gardea-Torresdey et al. reported the synthesis of AuNPs, also by live plants. Alfalfa plant seeds were prepared and grown for two weeks with various concentrations of $K(AuCl_4)$. The nanoparticles were then extracted and analysed by various methods which confirmed the production of elemental AuNPs [75]. Although an interesting study, the NP synthesis time was long, over two weeks including the NP extraction. In order for a biological process for NP synthesis to be commercially feasible, the production time would need to be shortened significantly. On the other hand this would be a cheap and green method for synthesising such nanoparticles.

Applications of Metallic Nanoparticles

This review focuses on a number of metallic nanoparticles including gold (Au), silver (Ag), copper (Cu), Platinum (Pt), Palladium (Pd) and magnetite (Fe_3O_4). There are many reports on metallic nanoparticles used for industrial and medical applications and all of them show promising

results. Catalysts, cancer treatment, cosmetics and electronics are just a few examples of all the applications that metallic nanoparticles can be used for.

Au nanoparticles have found use in modern electronics where they can be used to print low resistance Au conductors. Conductors made of such nanoparticles have certain advantages over their bulk metal equivalent as they can be more flexible and also have a lower sintering temperature. This makes them suitable for electronics in plastic as they can be hardened at lower temperature and hence form low resistance conductors [76]. Au has also been studied on its effects on breast cancer cells. Stuchinskaya et al., conjugated the Au nanoparticles with a phthalocyanine-antibody complex which proved to be a promising way of targeting and killing breast cancer cells by the Au nanoparticles and cytotoxic singlet oxygen producer phthalocyanine [77].

Ag nanoparticles have been extensively studied in the recent years due to their antibacterial and therapeutic potential. Ag has been used in much a similar way to Au nanoparticles where an antibody-photosensitizer-nanoparticle complex was fused and targeted to cancer cells in order to create free radicals which would then kill the affected cells [78]. Ag nanoparticles have also sparked interest in other biomedical uses as well due to their high versatility in different areas of research. Their powerful antibacterial effects have been studied extensively and offer promising results for future antimicrobials [79]. They have the ability to create reactive oxygen species which cause irreversible damage to bacteria and also have a strong affinity in binding to DNA or RNA which interferes with the microbial replication process [78].

A study by Zain et al. suggested that Cu nanoparticles can also be used as antibacterial agents. It was also found that when Cu and Ag nanoparticles were fused together to create bi-metallic nanoparticles, their antibacterial effects increased and that nanoparticle size played a key role in the strength of the bactericidal effect [79].

Pt nanoparticles have also been extensively studied as they possess superior catalytic activities. They are primarily used for catalysis and fuel cell technology as they have can control redox reactions effectively [80]. For fuel cell applications Pt is used in cathodes and acts as an oxygen reducer. However Pt can also be used as the anode in which case it oxidises different types of fuels such as methanol in the methanol oxidation reaction (MOR) [80]. Pt has also been applied in catalysis where it acts as the catalyst for chemical reactions such as hydrogenation processes [81]. Similarly to Pt nanoparticles, Pd nanoparticles have also been used for catalytic purposes [79]. Bunge et al. was able to isolate bacterial strains from Alpine sites and use them to synthesise biogenic Pd nanoparticles. These nanoparticles when tested; were found to be highly catalytically active during dehalogenation reactions of polychlorinated dioxins [79].

Conclusions

It is clear that metallic nanoparticles have great potential in many different industries. The need for a process to synthesise such nanoparticles in a reliable and green way is becoming more pressing. Current chemical and physical methods involve toxic chemicals and high temperatures that are not only dangerous to the environment but costly too. Numerous groups have focused on alternative ways of synthesising nanoparticles as described here. Biological systems have been investigated in an effort to provide a sustainable, resource efficient and cheap method of synthesis. Many different biological chassis have been studied for their ability to resist the toxic effects of metal ions whilst producing metallic nanoparticles.

Bacteria are relatively cheap to cultivate and have a high growth rate compared to other biological systems such as fungi or plants. Their ease of manipulation gives them the advantage over plants and fungi as the chassis of choice for the near-term bio-production of nanoparticles that require optimised synthesis through genetic engineering. Alternatively, fungi have the advantage of producing very high yields of secreted proteins, which may increase nanoparticle synthesis rate. Many fungi have mycelia that provide a much higher surface area than bacteria and this area could be used to support the interaction of metal ions and fungal reducing agent thus enhancing the conversion of ions to metallic nanoparticles. Fungi also have the advantage of ease of downstream processing when extracellular nanoparticles are produced, allowing for a more efficient way of extracting nanoparticles from them. Scalability, another factor for consideration in the case of commercial production of nanoparticles, gives fungi the edge as the chassis of choice for long-term development as they can be used more easily in large-scale reactors than bacteria. Finally plants have also been found to be nanoparticle producers. The plants physiology has allowed for many different types of studies on them. Single components of plant extracts to whole plants have been utilised for the synthesis of nanoparticles. However before any industrial relevance can be attributed to the synthesis of nanoparticles by plants many more examples must be identified and, especially in the case of whole plant synthesis, the risks must be thoroughly assessed.

Whatever the choice of biological chassis may be, whether it is a bacterium, fungus or plant, they all need to be studied comprehensively in order to gain a clearer understanding of mechanism and to close the knowledge gap in biological nanoparticle synthesis methods by different organisms. The risks of such nanoparticles must also be assessed, but here biological synthesis may offer yet another advantage. The rapidly developing field of synthetic biology aims to create predictable, standardised systems and with such new technologies directed towards the production of metallic nanoparticles, biogenic nanoparticle samples are likely to become more homogenous and more reproducible, therefore the environmental and health risks posed will be more easily and more reliably assessed.

The field of biological production of metallic nanoparticles is relatively new and underexplored, however it shows great potential in the biotechnology sector. There are many aspects of these biological methods to be discovered, and later manipulated, as the technology emerges.

Acknowledgment

We would like to thank the BBSRC and Diageo for the studentship of Nikolaos Pantidos and Dr. Matthew Edmundson and Michael Capeness for their comments on the manuscript.

References

1. Narayanan KB, Sakthivel N (2010) Biological synthesis of metal nanoparticles by microbes. Adv Colloid Interface Sci 156: 1-13.
2. Thakkar KN, Mhatre SS, Parikh RY (2010) Biological synthesis of metallic nanoparticles. Nanomedicine 6: 257-262.
3. Lyubchenko YL, Shlyakhtenko LS (1997) Visualization of supercoiled DNA with atomic force microscopy in situ. Proc Natl Acad Sci U S A 94: 496-501.
4. Wagner E, Plank C, Zatloukal K, Cotten M, Birnstiel ML (1992) Influenza virus hemagglutinin HA-2 N-terminal fusogenic peptides augment gene transfer by transferrin-polylysine-DNA complexes: toward a synthetic virus-like gene-transfer vehicle. Proceedings of the National Academy of Sciences 89: 7934-7938.
5. Katz A, Alimova A, Min X, Rudolph E, Shah MK, et al. (2003) Bacteria size determination by elastic light scattering. Selected Topics in Quantum Electronics, IEEE Journal of 9(2): 277-287.

6. Mohanraj VJ, Chen Y (2006) Nanoparticles – A Review. Tropical Journal of Pharmaceutical Research 5: 561-573.

7. Husseiny MI, El-Aziz MA, Badr Y, Mahmoud MA (2007) Biosynthesis of gold nanoparticles using Pseudomonas aeruginosa. Spectrochim Acta A Mol Biomol Spectrosc 67: 1003-1006.

8. Durán N, Marcato PD, De Souza DIH, Alves OL, Esposito E (2007) Antibacterial Effect of Silver Nanoparticles Produced by Fungal Process on Textile Fabrics and Their Effluent Treatment. Journal of Biomedical Nanotechnology 3: 203-208.

9. Guzman M, Dille J, Godet S (2012) Synthesis and antibacterial activity of silver nanoparticles against gram-positive and gram-negative bacteria. Nanomedicine: Nanotechnology, Biology and Medicine 8: 37-45.

10. Guzmán M, Jean GD, Stephan G (2009) Synthesis of silver nanoparticles by chemical reduction method and their antibacterial activity. International Journal of Chemical and Biomolecular Engineering 2: 104-111.

11. Krishnaraj C, Jagan EG, Rajasekar S, Selvakumar P, Kalaichelvan PT, et al. (2010) Synthesis of silver nanoparticles using Acalypha indica leaf extracts and its antibacterial activity against water borne pathogens. Colloids Surf B Biointerfaces 76: 50-56.

12. Lima E, Guerra R, Lara V, Guzmán A (2013) Gold nanoparticles as efficient antimicrobial agents for Escherichia coli and Salmonella typhi. Chem Cent J 7: 11.

13. McFarland AD, Van Duyne RP (2003) Single Silver Nanoparticles as Real-Time Optical Sensors with Zeptomole Sensitivity. Nano Letters 3: 1057-1062.

14. Waszczuk P, Barnard T, Rice MC, Masel RI, Wieckowsky A (2002) A nanoparticle catalyst with superior activity for electrooxidation of formic acid. Electrochemistry Communications 4: 599-603.

15. Li X, Xu H, Chen ZS, Chen G (2011) Biosynthesis of Nanoparticles by Microorganisms and Their Applications. Journal of Nanomaterials 2011: 1-16.

16. Suresh K, Prabagaran SR, Sengupta S, Shivaji S (2004) Bacillus indicus sp. nov., an arsenic-resistant bacterium isolated from an aquifer in West Bengal, India. Int J Syst Evol Microbiol 54: 1369-1375.

17. Bhainsa KC, D'Souza SF (2006) Extracellular biosynthesis of silver nanoparticles using the fungus Aspergillus fumigatus. Colloids Surf B Biointerfaces 47: 160-164.

18. Song JY, Kim BS (2009) Rapid biological synthesis of silver nanoparticles using plant leaf extracts. Bioprocess Biosyst Eng 32: 79-84.

19. Edmundson MC, Capeness M, Horsfall L (2014) Exploring the potential of metallic nanoparticles within synthetic biology. N Biotechnol 31: 572-578.

20. Deplanche K, Caldelari I, Mikheenko IP, Sargent F, Macaskie LE (2010) Involvement of hydrogenases in the formation of highly catalytic Pd(0) nanoparticles by bioreduction of Pd(II) using Escherichia coli mutant strains. Microbiology 156: 2630-2640.

21. Yong P, Rowson AN, Farr JPG, Harris IR, Mcaskie LE (2002) Bioaccumulation of palladium by Desulfovibrio desulfuricans. Journal of Chemical Technology and Biotechnology 55: 593-601.

22. Wiley B, Herricks T, Sun Y, Xia Y (2004) Polyol Synthesis of Silver Nanoparticles - Use of Chloride and Oxygen to Promote the Formation of Single-Crystal, Truncated Cubes and Tetrahedrons. Nano Letters 4: 1733-1739.

23. Montazer M, Shamei A, Alimohammadi F (2014) Synthesis of nanosilver on polyamide fabric using silver/ammonia complex. Mater Sci Eng C Mater Biol Appl 38: 170-176.

24. Mafuné F, Kohno JY, Takeda Y, Kondow T (2003) Formation of Stable Platinum Nanoparticles by Laser Ablation in Water. The Journal of Physical Chemistry B 107: 4218-4223.

25. He S, Guo Z, Zhang Y, Zhang S, Wang J, et al. (2007) Biosynthesis of gold nanoparticles using the bacteria Rhodopseudomonas capsulata. Materials Letters 61: 3984-3987.

26. Johnston CW, Wyatt MA, Li X, Ibrahim A, Shuster J, et al. (2013) Gold biomineralization by a metallophore from a gold-associated microbe. Nat Chem Biol 9: 241-243.

27. Ahmad A, Mukherjee P, Senapat S, Mandal D, Khan MI, et al. (2003) Extracellular biosynthesis of silver nanoparticles using the fungus Fsarium oxysporum. Colloids and Surfaces B: Biointerfaces 28: 313-318.

28. Schlüter M, Hentzel T, Suarez C, Koch M, Lorenz WG, et al. (2014) Synthesis of novel palladium(0) nanocatalysts by microorganisms from heavy-metal-influenced high-alpine sites for dehalogenation of polychlorinated dioxins. Chemosphere 117C: 462-470.

29. Lloyd JR, Yong P, Macaskie LE (1998) Enzymatic recovery of elemental palladium by using sulfate-reducing bacteria Appl Environ Microbiol 64: 4607-4609.

30. Kalimuthu K, Suresh Babu R, Venkataraman D, Bilal M, Gurunathan S (2008) Biosynthesis of silver nanocrystals by Bacillus licheniformis. Colloids Surf B Biointerfaces 65: 150-153.

31. Pugazhenthiran N, Anandan S, Kathiravan G, Udaya Prakash NK, Crawford S, et al. (2009) Microbial synthesis of silver nanoparticles by Bacillus sp. Journal of Nanoparticle Research 11: 1811-1815.

32. Shahverdi AR, Minaeian S, Shahverdi HR, Jamalifar H, Nohi AA (2007) Rapid synthesis of silver nanoparticles using culture supernatants of Enterobacteria: A novel biological approach. Process Biochemistry 42: 919-923.

33. Das V, Thomas R, Varghese R, Soniya EV, Mathew J, et al. (2014) Extracellular synthesis of silver nanoparticles by the Bacillus strain CS 11 isolated from industrialized area. 3 Biotech 4: 121-126.

34. Sintubin L, De Windt W, Dick J, Mast J, van der Ha D, et al. (2009) Lactic acid bacteria as reducing and capping agent for the fast and efficient production of silver nanoparticles. Appl Microbiol Biotechnol 84: 741-749.

35. Pollmann K, Raff J, Merroun M, Fahmy K, Selenska-Pobell S (2006) Metal binding by bacteria from uranium mining waste piles and its technological applications. Biotechnol Adv 24: 58-68.

36. Sleytr UB, Messner P, Pum D, Sára M (1993) Crystalline bacterial cell surface layers. Mol Microbiol 10: 911-916.

37. Baco-Carles V, Datas L, Tailhades P (2011) Copper Nanoparticles Prepared from Oxalic Precursors. ISRN Nanotechnology: 1-7.

38. Ramanathan R, Field MR, O'Mullane AP, Smooker PM, Bhargava SK, et al. (2013) Aqueous phase synthesis of copper nanoparticles: a link between heavy metal resistance and nanoparticle synthesis ability in bacterial systems. Nanoscale 5: 2300-2306.

39. Parikh RY, Singh S, Prasad BLV, Patole MS, Sastry M, et al. (2008) Extracellular Synthesis of Crystalline Silver Nanoparticles and Molecular Evidence of Silver Resistance fromMorganellasp.: Towards Understanding Biochemical Synthesis Mechanism. Chem Bio Chem 9: 1415-1422.

40. Mukherjee P, Ahmad A, Mandal D, Senapati S, Sainkar S, et al. (2001) Fungus-Mediated Synthess of Silver Nanoparticles and Their Immobilizaation in the Mycelial Matrix- A Novel Biological Apporach to Nanoparticle Synthesis. Nano Letters 1: 515-519.

41. Rai M, Yadav A, Gade A (2009) Silver nanoparticles as a new generation of antimicrobials. Biotechnol Adv 27: 76-83.

42. Ummartyotin S, Bunnak N, Juntaro J, Sain M, Manuspiya H (2012) Synthesis of colloidal silver nanoparticles for printed electronics. Comptes Rendus Chimie 15: 539-544.

43. Ahmad A, Mukherjee P, Mandal D, Senapati S, Khan MI, et al. (2002) Enzyme mediated extracellular synthesis of CdS nanoparticles by the fungus, Fusarium oxysporum. J Am Chem Soc 124: 12108-12109.

44. Vahabi K, Mansoori GA, Karimi S (2011) Biosynthesis of Silver Nanoparticles by Fungus Trichoderma Reesei (A Route for Large-Scale Production of AgNPs). Insciences Journal: 65-79.

45. Sanghi R, Verma P (2009) Biomimetic synthesis and characterisation of protein capped silver nanoparticles. Bioresour Technol 100: 501-504.

46. Eustis S, El-Sayed MA (2001) Why gold nanoparticles are more precious than pretty gold Noble metal surface plasmon resonance and its enhancement of the radiative and nonradiative properties of nanocrystals of different shapes. Chemical Society Reviews 35: 209-217.

47. Mukherjee P, Ahmad A, Mandal D, Senapati S, Sainkar SR, et al. (2001) Bioreduction of AuCl(4)(-) Ions by the Fungus, Verticillium sp. and Surface Trapping of the Gold Nanoparticles Formed D.M. and S.S. thank the Council of Scientific and Industrial Research (CSIR), Government of India, for financial assistance. Angew Chem Int Ed Engl 40: 3585-3588.

48. Castro-Longoria E, Moreno-Velázquez SD, Vilchis-Nestor AR, Arenas-Berumen E, Avalos-Borja M (2012) Production of platinum nanoparticles and nanoaggregates using Neurospora crassa. J Microbiol Biotechnol 22: 1000-1004.

49. Riddin TL, Gericke M, Whiteley CG (2006) Analysis of the inter- and extracellular formation of platinum nanoparticles by Fusarium oxysporum f. sp. lycopersici using response surface methodology. Nanotechnology 17: 3482-3489.

50. Bharde A, Rautaray D, Bansal V, Ahmad A, Sarkar I, et al. (2006) Extracellular biosynthesis of magnetite using fungi. Small 2: 135-141.

51. Sun S, Zeng H (2002) Size-controlled synthesis of magnetite nanoparticles. J Am Chem Soc 124: 8204-8205.

52. Thapa D, Palkar VR, Kurup MB, Malik SK (2004) Properties of magnetite nanoparticles synthesized through a novel chemical route. Materials Letters 58: 2692-2694.

53. Spadaro D, Gullino ML (2005) Improving the efficacy of biocontrol agents against soilborne pathogens. Crop Protection 24: 601-613.

54. Mukherjee P, Roy M, Mandal BP, Dey GK, Mukherjee PK, et al. (2008) Green synthesis of highly stabilized nanocrystalline silver particles by a non-pathogenic and agriculturally important fungus T. asperellum. Nanotechnology 19: 075103.

55. Nevalainen H, Suominen P, Taimisto K (1994) On the safety of Trichoderma reesei. J Biotechnol 37: 193-200.

56. Narayanan KB, Sakthivel N (2011) Green synthesis of biogenic metal nanoparticles by terrestrial and aquatic phototrophic and heterotrophic eukaryotes and biocompatible agents. Adv Colloid Interface Sci 169: 59-79.

57. Iravani S, Zolfaghari B (2013) Green synthesis of silver nanoparticles using Pinus eldarica bark extract. Biomed Res Int 2013: 639725.

58. Mittal AK, Chisti Y, Banerjee UC (2013) Synthesis of metallic nanoparticles using plant extracts. Biotechnol Adv 31: 346-356.

59. Bar H, Bhui DK, Sahoo GP, Sarkar P, De SP, et al. (2009) Green synthesis of silver nanoparticles using latex of Jatropha curcas. Colloids and Surfaces A: Physicochemical and Engineering Aspects 339: 134-139.

60. Lukman AI, Gong B, Marjo CE, Roessner U, Harris AT (2011) Facile synthesis, stabilization, and anti-bacterial performance of discrete Ag nanoparticles using Medicago sativa seed exudates. J Colloid Interface Sci 353: 433-444.

61. Mallikarjuna K, Narasimha G, Dillip GR, Praveen B, Shreedhar B, et al. (2011) Green Synthesis of Silver Nanoparticles Using Ocumum Leaf Extract and their Characterization. Digest Journal of Nanomaterials and Biostructures 6: 181-186.

62. Kasthuri J, Kathiravan K, Rajendiran N (2008) Phyllanthin-assisted biosynthesis of silver and gold nanoparticles: a novel biological approach. Journal of Nanoparticle Research 11: 1075-1085.

63. Park Y, Hong YN, Weyers A, Kim YS, Linhardt RJ (2011) Polysaccharides and phytochemicals: a natural reservoir for the green synthesis of gold and silver nanoparticles. IET Nanobiotechnol 5: 69-78.

64. Raveendran P, Fu J, Wallen SL (2003) Completely "green" synthesis and stabilization of metal nanoparticles. J Am Chem Soc 125: 13940-13941.

65. Laudenslager MJ, Schiffman JD, Schauer CL (2008) Carboxymethyl chitosan as a matrix material for platinum, gold, and silver nanoparticles. Biomacromolecules 9: 2682-2685.

66. Cai J, Kimura S, Wada M, Kuga S (2009) Nanoporous cellulose as metal nanoparticles support. Biomacromolecules 10: 87-94.

67. Ma Y, Li N, Yang C, Yang X (2005) One-step synthesis of amino-dextran-protected gold and silver nanoparticles and its application in biosensors. Anal Bioanal Chem 382: 1044-1048.

68. Saha S, Pal A, Kundu S, Basu S, Pal T (2010) Photochemical green synthesis of calcium-alginate-stabilized Ag and Au nanoparticles and their catalytic application to 4-nitrophenol reduction. Langmuir 26: 2885-2893.

69. Kemp MM, Kumar A, Mousa S, Park TJ, Ajayan P, et al. (2009) Synthesis of gold and silver nanoparticles stabilized with glycosaminoglycans having distinctive biological activities. Biomacromolecules 10: 589-595.

70. Song JY, Kim BS (2009) Rapid biological synthesis of silver nanoparticles using plant leaf extracts. Bioprocess Biosyst Eng 32: 79-84.

71. Shankar SS, Rai A, Ankamwar B, Singh A, Ahmad A, et al. (2004) Biological synthesis of triangular gold nanoprisms. Nat Mater 3: 482-488.

72. Shankar SS, Rai A, Ahmad A, Sastry M (2004) Rapid synthesis of Au, Ag, and bimetallic Au core-Ag shell nanoparticles using Neem (Azadirachta indica) leaf broth. J Colloid Interface Sci 275: 496-502.

73. Song JY, Kwon EY, Kim BS (2010) Biological synthesis of platinum nanoparticles using Diopyros kaki leaf extract. Bioprocess Biosyst Eng 33: 159-164.

74. Parker HL, Rylott EL, Hunt AJ, Dodson JR, Taylor AF, et al. (2014) Supported palladium nanoparticles synthesized by living plants as a catalyst for Suzuki-Miyaura reactions. PLoS One 9: e87192.

75. Gardea-Torresdey JL, Parsons JG, Gomez E, Peralta-Videa J, Toiani HE, et al. (2002) Formation and growth of Au nanoparticles inside live alfalfa plants. Nano Letters 2: 397-401.

76. Daniel H, Frank L, Steven M, David R, Vivek S (2003) Plastic-Compatible Low Resistance Printable Gold Nanoparticle Conductors for Flexible Electronics. Journal of the Electrochemical Society 150: G412-G417.

77. Stuchinskaya T, Moreno M, Cook MJ, Edwards DR, Russell DA (2011) Targeted photodynamic therapy of breast cancer cells using antibody-phthalocyanine-gold nanoparticle conjugates. Photochemical & Photobiological Sciences 10: 822-831.

78. dos Santos CA, Seckler MM, Ingle AP, Gupta I, Galdiero S, et al. (2014) Silver nanoparticles: therapeutical uses, toxicity, and safety issues. J Pharm Sci 103: 1931-1944.

79. Zain NM, Stapley AG, Shama G (2014) Green synthesis of silver and copper nanoparticles using ascorbic acid and chitosan for antimicrobial applications. Carbohydr Polym 112: 195-202.

80. Chen J, Lim B, Lee EP, Xia Y (2009) Shape-controlled synthesis of platinum nanocrystals for catalytic and electrocatalytic applications. Nano Today 4: 81-95.

81. Bratlie KM, Lee H, Komvopoulos K, Yang P, Somorjai GA (2007) Platinum nanoparticle shape effects on benzene hydrogenation selectivity. Nano Lett 7: 3097-3101.

Citation: Pantidos N, Horsfall LE (2014) Biological Synthesis of Metallic Nanoparticles by Bacteria, Fungi and Plants. J Nanomed Nanotechnol 5: 233. doi: 10.4172/2157-7439.1000233

Submit your next manuscript and get advantages of OMICS Group submissions

Unique features:

- User friendly/feasible website-translation of your paper to 50 world's leading languages
- Audio Version of published paper
- Digital articles to share and explore

Special features:

- 350 Open Access Journals
- 30,000 editorial team
- 21 days rapid review process
- Quality and quick editorial, review and publication processing
- Indexing at PubMed (partial), Scopus, EBSCO, Index Copernicus and Google Scholar etc
- Sharing Option: Social Networking Enabled
- Authors, Reviewers and Editors rewarded with online Scientific Credits
- Better discount for your subsequent articles

Submit your manuscript at: www.editorialmanager.com/biochem